Trajectory Tracking Control in Linear Complementarity Systems and Frictional Oscillators

Aya Younes

THÈSE

Pour obtenir le grade de

DOCTEUR DE L'UNIVERSITÉ GRENOBLE ALPES

École doctorale : EEATS - Electronique, Electrotechnique, Automatique, Traitement du Signal (EEATS)
Spécialité : Automatique - Productique
Unité de recherche : Centre de recherche Inria de l'Université Grenoble Alpes

Poursuite de Trajectoires dans les Systèmes Linéaires de Complémentarité et les Oscillateurs à Frottement.

Trajectory Tracking Control in Linear Complementarity Systems and Frictional Oscillators

Présentée par :

Aya YOUNES

Direction de thèse :

Bernard BROGLIATO DIRECTEUR DE RECHERCHE, INRIA	Directeur de thèse
Felix MIRANDA VILLATORO INRIA Grenoble-Rhône-Alpes	Co-encadrant de thèse

Rapporteurs :

Pierre RIEDINGER
PROFESSEUR DES UNIVERSITES, Université de Lorraine
Sophie TARBOURIECH
DIRECTRICE DE RECHERCHE, CNRS DELEGATION OCCITANIE OUEST

Thèse soutenue publiquement le **1 octobre 2024**, devant le jury composé de :

Didier GEORGES, PROFESSEUR DES UNIVERSITES, Grenoble INP - UGA	Président
Bernard BROGLIATO, DIRECTEUR DE RECHERCHE, CENTRE INRIA UNIVERSITE GRENOBLE ALPES	Directeur de thèse
Pierre RIEDINGER, PROFESSEUR DES UNIVERSITES, Université de Lorraine	Rapporteur
Sophie TARBOURIECH, DIRECTRICE DE RECHERCHE, CNRS DELEGATION OCCITANIE OUEST	Rapporteure
Vincent ANDRIEU, DIRECTEUR DE RECHERCHE, CNRS DELEGATION RHONE AUVERGNE	Examinateur

Invités :

Felix Miranda-Villatoro
CHARGE DE RECHERCHE, INRIA Grenoble Rhône-Alpes

"To my beloved family..."

Abstract/Résumé

Abstract- This thesis is concerned with trajectory tracking in Linear Complementarity Systems (LCSs). LCS is a subclass of Non-Smooth Dynamical Systems (NSDS) defined by the combination of differential equations and non-smooth constraints known as complementarity conditions. These conditions are represented by a Linear Complementarity Problem LCP, which has the form of $0 \leq w \perp \lambda \geq 0$, where both variables $w = M\lambda + q$ and λ are called complementarity variables. It is important to note that the difficulty in studying LCS stems from the non-smooth constraints represented by the complementarity problem, which can also induce state jumps. The main analytical tools for stability analysis and control design are passivity which is an input/output property, and the maximal monotonicity of the non-smooth part. The notion of passivity is studied before applying complementarity constraints between w, as the output of the system, and λ, considered as a virtual input. Matrix inequalities which arise from passivity play a crucial role in the control design process; thus, solving linear matrix inequalities (LMIs) is an important objective of this thesis.

The contributions of this work are theoretical results on the stability analysis of the error dynamics, where the error represents the difference between the trajectories of the real system and the desired system (*i.e.*, the system to be tracked). First, the nominal case without state jumps is tackled. Then, the study focuses on cases with state jumps, analyzing stability for both jumps at initial time and further state jumps. In this case, preserving passivity during the state jump is crucial for stability analysis. Furthermore, the analysis is extended to the case when parametric time-varying uncertainties are added to the dynamical system to be controlled, resulting in the boundedness of the error under strong passivity conditions, which can be relaxed under certain conditions. In addition, this thesis illustrates various numerical applications, with a particular focus on electrical circuits with ideal diodes. It also presents applications on networks with unilateral interactions and mechanical systems with unilateral springs.

Building on the theoretical contributions presented, this work is extended to address the challenges of trajectory tracking in frictional oscillators. Frictional oscillators with set-valued friction are studied due to their dynamics which are suitable for modeling within the LCS framework. Relaxing strong passivity conditions is essential for the analysis of trajectory tracking in the presence of uncertainties. Moreover, the set-valued friction model is enhanced by including the Stribeck effect which enables us to design a new control strategy based on passifying the friction model. The dynamics of the frictional oscillator introduce a complex control problem when incorporating pulley-belt dynamics into the analysis. This leads to a new contribution which is the design

of a controller based on backstepping strategy, since the previous theoretical results on trajectory tracking in the nominal case could not be applied when considering the entire dynamical system.

Résumé- Cette thèse se concentre sur la poursuite de trajectoires dans les Systèmes de Complémentarité Linéaire (LCS). Les LCS sont une classe de systèmes dynamiques non lisses (NSDS) définis par la combinaison d'équations différentielles et de contraintes non lisses aussi connues sous le nom de conditions de complémentarité. Ces conditions sont représentées par un problème de complémentarité linéaire (LCP), de la forme $0 \leq w \perp \lambda \geq 0$, où les deux variables $w = M\lambda + q$ et λ sont appelées variables de complémentarité. Il est important de noter que la difficulté de l'étude des LCS vient du caractère non-régulier des contraintes, qui peuvent également engendrer des sauts d'état. Le principal outil analytique pour l'analyse de la stabilité et la conception des commandes est la passivité, qui est une propriété entrée/sortie, ainsi que la monotonie maximale de la partie non-régulière. La notion de passivité est étudiée avant d'appliquer des contraintes de complémentarité entre w, la sortie du système, et λ, l'entrée virtuelle. Les inégalités matricielles qui découlent de la passivité jouent un rôle crucial dans le processus de conception des commandes; ainsi, la résolution des inégalités matricielles linéaires (LMIs) est un objectif important de cette thèse.

Les contributions de ce travail donnent des résultats théoriques sur l'analyse de stabilité de la dynamique d'erreur, où l'erreur représente la différence entre les trajectoires du système réel et celles du système désiré. Tout d'abord, le cas nominal sans sauts d'état est abordé. Ensuite, l'étude se concentre sur les cas avec sauts d'état, en analysant la stabilité pour des sauts au moment initial et des sauts d'état suivants. Dans ce cas, la préservation de la passivité pendant le saut d'état est cruciale pour l'analyse de stabilité. En outre, l'analyse est étendue au cas où des incertitudes paramétriques variant dans le temps sont ajoutées au modèle du système dynamique à commander, ce qui se traduit par une erreur bornée garantie par la passivité forte, que l'on peut relaxer sous certaines conditions. De plus, cette thèse illustre diverses applications numériques, avec un accent particulier sur les circuits électriques avec diodes idéales. Elle présente également des applications sur des réseaux à interactions unilatérales et des systèmes mécaniques à ressort unilatéral.

En s'appuyant sur les contributions théoriques présentées, ce travail est étendu pour relever les défis de la poursui de trajetoires dans les oscillateurs à frottement. Les oscillateurs à frottement, dont le frottement est supposé multi-valué lorsque la vitesse de glissement est nulle, sont étudiés en raison de leur dynamique, adaptée à la modélisation dans le cadre LCS. La relaxation des conditions de passivité forte est essentielle pour l'analyse du suivi de trajectoire en présence d'incertitudes. De plus, le modèle de frottement à valeurs multi-valué est amélioré en incluant l'effet Stribeck qui nous permet de concevoir une nouvelle stratégie de commande basée sur la passification du modèle de frottement. Les dynamiques de l'oscillateur à frottement posent un problème de commande complexe lors de l'incorporation des dynamiques de poulie-courroie dans l'analyse. Cela conduit à une nouvelle contribution, qui est la conception d'une commande basée sur une stratégie appelée backstepping, car les résultats théoriques précédents sur la poursuite de trajectoires dans le cas nominal ne peuvent pas être appliquées lorsque l'on considère l'ensemble du système dynamique.

Acknowledgments

The last three years of my PhD journey have resulted in this manuscript, which would not be possible without the support of many individuals. This work is funded by the French National Research Agency "ANR-15-IDEX-02" and LabEx PERSYVAL "ANR-11-LABX-0025-01".

First, I would like to thank my supervisors, Bernard Brogliato and Felix Miranda-Villatoro for their invaluable guidance and feedback throughout my PhD journey. Their expertise and knowledge helped me to understand the challenges of research and to improve the quality of my work. I also want to thank Franck Pérignon for introducing me to SICONOS and for his technical assistance in simulations.

I am deeply thankful to all my colleagues in TRIPOP at INRIA: Nicholas, Chloé, Rasool and many others I have met during the last three years. I especially want to thank my office mates: Louis and Minh for their support and help. Sincere gratitude goes for Diane for her kindness and assistance with administrative issues.

I would like to express my gratitude to my friends Zakia, Alaa and Zaman for the quality time we have shared and the supportive conversations that made this journey easier. The places we explored and the memories we created made Grenoble a special place to remember. I also want to thank Zahraa and Sarah for their motivation, support and all the valuable moments we have shared despite the distance.

Finally, special thanks to my family: my parents Ali and Fatima, my brothers and my cousin Khawla for their unconditional love and constant encouragement. Their motivations helped me overcome challenging times. I am truly thankful to my partner Ali for his constant support, patience and presence all the time.

Contents

Abstract/Résumé . . . iv
Acknowledgment . . . vi

1 Introduction and Preliminaries **1**
1.1 Introduction . . . 1
1.2 Preliminaries . . . 5
1.2.1 Notations and Definitions . . . 5
1.2.2 Well-posedness of Linear Complementarity Systems . . . 9

2 Trajectory Tracking in Linear Complementarity Systems **15**
2.1 Trajectory Tracking in the Nominal Case . . . 15
2.1.1 Controller Design . . . 15
2.1.2 Error Dynamics Stability Analysis (no state jumps) . . . 19
2.1.3 Error Dynamics Stability Analysis including State Jumps . . . 21
2.2 Simple Scalar Example with State Jumps . . . 27
2.2.1 Dynamics and Closed-loop System . . . 27
2.2.2 State-jumps Analysis . . . 28
2.2.3 Stability Analysis of Error Dynamics . . . 29
2.2.4 Numerical Applications . . . 33
2.2.5 Recapitulation . . . 36
2.3 Tracking Control for First-order Sweeping Process . . . 36
2.3.1 Dynamics under FOSwP . . . 37
2.3.2 Conditions for Post-Jump Equality: $x^+ = x_d^+$ . . . 37
2.4 Robustness Analysis: Tracking with Parametric Uncertainties 44
2.4.1 Controller Design . . . 44
2.4.2 Error Dynamics Stability Analysis . . . 45
2.4.3 Relaxing Strong Passivity to Strict State Passivity . . . 49

3 Numerical Applications and Simulations **53**
3.1 Electrical Circuit with Parametric Uncertainties . . . 53
3.1.1 Open-loop Passivity . . . 54
3.1.2 Passivity of the Closed-loop System without Uncertainties . . . 55
3.1.3 Passivity of the Closed-loop System in the Presence of Uncertainties 56
3.2 Enhancing Electrical Circuit Passivity through Current Source Integration . . . 59
3.2.1 Passivity Analysis with Voltage Sources: Motivation . . . 59
3.2.2 Passivity Analysis with Current Source . . . 61

3.3 Electrical Circuits with Possible State Jumps . . . 65
3.3.1 Building Strictly State Passive Circuit . . . 65
3.3.2 Analysis of State Jumps . . . 71
3.4 Diode Bridge Example . . . 79
3.5 Networks with Unilateral Interactions . . . 82
3.6 Nonsmooth Mechanical Systems with Unilateral Springs . . . 85

4 Trajectory Tracking in Frictional Oscillators **89**
4.1 Friction Modeling . . . 89
4.2 Controlled Frictional Oscillators . . . 90
4.2.1 The Complementarity System Framework . . . 91
4.2.2 Well-posedness issues . . . 93
4.2.3 Equilibrium Points of the Error System . . . 95
4.3 Analysis of the Desired Trajectories . . . 97
4.3.1 Properties of the Desired Trajectories . . . 97
4.3.2 Numerical Simulation of the Desired Trajectories . . . 100
4.4 Trajectory Tracking of Frictional Oscillator in Nominal Case . 104
4.4.1 Passivity-based Control Framework . . . 104
4.4.2 Closed-loop Error Stability Analysis . . . 105
4.4.3 Numerical Simulation . . . 107
4.5 Parametric Robustness Analysis . . . 109
4.5.1 In the Presence of Time-varying Bounded Uncertainties $\Delta\mu(\dot{q}_{rel})$ 110
4.5.2 In the Presence of Constant Bounded Uncertainties $\Delta\mu = \mu - \mu_0$ 116
4.5.3 Numerical simulations . . . 119
4.6 Controller Design and Stability Analysis with Stribeck Effect . 121
4.6.1 The Stribeck Model and its Properties . . . 121
4.6.2 Controller Calculation . . . 124
4.6.3 Error Dynamics Stability Analysis . . . 124
4.6.4 Numerical simulation . . . 126

5 Backstepping Tracking Control of Frictional Oscillators with Pulley-Belt Dynamics **128**
5.1 Frictional Oscillator with Pulley-Belt Dynamics . . . 128
5.2 First Control Approach: Motivation for Backstepping Strategy 129
5.3 Backstepping-Based Control Approach . . . 131
5.3.1 Controller Design and Stability Analysis . . . 131
5.3.2 Analysis of Pulley's Angle Error Dynamics . . . 136
5.3.3 Numerical Simulations . . . 138
5.4 The Backward-Euler Discrete-time Implementation of the Backstepping Controller . . . 149
5.4.1 Well-posedness . . . 149
5.4.2 Stability Analysis . . . 153

6 Conclusions and Perspectives **157**
6.1 Summary of Contributions . . . 157
6.2 Research Perspectives . . . 158

6.2.1 Perspectives in LCS . . . 158
6.2.2 Perspectives in frictional oscillators . . . 158

Appendix **160**

A Useful Mathematical Results **161**
A.1 Transformation of BMI to an LMI . . . 161
A.2 Uniform and Ultimate Boundedness . . . 161
A.3 Conditions for Positive (Semi) Definiteness . . . 162

B Supplementary Mathematical Developments **164**
B.1 Optimization problem in (1.11) for the example in section 2.2 . 164
B.1.1 Desired system in (2.23) . . . 164
B.1.2 Closed-loop system in (2.25) . . . 165
B.2 Proof of the DI in (2.16) . . . 166

C Numerical Simulations and Computations **167**
C.1 Numerical Simulations with SICONOS . . . 167
C.1.1 Modelling . . . 167
C.1.2 Integration of the Dynamics . . . 170
C.2 Numerical computation of state-jump times . . . 171

D Electrical Circuits' Dynamics **174**

Chapter 1

Introduction and Preliminaries

1.1 Introduction

Complementarity dynamical systems are a class of nonsmooth nonlinear systems, that has received attention in the Automatic Control and Applied Mathematics literature because of their applications in many fields like electrical circuits with nonsmooth components, mechanical systems with unilateral contact, networks with unilateral interactions, economics with projected dynamical systems, genetics, traffic flow and neural networks, *etc*, see [37, 23, 81]. A Linear Complementarity System (LCS) with inputs is a nonsmooth dynamical system defined as:

$$\begin{cases} (a) & \dot{x}(t) = Ax(t) + B\lambda(t) + Eu(t) \quad \text{(almost everywhere)} \\ (b) & 0 \leq \lambda(t) \perp w(t) = Cx(t) + D\lambda(t) + Fu(t) \geq 0 \end{cases} \tag{1.1}$$

where $x \in \mathbb{R}^n$, $\lambda \in \mathbb{R}^m$ and $w \in \mathbb{R}^m$, A, B, C, D, E and F are constant matrices of appropriate dimensions, $u : \mathbb{R}_+ \to \mathbb{R}^p$ is an exogenous signal or a control input. The constraint in (1.1) (b) is the short form of the following three conditions: *i)* $\lambda(t) \in \mathbb{R}^m_+$, *ii)* $w(t) = Cx(t) + D\lambda(t) + Fu(t) \in \mathbb{R}^m_+$, and *iii)* $\langle \lambda(t), w(t) \rangle = 0$. Such constraints describe a linear complementarity problem (LCP), denoted LCP$(D, Cx + Fu)$. The LCP (1.1) (b) states that for $i = 1, \ldots, k$, either $\lambda_i = 0$ or $w_i = 0$. The set of constraints corresponding to the indices where $w_i = 0$ is the set of active constraints and it varies as the system evolves over time. Thus, the LCS in (1.1) can transition from one operation mode to another.

The Lyapunov-based stability of linear complementarity systems (LCS) is studied in [46, 43, 30, 29, 74, 130, 11], and the output regulation is analyzed in [145]. Linear Passive Complementarity system (LPCS) are investigated in [43] with some insights provided on their stability. The trajectory tracking problem is given a solution in [115, 114, 116, 71, 70, 33, 32, 21, 118, 117, 98, 78, 131, 132] for different systems and using various strategies. The tracking control for mechanical systems with unilateral constraints and/or impacts is tackled in [117, 32, 33, 78, 116]. The tracking of cyclic trajectories which undergo constrained/unconstrained/impacting phases of motion, including multiple constraints and multiple impacts phenomena, is studied in [33, 32, 21, 118, 117] for n-degree-of-freedom (dof) systems. Basically, in these studies, the

controllers are extended passivity-based algorithms which switch between three sub-controllers (persistent contact with constant number of activated constraints, mode obtained from the deactivation of one or several constraints, and impacting transition phase between two persistent contact modes when the number of activated constraints increases). The authors introduce the notion of weak stability, which extends Lyapunov stability by disregarding the Lyapunov function variation during the transition phases (nonmonotonic Lyapunov functions are used). Trajectory tracking in planar billiards is studied in [115, 114, 116, 71, 70]. The objective is to control a two-dof particle inside a closed compact domain when trajectories collide with the domain's boundary and never undergo persistent contact with it (a kind of vibro-impact systems [26, section 1.3.2]). Tracking control for a class of hybrid systems with state jumps is studied in [68, 20, 132], where in [68] the state feedback controller is designed with the property that the plant's jump times coincide with those of the reference trajectory, while [20] proposes a novel tracking error definition that deals with the non-coinciding jump times. It is noteworthy that in most of these articles, the desired trajectory is suitably modified in the neighborhood of state jumps (impacts), and/or the tracking error dynamics 'stability is tailored to the problem.

Trajectory tracking in fully-actuated complementarity Lagrangian systems has been tackled in [115, 114, 71, 70, 33, 32, 21, 118, 117, 78, 131]. This thesis, however, is dedicated to trajectory tracking in LCS, which represent a class of complementarity systems different from the Lagrangian complementarity systems studied in the references mentioned before. The main differences between Lagrangian systems with unilateral constraints and impacts, and LCS as presented in this manuscript, are that impacts in mechanical systems are state-dependent, see (3.39), and passivity does not hold when the complementarity variables (*i.e.*, the contact force multiplier and the gap function, which is usually a nonlinear function of the position) are used as the input and output variables to define the supply rate (see Remark 3.6.1). In passive LCS, state jumps are essentially exogenous (*i.e.*, they are triggered by the signal $Fu(t)$ in the variable w in (1.1) above), and passivity holds between the complementarity variables. Moreover the complementarity variables are not of the same form in mechanical systems and in LCS. In the latter they take the form of a linear function of the state, the multiplier and an exogenous signal (see definition of LCS in (1.1)), while unilateral constraints in Lagrangian systems always have $D = 0$ and $F = 0$ (hence excluding the strong passivity of the closed-loop system), and usually are a nonlinear function of one part of the state only, *i.e.*, positions. However, even linear unilaterally constrained Lagrangian systems do not fit within the class of LCS studied in this thesis, because of the different nature of state jumps as explained above. One major consequence is that state jumps can be triggered instantaneously by the exogenous signal, which is not possible in mechanical systems where exogenous signals (external forces and torques) do not act directly in the complementarity constraints. The way the desired trajectories are designed in the above works and in this manuscript, are quite different as well. When the unilateral constraints are replaced by unilateral springs, things differ significantly as illustrated in section 3.6.

Certainly, the frameworks that are the closest to what is presented in the sequel, are in

[145] and [98] (though the class of studied systems is not the same, and the robustness analysis is not led in [98]). The output regulation problem tackled in [145] differs from the problem tackled in this work. First, the desired systems are different: The desired system to be tracked is defined by the dynamics of the quadruple (A_r, G_r, H_r, J_r) as mentioned in [145] which is different from the real system defined. It is noticeable that the controller u in [145] is introduced only in the ordinary differential equation (ODE) of the real system, but not in the variational inequality (VI). Besides, there is no presence of a desired controller u_d in the desired system, which is autonomous. Second, the objectives are different: In the presence of uncertainties, the real and the desired systems have different dynamics. Hence, in this case, the aim of the regulation problem in [145] is to design a controller using internal model principle that achieves a zero steady-state regulation error: $e \triangleq x - \Pi x_r$ for some matrix Π. But, the aim of the tracking problem tackled in this work, in the presence of uncertainties, is to ultimately bound the tracking error: $e \triangleq x - x_d$, where $x_d(\cdot)$ is generated by desired dynamics. Third, the controller in [145] is state feedback, while state and multiplier feedback are considered in this thesis.

The authors in [98] study tracking for Measure Differential Inclusions (MDIs), which differ from LCS investigated in this work. They give sufficient conditions for the uniform convergence of MDIs with maximal monotonicity properties. In the tracking control of MDIs, the authors considered a desired trajectory x_d of locally bounded variation, and control inputs with an impulsive part (which we avoid, see section 2.1.3 and condition **(C1)**). In our approach, the desired trajectory x_d is designed independently by a LCS as shown in (2.1). Another difference with [98] is that the authors are interested in designing a controller such that the MDI of the closed-loop system is uniformly convergent with zero tracking error, while this thesis is primarily concerned with studying the stability of the error dynamics without explicitly considering the convergence of the closed-loop system.

The second part of the thesis focuses on frictional oscillators, which are low-dimension mechanical systems where friction plays a prominent role due to its nonlinear and non-smooth effect. Frictional oscillators have gained significant attention in the Nonlinear Dynamics scientific community due to their applications in mechanical engineering. The friction in these oscillators is modeled by a set-valued signum function, specifically representing planar Coulomb's friction with constant normal contact force. The set-valued signum function is quite amenable for complementarity [42, 26], which allows the study of frictional oscillators within the complementarity framework. This connection with complementarity systems motivates us to apply some of the theoretical results derived in the first part and introduce original extensions to address some challenges.

One-degree-of-freedom oscillator have been widely studied in the Applied Mathematics and in the Bifurcation and Chaos scientific communities, see, *e.g.*, [91, Chapter 9] [99, 96, 95, 63, 65, 139, 16, 97]. It may also be linked to a simplified Burridge-Knopoff model in seismology (see [66]). Many authors studied the behaviour of the stick-slip oscillators with various frictional laws see, *e.g.*, [99, 96, 95, 7, 84, 104, 108, 129, 147, 148]. The construction and stability analysis of periodic solutions for periodically excited frictional oscillator was first presented by [65, 139], with further results on the

existence and stability of periodic solutions presented in [129, 107, 90, 108, 63]. Externally excited frictional oscillators, as studied in [147, 148, 7, 84], may exhibit chaotic behaviour and they usually undergo rich bifurcation behaviour, see, *e.g.*, [125, 62, 96, 95, 72, 113, 84, 107, 90, 100]. Stick-slip vibrations, which are self-sustained oscillations induced by dry friction are described in [148, 129]. Several control techniques have been proposed for the stability analysis of frictional oscillators, such as active feedback control to superimpose frictional force in [79], and control strategies based on delayed time feedback in [64, 101].

Contributions

The main contributions of this thesis are presented in two main parts:

- Part 1: Trajectory Tracking in Linear Complementarity Systems
- Part 2: Trajectory Tracking in Frictional Oscillators

In the first part, which is covered in Chapters 2 and 3, a solution for the trajectory tracking in LCS is proposed. The study addresses case when all parameters are known, and when parameter uncertainties are taken into account. In the case when all parameters are known, both absolutely continuous solutions and solutions with state jumps are treated. Passivity and maximal monotonicity of suitable operators are crucial tools used to design stable closed-loop systems. Solving matrix inequalities, which are derived from passivity is central for the controller design. The theoretical developments are illustrated by numerical examples on nonsmooth circuits, networks with unilateral interactions, and mechanics with unilateral springs. A significant focus is given to electrical circuits with ideal diodes, where the passivity of electrical circuits with ideal diodes is investigated, strongly passive circuits are presented, and different approaches are explained for building passive circuits.

The second part of this thesis is represented by Chapters 4 and 5. It contributes to solve the tracking control problem in frictional oscillators. First, the strong passivity assumption is relaxed to assume strict state passivity for robustness analysis in the presence of uncertainties. Then, an extended controller with a compensation term is designed to handle the Stribeck effect in the friction model. Another contribution addresses the tracking control problem when incorporating pulley-belt dynamics, proposing a backstepping strategy for the controller design. This approach ensures stability of the tracking error and boundedness of the pulley's angle dynamics, supported by numerical simulations for nominal and uncertain cases to guarantee some robustness for the controller. Furthermore, the controller is studied in discrete time when using the Backward-Euler (implicit) method. Stability results are proved.

Outline

This manuscript is divided into five chapters. The first chapter is dedicated to the general introduction of the thesis, along with useful preliminaries and definition for the

analysis in the following chapters. Chapters 2 and 3 represent the first part of the thesis. In Chapter 2, the problem of trajectory tracking control in LCS is given a solution for cases with and without state jumps, and with and without uncertainties. Also, a simple example is given to illustrate the case of state jumps. In Chapter 3, various numerical applications are provided to explain the theoretical results developed in Chapter 2 which are supported by numerical simulations. Most of Chapter 3 is concerned with the study of electrical circuits with ideal diodes, where different approaches are explained to enhance the passivity of electrical circuits and achieve strictly and strongly passive circuits. Other applications are introduced like networks with unilateral interactions and mechanical systems with unilateral springs.

Chapters 4 and 5 cover the second part of the thesis. In Chapter 4, the problem of trajectory tracking control in frictional oscillators is considered. The stability is analyzed for cases with and without uncertainties. Then, the friction model is refined by including Stribeck effect, and a new approach is tackled to design the controller, followed by stability analysis for the tracking error. Chapter 5 focuses on backstepping tracking control in frictional oscillators with pulley-belt dynamics. In this chapter, the controller is designed based on backstepping strategy and the stability analysis is performed in continuous time and discrete time domains. In addition, numerical simulations is carried out for the nominal case and the case when parametric uncertainties are presented.

Publications

1. A.Younes, F. Miranda-Villatoro, and B. Brogliato. "Trajectory tracking in linear complementarity systems with and without state jumps: A passivity approach". In: *Nonlinear Analysis: Hybrid Systems* 54 (2024), p.101520.DOI: https://doi.org/10.1016/j.nahs.2024.101520

2. A.Younes, F. Miranda-Villatoro, and B. Brogliato. "Passivity-based Trajectory Tracking in Frictional Oscillators with Set-valued Friction". Submitted to Nonlinear Analysis: Hybrid Systems, Special Issue: Nonsmooth Dynamical Systems: Analysis, Control, and Optimization.

3. B. Brogliato, F. Miranda-Villatoro, and A.Younes. "Backstepping passivity-based trajectory tracking control of frictional oscillators: continuous and discrete time analyses". Submitted to Automatica.

1.2 Preliminaries

1.2.1 Notations and Definitions

This section provides an overview of the notations and definitions used throughout the manuscript, which ensures clarity of the discussion in the following chapters.

Matrices. The elements of a matrix $M \in \mathbb{R}^{n\times m}$ are denoted M_{ij}. $M_{\bullet,j}$ is its jth column, and $M_{i,\bullet}$ is its ith row. A matrix $M \in \mathbb{R}^{n\times n}$, possibly nonsymmetric, is said to be positive definite, $M \succ 0$ (resp. positive semi-definite, $M \succcurlyeq 0$) if $x^\top Mx > 0$ for all $x \neq 0 \in \mathbb{R}^n$ (resp. $x^\top Mx \geq 0$). M is a P-matrix if all its principal minors are positive; a positive definite matrix is a P-matrix. The minimum and the maximum eigenvalues of M are denoted $\lambda_{\min}(M)$ and $\lambda_{\max}(M)$. The maximum singular value of $M \in \mathbb{R}^{n\times m}$ is denoted $\sigma_{\max}(M)$, $\mathrm{Im}(M)$ is its image, $\mathrm{Ker}(M)$ is its null space. The singular values are ordered as $\sigma_{\max}(M) = \sigma_1(M) \geq \sigma_2(M) > \ldots > \sigma_r(M) > 0$, where $r = \mathrm{rank}(M)$. Let $M = M^\top$, its eigenvalues are real and ordered as $\lambda_{\max}(M) = \lambda_1(M) \geq \lambda_2(M) \geq \ldots \geq \lambda_n(M) = \lambda_{\min}(M)$. $M^\dagger$ denotes the Moore-Penrose pseudo-inverse of M.

Functions. Let $1 \leq p < +\infty$, a Lebesgue integrable function $f : I \subseteq \mathbb{R}^n \to \mathbb{R}$ belongs to $\mathcal{L}^p_{loc}(I;\mathbb{R})$ if $(\int_I ||f(t)||^p dt)^{\frac{1}{p}} < +\infty$ for any open set I (extended spaces). If $I = \mathbb{R}^n$ then $f \in \mathcal{L}^p(\mathbb{R}^n;\mathbb{R})$. Also $f \in \mathcal{L}^\infty(\mathbb{R}^n;\mathbb{R})$ if $f(\cdot)$ is Lebesgue integrable and $||f(x)|| < +\infty$ almost everywhere on $\mathbb{R}^n$. We denote $||f||_{I,p} \triangleq (\int_I ||f(t)||^p dt)^{\frac{1}{p}}$ for $1 \leq p < +\infty$, and $||f||_{I,\infty} \triangleq \mathrm{esssup}_{t\in I}||f(t)||$ (when I is obvious from the context it may be avoided). The range of the function $f(\cdot)$ is $\mathrm{Im}(f)$, its domain is $\mathrm{dom}(f) = \{x \mid f(x) < +\infty\}$. Right and left limits of the function $f(\cdot)$ at t are denoted $f(t^+)$ and $f(t^-)$. AC is for absolute continuity, DI for differential inclusion, BV is for bounded variation, LBV is locally BV, and RCLBV is for right-continuous LBV.

Sets. Let S be a nonempty set, $\mathrm{rint}(S)$ is its relative interior [134]. Let S and S' be closed sets, $d_H(S,S')$ denotes the Hausdorff distance between S and S'. Let $S \subseteq \mathbb{R}^m$ be a closed convex set containing 0. Its polar cone $S^\circ = \{x \in \mathbb{R}^m \mid x^\top v \leq 0,\ \forall v \in S\} = -S^\star$ where $S^\star$ is the dual cone.

Let us recall some useful definitions [37, 134, 135, 61, 39].

Definition 1 (Normal Cone)**.** *Let $S \subset \mathbb{R}^n$ be a closed, non-empty and convex set. The normal cone to S at a point $x \in S$ is given by*

$$\mathcal{N}_S(x) = \left\{g \in \mathbb{R}^n \mid g^\top(z-x) \leq 0,\ \ \forall z \in S\right\}. \tag{1.2}$$

For $x \notin S$ one usually sets $\mathcal{N}_S(x) = \emptyset$. The tangent cone $\mathcal{T}_S(\cdot)$ is the polar to the normal cone.

The domain of a set-valued mapping $T : \mathbb{R}^n \rightrightarrows \mathbb{R}^n$ is $\mathrm{Dom}(T) = \{x \in \mathbb{R}^n \mid T(x) \neq \emptyset\}$.

Definition 2 (Monotonicity)**.** *A multivalued mapping $T : \mathrm{Dom}(T) \subseteq \mathbb{R}^n \rightrightarrows \mathbb{R}^n$ is monotone if for all $u_1, u_2 \in \mathrm{Dom}(T)$, for all $v_1 \in T(u_1)$, $v_2 \in T(u_2)$*

$$\langle u_1 - u_2, v_1 - v_2\rangle \geq 0.$$

It is hypomonotone if there exists a real $k > 0$ such that: $\langle u_1 - u_2, v_1 - v_2\rangle \geq -k||u_1 - u_2||^2$. It is maximal monotone if its graph cannot be enlarged without destroying monotonicity.

The normal cone to a convex closed nonempty set defines a maximal monotone set-valued mapping. More generally, let $\varphi : \mathbb{R}^n \to \mathbb{R} \cup \{+\infty\}$ be a proper, convex and lower semicontinuous function. Its subdifferential at x is defined as the set $\partial\varphi(x) = \{g \in \mathbb{R}^n \mid \varphi(v) - \varphi(x) \geq g^\top(v - x),\ \forall v \in \mathbb{R}^n\}$, and it defines a maximal monotone mapping. The normal cone in (1.2) is the subdifferential of the indicator function defined as $\Psi_S(x) = 0$ if $x \in S$, $\Psi_S(x) = +\infty$ if $x \notin S$. Another function plays an important role: the support function of the set S, defined as $\sigma_S(y) = \sup_{v \in S} v^\top y$. It is related to the indicator function as: $\eta \in \mathcal{N}_S(v) = \partial\Psi_S(v) \Leftrightarrow v \in \partial\sigma_S(\eta) = \mathcal{N}_S^{-1}(\eta)$ (the indicator and the support functions are conjugate functions, and their subdifferentials are inverse mappings). The set-valued signum function $\mathrm{sgn}(x)$ is:

$$\mathrm{sgn}(x) = \begin{cases} +1, & \text{if } x > 0 \\ -1, & \text{if } x < 0 \\ [-1, +1], & \text{if } x = 0 \end{cases} \tag{1.3}$$

Definition 3 (Generalized Equation)**.** *A Generalized Equation (GE) is a nonlinear problem characterized by set-valued mapping denoted as:*

$$0 \in F(x) \tag{1.4}$$

where $dom(F) \subseteq \mathbb{R}^n \rightrightarrows \mathbb{R}^p$. One common form is: $0 \in f(x) + N_K(x)$, where $f : \mathbb{R}^n \to \mathbb{R}^p$ is a single-valued function and $N_K(x)$ is the normal cone to the closed convex set K at x.

Definition 4 (LCCS)**.** *A linear cone complementarity system (LCCS) is a particular class of a nonsmooth dynamical system given by:*

$$\begin{cases} \dot{x}(t) = Ax(t) + B\lambda(t) + Eu(t) \\ K \ni \lambda(t) \perp w(t) = Cx(t) + D\lambda(t) + Fu(t) \in K^\star \end{cases} \tag{1.5}$$

where $K \subseteq \mathbb{R}^m$ is a nonempty closed convex cone, $K^\star = \{z \in \mathbb{R}^m \mid z^\top w \geq 0,\ \forall\ w \in K\}$ is its dual cone.

It is noteworthy that most of the results in this thesis apply to linear cone complementarity systems (LCCS).

Definition 5 (DI)**.** *A differential inclusion (DI) describes the time evolution of a state variable x and has the form:*

$$\begin{cases} \dot{x}(t) \in F(t, x(t)), & a.e.\ \ t \in [0, T] \\ x(0) = x_0 \in \mathbb{R}^n \end{cases}$$

where $F : [0, \infty) \times \mathbb{R}^n \rightrightarrows \mathbb{R}^n$ is a multi-valued mapping.

Using tools from convex analysis it is possible to rewrite equivalently the LCS in (1.1) as the differential inclusion (DI) [37]:

$$\dot{x}(t) \in Ax(t) + Eu(t) - B(D + \mathcal{N}_{\mathbb{R}^m_+}^{-1})^{-1}(Cx(t) + Fu(t)) \stackrel{\Delta}{=} -H(t, x(t)), \tag{1.6}$$

where $\lambda(t) \in -(D + \mathcal{N}_{\mathbb{R}^m_+}^{-1})^{-1}(Cx(t) + Fu(t))$. We shall see later that the DI may sometimes be written in a slightly different way when the input is given a specific form, see (2.8) below. A state x^* is an equilibrium point of (1.1) if and only if there exist λ^* and $w^* \in \mathbb{R}^n$ such that the mixed LCP (MLCP)

$$\begin{cases} 0 = Ax^* + B\lambda^* \\ 0 \leq \lambda^* \perp w^* = Cx^* + D\lambda^* \geq 0 \end{cases}$$

holds.

Passivity plays an important role in the sequel of this work.

Definition 6 (Passivity)**.** *A quadruple (A, B, C, D) is said to be passive, or dissipative with respect to the supply rate $u^\top y$, if there exists a non-negative function $V : \mathbb{R}^n \to \mathbb{R}_+$, called a storage function, such that for all $t_0 \leq t_1$ and all time functions $(u, x, y) \in \mathcal{L}_2([t_0, t_1]; \mathbb{R}^m \times \mathbb{R}^n \times \mathbb{R}^m)$ such that $\dot{x}(t) = Ax(t) + Bu(t)$, $y(t) = Cx(t) + Du(t)$, the following inequality holds:*

$$V(x(t_0)) + \int_{t_0}^{t_1} u^\top(t)y(t)\, dt \geq V(x(t_1)) \tag{1.7}$$

The inequality (1.7) is called the dissipation inequality. Equivalently, the following LMI

$$\begin{pmatrix} A^\top P + PA & PB - C^\top \\ B^\top P - C & -D - D^\top \end{pmatrix} \preccurlyeq 0 \tag{1.8}$$

has a solution $P = P^\top \succcurlyeq 0$. Then $V(x) = \frac{1}{2}x^\top Px$. The quadruple (A, B, C, D) is said strictly state passive if the LMI (1.8) holds with $P = P^\top \succ 0$ and $A^\top P + PA + \epsilon P \preccurlyeq 0$ for some $\epsilon > 0$. It is said strongly passive if the LMI (1.8) holds with strict inequality and $P = P^\top \succ 0$.

When LCS are considered, then the multiplier λ is chosen as the input u while w is chosen as the output y for the passivity property. Passivity is then to be seen as a structural property related to internal variables of the LCS, and motivated by the fact that it corresponds to a physical property in some applications like circuits.

Definition 7 (VIs)**.** *[67, Definition 1.1.1] Given a subset K of the Eucledian n-dimensional space $\mathbb{R}^n$ and a mapping $F : K \to \mathbb{R}^n$, the variational inequality, denoted $VI(K, F)$ is to find a vector $x \in K$ such that:*

$$(y - x)^\top F(x) \geq 0,\ \forall y \in K \Leftrightarrow -F(x) \in \mathcal{N}_K(x) \tag{1.9}$$

where $\mathcal{N}_K(x)$ is the normal cone to K at a point x. The set of solutions to this problem is denoted $SOL(K, F)$. In addition, if K is a polyhedral set, the variational inequality is called 'affine' and denoted $AVI(K, F)$.

Definition 8 (Transfer Functions)**.** *[39, Definitions 2.34, 2.58, 2.78] The transfer function $H(s) = C(sI - A)^{-1}B + D \in \mathbb{C}^{mxm}$ is positive real (PR) if: $H(s)$ has no pole in $\boldsymbol{Re}[s] > 0$, $H(s)$ is real for all positive real s, $H(s) + H^\star(s) \succcurlyeq 0$ for all $\boldsymbol{Re}[s] > 0$. The transfer function $H(s) \in \mathbb{C}^{mxm}$ is strictly positive real (SPR) if $H(s - \epsilon)$ is PR for some $\epsilon > 0$ [39, Definition 2.58] and it is strong SPR (SSPR) if $H(s)$ is analytic in $\boldsymbol{Re}[s] \geq 0$ and $\boldsymbol{Re}[H(j\omega)] \geq \delta > 0$, for all $\omega \in [-\infty, \infty]$ and some $\delta \in \mathbb{R}$ [39, Definition 2.78].*

Strict state passivity is related to SPR tranfer functions, while strong passivity is related to SSPR transfer functions [39, 109]. Using the Schur complement theorem (see *e.g.*, [39, Theorem A.65]), strong passivity implies that $D \succ 0$ and $-A^\top P - PA \succ 0$.

1.2.2 Well-posedness of Linear Complementarity Systems

LCS as in (1.1) are nonlinear nonsmooth dynamical systems with external inputs, whose well-posedness (existence, uniqueness, and continuous dependence of solutions) has been investigated. Let us provide a short summary of well-posedness results in [43, 46, 45, 44, 38, 40, 30, 145]. Most of them apply to larger classes of nonsmooth systems than LCS. Let us remind that a right-continuous function $f : I \subseteq \mathbb{R} \to \mathbb{R}$ of locally bounded variation (RCLBV), has a countable set of discontinuities on I (allowing for left accumulations of jump instants), and possesses a differential measure df, see [112]. The conditions associated with the results recalled below, are sufficient. However they are well fitted with the conditions imposed in this article for stability purposes, *i.e.*, passivity.

1. (Well-posedness based on reduction to an ODE)

   • Assume that D is a P-matrix. Then from the fundamental theorem of Complementarity Theory [61], it follows that λ is a piecewise continuous, Lipschitz single-valued function of x and u. Hence the LCS in (1.1) is the ODE:

   $$\dot{x}(t) = Ax(t) + B\lambda(x(t), u(t)) + Eu(t).$$

   Provided $u(\cdot)$ satisfies Lebesgue integrability conditions, an AC solution exists on $\mathbb{R}_+$ for any bounded initial condition, with uniqueness and continuous dependence on initial data [52, 50].

   • Assume that $D \succ 0$ (not necessarily symmetric), then using the formalism in (1.6), the result can be extended to systems with operators $(D + \mathcal{M}_t)^{-1}(\cdot)$ where $\mathcal{M}_t(\cdot)$ is a maximal monotone operator for each fixed t. Using [30, Proposition 1] or [5], the mapping $(D + \mathcal{M}_t)^{-1}(\cdot)$ is then single-valued, defined everywhere, and Lipschitz continuous with constant $\frac{1}{\lambda_{\min}(D+D^\top)}$for each fixed t. Therefore the mapping $H(t, x)$ in (1.6) is single-valued Lipschitz continuous in x and classical results on ODE's well-posedness apply.

2. (Well-posedness based on passivity and relaxations of passivity) Let us summarize the results presented in [43, 145, 45, 47, 30, 44], which deal with the case with external inputs.

   (a) [43, Theorem 7.5] Assume that:

   - i) $(B^\top, D + D^\top)^\top$ has full column rank,
   - ii) (A, B, C, D) is passive with $P = P^\top \succ 0$, and minimal,
   - iii) $u(\cdot)$ is piecewise continuous with rational Laplace transform.

   Then for any $x(0) = x_0$, there exists a unique global solution to (1.1) such that $(\lambda, x, w) \in \mathcal{L}^2_\delta(\mathbb{R}_+; \mathbb{R}^{m+n+m})$, the space of Schwartz' distributions, with

regular parts in $\mathcal{L}^2_{loc} \subseteq \mathcal{L}^1_{loc}$, and atomic part with isolated atoms (instants of state jumps) that is represented by sums of Dirac measures (higher degree distributions do not occur).

(b) [45, Theorems 7, 8, 9] Assume that:

- i) (A, B, C, D) is passive with $P = P^\top \succ 0$,
- ii) $Fu(t) \in Q_D^\star + \mathrm{Im}(C)$ for all $t \geq [0, T)$, $T > 0$ (see paragraph of State Jumps below for the definition of Q_D and of its dual cone),
- iii) $u(\cdot)$ is a Bohl function (*i.e.*, $u(t) = M \exp(Nt)R$ for some constant matrices M, N, R).

Then $x(0^+)$ is calculated as in (1.11), there exists a unique AC solution $x : (0, T) \to \mathbb{R}^n$, and $\lambda(\cdot)$ is locally Lebesgue integrable. The solution is a forward solution, *i.e.*, it is the concatenation of Bohl functions defined between state jumps. Left accumulations of state jumps are allowed.

(c) [145, Corollary 2] [37, Corollary 5.9] Assume that:

- i) $D \succcurlyeq 0$, $\mathrm{Ker}(D + D^\top) \subseteq \mathrm{Ker}(PB - C^\top)$ for some $P = P^\top \succ 0$,
- ii) $\mathrm{rint}(\mathbb{R}^m_+ - Fu(t)) \subseteq \mathrm{rint}(\mathrm{Im}(\partial\sigma_{\mathbb{R}^m_+ - Fu(t)} + D))$,
- iii) $D\mathbb{R}^m_+ \subseteq \mathrm{Im}(C)$,
- iv) $\mathrm{Im}(C) - \mathbb{R}^m_+ = \mathbb{R}^m$,
- v) for each $x \in \mathbb{R}^n$ and each $t \geq 0$, if the set $\Lambda = \{\lambda \in \mathbb{R}^m_+ \mid v = Cx + D\lambda + Fu(t) \geq 0,\ \lambda^\top v = 0\}$ has a nonzero element, and $\Lambda \cap \mathrm{Im}(D + D^\top) \neq \emptyset$.

Then if $Fu(\cdot)$ is AC (resp. RCLBV), there exists a unique AC (resp. RCLBV) solution to (1.1) for any $x(0)$ such that $Cx(0) \in \mathrm{Im}(\partial\sigma_{\mathbb{R}^m_+ - Fu(0)} + D)$.

(d) [44, Theorems 11, 26] Let:

- i) (A, B, C, D) be passive,
- ii) $\mathrm{Im}(C) \cap \mathrm{rint}(\mathrm{Im}(D + \mathcal{N}_{\mathbb{R}^m_+}) - Fu(t)) \neq \emptyset$,
- iii) $Fu(\cdot)$ be AC.

Then there exists a unique AC solution for any $x(0) = x_0 \in \mathrm{Dom}(H(0, \cdot))$.

(e) [30, Theorem 1, Corollaries 2, 3] Assume that:

- i) $D = \begin{pmatrix} 0 & 0 \\ 0 & D_2 \end{pmatrix} \in \mathbb{R}^{m_2 \times m_2}$, $m_2 \leq m$
- ii) $F = 0$,
- iii) $u(\cdot)$ is continuous with $\dot{u} \in \mathcal{L}^1_{loc}(\mathbb{R}_+; \mathbb{R}^p)$,
- iv) there exists a full-rank $R = R^\top \in \mathbb{R}^{n \times n}$ such that $R^2 B_1 = C_1^\top$, $B = (B_1\ B_2)$, $C = (C_1^\top\ C_2^\top)^\top$,
- v) there exists $w_0 \in \mathbb{R}^{m_1}$ at which the operator $w \mapsto \partial\Psi_{\mathbb{R}^{m_1}_+}(C_1 R^{-1} w)$ is continuous,
- vi) the operator $w \mapsto RB_2(D_2 + \partial\Psi_{\mathbb{R}^{m_2}_+})^{-1}(-C_2 R^{-1} w)$ is well-defined, single-valued and Lipschitz continuous.

Then there exists a unique continuous right-differentiable solution for any $x(0) \in \mathrm{Dom}(\partial\Psi_{\mathbb{R}^{m_1}_+}(C_1R^{-1}\cdot)) = \{w \in \mathbb{R}^n \mid C_1R^{-1}w \geq 0\}$, with $\dot{x} \in \mathcal{L}^\infty(\mathbb{R}_+;\mathbb{R}^n)$. The result holds if $m_2 = 0$ and i-v) are verified, or if $m_2 = m$ and vi) is verified (then item 1 applies). Condition vi) holds if D_2 is a P-matrix [30, Proposition 1, Corollary 1].

(f) [93, Theorems 5.3, 5.4] and [92, Theorems 1, 2] deal with DIs of the form:

$$\dot{x}(t) \in g(t, x(t)) - B(D + F^{-1}_{t,x})^{-1}(Cx(t)),$$

where $F_{t,x} : \mathbb{R}^m \rightrightarrows \mathbb{R}^m$ is maximal monotone for each (t, x). For briefness we focus on $F_{t,x}(\cdot) = \mathcal{N}_{K(t,x)}(\cdot)$ [92]. Assume that:

- i) $D \succcurlyeq 0$, $\mathrm{Im}(D) \subset \mathrm{Im}(C)$, $\mathrm{Ker}(D + D^\top) \subseteq \mathrm{Ker}(PB - C^\top)$ for some $P = P^\top \succ 0$,
- ii) $K(t, x)$ has closed convex values, $K(t, x) \cap \mathrm{Im}(C) \neq \emptyset$, $d_H(K(t, x) \cap \mathrm{Im}(C), K(s, y) \cap \mathrm{Im}(C)) \leq k_1|t - s| + l_2||x - y||$ for all t, s, x, y, $l_1 \geq 0$, $0 \leq l_2 \leq \frac{\lambda_2}{||C||}$, λ_2 the smallest positive eigenvalue of $CC^\top$,
- iii) $(\mathcal{N}^{-1}_{K(t,x)} + D)^{-1}(Cx) \neq \emptyset \Rightarrow \mathrm{Im}(D + D^\top) \cap (\mathcal{N}^{-1}_{K(t,x)} + D)^{-1}(Cx) \neq \emptyset$,
- iv) $\mathrm{Im}(C) \cap \mathrm{rint}(\mathrm{Im}(\mathcal{N}^{-1}_{K(t,x)} + D)) \neq \emptyset$,
- v) $g(\cdot, \cdot)$ is continuous in t and Lipschitz continuous in x.

Then existence and uniqueness of Lipschitz continuous solutions is guaranteed for each initial condition such that $(\mathcal{N}^{-1}_{K(0,x_0)} + D)^{-1}(Cx_0) \neq \emptyset$. Moreover, $\|\dot{x}(t)\| \leq \alpha + \beta\|x(0)\|$ for some $\alpha > 0$ and $\beta > 0$.

3. (Well-posedness by transformation to a sweeping process [38, 37, 22]) Assume that $D = 0$, and that:

   - i) $PB = C^\top$ for some $P = P^\top \succ 0$,
   - ii) $u \in \mathcal{L}^1_{loc}(\mathbb{R}_+;\mathbb{R}^p)$,
   - iii) $\mathrm{Im}(C) - \mathbb{R}^m_+ = \mathbb{R}^m$.

   Then the LCS in (1.1) can be rewritten equivalently as a FOSwP (see (2.32) in section 2.3, and [38, 37] for details on the transformation, and [112, 37] for details on FOSwP). The basic condition i) is implied by, but does not imply, the passivity of $(A, B, C, 0)$. Depending on the signal $u(\cdot)$ being AC (resp. RCLBV), the solution is shown to be AC (resp. RCLBV), defined on $\mathbb{R}_+$, and uniqueness holds. For AC to hold it is needed that $x(0) \in S(0)$ (no initial jump).

The various assumptions made in items 2 and 3 (which may be thought as constraint qualifications in many instances, a concept which is familiar in Optimization) have different meanings:

- property of the plant's model: item 2 (a) ii), (b) i), (c) i), (d) i), (e) i) ii) iv), item 3 i),
- constraints qualifications: item 2 (a) i), (b) ii), (c) ii), iii), iv), v), (e) v), (f) ii), iii), iv), item 3 iii),

- exogenous signals properties: item 2 (a) iii), (b) iii), conclusion of item 2 (c), item 2 (e) iii), (f) v), conclusion of item 3.

The condition in item 2 (b) ii) stems from a fundamental result in Complementarity Theory [61, Theorem 3.8.6, Corollary 3.8.10], which guarantees the existence of solutions to the LCP in (1.1). This assumption thus secures that there exists a bounded multiplier $\lambda(t)$ which solves the LCP (notice that at the end time T, there may be a state jump if this assumption does not hold). This is an assumption quite similar to item 2 (c) ii), and item 2 (d) ii). Roughly speaking, they all guarantee that the various operators have nonempty domains so that the problem makes sense. They stem from [135, Theorem 12.43] to guarantee maximal monotonicity (see [30, section 3.2.1]). Such CQ may not be easy to check and may require some developments [28]. Condition in item 2 (c) iii) and (f) i) ($\mathrm{Im}(D) \subset \mathrm{Im}(C)$) are used to compute Vladimirov's pseudo distance (see [150] for the definition, which is beyond the scope of this article) between time-varying and/or state-dependent sets.

Multipliers boundedness (AC solutions)

Well-posedness analyses usually focus solely on the state. However, the boundedness of the multiplier is an important feature, since it may be used for feedback in this article. The condition in item 2 (b) ii) guarantees the existence of a solution to the LCP in (1.1). If the conditions in item 3 are verified, then explicit upper-bounds $\|\dot{x}(t)\| \leq \dot{v}(t) + \alpha(t)\|x(t)\|$ can be obtained for some integrable $\alpha(\cdot)$ and AC $v(\cdot)$ [146, Theorem 4.3] [112, section 5.2, Theorem 2.1]. In our case, these upper-bounds depend on the properties of the set-valued map $t \mapsto S(t)$ (which in turn depend on $Fu(\cdot)$ being AC, or Lipschitz continuous, or LBV [38, Proposition 3.2]). Following the developments in [145] (see item 2. (c) in section 1.2.2), $\lambda = \lambda^{\mathrm{im}}(t,x) + \lambda^{\mathrm{ker}}$, where $x \mapsto \lambda^{\mathrm{im}}(t,x) \in \mathrm{Im}(D + D^\top)$ is Lipschitz continuous, while $\lambda^{\mathrm{ker}} \in \mathrm{Ker}(D + D^\top)$. Moreover, λ^{im} is the least norm element in the (possibly) set-valued right-hand side of the DI, see [145, Equ. (15), Lemma 3]. It is inferred that in case the existence of AC solutions is proved, then $B\lambda(\cdot)$ is a bounded selection of the (possibly set-valued) right-hand side in (1.1). The part of λ inside $\mathrm{Ker}(B)$ does not play any role in $x(\cdot)$, but we may need the whole multiplier vector for feedback purpose. It is therefore reasonable to assume that the minimum norm element is available and that it satisfies a linear growth condition in $\|x\|$. Finally, it is worth recalling that even if $x(\cdot)$ is AC, the multiplier $\lambda(\cdot)$ may have discontinuities at junction times when $w(\cdot)$ reaches the boundary (*i.e.*, $w = 0$), when D is not a P-matrix. In the case of item 1, the multipliers are AC when $Fu(t)$ is AC since they are a Lipschitz continuous function of AC functions.

From a more practical point of view, multipliers in LCS can be calculated by constructing the contact LCP [37, section 2.4.1]. Thus, they appear to be a nonsmooth function of both state and input. The uniqueness of λ can be deduced from the conditions in item 2 (a) and (b), where passivity is the main property, plus some constraints qualification.

State jumps

Let the solution $x(\cdot)$ of (1.1) be RCLBV. Then $x(\cdot)$ may undergo discontinuities and the LCS has to be interpreted in the Measure Differential Inclusion (MDI) formalism [112, 69, 37]. In other words, the DI (1.6) has to be embedded into an MDI: $dx \in (Ax(t) + Eu(t))dt - B(D + \mathcal{N}_{\mathbb{R}^m_+}^{-1})^{-1}(Cx(t^+) + Fu(t))d\nu$, where dx is the differential measure associated with the RCLBV function $x(\cdot)$ [112], dt is the Lebesgue measure, and $d\nu$ is a specific Radon measure, see [145, Definition 4] for a rigorous introduction. The dissipation inequality extends to MDI, see [26, section 5.4.4.5] [39, section 7.2.4.1]. Let the set of time instants at which the state undergoes a jump, be denoted as $\mathcal{J}_x$, and the set of time instants at which $Fu(\cdot)$ is discontinuous be denoted as $\mathcal{J}_{Fu}$. Then if conditions of item 2 (a) hold, $\mathcal{J}_x \subseteq \{0\} \cup \mathcal{J}_{Fu}$ [43, 38]. In other words, the state can jump only initially, or at times of discontinuity in $Fu(\cdot)$ (or in the set $S(t)$ in the FOSwP formalism). *This means that state jumps can be chosen and dwell times can be imposed (contrarily to complementarity mechanical systems), by suitably choosing* $Fu(t)$.
In the case of BV solutions, and under the conditions stated above, the term $B\lambda$ is a Dirac measure at times of state jumps, and we may denote $\lambda = \lambda^{imp} + \lambda^{reg}$. The input in (2.2) below, may be defined with the complete λ ("impulsive" input), or just with its function part λ^{reg}. In both cases, the stability analysis has to incorporate the jumps. At an instant of jump t, using (1.6) and [145, section 3.4], we have:

$$x(t^+) - x(t^-) \in -B(D + \partial\sigma_{S(t^+)})^{-1}(Cx(t^+)), \tag{1.10}$$

with $S(t^+) = \mathbb{R}^m_+ - Fu(t^+)$. State jump rules formulations are given in [37, Lemma 2.3], compiling results in [43, 38, 45, 75]. They are based on a maximum dissipation principle (a kind of plastic impact, inspired from [124]). Let us introduce such rules briefly. If (A, B, C, D) is passive with $P = P^\top \succ 0$ and if $0 \in \mathcal{K} \triangleq \{z \in \mathbb{R}^n \mid Cz + Fu(t^+) \in Q_D^\star\}$ (notice that the set $\mathcal{K} \neq \emptyset$ by the condition in item 2 (b) ii)), $Q_D = \{z \in \mathbb{R}^m \mid 0 \leq z \perp Dz \geq 0\}$, then the jumps dissipate "energy", *i.e.*, $V(x(t^+)) \leq V(x(t^-))$ [75, Lemma 3], and the state jump rule is given by:

$$x(t^+) = \text{argmin}_{x \in \mathcal{K}} \frac{1}{2}(x - x(t^-))^\top P(x - x(t^-)). \tag{1.11}$$

Notice that Q_D is a polyhedral set, and so is its dual cone [135, Lemma 6.45, Theorem 3.52]. If $D \succ 0$ then $Q_D = \{0\}$, $Q_D^\star = \mathbb{R}^m$, $\mathcal{K} = \mathbb{R}^n$ and using (1.11), $x(t^+) = x(t^-)$. If $D = 0$ then $Q_D = \mathbb{R}^m_+ = Q_D^\star$, $\mathcal{K} = \{z \in \mathbb{R}^n \mid Cz + Fu(t^+) \geq 0\}$, hence $0 \in \mathcal{K}$ if and only if $Fu(t) \geq 0$. Thus, strongly passive systems have continuous-time solutions, but strictly state passive systems may have state jumps. Notice that : $x(t^+) - x(t^-) = B\sigma$, with $\lambda^{imp} = \sigma\delta_t$, and $0 \leq \sigma \perp D\sigma \geq 0$. As shown in [43, 37, 75] the state jump does not depend on a particular choice of the storage function matrix P. The meaning of the complementarity conditions at discontinuity times is explained in [43, Theorems 6.1, 9.1], see also [37, Lemma 2.3].

Zeno behavior

LCS undergo two classes of events, *i.e.*, switching between modes of the LCP (1.1) (b) (AC solutions), and state discontinuities (BV solutions). Zenoness with AC solutions is

tackled in [141, 46, 140] when $Fu(\cdot) = 0$. It states that if $B\mathrm{SOL}(D, Cx)$ is a singleton, then the LCS (1.1) is Zeno-free. This holds if D is a P-matrix. Thus junction and detachment times are separated (dwell time). The conditions stated in [45, Theorem 7] also prevent Zeno behaviour in LCS with external inputs and state jumps, by imposing condition ii) in item 2 (b) between jumps.

Time-varying LCS (TVLCS)

We may also encounter TVLCS of the form:

$$\begin{cases} (a) & \dot{x}(t) = A(t)x(t) + B(t)\lambda(t) + E(t)u(t) \quad \text{(almost everywhere)} \\ (b) & 0 \leq \lambda(t) \perp w(t) = C(t)x(t) + D(t)\lambda(t) + F(t)u(t) \geq 0 \end{cases} \tag{1.12}$$

when we deal with uncertainties which may be time-varying. The TVLCS is rewritten equivalently as:

$$\begin{aligned} \dot{x}(t) \in \; & A(t)x(t) + E(t)u(t) - B(t)(D(t) + \mathcal{N}^{-1}_{\mathbb{R}^m_+})^{-1}(C(t)x(t) + F(t)u(t)) \\ = \; & A(t)x(t) + E(t)u(t) - B(t)(D(t) + \mathcal{N}^{-1}_{\mathbb{R}^m_+ - F(t)u(t)})^{-1}(C(t)x(t)) \end{aligned} \tag{1.13}$$

Clearly, some of the results described above can be used to analyse (1.13), in particular cases [38, 44]. One such case is as follows. Assume that $A = A(t)$, $E = E(t)$, $F = F(t)$, $D = 0$, C and B are constant. Assume that there exists $P = P^\top \succ 0$ such that $PB = C^\top$. Then, (1.13) is rewritten equivalently as:

$$\dot{x}(t) \in A(t)x(t) + E(t)u(t) - B\mathcal{N}_{\mathbb{R}^m_+ - F(t)u(t)}(Cx(t)) \tag{1.14}$$

After the classical state change $z = Rx$, $R^2 = P$, $R = R^\top \succ 0$ [37], (1.14) is rewritten equivalently as:

$$\dot{z}(t) \in RA(t)R^{-1}z(t) + RE(t)u(t) - \mathcal{N}_{\mathbb{R}^m_+ - F(t)u(t)}(z(t)),$$

which is a FOSwP with affine perturbation. Hence, the material in item 3 section 1.2.2 can be used to analyse the well-posedness with both AC and RCLBV solutions. The general problem of well-posedness of (1.13) is not tackled in this work.

Chapter 2

Trajectory Tracking in Linear Complementarity Systems

This chapter is dedicated to trajectory tracking in linear complementarity systems (LCS). It focuses mainly on the control design based on passivity and the stability analysis of the error dynamics. Several cases are addressed in the following sections of the chapter, including systems with and without state jumps in the known parameter case, and then the results are extended to the case when parametric uncertainties are considered. A simple example is provided to illustrate the trajectory tracking results in the case of state jumps. Furthermore, trajectory tracking in First-order Sweeping Process (FOSwP), which is equivalent to LCS with matrix $D = 0$ under some conditions, is investigated.

2.1 Trajectory Tracking in the Nominal Case

In this section, it is assumed that the plant model and parameters have no uncertainties. That is, the matrices A, B, C, D, E, F in (1.1) are known.

2.1.1 Controller Design

Let us consider the LCS with external input in (1.1). Let us define the system which generates the desired trajectory to be tracked, as follows:

$$\begin{cases} \dot{x}_d(t) = Ax_d(t) + B\lambda_d(t) + Eu_d(t) \\ 0 \leq \lambda_d(t) \perp w_d(t) = Cx_d(t) + D\lambda_d(t) + Fu_d(t) \geq 0 \end{cases} \tag{2.1}$$

where $u_d(\cdot)$ is the desired input. Following the LCS of the desired system in (2.1), the designer has to perform a preliminary analysis of the desired dynamics to determine a suitable trajectory for tracking. This analysis may involve numerical methods or the approaches presented in [138, 80]. The aim is to design a feedback controller such that the error dynamics with state vector $e \stackrel{\Delta}{=} x - x_d$ possesses some stability property, to be defined later. Let us state the following assumptions which will be used later:

Assumption 2.1.1. *The solution $x_d : \mathbb{R}_+ \to \mathbb{R}^n$ of the LCS (2.1) is AC and uniformly bounded, and the multiplier vector $\lambda_d(u_d, x_d)$ is a bounded function of time.*

Conditions such that this holds can be obtained from the results stated in section 1.2.2.

Assumption 2.1.2. *The state $x(\cdot)$ and the multiplier $\lambda(\cdot)$ are available for measurement.*

In practice, the multiplier may be a physical quantity (like voltages and currents in circuits, contact force in mechanics), and Assumption 2.1.2 is reasonable (and studying state observers in the loop is outside the scope of this thesis). Thus, the feedback controller in the plant (1.1) is chosen generically as:

$$u(x, \lambda, t) = K[x - x_d(t)] + G[\lambda - \lambda_d(t)] + u_d(t). \tag{2.2}$$

where the example in Remark 2.1.3 plays the role of a motivating example for introducing a feedback from λ in the controller (2.2).

Remark 2.1.3. *To motivate the addition of a feedback from λ in the controller (2.2), consider the LCS in (1.1) with the following matrices:*

$$A = \begin{pmatrix} -1 & 0 \\ 0 & -2 \end{pmatrix}, \quad B = \begin{pmatrix} 1 \\ 0 \end{pmatrix}, \quad C = \begin{pmatrix} 1 & 0 \\ 0 & 1 \end{pmatrix}, \quad D = \begin{pmatrix} 1 & 0 \\ 0 & 0 \end{pmatrix}, \quad E = 0, \quad F = \begin{pmatrix} 0 \\ 1 \end{pmatrix}$$

Let $u = K(x - x_d) + u_d$, then the closed-loop system's quadruple $(A, B, C + FK, D)$ is strictly state passive with $K = (1.12, \ -1)$, $P = \begin{pmatrix} 1.12 & -0.006 \\ -0.006 & 2.012 \end{pmatrix}$ given by solving the BMI in (4.10) after transforming it to LMI according to Appendix A.1. However, the LMI for strong passivity in (2.7) does not have a solution for the closed-loop quadruple $(A, B, C + FK, D)$.

Let us introduce feedback from the complementarity variable λ, resulting in the extended controller in (2.2): $u = K(x - x_d) + G(\lambda - \lambda_d) + u_d$. In order to check if the closed-loop quadruple $(A, B, C + FK, D + FG)$ with the extended controller is strongly passive, let us check if the BMI in (2.7) has a solution. It appears that the transformed BMI in (2.7) for strong passivity has a solution given by:

$$K = \begin{pmatrix} 1.13 & -0.99 \end{pmatrix}, \quad G = 0.59, \quad P = \begin{pmatrix} 1.17 & -0.014 \\ -0.014 & 2.16 \end{pmatrix}$$

Strong passivity of the closed-loop system is a fundamental assumption in robustness analysis in section 2.4 in order to guarantee the boundedness of the tracking error e. Therefore, there is a need to introduce a feedback from λ in the controller u to enhance the passivity of the closed-loop system in certain applications.

Inserting (2.2) into (1.1) for some feedback gains $K \in \mathbb{R}^{p \times n}$ and $G \in \mathbb{R}^{p \times m}$ gives rise to the closed-loop LCS:

$$\begin{cases} \dot{x}(t) = (A + EK)x(t) + (B + EG)\lambda(t) - EKx_d(t) - EG\lambda_d(t) + Eu_d(t) & \text{(a.e.)} \\ 0 \le \lambda(t) \perp w(t) = (C + FK)x(t) + (D + FG)\lambda(t) - FKx_d(t) - FG\lambda_d(t) \\ \qquad\qquad + Fu_d(t) \ge 0 \end{cases} \tag{2.3}$$

It is important to note that, in general, both $\lambda_d(\cdot)$ and $u_d(\cdot)$ in (2.1) may be discontinuous time-functions, hence (2.3) is in general an LCS as (1.1) with a potentially discontinuous term $-FKx_d(t) - FG\lambda_d(t) + Fu_d(t)$ inside the complementarity constraints. As a consequence, jumps in $x(\cdot)$ may occur unless some conditions hold (see the end of section 2.1.2). We shall come back to state jumps in section 2.1.3. Rewriting (2.1) equivalently as

$$\begin{cases} \dot{x}_d(t) = (A+EK)x_d(t) + (B+EG)\lambda_d(t) + Eu_d(t) - EKx_d(t) - EG\lambda_d(t) \\ 0 \leq \lambda_d(t) \perp w_d(t) = (C+FK)x_d(t) + D\lambda_d(t) + Fu_d(t) - FKx_d(t) \geq 0 \end{cases} \tag{2.4}$$

gives rise to the error dynamics:

$$\begin{aligned} \dot{e}(t) &= (A+EK)e(t) + (B+EG)(\lambda(t) - \lambda_d(t)) \\ 0 \leq \begin{pmatrix} w(t) \\ w_d(t) \end{pmatrix} &= \begin{pmatrix} C+FK \\ -C-FK \end{pmatrix} e(t) + \begin{pmatrix} D+FG & -FG \\ 0 & D \end{pmatrix} \begin{pmatrix} \lambda(t) \\ \lambda_d(t) \end{pmatrix} \\ &\quad + \begin{pmatrix} 0 & C \\ C+FK & -FK \end{pmatrix} \begin{pmatrix} x(t) \\ x_d(t) \end{pmatrix} + \begin{pmatrix} Fu_d(t) \\ Fu_d(t) \end{pmatrix} \perp \begin{pmatrix} \lambda(t) \\ \lambda_d(t) \end{pmatrix} \geq 0 \end{aligned} \tag{2.5}$$

Clearly, the LCS in (2.5) is well-posed if both (2.1) and (2.3) are. However, the LCS in (2.5) cannot be used for well-posedness directly, because $x(\cdot)$ acts as an exogenous signal in the complementarity constraints, whose properties have to be proved. The closed-loop's well-posedness has to be tackled with (2.3) and (2.4) (or (2.1)). In view of the structure of the closed-loop LCS in (2.3), let us state the following assumptions, which will be used in the sequel for both well-posedness and stability purposes.

Assumption 2.1.4. *There exist matrices K and G such that the plant's closed-loop quadruple $(A+EK, B+EG, C+FK, D+FG)$ is strictly state passive.*

From Assumption 2.1.4, there exist gain matrices K and G such that the following nonlinear matrix inequality with unknowns P, K and G:

$$M \triangleq \begin{pmatrix} (A+EK)^\top P + P(A+EK) & P(B+EG) - (C+FK)^\top \\ (B+EG)^\top P - (C+FK) & -(D+FG) - (D+FG)^\top \end{pmatrix} \preccurlyeq \begin{pmatrix} -\epsilon P & 0 \\ 0 & 0 \end{pmatrix}, \tag{2.6}$$

has a solution $P = P^\top \succ 0$. This may be replaced by the more stringent assumption:

Assumption 2.1.5. *There exist matrices K and G such that the plant's closed-loop quadruple $(A+EK, B+EG, C+FK, D+FG)$ is strongly passive.*

From Assumption 2.1.5, there exist gain matrices K and G such that the nonlinear matrix inequality:

$$M \prec 0 \tag{2.7}$$

has a solution $P = P^\top \succ 0$. For numerical purposes, it is important to note that the BMIs in (4.10) and (2.7) are transformed into LMIs, as detailed in Appendix A.1.

Using Convex Analysis, the closed-loop system (2.3) is rewritten equivalently as the DI:

$$\begin{aligned} \dot{x}(t) \quad &\in (A+EK)x(t) - (B+EG)((D+FG) + \partial\sigma_{S(t)})^{-1}((C+FK)x(t)) \\ &\quad -EKx_d(t) - EG\lambda_d(t) + Eu_d(t) \end{aligned} \tag{2.8}$$

where $S(t) = \{v \in I\!R^m_+ \mid v + FKx_d(t) + FG\lambda_d(t) - Fu_d(t) \geq 0\}$ is closed nonempty convex for each t, and $\sigma_{S(t)}(\cdot)$ is the support function of $S(t)$. The DI in (2.8) has the form

$$\dot{x}(t) \in -\mathcal{M}(t, x(t)) + f(t), \tag{2.9}$$

with $f(t) = -EKx_d(t) - EG\lambda_d(t) + Eu_d(t)$ and $\mathcal{M}(\cdot,\cdot)$ is a set-valued operator. In view of (2.1) and Assumption 2.1.1, depending on the system's parameters, the multiplier $\lambda_d(\cdot)$ may be discontinuous at some instants, hence the set $S(t)$ may also be discontinuous at those instants ($D \succ 0$ prevents such jumps). The LCS in (2.1) is also equivalently rewritten as the DI:

$$\dot{x}_d(t) \in Ax_d(t) - B(D + \partial\sigma_{S_d(t)})^{-1}(Cx_d(t)), \tag{2.10}$$

with $S_d(t) = \{v \in I\!R^m \mid v - Fu_d(t) \geq 0\}$, and the set $S_d(t)$ is continuous as long as $u_d(t)$ is. Therefore, the DI in (2.10) also fits with (2.9). Let us now examine (2.5). Using that $x(t) = e(t) + x_d(t)$, the error dynamics may be rewritten as:

$$\dot{e}(t) \in \tilde{A}e(t) - \tilde{B}(\tilde{D} + \mathcal{N}^{-1}_{\tilde{S}(t,e(t))})^{-1}(\tilde{C}e(t)) \tag{2.11}$$

with $\tilde{S}(t,e) = \{z \in I\!R^{2m} \mid z + \tilde{E}e + \tilde{F}(t) \geq 0\}$, $\tilde{E} = \begin{pmatrix} 0 \\ C + FK \end{pmatrix}$,
$\tilde{F}(t) = \begin{pmatrix} Cx_d(t) + Fu_d(t) \\ Cx_d(t) + Fu_d(t) \end{pmatrix}$, $\tilde{D} = \begin{pmatrix} D + FG & -FG \\ 0 & D \end{pmatrix}$, $\tilde{C} = \begin{pmatrix} C + FK \\ -C - FK \end{pmatrix}$,
$\tilde{B} = (B + EG \quad -B - EG)$, $\tilde{A} = A + EK$.

The DI in (2.11) has a state and time-dependent polyhedral set $\tilde{S}(\cdot,\cdot)$ which renders its study more complex. For each t and e, the normal cone $\mathcal{N}_{S(t,e)}$ defines a maximal monotone mapping, which may allow to recast (2.11) in the framework of item 2 (f) in section 1.2.2, and deduce conditions such that (2.11) has a Lipschitz solution. A second equivalent way to write the LCS (2.5) is:

$$\dot{e}(t) \in \bar{A}e(t) - \bar{B}(\bar{D} + \mathcal{N}^{-1}_{\bar{S}(t)})^{-1}(\bar{C}e(t)) \quad \Leftrightarrow \quad \begin{cases} \dot{e}(t) = \bar{A}e(t) + \bar{B}\tilde{\lambda}(t) \\ 0 \leq \tilde{\lambda}(t) \perp \bar{C}e(t) + \bar{D}\tilde{\lambda}(t) + \bar{F}(t) \geq 0 \end{cases}, \tag{2.12}$$

with $\bar{A} = \tilde{A}$, $\bar{B} = \tilde{B}$, $\bar{C} = \begin{pmatrix} C + FK \\ 0 \end{pmatrix}$, $\bar{D} = \tilde{D}$, $\bar{S}(t) = \{z \in I\!R^{2m} \mid z + \bar{F}(t) \in I\!R^{2m}_+\}$,
$\bar{F}(t) = \begin{pmatrix} Cx_d(t) + Fu_d(t) \\ Cx_d(t) + Fu_d(t) \end{pmatrix}$. It is noteworthy that some conditions have to be imposed so that the construction of the DIs in (2.11) and (2.12) is possible, see section 2.1.3 for more details. Now, we have at our disposal several (equivalent) formalisms for the closed-loop plant dynamics (2.3) and (2.8), the desired trajectory generator (2.1) and (2.10), and the error dynamics (2.5), (2.11) and (2.12). This is useful for the well-posedness analyses relying on the various results recalled in section 1.2.2. A difficulty is to determine under which conditions the passivity in Assumptions 2.1.4 or 2.1.5, implies the passivity of the quadruples $(\tilde{A}, \tilde{B}, \tilde{C}, \tilde{D})$, or $(\bar{A}, \bar{B}, \bar{C}, \bar{D})$, see (2.18).

Remark 2.1.6 (Closed-loop system's well-posedness)**.** *In the framework of this thesis, the well-posedness of the plant dynamics is not a fundamental issue, since it is only*

the closed-loop system which is used in the analysis. In a similar way as feedback can be used to make an unstable system stable in closed-loop, it may be used to render an ill-posed plant's model well-posed in closed loop. The well-posedness of the closed-loop plant LCS (2.3) (equivalently the DI in (2.8)) can be inferred from [38, 44, 145, 93, 30], assuming that the desired signals $x_d(\cdot)$, $\lambda_d(\cdot)$ and $u_d(\cdot)$ are AC or $\mathcal{L}^2_{loc}(\subseteq \mathcal{L}^1_{loc})$, and that some basic constraint qualification conditions hold. Clearly, in this setting, Assumption 2.1.1 is important. When $D + FG \succ 0$ (this is the case if Assumption 2.1.5 holds), then the results reported in item 1 in section 1.2.2 apply. If $D + FG = 0$ (which may be the case if Assumption 2.1.4 holds), then the results in item 3 in section 1.2.2 apply. When $D + FG \succcurlyeq 0$ but not null, then the various results in item 2 in section 1.2.2 can be used. This requires to check the constraint qualifications listed in item 2 (a) through (f). This is not tackled in this thesis whose primary goal is tracking control.

Remark 2.1.7. *The trajectory tracking problem as tackled in this work, can be interpreted as a synchronization problem between the master system (2.1), and the plant (1.1).*

2.1.2 Error Dynamics Stability Analysis (no state jumps)

This section is dedicated to the stability analysis of the error dynamics (2.5), and it is assumed that all trajectories are at least absolutely continuous. The arguments used for the proof of Proposition 2.1.8 are similar to those employed in [31, 6, 30], and are given for completeness.

Proposition 2.1.8. *Suppose that Assumptions 2.1.1, 2.1.2 and 2.1.4 hold, and that the solution $x(\cdot)$ of the closed-loop LCS (2.3) is AC on $\mathbb{R}_+$. Then, the error dynamics in (2.5) has a globally exponentially stable equilibrium point $e^* = 0$.*

Proof. Let $\Delta\lambda(t) \triangleq \lambda(t) - \lambda_d(t)$ and $\Delta w(t) \triangleq w(t) - w_d(t) = (C + FK)e(t) + (D + FG)\Delta\lambda(t)$. Consider the Lyapunov function candidate $V(e) = e^\top Pe$, where $P = P^\top \succ 0$ satisfies (4.10). From the assumptions, $e(\cdot)$ is absolutely continuous and thus it has a derivative almost everywhere. Along the error dynamics trajectories (2.5), it holds that:

$$\dot{V}(t) = e^\top[(A + EK)^\top P + P(A + EK)]e + 2e^\top P(B + EG)\Delta\lambda(t)$$

From the complementarity conditions in (2.3) and (2.4), we obtain equivalently:

$$\lambda(t) \in -\mathcal{N}_{S(t)}((C + FK)x(t) + (D + FG)\lambda(t))$$

and

$$\lambda_d(t) \in -\mathcal{N}_{S(t)}((C + FK)x_d(t) + (D + FG)\lambda_d(t))$$

with $S(t)$ defined after (2.8). It follows from the monotonicity of the normal cone mapping that:

$$[w(t) - w_d(t)]^\top[\lambda(t) - \lambda_d(t)] = \Delta w(t)^\top\Delta\lambda(t) \leq 0. \tag{2.13}$$

In matrix form (the time argument is dropped on the right-hand side):

$$\begin{aligned}\dot{V}(t) &= \begin{pmatrix} e \\ \Delta\lambda \end{pmatrix}^\top M \begin{pmatrix} e \\ \Delta\lambda \end{pmatrix} + \begin{pmatrix} e \\ \Delta\lambda \end{pmatrix}^\top \begin{pmatrix} 0 & (C+FK)^\top \\ C+FK & D+FG+(D+FG)^\top \end{pmatrix} \begin{pmatrix} e \\ \Delta\lambda \end{pmatrix} \\ &= \begin{pmatrix} e \\ \Delta\lambda \end{pmatrix}^\top M \begin{pmatrix} e \\ \Delta\lambda \end{pmatrix} + 2\Delta\lambda^\top \Delta w \leq \begin{pmatrix} e \\ \Delta\lambda \end{pmatrix}^\top M \begin{pmatrix} e \\ \Delta\lambda \end{pmatrix} \leq 0,\end{aligned} \tag{2.14}$$

where $(C+FK)e = \Delta w - (D+FG)\Delta\lambda$. So, for all e and $\Delta\lambda$ and using the strict state passivity, it is inferred:

$$\dot{V}(t) \leq -\epsilon\, e(t)^\top P e(t) = -\epsilon\, V(t).$$

Classical arguments yield $V(t) \leq V(0)\exp(-\epsilon t)$. Using the inequality: $\lambda_{\min}(P)\|e\|^2 \leq e^\top P e$, the following is obtained

$$\|e(t)\|^2 \leq \frac{V(t)}{\lambda_{\min}(P)} \leq \frac{V(0)}{\lambda_{\min}(P)}\exp(-\epsilon t)$$

Therefore, the equilibrium point of the error dynamics is globally exponentially stable. □

Notice that using (2.5) it follows that $\lambda(t) - \lambda_d(t)$ converges exponentially fast to $\mathrm{Ker}(B - EG)$.

Comments on passivity Following on from the proof of Proposition 2.1.8, the supply rate in (2.13) indicates that the passivity, in this case, is studied between the input $\lambda - \lambda_d$ and the output $w - w_d$. The variation of the storage function in (2.14) is written as $\dot{V}(t) \leq 2\Delta\lambda^\top \Delta w$. This shows the incremental passivity [127, 39] of the LCS defined in (2.3).

Continuity of the solutions A sufficient condition for no state-jump is that both matrices D and $D+FG$ are P-matrices, and $u_d(\cdot)$ is continuous. Then (2.1) has continuously differentiable solutions $x_d(\cdot)$ with uniqueness for any initial data, and $\lambda_d(\cdot)$ is time-continuous (being a Lipschitz continuous function of x_d and u_d). Thus, the trajectories of the closed-loop system (2.3) (or (2.8)) are also state-jump free. Let now $G = 0$ in (2.2). Then $\lambda_d(\cdot)$ does not appear in (2.3). Thus, provided both $x_d(\cdot)$ and $u_d(\cdot)$ are continuous, no state jump occurs, except possibly at the initial time. These results follow by applying, *e.g.*, items 1 or 2 (a) in section 1.2.2. When $D = 0$ and/or $D + FG = 0$ (which cannot be excluded by Assumption 2.1.4), item 3 in section 1.2.2 can be used. We may also rely on item 2 (f) to analyse (2.11) and guarantee that it has Lipschitz continuous solutions for the admissible initial state. Let us check conditions i) of item 2 (f) 1.2.2 under Assumption 2.1.4 ($\Rightarrow D + FG \succcurlyeq 0$) and $D \succcurlyeq 0$ (most of the conditions assuring Assumption 2.1.1 imply it):

(a) $\tilde{D} \succcurlyeq 0 \Leftrightarrow \tilde{D} + \tilde{D}^\top \succcurlyeq 0$. Using Lemma A.3.1, equivalently we have:

1. $\mathrm{Im}(G^\top F^\top) \subseteq \mathrm{Im}(D + D^\top)$,

2. $D + FG + (D + FG)^\top \succcurlyeq FG(D + D^\top)^\dagger G^\top F^\top$. A sufficient condition for this to hold is $D + FG \succ 0$, and $\sigma_{\max}(FG(D + D^\top)^\dagger G^\top F^\top) < \sigma_{\max}(D + FG + (D + FG)^\top) = \lambda_{\max}(D + FG + (D + FG)^\top)$. From [17, Corollary 9.6.5], we have: $\sigma_{\max}(FG(D + D^\top)^\dagger G^\top F^\top) \leq \sigma^2_{\max}(FG)\sigma_{\max}((D + D^\top)^\dagger)$. If $D + D^\top = 0$, the matrix inequality is satisfied. If $D + D^\top \neq 0$ and $\text{rank}(D + D^\top) = d$, then $\sigma_{\max}((D+D^\top)^\dagger) = \sigma_d^{-1}(D+D^\top)$ [17, Fact 6.3.28], and $\sigma_d(D+D^\top) = \lambda_d(D+D^\top)$ since $D + D^\top \succcurlyeq 0$ is symmetric. Thus, a sufficient condition is $\sigma^2_{\max}(FG) < \lambda_d(D + D^\top)\lambda_{\max}(D + FG + (D + FG)^\top)$. Another sufficient condition, following similar steps, is $D+D^\top \succ 0$, $\sigma_{\max}(FG) < \lambda_d(D+FG+(D+FG)^\top)\lambda_{\max}(D+D^\top)$. We see that in both cases we allow for $D + D^\top$ of $D + FG + (D + FG)^\top$ to be low rank, which hampers $\tilde{D} \succ 0$. Finally, we may use Lemmas A.3.1, A.3.2, as well as the matrix decompositions described after Lemma A.3.2, to get necessary and sufficient conditions.

(b) $\text{Im}(\tilde{D}) \subseteq \text{Im}(\tilde{C})$: $\Leftrightarrow \text{Im}(D + FG) + \text{Im}(FG) \subseteq \text{Im}(C + FK)$ and $\text{Im}(D) \subseteq \text{Im}(C + FK)$.

(c) $\text{Ker}(\tilde{D} + \tilde{D}^\top) \subseteq \text{Ker}(P\tilde{B} - \tilde{C}^\top)$ for some $\mathbb{R}^{n\times n} \ni P = P^\top \succ 0$: $\Leftrightarrow \{(x, y) \in \mathbb{R}^{m\times m} \mid ((D + FG) + (D + FG)^\top)x - FGy = 0, -G^\top F^\top x + (D + D^\top)y = 0\} \subseteq \{(x, y) \in \mathbb{R}^{m\times m} \mid x-y \in \text{Ker}(P(B+EG)-(C+FK)^\top)\}$. This is verified if $FG = 0$ and Assumption 2.1.4 holds, since in this case $\text{Ker}(D+D^\top) \subseteq \text{Ker}(P(B+EG)-(C+FK)^\top)$ [45] [39, section 3.8]. If D and $D + FG$ are P-matrices, and if $FG(D + D^\top)^{-1}G^\top F^\top \neq D + FG + (D + FG)^\top$, then $\text{Ker}(\tilde{D} + \tilde{D}^\top) = \{0\}$, hence the inclusion holds. If $FG(D + D^\top)^{-1}G^\top F^\top = D + FG + (D + FG)^\top$, then $\text{Ker}(\tilde{D} + \tilde{D}^\top) = \mathbb{R}^m \times \mathbb{R}^m$, hence the inclusion holds only if $P(B + EG) = (C + FK)^\top$.

The various conditions stated in section 1.2.2 are sufficient only, so it may be that some of them are unnecessary in some cases (*e.g.*, condition **b**)) above is needed for continuity arguments using the Vladimirov's pseudo-distance defined in [150] as done in [145, 93, 92], but it is not necessary at all [37, section 5.3] [44]). Condition **b**) is not necessary for the well-posedness of (2.5) when both D and $D + FG$ are P-matrices. The point is also that the error system (2.5) or (2.11) is a specific interconnection of both subsystems, which does not necessarily inherits good properties of the subsystems (*e.g.*, $D \succcurlyeq 0$ and $D + FG \succcurlyeq 0$ may not imply $\tilde{D} \succcurlyeq 0$). Conditions in **a**) and **c**) are necessary for the passivity of $(\tilde{A}, \tilde{B}, \tilde{C}, \tilde{D})$ [45] [39, section 3.8].

The stability proof shows that under the proposition's assumptions (like the continuity of the solutions) the generalized equation $0 \in \bar{A}e^* - \bar{B}(\bar{D} + \mathcal{N}^{-1}_{\bar{S}(t)})^{-1}(\bar{C}e^*)$ has the unique solution $e^* = 0$ for all $t \geq 0$.

2.1.3 Error Dynamics Stability Analysis including State Jumps

An important question is whether or not the tracking control framework developed above is suitable for trajectories with discontinuities. Let us study how to relax Assumption 2.1.1 and the continuity of the closed-loop state $x(\cdot)$. State jumps are known to add difficulty to the trajectory tracking problem, especially when the jump times are unknown. The so-called peaking phenomenon, due to non-synchronized jumps in the plant and the desired trajectories, has long been known to be one of the obstacles. The jumps in $x(\cdot)$ and $x_d(\cdot)$ may arise from different reasons:

1. Let the conditions in section 1.2.2 item 2 (a) or item 3 hold for (A, B, C, D). Jumps at t in $x_d(\cdot)$ occur only if Fu_d is discontinuous at t and $\text{rank}(D) < m$.

2. Let the conditions in section 1.2.2 item 2 (a) or item 3 hold for $(A + EK, B + EG, C + FK, D + FG)$. Jumps at t in the closed-loop state occur only if $\text{rank}(D + FG) < m$ and $-FKx_d - FG\lambda_d + Fu_d$ is discontinuous at t.

The following is deduced, where $\mathcal{T}_f$ denotes the set of discontinuity times of the function $f(\cdot)$:

Lemma 2.1.9. *Let $FG\lambda_d(\cdot)$ and $u_d(\cdot)$ be bounded functions of time. (a) $\mathcal{T}_{x_d} \subseteq \{t_0\} \cup \mathcal{T}_{Fu_d}$ and (b) $\mathcal{T}_x \subseteq \{t_0\} \cup \mathcal{T}_{Fu_d} \cup \mathcal{T}_{FG\lambda_d}$.*

Proof. (a) is obvious. (b): $\mathcal{T}_x \subseteq \{t_0\} \cup \mathcal{T}_{-FKx_d - FG\lambda_d + Fu_d} \subseteq \{t_0\} \cup \mathcal{T}_{FKx_d} \cup \mathcal{T}_{FG\lambda_d} \cup \mathcal{T}_{Fu_d} \subseteq \{t_0\} \cup \mathcal{T}_{FG\lambda_d} \cup \mathcal{T}_{Fu_d}$ since $\mathcal{T}_{FKx_d} \subseteq \mathcal{T}_{Fu_d}$. □

Lemma 2.1.9 indicates that when $FG\lambda_d$ is continuous, then either $x_d(\cdot)$ jumps while $x(\cdot)$ is continuous, or the inverse, or they jump simultaneously. This will be illustrated on examples. Notice that when $x_d(\cdot)$ jumps, then λ_d is a Dirac measure, and the meaning of the feedback in (2.2) has to be carefully studied, as well as the mere meaning of the complementarity constraints in (2.3) which contain the term $FG\lambda_d$. Also, depending on FG, the sum of two Dirac measures, one stemming from λ_d (due to a jump in $u_d(t)$) and one stemming from λ (due to a jump in $-FKx_d - FG\lambda_d + Fu_d$) could occur in the differential part of the closed-loop dynamics (see section 2.2): we may call this a forbidden situation (this is not to be confused with the case of Measure Differential Inclusions, or with passive LCS with state jumps [37, 38, 43]). It is inferred that:

(C1) *If $x_d(\cdot)$ jumps, we impose $FG = 0$. A sufficient condition to prevent forbidden situations, is that $FG = 0$ if $u_d(\cdot)$ is discontinuous. In other words, only continuous $u_d(\cdot)$ is allowed if $FG \neq 0$.*

In view of condition **(C1)**, we can refine item 2: Jumps in the closed-loop state can occur at t if:

1. $FG = 0$ and $-FKx_d + Fu_d$ is discontinuous at t,

2. or $FG \neq 0$, x_d is continuous at t and λ_d jumps at t (which can occur if u_d is continuous at t at a junction time with the constraint boundary $(Cx_d + D\lambda_d + Fu_d)_i = 0$ for some $1 \leq i \leq m$).

Conditions in item 2 are not straightforward, because we want that $FG \neq 0$, but FG also multiplies λ, see (2.3), and passivity implies $D + FG \succcurlyeq 0$. The scalar case $m = 1$ is analysed in section 2.2.

The first step is to characterize the jumps in (2.5), then to study the variation $\Delta V(e(t)) = V(e(t^+)) - V(e(t^-)) = (e(t^+) - e(t^-))^\top P(e(t^+) - e(t^-))$.

Case $G = 0$ and $D = 0$

In this case λ_d does not enter (2.3), and $\tilde{D} = 0$. Let Assumptions 2.1.1 and 2.1.4 hold, and let us study the case when $x(\cdot)$ jumps while $x_d(\cdot)$ is continuous. Then, $(A + EK, B, C + FK, 0)$ is strictly state passive and $PB = (C + FK)^\top$ for some $P = P^\top \succ 0$. The closed-loop system in (2.8) becomes:

$$\dot{x}(t) \in (A + EK)x(t) - B\mathcal{N}_{S(t)}((C + FK)x(t)) - EKx_d(t) + Eu_d(t). \tag{2.15}$$

where $S(t) = \{v \in \mathbb{R}^m_+ \mid v - FKx_d(t) + Fu_d(t) \geq 0\}$. This DI can be rewritten equivalently as a FOSwP, see item 3 in section 1.2.2, [37, 38, 22], and section B.2 as:

$$\dot{\zeta}(t) \in R(A + EK)R^{-1}\zeta(t) + RE(-Kx_d(t) + u_d(t)) - \mathcal{N}_{\Phi(t)}(\zeta(t)) \tag{2.16}$$

where $R^2 = P$, $R = R^\top \succ 0$, $\zeta = Rx$, $\Phi(t) = \{Rx \mid (C + FK)x - FKx_d(t) + Fu_d(t) \in S(t)\}$. We see that $\Phi(t) \neq \emptyset$ for each t if and only if there exists x such that $(C+FK)x-FKx_d(t)+Fu_d(t) \geq 0$. This is guaranteed if a condition as in item 3 iii) holds, *i.e.*, $\mathrm{Im}(C + FK) - \mathbb{R}^m_+ = \mathbb{R}^m$ (which is a constraint qualification). Assume in addition that $u_d(\cdot)$ is continuous on $\mathbb{R}_+$. Suppose that $Cx_d(0)+Fu_d(0) \geq 0$, hence $x_d(\cdot)$ is continuous at $t = 0$. Then, a jump in $x(\cdot)$ (thus in $e(\cdot)$) can occur only at the initial time and $V(0^+)-V(0^-) = e(0^+)^\top Pe(0^+)-e(0^-)^\top Pe(0^-) = (e(0^+)+e(0^-))^\top P(e(0^+)-e(0^-)) = (x(0^+)+x(0^-)-2x_d(0))^\top P(x(0^+)-x(0^-)) = x(0^+)^\top Px(0^+)-x(0^-)^\top Px(0^-)-2x_d(0))^\top P(x(0^+) - x(0^-))$. Now, using the passivity of $(A + EK, B, C + FK, 0)$, we have (see the paragraph State Jumps at the end of section 1.2.2): $x(0^+)^\top Px(0^+) - x(0^-)^\top Px(0^-) \leq 0$, provided that $0 \in \{z \in \mathbb{R}^n \mid (C+FK)z-FKx_d(0)+Fu_d(0) \geq 0\}$, equivalently $0 \in \Phi(0)$, equivalently $-FKx_d(0) + Fu_d(0) \geq 0$. In this case, $V(0^+) - V(0^-) \leq -2x_d(0))^\top P(x(0^+) - x(0^-))$. We have $P(x(0^+) - x(0^-)) \in -\mathcal{N}_\mathcal{K}(x(0^+))$ [37, Lemma 2.3]. Thus, it is necessary and sufficient that $x_d(0) \in (\mathcal{N}_\mathcal{K}(x(0^+)))^\circ = \mathcal{T}_\mathcal{K}(x(0^+))$ to guarantee that the right-hand side is nonpositive. Therefore, the following has been proved:

Lemma 2.1.10. *Assume that $u_d(\cdot)$ is time-continuous, $G = 0$, $D = 0$, $-FKx_d(0) + Fu_d(0) \geq 0$, and $x_d(0) \in \mathcal{T}_\mathcal{K}(\mathrm{proj}_P[\mathcal{K}; x(t_0^-)])$. Then, at an initial state jump, we have $V(0^+) - V(0^-) \leq 0$, where $P = P^\top \succ 0$ is a solution of the passivity LMI associated with the triple $(A + EK, B, C + FK)$ and $V(t) = V(e(t))$.*

The condition on $x_d(0)$ is certainly not easy to check in general (but $x_d(0) = 0$ is always suitable). The interest of Lemma 2.1.10 is that it allows for a jump in $x(0)$ while $x_d(0)$ does not jump. But applying it at any time of state jump $t_k > 0$ implies to impose a suitable desired state, which may not be possible in our framework where x_d is generated by (2.1). Under the same conditions, assume that $Fu_d(\cdot)$ has a discontinuity at time t_c. From (2.1) and (2.3), both $x(\cdot)$ and $x_d(\cdot)$ may jump at t_c, so λ and λ_d are Dirac measures at t_c. From (2.3), the discontinuity may act in both terms FKx_d and Fu_d. Using (2.8) and (2.10), this implies that the jumps' magnitudes in the sets $S(t)$ and $S_d(t)$, may not be equal. The post-jump states are computed using (1.11), where $\mathcal{K} = \{z \in \mathbb{R}^n \mid (C + FK)z - FKx_d(t) + Fu_d(t) \geq 0\}$ for the closed-loop plant, and $\mathcal{K}_d = \{z \in \mathbb{R}^n \mid Cz + Fu_d(t) \geq 0\}$ for the desired system.

Extension for further jumps at $t > 0$

Let us now place ourselves in another perspective. Until now we have assumed that $x_d(\cdot)$ is time-continuous. First notice that condition **(C1)** can be relaxed, if we admit that the state $x_d(\cdot)$ of the dynamics in (2.1) can be arbitrarily reset to some value at arbitrary times, without considering λ_d as a Dirac measure. This has important consequences because as we shall see, this means that the desired dynamics is no longer autonomous (the desired state has to be modified online, a common feature in trajectory tracking for systems undergoing state jumps [118, 117, 131]). Consider (2.3), with Assumption 2.1.4.

Proposition 2.1.11. *Let $V(e) = e^\top Pe$, with P a solution of the closed-loop passivity LMI, and let $\{0\} \in \mathcal{K} = \{z \in I\!R^n \mid (C+FK)z - FKx_d - FG\lambda_d(t^+) + Fu_d(t) \in Q^*_{D+FG}\}$. Assume that $x_d(t^+) \in \mathcal{T}_\mathcal{K}(\mathrm{proj}_P[\mathcal{K}; x(t^-)])$ and $x_d(t^+)^\top Px(t^-) \geq x_d(t^-)^\top Px(t^-)$, then $\Delta V(e(t)) \leq (x_d(t^+) - x_d(t^-))^\top P(x_d(t^+) + x_d(t^-))$.*

Proof. At a state jump time:

$$\begin{aligned}
\Delta V(e(t)) \quad &= (x(t^+) - x(t^-))^\top P(x(t^+) + x(t^-)) - (x(t^+) - x(t^-))^\top P(x_d(t^+) + x_d(t^-)) \\
&\quad -(x_d(t^+) - x_d(t^-))^\top P(x(t^+) + x(t^-)) + (x_d(t^+) - x_d(t^-))^\top P(x_d(t^+) + x_d(t^-)) \\
&\leq -(x(t^+) - x(t^-))^\top P(x_d(t^+) + x_d(t^-)) - (x_d(t^+) - x_d(t^-))^\top P(x(t^+) + x(t^-)) \\
&\quad +(x_d(t^+) - x_d(t^-))^\top P(x_d(t^+) + x_d(t^-)) \\
&= -(x_d(t^+) + x_d(t^-))^\top P(x(t^+) - x(t^-)) - (x_d(t^+) - x_d(t^-))^\top P(x(t^+) - x(t^-)) \\
&\quad -2(x_d(t^+) - x_d(t^-))^\top Px(t^-) + (x_d(t^+) - x_d(t^-))^\top P(x_d(t^+) + x_d(t^-)) \\
&= -2x_d(t^+)^\top P(x(t^+) - x(t^-)) - 2(x_d(t^+) - x_d(t^-))^\top Px(t^-) \\
&\quad +(x_d(t^+) - x_d(t^-))^\top P(x_d(t^+) + x_d(t^-))
\end{aligned} \tag{2.17}$$

The first term in the first equality in (2.17) is nonpositive from the passivity. It is noteworthy that we cannot infer the same conclusions about the last term in (2.17) from (2.4) because these dynamics are equivalent to that in (2.1). Let us consider the last equality in (2.17). We know that $P(x(t^+) - x(t^-)) \in -\mathcal{N}_\mathcal{K}(x(t^+))$ [37, Lemma 2.3]. Thus, the nonpositivity of the first term is equivalent to $x_d(t^+) \in (\mathcal{N}_\mathcal{K}(x(t^+)))^\circ = \mathcal{T}_\mathcal{K}(x(t^+))$. Using (1.11), the first condition follows. The second condition is obvious. □

Thus, under the conditions of Proposition 2.1.11, $\Delta V(e(t)) \leq 0$ if and only if

$$x_d(t^+)^\top Px_d(t^+) \leq x_d(t^-)^\top Px_d(t^-),$$

which means that the desired state jump is dissipative with respect to the closed-loop storage function (in general there is no reason that it should satisfy this property). This makes a set of constraints that the reset desired state $x_d(t^+)$ has to satisfy. Note that the conditions of Proposition 2.1.11 are sufficient only. Examples show that they may not be satisfied, while $\Delta V(e(t)) \leq 0$, see section 2.2.4. Also, we note that the reset mechanism is not needed when $G = 0$ (then condition **C1)** holds true), while the characterization of $\Delta V(e(t))$ as in (2.17) remains valid.

Using the DI (2.12)

The formalism in (2.11) is not convenient for the state jumps analysis, because it involves a state-dependent set. Let us recall the error dynamics in (2.12) to analyze the state discontinuities.

$$\dot{e}(t) \in \bar{A}e(t) - \bar{B}(\bar{D} + \mathcal{N}^{-1}_{\bar{S}(t)})^{-1}(\bar{C}e(t)) \quad \Leftrightarrow \quad \begin{cases} \dot{e}(t) = \bar{A}e(t) + \bar{B}\lambda(t) \\ 0 \leq \lambda(t) \perp \bar{C}e(t) + \bar{D}\lambda(t) + \bar{F}(t) \geq 0 \end{cases},$$

with $\bar{A} = \tilde{A}$, $\bar{B} = \tilde{B}$, $\bar{C} = \begin{pmatrix} C + FK \\ 0 \end{pmatrix}$, $\bar{D} = \tilde{D}$, $\bar{S}(t) = \{z \in I\!R^{2m} \mid z + \bar{F}(t) \in I\!R^{2m}_{+}\}$, $\bar{F}(t) = \begin{pmatrix} Cx_d(t) + Fu_d(t) \\ Cx_d(t) + Fu_d(t) \end{pmatrix}$. At a state jump time t, the DI in (2.12) may be written as:

$$e(t^+) - e(t^-) \in -\bar{B}(\bar{D} + \mathcal{N}^{-1}_{\bar{S}(t^+)})^{-1}(\bar{C}e(t^+)).$$

which has a solution (possibly with jumps) if the quadruple $(\bar{A}, \bar{B}, \bar{C}, \bar{D})$ is passive with positive definite storage function. Then, (1.11) holds. Thus, it is inferred that $\Delta V(e(t)) \leq 0$ provided that $0 \in \mathcal{K} = \{e \in I\!R^n \mid \bar{C}e + \bar{F}(t) \in Q^{\star}_{\bar{D}}\}$, and:

$$\begin{pmatrix} -P(A+EK) - (A+EK)^\top P & -P(B+EG) + (C+FK)^\top & P(B+EG) \\ -(B+EG)^\top P + C + FK & D + FG + (D+FG)^\top & FG \\ (B+EG)^\top P & (FG)^\top & D + D^\top \end{pmatrix} \succcurlyeq 0, \tag{2.18}$$

where $P = P^\top \succ 0$ is a solution to $-M \succcurlyeq 0$ with M in (2.7). Notice that (2.18) holds only if $M \preceq 0$, hence only if P is also a solution of the plant's closed-loop LMI. Thus, the solution P of (2.18) must be the solution of BMI in (2.7). From Assumption 2.1.4, we have $-M \succcurlyeq 0$. Using Lemma A.3.1, we infer that (2.18) holds if and only if:

1. $\bar{D} + \bar{D}^\top \succcurlyeq 0$ (see item a) at the end of section 2.1.2 for sufficient conditions),
2. $\text{Im} \begin{pmatrix} -(B+EG)^\top P + C + FK \\ (B+EG)^\top P \end{pmatrix} \subseteq \text{Im}(\bar{D} + \bar{D}^\top)$,
3. $$-M \succcurlyeq \begin{pmatrix} -P(B+EG) + (C+FK)^\top & P(B+EG) \end{pmatrix} (\bar{D} + \bar{D}^\top)^\dagger \begin{pmatrix} -(B+EG)^\top P + C + FK \\ (B+EG)^\top P \end{pmatrix} \tag{2.19}$$

Some comments arise:

- A sufficient condition for (2.19) to hold is $\bar{D} = -\bar{D}^\top \iff D + FG = -(D+FG)^\top$, $D = -D^\top$, $FG = 0$. This is allowed by strict state passivity in Assumption 2.1.4. However, item 2 then implies that $-(B+EG)^\top P + C + FK = 0$ and $(B+EG)^\top P = 0$, hence $C + FK = 0$ and $B + EG = 0$ since P is full-rank. Thus, in (2.3) the ODE part and the complementarity part are decoupled.
- Assume that $D = \begin{pmatrix} D_1 & 0 \\ 0 & 0 \end{pmatrix}$, $D_1 \succ 0$. Item 1 implies that $FG = \begin{pmatrix} (FG)_1 & 0 \\ 0 & 0 \end{pmatrix}$. Then, $\bar{D} + \bar{D}^\top = \begin{pmatrix} \bar{D}_1 + \bar{D}_1^\top & 0 \\ 0 & 0 \end{pmatrix}$, and $(\bar{D} + \bar{D}^\top)^\dagger = \begin{pmatrix} (\bar{D}_1 + \bar{D}_1^\top)^\dagger & 0 \\ 0 & 0 \end{pmatrix}$, with

$\bar{D}_1 + \bar{D}_1^\top = \begin{pmatrix} D_1 + (FG)_1 + D_1 + (FG)_1^\top & 0 & -(FG)_1 \\ 0 & 0 & 0 \\ -(FG)_1^\top & 0 & D_1 + D_1^\top \end{pmatrix}$. Similar calculations can be done for M in (2.7), and also for the ranges inclusion in item 2. Pursuing the calculations and matrices partitions allows to simplify (2.19).

- Assume that $(\bar{A}, \bar{B}, \bar{C}, \bar{D})$ is passive. A jump in $e(\cdot)$ occurs at t only if $\bar{F}(\cdot)$ jumps at t. In turn, $\bar{F}(\cdot)$ jumps at t if and only if $Cx_d + Fu_d$ jumps at t, while $x_d(\cdot)$ jumps only if $u_d(\cdot)$ does. Hence, $e(\cdot)$ jumps at t only if $u_d(\cdot)$ does. How is this related to the jumps in $x(\cdot)$ in (2.3) and in $x_d(\cdot)$ in (2.1) ? As we saw above, if $x_d(\cdot)$ jumps at t_c then λ_d is a Dirac measure at t_c and the complementarity constraints in (2.3) are meaningless at t_c. This means that applying an impulsive feedback control to an LCS (1.1) with $FGu \neq 0$, has to be avoided as pointed out in condition **(C1)**. In fact, the DIs in (2.11), (2.12), (2.8), and (2.9) are constructed with the underlying assumption that the complementarity conditions can be rewritten equivalently as inclusion into a normal cone (see, *e.g.*, [37, Equ. (B.1)] [134, Corollary 23.5.4]). For instance, $f(t)$ in (2.9) is a Dirac measure if $EG\lambda_d$ is. This might let one think that in this case, $x(\cdot)$ jumps at t_c. We set that this is true if $F = 0$ only, in which case $x_d(\cdot)$ can jump only initially, see (2.1). Obviously, if λ_d is a Dirac measure, both formalisms (complementarity and inclusion) require further analysis for their understanding if $FG \neq 0$.

- The conditions in this paragraph are different from those of the foregoing paragraph, because now we consider both the desired system and the closed-loop plant simultaneously, instead of looking at (2.15) only. However, jumps in both $x(\cdot)$ and $x_d(\cdot)$ are permitted under some conditions as stated above. A quick examination of the LMI in (2.18) shows that the occurrence of state jumps is quite restricted in this context. Indeed, if $D + D^\top = 0$, then (2.18) implies that $B + EG = 0$ and $FG = 0$. In fact, the LMI in (2.18) shows that studying state jumps from the passivity error dynamics in (2.12) is almost impossible.

- The controller may be impulsive if $G \neq 0$ and a jump occurs in $x(\cdot)$. Condition **(C1)** still applies.

Analysis of jump sets $\mathcal{K}$ and $\mathcal{K}_d$

These sets are crucial in the state jump characterization and computation, see (1.10). We have:

$$\mathcal{K} = \{z \in I\!R^n \mid Cz + Fu_d(t^+) + FK(z - x_d(t^+)) \in Q^\star_{D+FG}\} \tag{2.20}$$

and

$$\mathcal{K}_d = \{z \in I\!R^n \mid Cz + Fu_d(t^+) \in Q^\star_D\} \tag{2.21}$$

In general, both sets are different. However, if $FG = 0$ then they differ only by the term $FK(z - x_d(t^+))$. Since $x(t^+)$ belongs to $\mathcal{K}$, both sets are almost equal if the tracking error $x(t^-) - x_d(t^-)$ and FK are very small. So, if in addition both storage functions matrices P (calculated from the closed-loop system LMI) and P_d (computed

from the desired dynamics LMI when this dynamics is passive) are closed one to each other, both state jumps are almost the same as well. On the other hand, the state jump as computed in (1.10) is independent of P (or P_d, respectively), provided it is a solution of the passivity LMI. Thus, if $EG = 0$, which implies that the "input" matrix of the closed-loop system is equal to the input matrix of the desired system, the forms of $\mathcal{K}$ and $\mathcal{K}_d$ in (2.20) and (2.21) will imply that both jumps in x and x_d are close one to each other.

The jump-mismatch (peaking) phenomenon

This is a well-known phenomenon in trajectory tracking when state jumps are present, as recalled in the introduction. The problem that is faced in this study is twofold: 1) is the discontinuity mismatch issue present? If it is, how can it be coped with? In the scalar case treated in section 2.2, it will be shown that if both states jump then they jump at the same time. However, it is also possible that x jumps while x_d does not, and *vice versa*. Lemma 2.1.9 shows that when $FG\lambda_d$ is continuous, then if both states jump they jump simultaneously.

2.2 Simple Scalar Example with State Jumps

This section is dedicated to analyse and mainly to present numerical simulations of the theoretical development on state jumps presented in section 2.1.3. The numerical simulations are done with the INRIA software package SICONOS[1] [3], and the LMIs are solved with MOSEK 9.3.14 solver [9].

2.2.1 Dynamics and Closed-loop System

Consider the scalar LCS with $d = 0$:

$$\begin{cases} \dot{x}(t) = ax(t) + b\lambda(t) + u_1(t) \\ 0 \leq \lambda(t) \perp w(t) = cx(t) + u_2(t) \geq 0 \end{cases} \tag{2.22}$$

where a, b, and $c \in \mathbb{R}$, $u = (u_1, u_2)^\top$, $u_1 = Eu$, $u_2 = Fu$ with $E = (1, 0)$ and $F = (0, 1)$. The desired system is represented by an LCS as follows:

$$\begin{cases} \dot{x}_d(t) = ax_d(t) + b\lambda_d(t) + u_{1d}(t) \\ 0 \leq \lambda_d(t) \perp w_d(t) = cx_d(t) + u_{2d}(t) \geq 0 \end{cases} \tag{2.23}$$

If $a > 0$, then the real system in (2.22) and the desired system (2.23) are unstable (*i.e*, the quadruple $(a, b, c, 0)$ has a real positive pole). But, in the context of trajectory tracking, the stability of the error dynamics is the main concern and not the stability of the plant and desired dynamics. Let

$$\begin{aligned} u_1 &= k_1(x - x_d) + g_1(\lambda - \lambda_d) + u_{1d} \\ u_2 &= k_2(x - x_d) + g_2(\lambda - \lambda_d) + u_{2d} \end{aligned} \tag{2.24}$$

[1] https://nonsmooth.gricad-pages.univ-grenoble-alpes.fr/siconos/index.html

so that $K = (k_1, k_2)^\top$ and $G = (g_1, g_2)^\top$. By substituting the expressions of u and v in (2.22), the closed-loop system is written in the form of (2.3) as follows:

$$\begin{cases} \dot{x}(t) = (a + k_1)x(t) + (b + g_1)\lambda(t) - k_1 x_d(t) - g_1\lambda_d(t) + u_{1d}(t) \\ 0 \leq \lambda(t) \perp w(t) = (c + k_2)x(t) + g_2\lambda(t) - k_2 x_d(t) - g_2\lambda_d(t) + u_{2d}(t) \geq 0. \end{cases} \tag{2.25}$$

Remark 2.2.1. *Consider $G = 0$. Recall the conditions of well-posedness given in section 1.2.2, item 3 for the case when $d = 0$. Assume that there exists $p > 0$ such that the quadruple $(a, b, c, 0)$ is passive (i.e., the LMI in (1.8) has a solution). Then the condition $pb = c$ holds. In addition, if the closed-loop system in (2.25) is well-posed, then the condition $pb = c + k_2$ holds. Therefore, knowing that $p > 0$, the variables b, c and $c + k_2$ should have the same sign. Notice also that the contact LCPs have the matrix cb, hence $cb < 0$ implies no or several solutions for some $u_{1d}(t)$ and $u_{2d}(t)$: passivity avoids this.*

2.2.2 State-jumps Analysis

State-jumps in $x(\cdot)$ and $x_d(\cdot)$ can occur for different reasons discussed in section 2.1.3. The purpose of this section is to analyze state jumps in the desired and closed-loop systems in different cases which illustrate the general developments.

If the controller gain $G = 0$

Notice that the dynamics (2.25) may not be well-posed due to the possible presence of Dirac measures that stem from both the complementarity conditions in (2.25) which create an impulsive multiplier λ and from the complementarity in (2.23) which implies an impulsive multiplier λ_d. Therefore, we shall consider $G = 0$ (which means that (**C1**) in section 2.1.3 is satisfied). In order to analyze state jumps, the following sets are calculated as follows (see section 1.2.2). For the desired system in (2.23):

$$\begin{aligned} Q_{d,D} &= \{\lambda_d \in I\!R \mid 0 \leq \lambda_d \perp d\lambda_d \geq 0\} = \{\lambda_d \in I\!R \mid 0 \leq \lambda_d \perp 0 \geq 0\} \\ &= \{\lambda_d \in I\!R \mid \lambda_d \in I\!R_+\} \\ Q^\star_{d,D} &= \{w_d \in I\!R \mid \langle w_d, \lambda_d \rangle \geq 0\} = \{w_d \in I\!R \mid w_d \in I\!R_+\} \\ \mathcal{K}_d &= \{x_d \in I\!R \mid cx_d + u_{2d}(t^+) \in Q^\star_{d,D}\} = \{x_d \in I\!R \mid cx_d \geq -u_{2d}(t^+)\} \end{aligned} \tag{2.26}$$

A jump can occur in the desired state x_d at time $t = t_c$, $t_c \in [0, +\infty)$, if and only if $cx_d(t_c^-) < -u_{2d}(t_c^+)$. For the closed-loop system in (2.25):

$$\begin{aligned} Q_D &= \{\lambda \in I\!R \mid 0 \leq \lambda \perp d\lambda \geq 0\} = \{\lambda \in I\!R \mid \lambda \in I\!R_+\} \\ Q^\star_D &= \{w \in I\!R \mid \langle w, \lambda \rangle \geq 0\} = \{w \in I\!R \mid w \in I\!R_+\} \\ \mathcal{K} &= \{x \in I\!R \mid (c + k_2)x - k_2 x_d(t^+) + u_{2d}(t^+) \in Q^\star_{d,D}\} \\ &= \{x \in I\!R \mid (c + k_2)x \geq k_2 x_d(t^+) - u_{2d}(t^+)\} \end{aligned} \tag{2.27}$$

The state x of the closed-loop system in (2.25) jumps at any $t = t_c$, $t_c \in [0, +\infty)$, if and only if $cx(t_c^-) + k_2[x(t_c^-) - x_d(t_c^+)] < -u_{2d}(t_c^+)$. Thus, when $G = 0$, the jumps at $t > 0$ in $x(\cdot)$ and $x_d(\cdot)$ occur only if u_{2d} is discontinuous at t, as expected.

If the controller gain $G \neq 0$ and x_d is continuous

In this case, a state jump in x (if any) is caused by the discontinuity in λ_d, which can arise when the complementarity problem switches mode (*i.e.*, $w(t) = cx(t) + u_2(t)$ vanishes). The desired system's state is considered continuous to avoid a Dirac measure λ_d in complementarity conditions in (2.25). For the closed-loop system represented by $(a + k_1, b + g_1, c + k_2, g_2)$ to be strictly passive, one must have $g_2 > 0$ given that $d = 0$. But, g_2 multiplies λ as shown in (2.25). The LCP of the closed-loop system (2.25) is

$$0 \leq \lambda(t) \perp w(t) = (c + k_2)x(t) + g_2\lambda(t) - k_2x_d(t) - g_2\lambda_d(t) + u_{2d}(t) \geq 0$$

has a unique piecewise continuous solution λ. Hence, the LCS in (2.25) is an ODE with an AC solution on $\mathbb{R}_+$ provided that $u_1(t)$ and $u_2(t)$ are continuous (see section 1.2.2, item 1). Thus, the closed-loop system's state is jump-free in the scalar case with $G \neq 0$ and the desired system's state x_d is continuous. Therefore, the error dynamics $e(t)$ is continuous in this case. The explanation of this result can be further understood by analyzing the following sets of the closed-loop system:

$$Q_D = \{\lambda \in \mathbb{R} \mid 0 \leq \lambda \perp (d + g_2)\lambda \geq 0\} = \{0\}$$

$$Q_D^\star = \{w \in \mathbb{R} \mid \langle w, \lambda \rangle \geq 0\} = \{\mathbb{R}\}$$

$$\mathcal{K} = \{x \in \mathbb{R} \mid (c + k_2)x(t) + g_2\lambda(t) - k_2x_d(t) - g_2\lambda_d(t) + u_{2d}(t) \in Q_{d,D}^\star\} = \{\mathbb{R}\}$$

Using the optimization problem in (1.11), $x(t^+) = x(t^-)$. Thus, the closed-loop system's state $x(t)$ is continuous even if λ_d is discontinuous. Therefore, the error dynamics $e(t)$ is continuous.

2.2.3 Stability Analysis of Error Dynamics

This section is dedicated to the stability analysis of the error dynamics in (2.28) when state jumps occur. Consider that $G = 0$, then the error dynamics $e(t) = x(t) - x_d(t)$ is written in the form of (2.5) as:

$$\dot{e}(t) = (a + k_1)e(t) + b\,(\lambda(t) - \lambda_d(t))$$

$$0 \leq \begin{pmatrix} \lambda(t) \\ \lambda_d(t) \end{pmatrix} \perp \begin{pmatrix} w(t) \\ w_d(t) \end{pmatrix} = \begin{pmatrix} c + k_2 \\ -c - k_2 \end{pmatrix} e(t) + \begin{pmatrix} 0 & c \\ c + k_2 & -k_2 \end{pmatrix} \begin{pmatrix} x(t) \\ x_d(t) \end{pmatrix} + \begin{pmatrix} u_{2d}(t) \\ u_{2d}(t) \end{pmatrix} \geq 0 \tag{2.28}$$

Let us now try the passivity criterion introduced in (2.18) to cope with state jumps directly from the error dynamics passivity. Let $\bar{a} = a + k_1$, $\bar{b} = \begin{pmatrix} b & -b \end{pmatrix}$ and $\bar{c} = \begin{pmatrix} c + k_2 \\ 0 \end{pmatrix}$. The passivity of the error dynamics represented by the quadruple $(\bar{a}, \bar{b}, \bar{c}, 0)$

is determined by checking analytically if the BMI in (2.18) has a solution for the system (2.28). Consider

$$M_{ext} \triangleq \begin{pmatrix} -2p(a+k_1) & -pb+c+k_2 & pb \\ -bp+c+k_2 & 0 & 0 \\ bp & 0 & 0 \end{pmatrix} \succeq 0.$$

From Lemma A.3.1, it follows that $M_{ext} \succcurlyeq$ only if $-pb+c+k_2 = pb = 0$. Therefore, it is inferred that this approach (imposing the passivity of the error dynamics with the LMI in (2.18)) is not fruitful in this case.

The following Lemma states the stability result.

Lemma 2.2.2. *Consider the dynamical systems in (2.25) and in (2.23). Suppose that Assumptions 2.1.2 and 2.1.4 hold. Assume that the states $x(\cdot)$ and $x_d(\cdot)$ have jumps for $t > 0$ (which is possible since $d = 0$ in the complementarity constraint). Then, the error dynamics in (2.28) has a globally asymptotically stable equilibrium point $e^\star = 0$.*

Proof. Consider the Lyapunov candidate function $V(e(t)) = e(t)^\top P e(t)$. Recall from section 2.1.2, Proposition 2.1.8, that the error dynamics in (2.28) has a globally exponentially stable equilibrium point $e^* = 0$ when both the states $x(\cdot)$ and $x_d(\cdot)$ are continuous. This result is proved by showing the variation of the storage function of the error dynamics $\dot{V}(e(t)) < 0$ for all $e \neq 0$.

In view of the desired dynamics (2.23), the closed-loop dynamics (2.25) and the controllers (2.24), let t_k where $k > 0$ be the set of time instants at which $u_{2d}(\cdot)$ is discontinuous. The states x and x_d undergoes a jump at $t \in \{0\} \cup \{t_k\}$. The goal is to study the sign of $\Delta V(e(t))$ at the jump time which is written as follows in scalar case:

$$\begin{aligned} \Delta V(e(t)) &= V(e(t^+)) - V(e(t^-)) \\ &= \left(x(t^+) - x_d(t^+)\right)^\top p \left(x(t^+) - x_d(t^+)\right) - \left(x(t^-) - x_d(t^-)\right)^\top \left(x(t^-) - x_d(t^-)\right) \\ &= p\left(x(t^+) - x_d(t^+)\right)^2 - p\left(x(t^-) - x_d(t^-)\right)^2 \end{aligned} \tag{2.29}$$

There are three cases to consider when analyzing the sign of $\Delta V(e(t))$. To lighten notations we denote $f^+ = f(t^+)$ and $f^- = f(t^-)$.

First case In this case, both x and x_d jump at the same time t. The values of the state jump for the desired and the closed-loop system are given by $x_d^+ = -\frac{1}{c}u_{2d}^+$ and $x^+ = \frac{k_2 x_d^+ - u_{2d}^+}{c+k_2}$ respectively by referring to Appendix B.1. If we substitute the value of x_d^+ in x^+, then $x^+ = -\frac{1}{c}u_{2d}^+$. The variation of the storage function at the jump time is:

$$\begin{aligned} \Delta V(e(t)) &= p\left(x(t^+) - x_d(t^+)\right)^2 - p\left(x(t^-) - x_d(t^-)\right)^2 \\ &= p\left(-\tfrac{1}{c}u_{2d}^+ + \tfrac{1}{c}u_{2d}^+\right) - p\left(x(t^-) - x_d(t^-)\right)^2 \\ &= -p\left(x(t^-) - x_d(t^-)\right)^2 \leq 0 \end{aligned}$$

Thus, when both x and x_d jump, the variation of the storage function of the error dynamics $\Delta V(e) < 0$ for all $e \neq 0$.

Second case In this case, the closed-loop system's state x jumps and the desired system's state x_d is continuous such that $x_d^+ = x_d^- = x_d$. The value of the closed-loop system's state jump is given by $x^+ = \frac{k_2 x_d - u_{2d}^+}{c+k_2}$ (see Appendix B.1). If these values are substituted in $\Delta V(e(t))$ in (2.29), then

$$\begin{aligned}
\Delta V(e(t)) &= p\left(\tfrac{k_2 x_d - u_{2d}^+}{c+k_2} - x_d\right)^2 - p(x^- - x_d)^2 = p\left(\left(\tfrac{-cx_d - u_{2d}^+}{c+k_2}\right)^2 - (x^- - x_d)^2\right) \\
&= p\left(\left(\tfrac{-cx_d - u_{2d}^+}{c+k_2} - x^- + x_d\right)\left(\tfrac{-cx_d - u_{2d}^+}{c+k_2} + x^- - x_d\right)\right) \\
&= p\left(\left(\tfrac{-(c+k_2)x^- + k_2 x_d - u_{2d}^+}{c+k_2}\right)\left(\tfrac{(c+k_2)x^- - (2c+k_2)x_d - u_{2d}^+}{c+k_2}\right)\right) \\
&= \tfrac{p}{(c+k_2)^2}\left(\left(-(c+k_2)x^- + k_2 x_d - u_{2d}^+\right)\left((c+k_2)x^- - (2c+k_2)x_d - u_{2d}^+\right)\right)
\end{aligned}$$

Let $h(x) \triangleq -(c+k_2)x^- + k_2 x_d - u_{2d}^+$ and $r(x) \triangleq (c+k_2)x^- - (2c+k_2)x_d - u_{2d}^+$. Let us study the signs of $h(x)$ and $r(x)$.

Knowing that $x^- \notin \mathcal{K}$, the following inequality holds:

$$(c+k_2)x^- - k_2 x_d + u_{2d}^+ < 0 \Leftrightarrow -(c+k_2)x^- + k_2 x_d - u_{2d}^+ > 0 \Leftrightarrow h(x) > 0$$

Now, let us check the sign of $r(x)$. If we add and subtract u_{2d}^+, then

$$\begin{aligned}
r(x) \pm u_{2d}^+ &\triangleq (c+k_2)x^- - k_2 x_d + u_{2d}^+ - 2cx_d - 2u_{2d}^+ \\
&\triangleq -h(x) - 2cx_d - 2u_{2d}^+
\end{aligned}$$

Provided that $-h(x) < 0$ and $cx_d + u_{2d}^+ \geq 0$ (*i.e.*, $x_d \in \mathcal{K}_d$) $\Leftrightarrow -2cx_d - 2u_{2d}^+ \leq 0$. So, $r(x) < 0$.

Thus, $h(x) > 0$ and $r(x) < 0$. Therefore, $\Delta V(e(t)) \triangleq \frac{p}{(c+k_2)^2}\left(h(x)r(x)\right) < 0$.

Third case In this case, the desired system's state x_d jumps and the closed-loop system's state x is continuous such that $x^+ = x^- = x(t)$. The value of the desired system's state jump is $x_d^+ = -\frac{1}{c}u_{2d}^+$ (see Appendix B.1). If these values are substituted in $\Delta V(e(t))$ in (2.29), then

$$\Delta V(e(t)) = p\left(x + \tfrac{u_{2d}^+}{c}\right)^2 - p(x - x_d^-)^2 = p\left(\left(x + \tfrac{u_{2d}^+}{c} + x - x_d^-\right)\left(\tfrac{u_{2d}^+}{c} + x_d^-\right)\right)$$

Let $h(x) \triangleq x + \frac{u_{2d}^+}{c} + x - x_d^-$ and $r(x) \triangleq \frac{u_{2d}^+}{c} + x_d^-$. Let us study the signs of $h(x)$ and $r(x)$. Knowing that $x_d^- \notin \mathcal{K}_d$, then

$$cx_d^- + u_{2d}^+ < 0 \Leftrightarrow x_d^- + \frac{u_{2d}^+}{c} < 0 \Leftrightarrow r(x) < 0$$

Now, let us check the sign of $h(x)$ by adding and subtracting u_{2d}^+. Then,

$$h(x) \pm u_{2d}^+ \triangleq 2(cx + u_{2d}^+) - cx_d^- - u_{2d}^+ \triangleq 2(cx + u_{2d}^+) - r(x)$$

The following holds:

$$\begin{aligned} x \in \mathcal{K} &\Leftrightarrow (c+k_2)x - k_2 x_d^+ + u_{2d}^+ \geq 0 \\ &\Leftrightarrow (c+k_2)x + \tfrac{k_2}{c}u_{2d}^+ + u_{2d}^+ \geq 0 \\ &\Leftrightarrow \tfrac{(c+k_2)}{c}(cx + u_{2d}^+) \geq 0. \end{aligned}$$

According to Remark 2.2.1, $\frac{c+k_2}{c} > 0$. So, $cx+u_{2d}^+ \geq 0 \Leftrightarrow 2cx+2u_{2d}^+ \geq 0$ and $-r(x) > 0$, and $h(x) > 0$. Thus, $h(x) > 0$ and $r(x) < 0$ and $\Delta V(e(t)) \stackrel{\Delta}{=} p\,(h(x)r(x)) < 0$. Therefore, the storage function is strictly decreasing (*i.e.,* $\dot{V} < 0$ when $t \neq t_k$ and $\Delta V < 0$ when $t = t_k$ for all $e \neq 0$ where t_k are the time instants of jumps) on $\mathbb{R}_+$. □

The next lemma states the existence of finite-time tracking.

Corollary 2.2.3. *Following on from Lemma 2.2.2, assume that $u_{2d}(\cdot)$ is discontinuous at time instants t_k, with $k = \{1, 2, ..., n\}$ where $n \in \mathbb{N}^\star$. For any t_k, if there exists $u_{2d}(t_k^+) < \min\left\{-cx(t_k^-), -cx_d(t_k^-)\right\}$, then both x and x_d jump to the value $x_d(t_k^+) = x(t_k^+) = -\frac{1}{c}u_{2d}(t_k^+)$. Therefore, there is perfect tracking for all $t \geq t_k$ (*i.e., *finite-time tracking is achieved).*

Proof. Let the time instants at which $u_{2d}(\cdot)$ is discontinuous be denoted by t_k with $k = \{1, 2, \ldots, n\}$. The goal is to show that if the input $u_{2d}(t_k^+) < \min\{-cx(t_k^-), -cx_d(t_k^-)\}$, then both x and x_d jump to the same value at $t = t_k$. According to the set $\mathcal{K}_d$ in (2.26), the state x_d performs a jump at $t = t_k$ if and only if $x_d(t_k^-) \notin \mathcal{K}_d$, which is written as follows:

$$x_d(t_k^-) \notin \mathcal{K}_d \Leftrightarrow cx_d(t_k^-) + u_{2d}(t_k^+) < 0 \Leftrightarrow u_{2d}(t_k^+) < -cx_d(t_k^-)$$

Also, the state x in (2.25) performs a jump at $t = t_k$ if and only if $x(t_k^-) \notin \mathcal{K}$ in (2.27). Let us write the following:

$$x(t_k^-) \notin \mathcal{K} \Leftrightarrow (c+k_2)x(t_k^-) - k_2 x_d(t_k^+) + u_{2d}(t_k^+) < 0 \tag{2.30}$$

Given that x_d jumps at $t = t_k$, let us substitute $x_d(t_k^+) = -\frac{1}{c}u_{2d}(t_k^+)$ (see (B.1) in Appendix B.1) in (2.30). Then,

$$(c+k_2)x(t_k^-) + \tfrac{k_2}{c}u_{2d}(t_k^+) + u_{2d}(t_k^+) < 0 \Leftrightarrow \tfrac{c+k_2}{c}\left(cx(t_k^-) + u_{2d}(t_k^+)\right) < 0$$

Let c and $c+k_2$ have the same sign (see Remark 2.2.1). It is inferred that equivalently

$$u_{2d}(t_k^+) < -cx(t_k^-).$$

According to the solution of the optimization problem (1.11) presented in Appendix B.1, the closed-loop system's state x jumps at t_k such that $x(t_k^+) = \frac{k_2 x_d(t_k^+) - u_{2d}(t_k^+)}{c+k_2} = -\frac{1}{c}u_{2d}(t_k^+)$ where $x_d(t_k^+) = -\frac{1}{c}u_{2d}(t_k^+)$. Therefore, both x and x_d jump at t_k to the same value $x_d(t_k^+) = x(t_k^+) = -\frac{1}{c}u_{2d}(t_k^+)$ (see Appendix B.1) if and only if $u_{2d}(t_k^+) < \mu$, where μ is given by $\mu = \min\left\{-cx_d(t_k^-), -cx(t_k^-)\right\}$. □

2.2.4 Numerical Applications

Let us consider that the open-loop system with $u_1 = u_2 = 0$ is not strictly passive but there exist k_1, k_2, and p such that the closed-loop quadruple $(a + k_1, b, c + k_2, 0)$ is strictly state passive, equivalently the bilinear matrix inequality in (4.10) has a solution $p > 0$ with $\epsilon > 0$. According to Appendix A.1, the following LMI is obtained with $G = 0$

$$\begin{pmatrix} -2qa - 2N_1 - \epsilon q & -b + qc + N_2 \\ -b + cq + N_2 & 0 \end{pmatrix} \succeq 0 \tag{2.31}$$

where $q = p^{-1}$, $N_1 = k_1 q$ and $N_2 = k_2 q$. The LMI in (2.31) has a solution such that:

$$k_1 = -1.198, \quad k_2 = 0.96 \quad \text{and} \quad p = 1.9607$$

for $a = 0.5$, $b = 1$ and $c = 1$. For the sake of numerical simulation, take $a = 0.5$ (so that the solutions of systems in (2.23) and (2.22) diverge slowly).

Example 1. *Let us take $b = 1$, and $c = 1$. The numerical simulation below for the closed-loop system and the desired system is implemented with a discontinuous controller $u_{2d}(t)$ at t_k with $k = \{1, 2, 3, 4\}$. Take $x(0) = 3$, $x_d(0) = -3$, $u_{1d} = 5 \sin 3t$ and $u_{2d} = 4$ for $t \leq 1s$ with the time step $h = 0.01$. Given that $x_d(1^-) = -0.7$ and $x(1^-) = 2.28$, and following Corollary 2.2.3, let us choose $u_{2d}(1^+)$ such that $u_{2d}(1^+) = \min\{-x_d(1^-) - \delta, -x(1^-) - \delta\} < \min\{-x_d(1^-), -x(1^-)\}$ with $\delta = 0.5$. Based on the value of δ, $u_{2d}(1^+) = \min\{0.2, -2.78\} = -2.78$.*

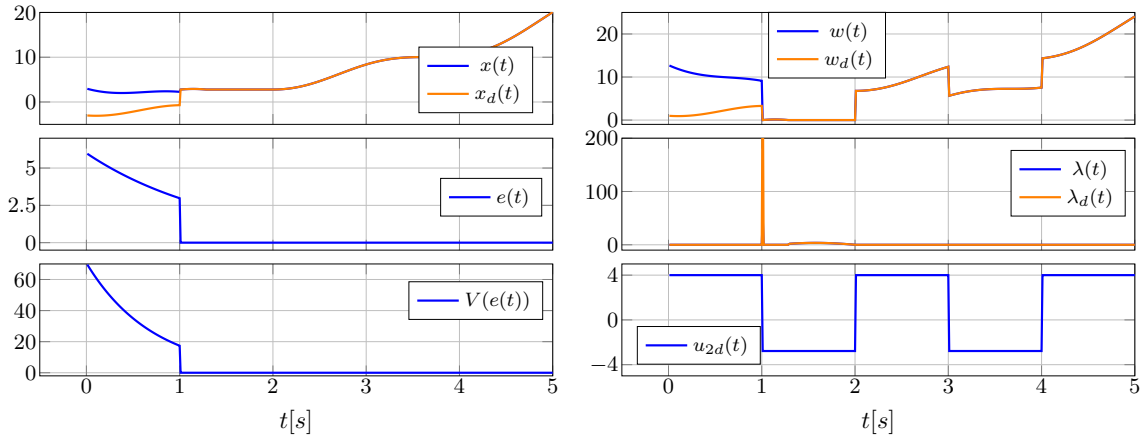

Figure 2.1: Numerical simulation of LCS where both x and x_d jump

*Both x and x_d jumps at $t = 1$ to the same value of $-u_{2d}(t_1^+) = 2.87$. Notice that the storage function's variation ΔV is non-positive at the time of the state jump (*i.e., *$V(e(1^+)) - V(e(1^-)) \leq 0$). After the first jump of both states x and x_d at the same time $t = 1$ and following Corollary 2.2.3, the controller u_{2d} can take any value at the time of discontinuities such that $u_{2d}(t_{k+1}^+) \in \mathbb{R}$ and perfect tracking is preserved (*i.e., *$e = 0$).*

Example 2. *Let us illustrate the case when x_d jumps but x does not jump. Take $x(0) = 3$, $x_d(0) = -3$. Knowing that $x_d(1^-) = -0.7$ and $x(1^-) = 2.28$ from the*

simulation in Figure 2.1, let us choose $u_{2d}(1^+)$ *such that* $x_d(1^-) \notin \mathcal{K}_d$ *in (2.26) and* $x(1) \in \mathcal{K}$ *in (2.27). Thus,*

$$x_d(1^-) \notin \mathcal{K}_d \;\Leftrightarrow\; cx_d(1^-) + u_{2d}(1^+) < 0 \;\Rightarrow\; u_{2d}(1^+) < 0.7$$

and

$$x(1) \in \mathcal{K} \;\Leftrightarrow\; (c+k_2)x(1) - k_2 x_d(1^+) + u_{2d}(1^+) \geq 0 \;\Rightarrow\; u_{2d}(1^+) \geq -2.28$$

with $c = 1$ *and* $k_2 = 0.96$ *(the solution of LMI in (2.31)). Take* $u_{2d}(1^+) = -1$.

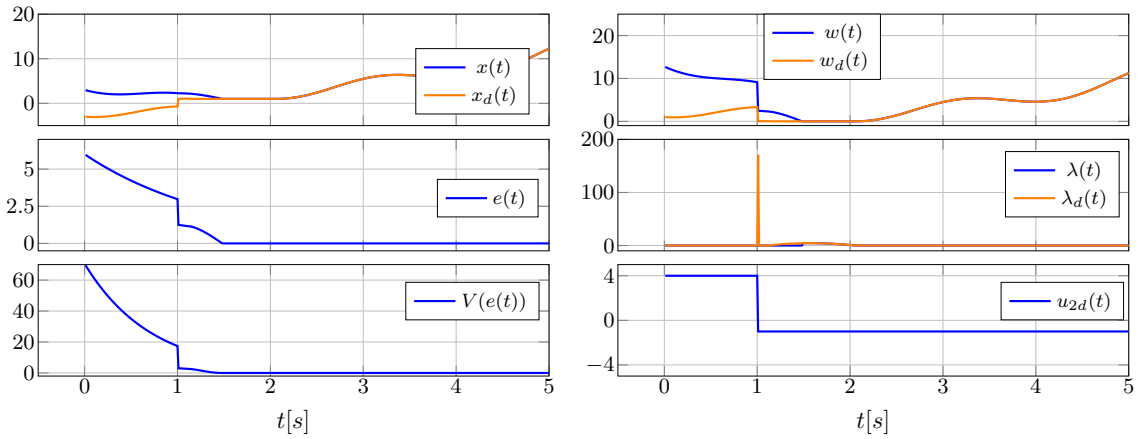

Figure 2.2: Numerical simulation of LCS when only x_d jumps

It is noticed from Figure 2.2 that the variation of the storage function $V = pe^2$ *is negative when* x_d *jumps at* $t = 1s$ *even though the closed-loop system's state* x *does not jump at* $t = 1s$. *Let us create another jump in* x_d *in the transient regime of the error dynamics (*i.e., *before* $e = 0$ *at* $t = 1.5s$*). Knowing that* $x_d(1.2^-) = 1$ *and* $x(1.2^-) = 2.057$, *choose* $-2.057 \leq u_{2d}(1.2^+) < -1$ *so that* $x_d(1.2^-) \notin \mathcal{K}_d$ *and* $x(1.2) \in \mathcal{K}$. *Take* $u_{2d}(1.2^+) = -1.5$.

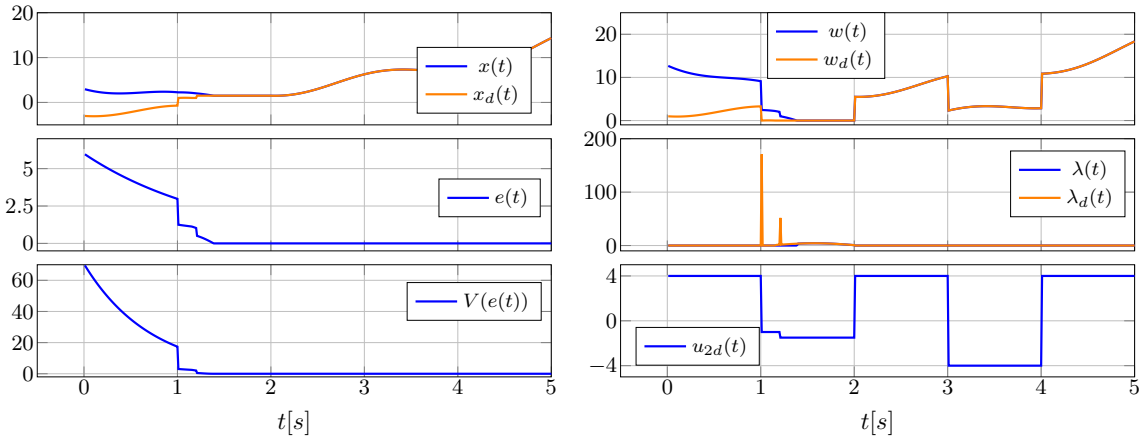

Figure 2.3: Numerical simulation of LCS where only x_d jumps

*In Figure 2.3, the desired state x_d jumps at $t = 1.2s$ such that $x_d(1.2^+) = -u_{2d}(1.2^+) = 1.5$. The value of the error $e(1.2^+) = 0.557 < e(1^-) = 1.057$, so the variation of the storage function V, computed in (2.29), is negative at the jump time $t = 1.2$. It is observed in Figure 2.3 that the error has an asymptotically stable equilibrium point $e^\star = 0$ which is consistent with the result in Lemma 2.2.2. It is important to state that, in the case of Figures 2.2 and 2.3, the necessary and sufficient conditions to have a jump in the closed-loop state x (*i.e., *$u_{2d}(1^+) < -2.28$*) generate a jump as well in the desired state x_d at the same time, illustrating Corollary 2.2.3.*

Example 3. *The above conditions that guarantee a negative Lyapunov function jump, may not match with the sufficient conditions of Proposition 2.1.11. The goal is to find an example such that the sufficient conditions of Proposition 2.1.11 are satisfied, as an illustration. Recall that $a = 0.5$, $b = 1$, $c = 1$, $p = 1.96$ and $k_2 = 0.96$.*

*Let $x(0) = -15$, $x_d(0) = 1$, $u_{1d}(t) = 5\sin 3t$ and u_{2d} is a discontinuous function as shown in Figure 2.4. Let us create a jump at $t = 1s$ such that the conditions in Proposition 2.1.11 are satisfied. At $t = 1^-$, the values of the states are $x(1^-) = -2.06$ and $x_d(1^-) = 5.89$. Let us consider the case when x_d is continuous at $t = 1s$ (*i.e., *$x_d(1^+) = x_d(1^-) = x_d(1)$) and x is discontinuous at $t = 1$ (*i.e., *$x(1^+) = \frac{k_2 x_d^+ - u_{2d}^+}{c+k_2}$ from Appendix B.1). Assume that at $t = 1s$:*

$$0 \in \mathcal{K} \Leftrightarrow -k_2 x_d(1^+) + u_{2d}(1^+) \geq 0 \Leftrightarrow u_{2d}(1^+) \geq 5.65$$

and

$$x_d(1^+)px(1^-) \geq x_d(1^-)px(1^-) \Leftrightarrow x_d(1)px(1^-) = x_d(1)px(1^-)$$

and

$$x_d(t^+) \in \mathcal{T}_\mathcal{K}(\text{proj}_P[\mathcal{K}; x(t^-)]) \Leftrightarrow x_d(t^+) \in \mathcal{T}_\mathcal{K}(x(t^+)) \Leftrightarrow x_d(t^+) \in (\mathcal{N}_\mathcal{K}(x(t^+)))^\circ.$$

Knowing that $-p(x(1^+) - x(1^-)) \in \mathcal{N}_\mathcal{K}(x(1^+))$, then the last condition is written as

$$\begin{aligned} x_d(1^+) \in (\mathcal{N}_\mathcal{K}(x(1^+)))^\circ \quad &\Rightarrow \quad -x_d(1^+)p(x(1^+) - x(1^-)) \leq 0 \\ &\Rightarrow \quad x_d(1^+)p\left(\tfrac{k_2 x_d^+ - u_{2d}^+}{c+k_2} - x(1^-)\right) \leq 0 \\ &\Rightarrow \quad u_{2d}(1^+) \geq 1.5 \end{aligned}$$

*Let $u_{2d}(1^+) \geq 5.56$ such that the above conditions (*i.e., *the conditions of Proposition 2.1.11) are satisfied and $-5 \leq u_{2d}(1^+) < 9.6$ (*i.e., *$x_d(1) \in \mathcal{K}_d$ and $x(1^-) \notin \mathcal{K}$ at $t = 1s$), thus choose $u_{2d}(1^+) = 6$. The numerical simulation is shown in the Figure 2.4 with a time step $h = 0.01s$.*

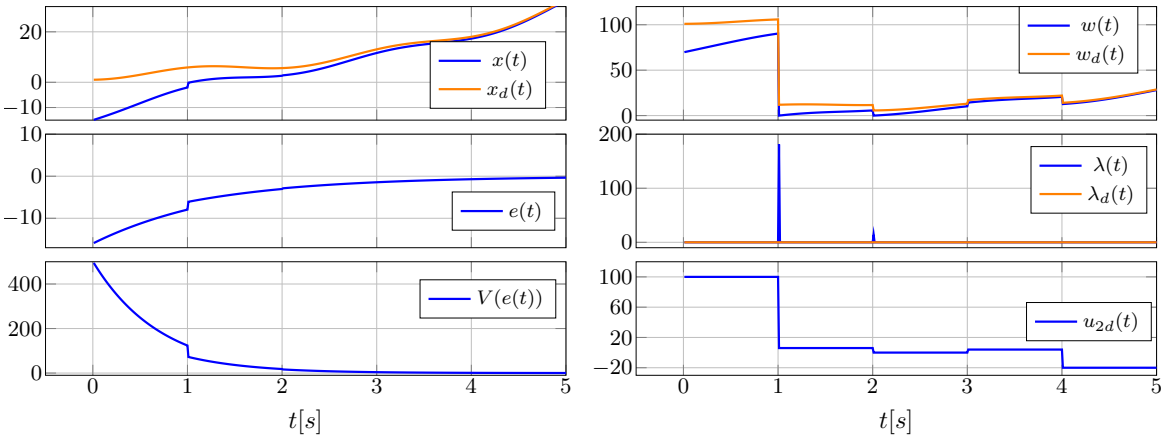

Figure 2.4: Numerical simulation of LCS where only x jumps

As shown in Figure 2.4, at the jump time $t = 1s$, the variation of the storage function $\Delta V(e(1)) = V(e(1^+)) - V(e(1^-)) \leq 0$ which agrees with the result stated in Proposition 2.1.11.

2.2.5 Recapitulation

The occurrence of "peaking phenomenon", which occurs when the jump times of two trajectories do not coincide, is not observed in our case. This is due to the fact that the desired system in (2.23) is derived from the dynamics of the real system in (2.22) and that both systems are passive.

*The challenge in our work results from the different situations leading to state jumps (*i.e., *discontinuities in $v_d(t)$ or in $\lambda_d(t)$). It is noteworthy that, in the scalar case, the jumps only occur due to discontinuities in $u_{2d}(t)$ as discussed in section 2.2.2. The closed-loop system's state $x(t)$ in (2.25) jumps when either $x_d(t)$ or $u_{2d}(t)$ jumps, and since the desired system's state $x_d(t)$ only jumps when $u_{2d}(t)$ jumps, it follows that both states jump at the same time (*i.e., *no jump mismatch occur).*

The electrical circuits with ideal diodes, presented as examples in Chapter 3, section 3.3.2 provide a more advanced analysis for state jumps and show the stability of the error dynamics in the presence of state jumps through numerical simulations.

2.3 Tracking Control for First-order Sweeping Process

The first order sweeping process (FOSwP) is a differential inclusion of the form:

$$\dot{x}(t) \in -\mathcal{N}_{S(t)}(x(t)) + f(t, x) \tag{2.32}$$

where $\mathcal{N}_{S(t)}(x(t))$ is the normal cone to the closed convex non-empty set $S(t) \subseteq \mathbb{R}^n$ at $x(t)$, defined in Definition 1, and $f(t, x)$ is a single-valued map such that $f : \mathbb{R} \times \mathbb{R}^n \to \mathbb{R}^n$. This type of differential inclusion is first introduced by J.J. Moreau in [123, 122,

120] and motivated by the problems of elastoplasticity. Indeed, the control of FOSwP has recently received much attention, especially its optimal control [56, 10, 48, 49, 54]. Many papers focused on deriving necessary and optimal conditions for different types of sweeping processes (*i.e.*, perturbed, unperturbed, *etc.*) using the method of discrete approximations [49, 55, 57, 58, 76, 77, 119]. Optimal control problems governed by sweeping process have been addressed with various applications, such as marine surface vehicles [49], robotics and pedestrian traffic [54], and crowd motions with obstacles [48]. Additionally, the existence of periodic solutions for FOSwP is discussed in [86], with further studies performed on the stability of these solutions in [151, 53]. Thus, it is of interest to investigate the trajectory tracking issue for such DIs.

Under some conditions (see, *e.g.*, section B.2), LCS can be equivalently rewritten as a First-order Sweeping Process (FOSwP). Here we are interested to see how the material in section 2.2 is generalized to trajectory tracking in FOSwP, considering the analysis of state jumps discussed in section 2.1.3.

2.3.1 Dynamics under FOSwP

Let us first rewrite both the closed-loop plant and the desired dynamics under the perturbed FOSwP format, when $D = 0$ in (2.1) and $D + FG = 0$ in (2.3). The LCS of the desired system in (2.1) can be represented equivalently as a FOSwP when $D = 0$ if the conditions in section 1.2.2, item 3 are satisfied. These conditions require the system represented by the quadruple $(A, B, C, 0)$ to be passive which implies the condition $PB = C^\top$ where $P = P^\top \succ 0$ is the solution of the matrix inequality of strict passivity in (4.10), the controller $u \in \mathcal{L}^1_{loc}(\mathbb{R}_+ : \mathbb{R}^p)$ and the constraint qualification $\mathrm{Im}(C) - \mathbb{R}^m_+ = \mathbb{R}^m$ holds. The desired FOSwP is represented as follows (see section B.2):

$$\dot{\zeta}_d(t) \in R_d A R_d^{-1} \zeta_d(t) - \mathcal{N}_{\phi_d(t)}(\zeta_d(t)) \tag{2.33}$$

where $R_d^2 = P_d$, $R_d = R_d^\top$, $\zeta_d = R_d x_d$ and $\phi_d(t) = \{R_d x_d \mid C x_d \in S_d(t)\}$ with $S_d(t) = \{v \in \mathbb{R}^m \mid v + F u_d(t) \geq 0\}$. Given that $x_d(t) = R_d^{-1}\zeta_d(t)$, then $\phi_d(t) = \{\zeta_d \in \mathbb{R}^n \mid C R_d^{-1}\zeta_d + F u_d(t) \geq 0\}$.

Recall that the closed-loop system in (2.16) when $D + FG = 0$ is the following FOSwP:

$$\dot{\zeta}(t) \in R(A + EK)R^{-1}\zeta(t) + RE(-K R_d^{-1}\zeta_d(t) + u_d(t)) - \mathcal{N}_{\Phi(t)}(\zeta(t)) \tag{2.34}$$

where $\phi(t) = \{Rx \mid (C + FK)x \in S(t)\}$ with $S(t) = \{v \in \mathbb{R}^m \mid v - FK x_d(t^+) + F u_d(t) \geq 0\}$ and $\zeta(t) = Rx(t)$. It is noteworthy that the set $\phi(t)$ depends on the post-jump of the desired state x_d^+. This means that it can be characterized only once the desired state's jump has been calculated. Thus, $\phi(t) = \{\zeta \in \mathbb{R}^n \mid (C+FK)R^{-1}\zeta - FK R_d^{-1}\zeta_d(t^+) + F u_d(t) \geq 0\}$. Note that $x \in \mathcal{K}$ if and only if $\zeta \in \phi(t)$ and $x_d \in \mathcal{K}_d$ if and only if $\zeta_d \in \phi_d(t)$.

2.3.2 Conditions for Post-Jump Equality: $x^+ = x_d^+$

Recall that $f(t^+) = \lim_{\substack{s \to t \\ s > t}} f(s)$ and $f(t^-) = \lim_{\substack{s \to t \\ s < t}} f(s)$. Taking advantage of the FOSwP formalism, the aim in the following is to show under which conditions $x_d^+ = x^+$

holds. As a first step, let us check if $x_d^+ \in \partial\mathcal{K}$. It is required to show that $x_d^+ \in \mathcal{K}$ (the set $\mathcal{K}$ is defined for (2.3)). Given that $x_d^+ \in \mathcal{K}_d$, then

$$Cx_d^+ + Fu_d \geq 0 \Leftrightarrow (C+FK)x_d^+ - FKx_d^+ + Fu_d \geq 0 \tag{2.35}$$

This means that x_d^+ satisfies the condition of the set $\mathcal{K}$. Hence, $x_d^+ \in \mathcal{K}$.
In addition, given that $x_d^+ \in \partial\mathcal{K}_d$, it follows that

$$\left[Cx_d^+ + Fu_d^+\right]_k = 0 \Leftrightarrow \left[(C+FK)x_d^+ - FKx_d^+ + Fu_d^+\right]_k = 0 \quad \text{for some } \; k \in \{1,\dots,m\} \tag{2.36}$$

Thus, the following is proved:

Lemma 2.3.1. *The post-jump desired state satisfies: $x_d^+ \in \partial\mathcal{K} \cap \partial\mathcal{K}_d$. So, a necessary condition to have $x^+ = x_d^+$ is that $x^+ \in \partial\mathcal{K}$, which is equivalent to $x^- \notin \text{Int}(\mathcal{K})$.*

If it is assumed that $P(x^- - x_d^+) \in \mathcal{N}_{\mathcal{K}}(x_d^+)$, equivalently $x_d^+ = \text{Proj}_P[\mathcal{K}; x^-] = x^+$ (the last equality holds from (1.11)). The question that arises is: what are the conditions such that the first inclusion holds?
Let us present the given information in the following. The optimization problem in (1.11) for the desired system leads to the following:

$$x_d^+ = \text{Proj}_{P_d}[\mathcal{K}_d; x_d^-] \Leftrightarrow P_d(x_d^- - x_d^+) \in \mathcal{N}_{\mathcal{K}_d}(x_d^+) \tag{2.37}$$

Similarly, according to the optimization problem in (1.11) for the closed-loop system, the following is derived:

$$P(x^- - x^+) \in \mathcal{N}_{\mathcal{K}}(x^+) \tag{2.38}$$

Using the definition of the normal cone in (1.2), the equations in (2.37) and (2.38) are written as follows, for the desired and closed-loop systems, respectively:

$$(x_d^- - x_d^+)^\top P_d(x_d - x_d^+) \leq 0 \;\; \forall\, x_d \in \mathcal{K}_d$$

$$(x^- - x^+)^\top P(x - x^+) \leq 0 \;\; \forall\, x \in \mathcal{K}$$

And the third inclusion for $x_d^+ = x^+$ is equivalent to the variational inequality VI (see Definition 7):

$$(x^- - x_d^+)^\top P(x - x_d^+) \leq 0 \;\; \forall\, x \in \mathcal{K}$$

Note that $x_d^+ \in \partial\mathcal{K}$ if and only if $Rx_d^+ \in \partial\phi(t) \Leftrightarrow RR_d^{-1}\zeta_d^+ \in \partial\phi(t)$, where $\zeta_d = R_d x_d$ and $\zeta = Rx$. Hence, the state $RR_d^{-1}\zeta_d$ becomes relevant and the set $RR_d^{-1}\phi_d(t)$ is considered in the following since $RR_d^{-1}\zeta_d \in RR_d^{-1}\phi_d(t)$. Let $\zeta_d' = RR_d^{-1}\zeta_d = Rx_d$ and $\phi_d'(t) = RR_d^{-1}\phi_d(t) = R\mathcal{K}_d$ which is defined as:

$$\phi_d'(t) = \{\zeta_d' \in I\!R^2 \mid CR^{-1}\zeta_d' + Fu_d \geq 0\} \tag{2.39}$$

The desired system in (2.33) is written, in the terms of the new variable $\zeta_d' = RR_d^{-1}\zeta_d$, as follows:

$$\dot{\zeta}_d' \in RAR^{-1}\zeta_d' - RP_d^{-1}R\mathcal{N}_{\phi_d'(t)}(\zeta_d') \tag{2.40}$$

Similarly, $x^+ \in \partial\mathcal{K}$ if and only if $\zeta^+ \in \partial\phi((t)$. Hence, equivalently the three VIs are obtained:

$$(\zeta_d'^- - \zeta_d'^+)^\top(\zeta_d' - \zeta_d'^+) \leq 0 \;\; \forall\, \zeta_d' \in \phi_d'(t) \tag{2.41}$$

$$(\zeta^- - \zeta^+)^\top(\zeta - \zeta^+) \leq 0 \;\; \forall\, \zeta \in \phi(t) \tag{2.42}$$

$$(\zeta^- - \zeta_d'^+)^\top(\zeta - \zeta_d'^+) \leq 0 \;\; \forall\, \zeta \in \phi(t) \tag{2.43}$$

The optimization problem in (2.38) for the closed-loop FOSwP in (2.34) is written as follows:

$$\zeta^+ = \text{Proj}[\phi(t), \zeta^-] \Leftrightarrow \zeta^- - \zeta^+ \in \mathcal{N}_{\phi(t)}(\zeta^+) \tag{2.44}$$

Then, it is required to prove under which conditions $\zeta^- - \zeta_d'^+ \in \mathcal{N}_{\phi(t)}(\zeta_d'^+)$ (which is the VI (2.43)) holds, equivalently $\zeta_d'^+ = \zeta^+$ (*i.e.*, $R^{-1}\zeta^+ = R_d^{-1}\zeta^+ \Leftrightarrow x_d^+ = x^+$). Let us study this on a particular example.

Example 4. *Consider the desired FOSwP in (2.33). Take $A = -I$, $B = I$, and $C = I$ where I is the 2×2 identity matrix. Let $E = \begin{pmatrix} 1 & 0 \end{pmatrix}^\top$ and $F = \begin{pmatrix} 2 & 1 \end{pmatrix}^\top$. The LMI of strict passivity in (4.10), related to the desired system's quadruple $(A, B, C, 0)$, has a solution $P_d = P_d^\top = I \succ 0$. Thus, the desired system is strictly state passive. Given that $R_d^2 = P_d$, then $R_d = I$.*

Let us check if there exist K and P such that the closed-loop system's quadruple $(A + EK, B, C + FK, 0)$ is strictly passive. This means that it is required to check if the matrix inequality in (4.10) has a solution. In order to solve the BMI in (4.10), it is transformed into an LMI (see Appendix A.1) and the solution is given by the software MOSEK *9.3.14 [9]:*

$$K = \begin{pmatrix} 0.07 & 0.035 \end{pmatrix} \quad \textit{and} \quad P = \begin{pmatrix} 1.14 & 0.07 \\ 0.07 & 1.035 \end{pmatrix}$$

Given that $R^2 = P$, then $R = \begin{pmatrix} 1.07 & 0.034 \\ 0.034 & 1.017 \end{pmatrix}$. Thus, the FOSwP associated with the closed-loop system in (2.34) is written as follows:

$$\begin{pmatrix} \dot{\zeta}_1 \\ \dot{\zeta}_2 \end{pmatrix} \in \begin{pmatrix} -0.93 & 0.034 \\ 0.034 & -1 \end{pmatrix} \begin{pmatrix} \zeta_1 \\ \zeta_2 \end{pmatrix} - \begin{pmatrix} 0.14 & 0.07 \\ 0.07 & 0.034 \end{pmatrix} \begin{pmatrix} \zeta_{1d}^{+\prime} \\ \zeta_{2d}^{+\prime} \end{pmatrix} + \begin{pmatrix} 1.07 \\ 0.034 \end{pmatrix} u_d - \mathcal{N}_{\phi(t)}(\zeta) \tag{2.45}$$

where $\mathcal{N}_{\phi(t)}(\zeta) = \{v \in \mathbb{R}^2 \mid v^\top(\zeta - \eta) \leq 0 \;\; \forall\, \eta \in \phi(t)\}$ and the set $\phi(t)$ is given by:

$$\begin{aligned} \phi(t) \;\; &= \{\zeta \in \mathbb{R}^2 \mid (C + FK)R^{-1}\zeta - FKR^{-1}\zeta_d'(t^+) + Fu_d(t) \geq 0\} \\ &= \left\{ \zeta \in \mathbb{R}^2 \;\middle|\; \begin{pmatrix} 1.065 & 0.034 \\ 0.034 & 1.016 \end{pmatrix} \begin{pmatrix} \zeta_1 \\ \zeta_2 \end{pmatrix} - \begin{pmatrix} 0.129 & 0.065 \\ 0.064 & 0.032 \end{pmatrix} \begin{pmatrix} \zeta_{1d}^{+\prime} \\ \zeta_{2d}^{+\prime} \end{pmatrix} + \begin{pmatrix} 2 \\ 1 \end{pmatrix} u_d \geq \begin{pmatrix} 0 \\ 0 \end{pmatrix} \right\} \end{aligned} \tag{2.46}$$

The desired FOSwP in (2.40) is written as follows:

$$\begin{pmatrix} \dot{\zeta}_{1d}' \\ \dot{\zeta}_{2d}' \end{pmatrix} \in \begin{pmatrix} \zeta_{1d}' \\ \zeta_{2d}' \end{pmatrix} - \begin{pmatrix} 1.14 & 0.07 \\ 0.07 & 1.035 \end{pmatrix} \mathcal{N}_{\phi_d'(t)}(\zeta_d') \tag{2.47}$$

where $\mathcal{N}_{\phi'_d(t)}(\zeta'_d) = \{v \in I\!R^2 \mid v^\top(\zeta'_d - \eta_d) \leq 0 \ \ \forall\, \eta_d \in \phi'_d(t)\}$ *and the desired set* $\phi'_d(t)$ *is given by:*

$$\begin{aligned}\phi'_d(t) &= \{\zeta_d \in I\!R^2 \mid CR^{-1}\zeta'_d + Fu_d \geq 0\} \\ &= \left\{\zeta'_d \in I\!R^2 \;\middle|\; \begin{pmatrix} 0.936 & -0.031 \\ -0.031 & 0.984 \end{pmatrix}\begin{pmatrix}\zeta'_{1d} \\ \zeta'_{2d}\end{pmatrix} + \begin{pmatrix}2u_d \\ u_d\end{pmatrix} \geq \begin{pmatrix}0 \\ 0\end{pmatrix}\right\}\end{aligned} \tag{2.48}$$

Let us define the set of active constraints for the desired system in (2.47) as:

$$A_d(\phi'_d(t)) = \{i \in \{1,2\} \mid (CR^{-1})_{i,\bullet}\zeta_d'^{+} + F_{i,\bullet}u_d(t) = 0 \ \ \textit{and}\ \zeta_d'^{+} \in \phi'_d(t)\} \tag{2.49}$$

and we define

$$\Omega_{id} \triangleq \left\{\zeta_d'^{+} \in I\!R^2 \middle| \begin{pmatrix} 0.936 & -0.031 \\ -0.031 & 0.984 \end{pmatrix}_{i,\bullet}\zeta_d'^{+} + \begin{pmatrix}2u_d \\ u_d\end{pmatrix}_{i,\bullet} = 0 \quad \textit{and}\ \zeta_d'^{+} \in \phi'_d(t)\right\},$$

for $i \in \{1,2\}$.
Let us draw the set $\phi'_d(t)$ *in (2.48) as shown in Figure 2.5 below*

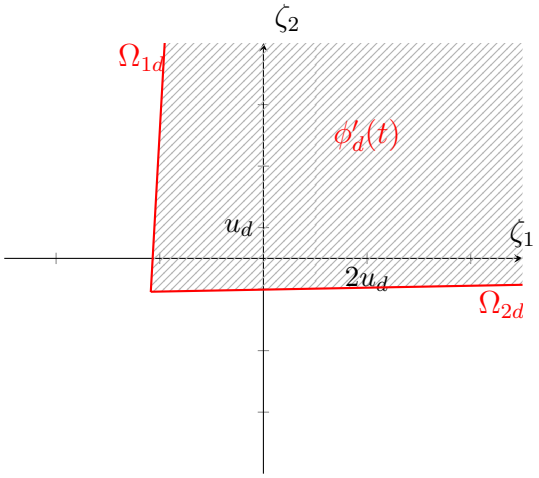

Figure 2.5: Plot of set $\phi'_d(t) in (2.48)$

It is noticeable that the set $\phi(t)$ *in (2.46) depends on the value of the state* $\zeta_d'^{+}$. *This implies that there exists a unique set* $\phi(t)$ *associated with each* $\zeta_d'^{+}$ *which is the solution to the optimization problem in (2.37) with a specific set of active constraints applied.*

Let us consider the following cases based on the different values of $\zeta_d'^{+}$, *each resulting in a different set of* $\phi(t)$.

Case 1: the state $\zeta_d'^{+} \in \Omega_{1d} \cap \Omega_{2d}$

In this case, both constraints Ω_{1d} *and* Ω_{2d} *in (2.49) for the desired system are considered active. According to the set of active constraints* $A_d(\phi'_d(t))$ *in (2.49) and given that the matrix* CR^{-1} *is invertible in this example, it follows that the state variable* $\zeta_d'^{+}$ *is*

expressed as $\zeta_d'^{+} = -RC^{-1}Fu_d \in \Omega_{1d} \cap \Omega_{2d}$. *By substituting the value of* $\zeta_d'^{+}$ *in the set* $\phi(t)$ *in* (2.46), *it gives the following expression of* $\phi(t)$:

$$\phi(t) = \{\zeta \in I\!R^2 \mid ((C + FK)R^{-1})\zeta + (FKC^{-1}F)u_d(t) + Fu_d(t) \geq 0\} \tag{2.50}$$

Figure 2.6 below shows both sets $\phi(t)$ *and* $\phi_d(t)$.

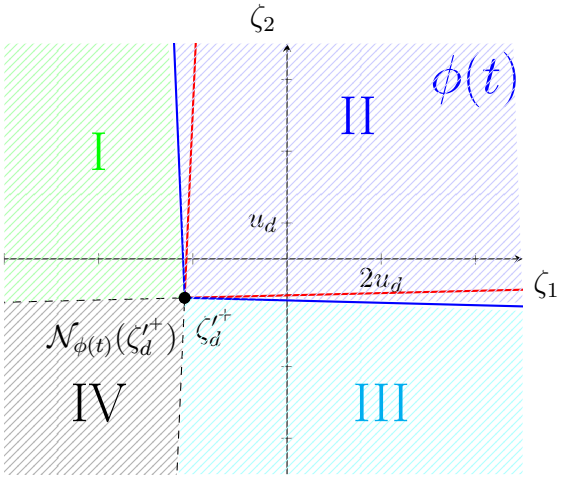

Figure 2.6: Plots of sets $\phi(t)$ in (2.50) and $\phi_d'(t)$

By observing the plots in Figure 2.6, it is noticeable that the state $\zeta_d'^{+}$ *is located at the corner of the set* $\phi_d'(t)$ (i.e., $\zeta_d'^{+} \in \Omega_{1d} \cap \Omega_{2d}$ *defined in* (2.49)). *This corner represented by* $\zeta_d'^{+}$ *is shared by both sets* $\phi_d'(t)$ *and* $\phi(t)$ *such that* $\zeta_d'^{+} \in \partial\phi(t) \cap \partial\phi_d'(t)$. *Let us define the active constraints for the closed-loop system in* (2.45) *as follows:*

$$A(\phi(t)) = \{i \in \{1,2\} \mid ((C + FK)R^{-1})_{i,\bullet}\zeta^{+} + (FKC^{-1}F)_{i,\bullet}u_d(t) + F_{i,\bullet}u_d(t) = 0, \text{ for } \zeta^{+} \in \phi(t)\} \tag{2.51}$$

and we define

$$\Omega_i \triangleq \left\{\zeta^{+} \in I\!R^2 \;\middle|\; \begin{pmatrix} 1.065 & 0.034 \\ 0.034 & 1.016 \end{pmatrix}_{i,\bullet} \zeta^{+} + \begin{pmatrix} 2.35u_d \\ 1.75u_d \end{pmatrix}_{i,\bullet} = 0 \;\; \text{for } \zeta^{+} \in \partial\phi(t)\right\},$$

for $i \in \{1,2\}$.

- *If* $\zeta^{-} \in$ *Region I* (i.e., $\zeta^{-} \notin \phi(t)$) *and the active constraint is* Ω_1 *defined in* (2.51), *then the post-jump state* $\zeta^{+} \in \Omega_1$ *and is defined as* $\zeta^{+} = \text{Proj}[\Omega_1; \zeta^{-}]$.
- *If* $\zeta^{-} \in$ *Region II* (i.e., $\zeta^{-} \in \text{int}\,\phi(t)$), *then* $\zeta^{+} = \zeta^{-} \in \text{int}\,\phi(t)$.
- *If* $\zeta^{-} \in$ *Region III* (i.e., $\zeta^{-} \notin \phi(t)$) *and the active constraint is* Ω_2 *as defined in* (2.51), *then* $\zeta^{+} \in \Omega_2$.
- *If* $\zeta^{-} \in$ *Region IV* (i.e., $\zeta^{-} - \zeta_d'^{+} \in \mathcal{N}_{\phi(t)}(\zeta_d'^{+})$) *and both constraints* Ω_1 *and* Ω_2 *are active as defined in* (2.51), *then* $\zeta^{+} = \zeta_d'^{+}$

Thus, regardless of the active constraint, $\zeta^{+} = \zeta_d'^{+}$ *if and only if* $\zeta^{-} - \zeta_d'^{+} \in \mathcal{N}_{\phi(t)}(\zeta_d'^{+})$.

Case 2: the state $\zeta_d'^{+} \in \Omega_{1d}$

In this case, only one of the constraints for the desired system is considered active which is Ω_{1d} as defined in (2.49). Let $\zeta_d'^{+} = (-2.104\, u_d, u_d)^\top \in \Omega_{1d}$ and let us substitute the value of $\zeta_d'^{+}$ in the set $\phi(t)$ in (2.46), then:

$$\phi(t) = \left\{ \zeta \in I\!R^2 \;\middle|\; \begin{pmatrix} 1.065 & 0.034 \\ 0.034 & 1.016 \end{pmatrix} \begin{pmatrix} \zeta_1 \\ \zeta_2 \end{pmatrix} - \begin{pmatrix} 0.129 & 0.065 \\ 0.064 & 0.032 \end{pmatrix} \begin{pmatrix} -2.1036 u_d \\ u_d \end{pmatrix} + \begin{pmatrix} 2u_d \\ u_d \end{pmatrix} \geq 0 \right\} \tag{2.52}$$

and it is represented graphically in Figure 2.7 below

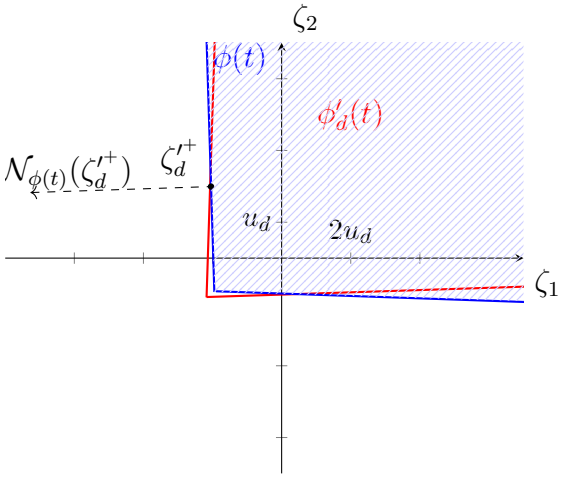

Figure 2.7: Plots of sets $\phi(t)$ in (2.52) and $\phi_d'(t)$

By observing Figure 2.7, the state $\zeta_d'^{+}$ is shared between the active constraint of the desired system Ω_{1d} and the set $\phi(t)$. It can be noticed that the set $\phi(t)$ in Figure 2.7 is different from that in Figure 2.5 due to the new selection of $\zeta_d'^{+}$. Let us define the active constraints for the closed-loop system in (2.45) as follows:

$$A(\phi(t)) = \Big\{ i \in \{1,2\} \mid ((C+FK)R^{-1})_{i\bullet}\zeta^+ + (FKR^{-1})_{i\bullet}\zeta_d'^{+}(t) + F_{i\bullet}u_d(t) = 0, \;\; for\, \zeta^+ \in \phi(t) \Big\} \tag{2.53}$$

and we define

$$\Omega_i = \left\{ \zeta^+ \in I\!R^2 \;\middle|\; \Omega_i \triangleq \begin{pmatrix} 1.065 & 0.034 \\ 0.034 & 1.016 \end{pmatrix}_{i\bullet} \zeta^+ + \begin{pmatrix} 2.206 u_d \\ 0.815 u_d \end{pmatrix}_{i\bullet} = 0 \;\; for\, \zeta^+ \in \phi(t) \right\},$$

for $i \in \{1,2\}$.

The same reasoning as before is applicable in this case. It is worth noting that the equality $\zeta^+ = \zeta_d'^{+}$ holds if and only if ζ^- is selected such that $\zeta^- - \zeta_d'^{+} \in \mathcal{N}_{\phi(t)}(\zeta_d'^{+})$. Otherwise, the resulting feasible solution $\zeta^+ \neq \zeta_d'^{+}$ but it belongs to the boundary of the set $\phi(t)$. That is, $\zeta^+ \in \partial\phi(t)$, which can be any of the three possible domains: Ω_1, Ω_2, or $\Omega_1 \cap \Omega_2$ as defined in (2.53).

Case 3: the state $\zeta_d'^{+} \in \Omega_{2d}$

In this case, only one of the constraints for the desired system is considered active which is Ω_{2d} defined in (2.49). Let $\zeta_d'^{+} = (4\ u_d, -0.89\ u_d)^\top \in \Omega_{2d}$ and let us substitute the value of $\zeta_d'^{+}$ in the set $\phi(t)$ in (2.46), then:

$$\phi(t) = \left\{ \zeta \in I\!R^2 \;\middle|\; \begin{pmatrix} 1.065 & 0.034 \\ 0.034 & 1.016 \end{pmatrix} \begin{pmatrix} \zeta_1 \\ \zeta_2 \end{pmatrix} - \begin{pmatrix} 0.129 & 0.065 \\ 0.064 & 0.032 \end{pmatrix} \begin{pmatrix} 4u_d \\ -0.89u_d \end{pmatrix} + \begin{pmatrix} 2u_d \\ u_d \end{pmatrix} \geq 0 \right\} \tag{2.54}$$

which is represented in Figure 2.8

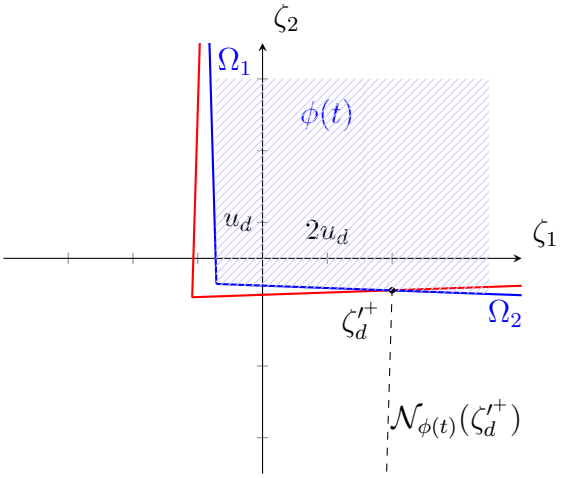

Figure 2.8: Plots of sets $\phi(t)$ in (2.54) and $\phi_d'(t)$

The state $\zeta_d'^{+}$ is shared by both sets $\phi(t)$ and $\phi_d(t)$, as shown in Figure 2.8. More precisely, $\zeta_d'^{+} \in \Omega_{2d} \cap \phi(t)$. Let us define the active constraints for the closed-loop system in (2.45) as follows:

$$A(\phi(t)) \;=\; \left\{ i \in \{1,2\} \mid ((C+FK)R^{-1})_{i\bullet}\zeta^+ + (FKR^{-1})_{i\bullet}\zeta_d'^{+}(t) + F_{i\bullet}u_d(t) = 0 \ \text{ for } \zeta^+ \in \phi(t) \right\}$$

and let $\Omega_i \triangleq \left\{ \zeta^+ \in I\!R^2 \;\middle|\; \begin{pmatrix} 1.065 & 0.034 \\ 0.034 & 1.016 \end{pmatrix}_{i\bullet} \zeta^+ + \begin{pmatrix} 1.542u_d \\ 0.773u_d \end{pmatrix}_{i\bullet} = 0 \ \text{ for } \zeta^+ \in \phi(t) \right\}$, *for* $i \in \{1,2\}$.

The same result as in the previous cases is determined: $\zeta^+ = \zeta_d'^{+}$ if and only if $\zeta^- - \zeta_d'^{+} \in \mathcal{N}_{\phi(t)}(\zeta_d'^{+})$.

In this section, an equivalence between LCS and FOSwP under certain conditions is demonstrated. Significantly, Lemma 2.3.1 gives a necessary condition to ensure that the equality $x^+ = x_d^+$ holds. Example 4 illustrates the conditions under which the post-jump states of the desired and the closed-loop systems are equal. However, further investigation is required on trajectory tracking in FOSwP, particularly on the conditions that guarantee that the assumption $P(x^- - x_d^+) \in \mathcal{N}_{\mathcal{K}}(x_d^+)$ is satisfied.

2.4 Robustness Analysis: Tracking with Parametric Uncertainties

It is of interest to analyse the tracking problem when the plant's dynamics have uncertainties. In this case, the desired dynamics' matrices in (2.1), and the plant's model matrices, differ. The desired dynamics (2.1) has to be designed using a nominal plant model.

2.4.1 Controller Design

The controller $u(t) = K_0[x(t) - x_d(t)] + G_0[\lambda(t) - \lambda_d(t)] + u_d(t)$ is designed from the plant's nominal quadruple (A_0, B_0, C_0, D_0), along the same procedure as in the foregoing section. Therefore the desired system (2.1) is represented by the following LCS:

$$\begin{cases} \dot{x}_d(t) = A_0 x_d(t) + B_0 \lambda_d(t) + E_0 u_d(t) \\ 0 \leq \lambda_d(t) \perp w_d(t) = C_0 x_d(t) + D_0 \lambda_d(t) + F_0 u_d(t) \geq 0. \end{cases} \tag{2.55}$$

If strong passivity is used (Assumption 2.1.5) instead of strict state passivity as in the foregoing section (Assumption 2.1.4), the controller gains are computed assuming there exist matrices K_0 and G_0 such that the inequality (2.7) is satisfied for the nominal plant, *i.e.*,

$$M_0 \triangleq \begin{pmatrix} (A_0 + E_0K_0)^\top P_0 + P_0(A_0 + E_0K_0) & P_0(B_0 + E_0G_0) - (C_0 + F_0K_0)^\top \\ (B_0 + E_0G_0)^\top P_0 - (C_0 + F_0K_0) & -D_0 - F_0G_0 - (D_0 + F_0G_0)^\top \end{pmatrix} \prec 0 \tag{2.56}$$

has a solution $P_0 = P_0^\top \succ 0$. The plant dynamics is represented as follows

$$\begin{cases} \dot{x}(t) = (A_0 + \Delta A)x(t) + (B_0 + \Delta B)\lambda(t) + (E_0 + \Delta E)u(t) \\ 0 \leq \lambda(t) \perp w(t) = (C_0 + \Delta C)x(t) + (D_0 + \Delta D)\lambda(t) + (F_0 + \Delta F)u(t) \geq 0 \end{cases}$$

where ΔA, ΔB, ΔC, ΔD, ΔE and ΔF represent additive uncertainties. Sufficient conditions on the uncertainties upperbounds are calculated in the next section, so that some stability is guaranteed. The closed-loop system is given by:

$$\begin{cases} \dot{x}(t) = (A_0 + \Delta A + (E_0 + \Delta E)K_0)x(t) + (B_0 + \Delta B + (E_0 + \Delta E)G_0)\lambda(t) \\ \qquad -(E_0 + \Delta E)(K_0 x_d(t) + G_0\lambda_d(t) - u_d(t)) \\ 0 \leq \lambda(t) \perp w(t) = (C_0 + \Delta C + (F_0 + \Delta F)K_0)x(t) + (D_0 + \Delta D + (F_0 + \Delta F)G_0)\lambda(t) \\ \qquad -(F_0 + \Delta F)(K_0 x_d(t) + G_0\lambda_d(t) - u_d(t)) \geq 0 \end{cases} \tag{2.57}$$

It is noteworthy that the well-posedness of (2.57) may not be guaranteed for any uncertainties. Some of the results in section 1.2.2 can be used. The following assumption is supposed to hold in this section:

Assumption 2.4.1. *The closed-loop system (2.57) is well-posed,* i.e., *it has unique AC*

solutions for any initial condition $x(t_0) = x_0$ *satisfying* $w(t_0, x_0) \geq 0$, *equivalently:*

$$\begin{aligned} x_0 \quad &\in \mathrm{Dom}\left((D_0 + \Delta D + (F_0 + \Delta F)G_0 + \partial\sigma_{S(t)})^{-1}\right) \\ &= \mathrm{Im}\left((D_0 + \Delta D + (F_0 + \Delta F)G_0 + \partial\sigma_{S(t)})\right), \end{aligned}$$

with $S(t) = \{\nu \in I\!R^m \mid \nu + (F_0 + \Delta F)(K_0 x_d + G_0\lambda_d - u_d) \geq 0\}$.

Remark 2.4.2. *It is clear that time-varying uncertainties give rise to a time-varying LCS in (2.57). As pointed out in section 1.2.2, it is only in few particular cases that the well-posedness of time-varying LCS has been studied. In this section, stability relies on the fact that the closed-loop nominal system is strongly passive, and that the closed-loop plant feedthrough matrix* $(D_0 + \Delta D + (F_0 + \Delta F)G_0) \succ 0$. *Thus, item 1 in 1.2.2 applies if this matrix is constant.*

2.4.2 Error Dynamics Stability Analysis

The error dynamics is given by:

$$\left\{\begin{array}{ll} \dot{e}(t) = & (A_0 + E_0K_0)e(t) + (B_0 + E_0G_0)\Delta\lambda(t) + \Delta Ax(t) + \Delta B\lambda(t) + \Delta EK_0e(t) \\ & +\Delta EG_0\Delta\lambda(t) + \Delta Eu_d(t) \\ \Delta w(t) = & w(t) - w_d(t) = (C_0 + F_0K_0)e(t) + (D_0 + F_0G_0)\Delta\lambda(t) + \Delta Cx(t) \\ & +\Delta D\lambda(t) + \Delta FK_0e(t) + \Delta FG_0\Delta\lambda(t) + \Delta Fu_d(t) \\ 0 \leq w(t) \perp \lambda(t) \geq 0 \quad \text{and} \quad & 0 \leq w_d(t) \perp \lambda_d(t) \geq 0. \end{array}\right. \tag{2.58}$$

with $\Delta\lambda(t) = \lambda(t) - \lambda_d(t)$. Let:

$$p(x, t, \lambda) \triangleq \Delta Ax(t) + \Delta B\lambda(t) + \Delta EK_0e(t) + \Delta EG_0\Delta\lambda(t) + \Delta Eu_d(t)$$

and

$$q(x, t, \lambda) \triangleq \Delta Cx(t) + \Delta D\lambda(t) + \Delta FK_0e(t) + \Delta FG_0\Delta\lambda(t) + \Delta Fu_d(t).$$

Let us now state the stability result.

Proposition 2.4.3. *Let Assumptions 2.1.1, 2.1.2, 2.1.5 hold for the nominal system, and Assumption 2.4.1 hold for the closed-loop system. Let the inequalities*

$$\begin{array}{lll} \Delta A^\top\Lambda_A^{-1}\Delta A \preccurlyeq I_n, & \Delta B^\top\Lambda_B^{-1}\Delta B \preccurlyeq I_m, & \Delta C^\top\Lambda_C^{-1}\Delta C \preccurlyeq I_n \\ \Delta D^\top\Lambda_D^{-1}\Delta D \preccurlyeq I_m, & \Delta E^\top\Lambda_E^{-1}\Delta E \preccurlyeq I_p, & \Delta F\Lambda_F^{-1}\Delta F^\top \preccurlyeq I_m \end{array} \tag{2.59}$$

hold for any $\Lambda_k = \Lambda_k^\top \succ 0$, $k \in \{A, B, C, D, E, F\}$, *and assume there exist* P_0, K_0 *and* G_0 *such that the matrix inequality*

$$\left(\begin{array}{cc|ccccccc} -(M_0)_{11} & -(M_0)_{12} & P_0 & P_0 & K_0^\top & I_n & 0 & 0 & 0 \\ -(M_0)_{12} & -(M_0)_{22} & 0 & 0 & 0 & 0 & G_0^\top & I_m & I_m \\ \hline P_0 & 0 & \Lambda_1^{-1} & 0 & 0 & 0 & 0 & 0 & 0 \\ P_0 & 0 & 0 & \tilde{\Lambda}_1^{-1} & 0 & 0 & 0 & 0 & 0 \\ K_0 & 0 & 0 & 0 & \tilde{\Lambda}_F^{-1} & 0 & 0 & 0 & 0 \\ I_n & 0 & 0 & 0 & 0 & \frac{1}{2}I_n & 0 & 0 & 0 \\ 0 & G_0 & 0 & 0 & 0 & 0 & \tilde{\Lambda}_F^{-1} & 0 & 0 \\ 0 & I_m & 0 & 0 & 0 & 0 & 0 & \Lambda_2^{-1} & 0 \\ 0 & I_m & 0 & 0 & 0 & 0 & 0 & 0 & \tilde{\Lambda}_2^{-1} \end{array}\right) \succ 0 \tag{2.60}$$

and $P_0 = P_0^\top \succ 0$*, with* $\tilde{\Lambda}_F \triangleq I_p + \Lambda_F$, $\tilde{\Lambda}_1 \triangleq \Lambda_A + 2\Lambda_E + \Lambda_B$, $\tilde{\Lambda}_2 \triangleq \Lambda_C + \Lambda_D + 4I_m$*, holds. Then, the solution of the error dynamics in* (2.58) *is globally uniformly ultimately bounded. Note that* $(M_0)_{ij}$ *denotes the element of the matrix* M_0 *in* (2.56) *located at the* i*th row and* j*th column where* $i, j \in \{1, 2\}$*.*

Proof. The derivative of the Lyapunov function candidate $V(t) = e^\top P_0 e$ along the closed-loop trajectories is calculated as follows:

$$\dot{V} = e^\top \left[(A_0 + E_0K_0)^\top P_0 + P_0(A_0 + E_0K_0)\right] e + 2e^\top P_0(B_0 + E_0G_0)\Delta\lambda + 2e^\top P_0 p(x,t,\lambda)$$

In matrix form

$$\dot{V}(t) = \begin{pmatrix} e \\ \Delta\lambda \end{pmatrix}^\top \begin{pmatrix} (A_0 + E_0K_0)^\top P_0 + P_0(A_0 + E_0K_0) & P_0(B_0 + E_0G_0) \\ (B_0 + E_0G_0)^\top P_0 & 0 \end{pmatrix} \begin{pmatrix} e \\ \Delta\lambda \end{pmatrix}$$

$$+2e^\top P_0 p(x,t,\lambda)$$
$$\pm \begin{pmatrix} e \\ \Delta\lambda \end{pmatrix}^\top \begin{pmatrix} 0 & (C_0 + F_0K_0)^\top \\ C_0 + F_0K_0 & D_0 + F_0G_0 + (D_0 + F_0G_0)^\top \end{pmatrix} \begin{pmatrix} e \\ \Delta\lambda \end{pmatrix}$$

The purpose of the $\pm$ term is to obtain the matrix in (2.56) and

$$\begin{pmatrix} e \\ \Delta\lambda \end{pmatrix}^\top \begin{pmatrix} 0 & (C_0 + F_0K_0)^\top \\ C_0 + F_0K_0 & D_0 + F_0G_0 + (D_0 + F_0G_0)^\top \end{pmatrix} \begin{pmatrix} e \\ \Delta\lambda \end{pmatrix} =$$

$$2\Delta\lambda^\top \left[(C_0 + F_0K_0)e + (D_0 + F_0G_0)\Delta\lambda\right] = 2\Delta\lambda^\top(\Delta w - q(x,t,\lambda))$$

Then,

$$\dot{V}(t) = \begin{pmatrix} e \\ \Delta\lambda \end{pmatrix}^\top M_0 \begin{pmatrix} e \\ \Delta\lambda \end{pmatrix} + 2e^\top P_0 p(x,t,\lambda) + 2\Delta\lambda^\top(\Delta w - q(x,\lambda)).$$

Let us substitute the values of p and q and write explicitly the following

$$\begin{aligned} 2e^\top P_0 p(x,t,\lambda) - 2\Delta\lambda^T q(x,\lambda) = \; & 2e^\top P_0[\Delta Ax + \Delta B\lambda + \Delta EK_0 e + \Delta EG_0\Delta\lambda + \Delta Eu_d \\ & \pm \Delta Ax_d \pm \Delta B\lambda_d)] \\ & -2\Delta\lambda^T[\Delta Cx + \Delta D\lambda + \Delta FK_0 e + \Delta FG_0\Delta\lambda \\ & +\Delta Fu_d \pm \Delta Cx_d \pm \Delta D\lambda_d]. \end{aligned}$$

Hence,

$$2e^\top P_0 p(x,t,\lambda) - 2\Delta\lambda^\top q(x,\lambda) =$$

$$\begin{pmatrix} e \\ \Delta\lambda \end{pmatrix}^\top \begin{pmatrix} (\Delta A + \Delta EK_0)^\top P_0 + P_0(\Delta A + \Delta EK_0) & P_0(\Delta B + \Delta EG_0) - (\Delta C + \Delta FK_0)^\top \\ (\Delta B + \Delta EG_0)^\top P_0 - (\Delta C + \Delta FK_0) & -\Delta D - \Delta FG_0 - (\Delta D + \Delta FG_0)^\top \end{pmatrix} \begin{pmatrix} e \\ \Delta\lambda \end{pmatrix}$$

$$+2e^\top P_0(\Delta Ax_d + \Delta B\lambda_d + \Delta Eu_d) - 2\Delta\lambda^\top(\Delta Cx_d + \Delta D\lambda_d + \Delta Fu_d)$$

Let

$$\Delta M_0 \triangleq \begin{pmatrix} -(\Delta A + \Delta EK_0)^\top P_0 - P_0(\Delta A + \Delta EK_0) & -P_0(\Delta B + \Delta EG_0) + (\Delta C + \Delta FK_0)^\top \\ -(\Delta B + \Delta EG_0)^\top P_0 + (\Delta C + \Delta FK_0) & \Delta D + \Delta FG_0 + (\Delta D + \Delta FG_0)^\top \end{pmatrix}$$

Thus,

$$\dot{V} \leq -\begin{pmatrix} e \\ \Delta\lambda \end{pmatrix}^{\top} (-M_0 + \Delta M_0) \begin{pmatrix} e \\ \Delta\lambda \end{pmatrix} + 2e^{\top} P_0(\Delta A x_d + \Delta B \lambda_d + \Delta E u_d)$$

$$-2\Delta\lambda^{\top}(\Delta C x_d + \Delta D \lambda_d + \Delta F u_d)$$

Let $a(t) \triangleq \Delta A x_d + \Delta B \lambda_d + \Delta E u_d$ and $b(t) \triangleq \Delta C x_d + \Delta D \lambda_d + \Delta F u_d$. For any $\Lambda_1^{\top} = \Lambda_1 \succ 0$ and $\Lambda_2^{\top} = \Lambda_2 \succ 0$, it holds that:

$$\left|2e^{\top} P_0 a(t)\right| \leq e^{\top} P_0 \Lambda_1 P_0 e + a^{\top}(t)\Lambda_1^{-1} a(t)$$

$$\left|2\Delta\lambda^{\top} b(t)\right| \leq \Delta\lambda^{\top}\Lambda_2 \Delta\lambda + b^{\top}(t)\Lambda_2^{-1} b(t)$$

So,

$$\dot{V} \leq -z^{\top}\left[-M_0 + \Delta M_0 - \begin{pmatrix} P_0\Lambda_1 P_0 & 0 \\ 0 & \Lambda_2 \end{pmatrix}\right] z + a^{\top}(t)\Lambda_1^{-1} a(t) + b^{\top}(t)\Lambda_2^{-1} b(t)$$

$$\leq -\lambda_{\min}\left[-M_0 + \Delta M_0 - \begin{pmatrix} P_0\Lambda_1 P_0 & 0 \\ 0 & \Lambda_2 \end{pmatrix}\right] \|z\|^2 + \lambda_{\min}^{-1}(\Lambda_1)\|a(t)\|^2 + \lambda_{\min}^{-1}(\Lambda_2)\|b(t)\|^2$$

where $z(t) \triangleq \begin{pmatrix} e \\ \Delta\lambda \end{pmatrix}$. Let us prove that if the conditions, (2.59) and (2.60) hold, then the matrix $-M_0 + \Delta M_0 - \begin{pmatrix} P_0\Lambda_1 P_0 & 0 \\ 0 & \Lambda_2 \end{pmatrix}$ is positive definite. For this purpose, the upper-bounding of ΔM_0 can be done term by term as:

$$\begin{pmatrix} e \\ \Delta\lambda \end{pmatrix}^{\top} \Delta M_0 \begin{pmatrix} e \\ \Delta\lambda \end{pmatrix} = -2e^{\top} P_0(\Delta A + \Delta E K_0)e - 2e^{\top} P_0(\Delta B + \Delta E G_0)\Delta\lambda$$
$$+2e^{\top}(\Delta C + \Delta F K_0)^{\top}\Delta\lambda + 2\Delta\lambda^{\top}(\Delta D + \Delta F G_0)\Delta\lambda$$

Thus, for any $\Lambda_k = \Lambda_k^{\top} \succ 0$, $k \in \{A, B, C, D, E, F\}$, the following hold

- $2e^{\top} P_0(\Delta A + \Delta E K_0)e \geq -e^{\top}\left[P_0(\Lambda_A + \Lambda_E)P_0 + \Delta A^{\top}\Lambda_A^{-1}\Delta A + K_0^{\top}\Delta E^{\top}\Lambda_E^{-1}\Delta E K_0\right] e$
- $2\Delta\lambda^{\top}(\Delta B + \Delta E G_0)^{\top} P_0 e \geq -e^{\top}\left[P_0(\Lambda_B + \Lambda_E)P_0\right] e$
$$-\Delta\lambda^{\top}\left[\Delta B^{\top}\Lambda_B^{-1}\Delta B + G_0^{\top}\Delta E^{\top}\Lambda_E^{-1}\Delta E G_0\right]\Delta\lambda$$
- $2\Delta\lambda^{\top}(\Delta C + \Delta F K_0)e \geq -\Delta\lambda^{\top}\left[\Lambda_C + \Delta F\Lambda_F^{-1}\Delta F^{\top}\right]\Delta\lambda$
$$-e^{\top}\left[\Delta C^{\top}\Lambda_C^{-1}\Delta C + K_0^{\top}\Lambda_F K_0\right] e$$
- $2\Delta\lambda^{\top}(\Delta D + \Delta F G_0)\Delta\lambda \geq -\Delta\lambda^{\top}\left[\Lambda_D + \Delta D^{\top}\Lambda_D^{-1}\Delta D + G_0^{\top}\Lambda_F G_0 + \Delta F\Lambda_F^{-1}\Delta F^{\top}\right]\Delta\lambda$

Assume that the constraints on uncertainties in (2.59) stated in Proposition 2.4.3 are satisfied, then:

$$\begin{pmatrix} e \\ \Delta\lambda \end{pmatrix}^\top \Delta M_0 \begin{pmatrix} e \\ \Delta\lambda \end{pmatrix} \geq - \begin{pmatrix} e \\ \Delta\lambda \end{pmatrix}^\top \begin{pmatrix} P_0\tilde{\Lambda}_1 P_0 + K_0^\top \tilde{\Lambda}_F K_0 + 2I_n & 0 \\ 0 & \tilde{\Lambda}_2 + G_0^\top \tilde{\Lambda}_F G_0 \end{pmatrix} \begin{pmatrix} e \\ \Delta\lambda \end{pmatrix}$$

Thus:

$$z^\top \left[-M_0 + \Delta M_0 - \begin{pmatrix} P_0\Lambda_1 P_0 & 0 \\ 0 & \Lambda_2 \end{pmatrix} \right] z \geq$$

$$z^\top \begin{pmatrix} (-M_0)_{11} - P_0\Lambda_1 P_0 - P_0\tilde{\Lambda}_1 P_0 - K_0^\top \tilde{\Lambda}_F K_0 - 2I_n & -(M_0)_{12} \\ -(M_0)_{12} & -(M_0)_{22} - \tilde{\Lambda}_2 - \Lambda_2 - G_0^\top \tilde{\Lambda}_F G_0 \end{pmatrix} z \tag{2.61}$$

Applying the Schur complement Theorem for positive definiteness [39, Theorem A.65], it is inferred that the matrix obtained in (2.61) is positive definite if and only if the matrix inequality (2.60) in Proposition 2.4.3 holds. The inequality obtained in (2.60) is a bilinear matrix inequality BMI due to the upper-left sub-matrix M_0. Then, in order to solve this inequality, it must be transformed into LMI (see A.1). It follows that

$$M_{0_{lin}} \triangleq - \begin{pmatrix} -Q_0 A_0^\top - Q_0 A_0 - N_0^\top E_0^\top - E_0 N_0 & -B_0 - E_0 G_0 + Q_0 C_0^\top + N_0^\top F_0^\top \\ -B_0^\top - G_0^\top E_0^\top + C_0 Q_0 + F_0 N_0 & D_0 + F_0 G_0 + (D_0 + F_0 G_0)^\top \end{pmatrix} \tag{2.62}$$

with $Q_0 = P_0^{-1}$ and $N_0 = K_0 Q_0$. So, the BMI in (2.60) is written as:

$$\left(\begin{array}{cc|cccccccc} -(M_{0_{lin}})_{11} & -(M_{0_{lin}})_{12} & I_n & I_n & N_0^\top & Q_0 & 0 & 0 & 0 \\ -(M_{0_{lin}})_{21} & -(M_{0_{lin}})_{22} & 0 & 0 & 0 & 0 & G_0^\top & I_m & I_m \\ \hline I_n & 0 & \Lambda_1^{-1} & 0 & 0 & 0 & 0 & 0 & 0 \\ I_n & 0 & 0 & \tilde{\Lambda}_1^{-1} & 0 & 0 & 0 & 0 & 0 \\ N_0 & 0 & 0 & 0 & \tilde{\Lambda}_F^{-1} & 0 & 0 & 0 & 0 \\ Q_0 & 0 & 0 & 0 & 0 & \frac{1}{2} I_n & 0 & 0 & 0 \\ 0 & G_0 & 0 & 0 & 0 & 0 & \tilde{\Lambda}_F^{-1} & 0 & 0 \\ 0 & I_m & 0 & 0 & 0 & 0 & 0 & \Lambda_2^{-1} & 0 \\ 0 & I_m & 0 & 0 & 0 & 0 & 0 & 0 & \tilde{\Lambda}_2^{-1} \end{array} \right) \succ 0 \tag{2.63}$$

where $(M_{0_{lin}})_{ij}$ denotes the element of the matrix $M_{0_{lin}}$ in (2.62) located at the ith row and jth column with $i, j \in \{1, 2\}$. The LMI in (2.63) can be solved, under some conditions, in the new variables $Q_0 = Q_0^\top \succ 0$, N_0 and G_0. Thus, it is possible to say that the inequality: $z^\top \left[-M_0 + \Delta M_0 - \begin{pmatrix} P_0\Lambda_1 P_0 & 0 \\ 0 & \Lambda_2 \end{pmatrix} \right] z \succ 0$ holds. As a consequence of the result obtained about positive definiteness of the matrix obtained in (2.61) and due to symmetry, there exists $\mu > 0$ such that $-\lambda_{\min} \left[M_0 + \Delta - M_0 - \begin{pmatrix} P_0\Lambda_1 P_0 & 0 \\ 0 & \Lambda_2 \end{pmatrix} \right] = -\mu < 0$. According to Assumption 2.1.1 where u_d, x_d and λ_d are bounded, the terms $\|a(t)\|^2$ and $\|b(t)\|^2$ are bounded such that $\|a(t)\|^2 < \beta_1$ and $\|b(t)\|^2 < \beta_2$ for some

β_1,$\beta_2 > 0$. Then, it is inferred that:

$$\begin{aligned}\dot{V} &\leq -\mu\|z\|^2 + \lambda_{\min}^{-1}(\Lambda_1)\beta_1 + \lambda_{\min}^{-1}(\Lambda_2)\beta_2 \\ &\leq -\mu\|e\|^2 - \mu\|\Delta\lambda\|^2 + \lambda_{\min}^{-1}(\Lambda_1)\beta_1 + \lambda_{\min}^{-1}(\Lambda_2)\beta_2 \\ &\leq -\mu\|e\|^2 + \lambda_{\min}^{-1}(\Lambda_1)\beta_1 + \lambda_{\min}^{-1}(\Lambda_2)\beta_2.\end{aligned}$$

It shows that $\dot{V} < 0$ outside the ball $B_r(0) \subset \mathbb{R}^n$, with $r \triangleq \sqrt{\frac{\lambda_{\min}^{-1}(\Lambda_1)\beta_1 + \lambda_{\min}^{-1}(\Lambda_2)\beta_2}{\mu}}$. Then, the solution of (2.58) is GUUB [87, 60]. According to Theorem A.2.1, the ultimate bound with $\alpha_1(\|e\|) = \lambda_{\min}(P_0)\|e\|^2$ and $\alpha_2(\|e\|) = \lambda_{\max}(P_0)\|e\|^2$ is given by

$$\|e\| \leq \alpha_1^{-1}(\alpha_2(r)) = \sqrt{\frac{\lambda_{\max}(P_0)r^2}{\lambda_{\min}(P_0)}} = \sqrt{\frac{\lambda_{\max}(P_0)\left(\lambda_{\min}^{-1}(\Lambda_1)\beta_1 + \lambda_{\min}^{-1}(\Lambda_2)\beta_2\right)}{\lambda_{\min}(P_0)\mu}}$$

□

Notice that under the conditions of the proposition, then $M_0 + \Delta M_0 \succ 0$. This implies that the closed-loop system's quadruple in (2.57) is strongly passive (in other words the uncertainties do not destroy the strong passivity of the nominal closed-loop system). In particular this implies that $D_0 + \Delta D + (F_0 + \Delta F)G_0 \succ 0$. Consequently, Assumption 2.1.1 and item 1 in section 1.2.2 guarantee that the solutions of (2.57) are AC as long as uncertainties are constant matrices. Time-varying uncertainties yield a closed-loop system which can be analyzed along the lines of section 1.2.2.

2.4.3 Relaxing Strong Passivity to Strict State Passivity

It is of interest to relax the strong passivity condition (Assumption 2.1.5) of Proposition 2.4.3, with strict state passivity (Assumption 2.1.4). The strict state passivity BMI in (2.56) modified to $M_0 \preccurlyeq \begin{pmatrix} -\epsilon P_0 & 0 \\ 0 & 0 \end{pmatrix}$. This means that the nominal closed-loop system may have $D_0 + F_0G_0 \succcurlyeq 0$, hence $M_0 \preccurlyeq 0$. Therefore we have to find conditions which guarantee

$$-M_0 + \Delta M_0 - \begin{pmatrix} \epsilon' P_0 & 0 \\ 0 & 0 \end{pmatrix} - \begin{pmatrix} P_0\Lambda_1 P_0 & 0 \\ 0 & \Lambda_2 \end{pmatrix} \succcurlyeq 0 \tag{2.64}$$

for some $0 < \epsilon' < \epsilon$, where M_0 corresponds to the strict state passivity LMI. To this end, we may rely on Lemma A.3.1 in Appendix A.3.

Proposition 2.4.4. *Let Assumptions 2.1.1, 2.1.2, 2.1.4 hold for the nominal system, and Assumption 2.4.1 holds for the closed-loop system. Then the matrix inequality in (2.64) holds if and only if:*

1. $R \triangleq (D_0 + F_0G_0) + (D_0 + F_0G_0)^\top + (\Delta D + \Delta F G_0) + (\Delta D + \Delta F G_0)^\top - \Lambda_2 \succcurlyeq 0$,
2. $Q \triangleq -(A_0 + E_0K_0 + \frac{\epsilon'}{2}I_n)^\top P_0 - P_0(A_0 + E_0K_0 + \frac{\epsilon'}{2}I_n) - (\Delta A + \Delta E K_0)^\top P_0 - P_0(\Delta A + \Delta E K_0) - P_0\Lambda_1 P_0 \succcurlyeq 0$, *with* $-(A_0 + E_0K_0)^\top P_0 - P_0(A_0 + E_0K_0) \succcurlyeq \epsilon P_0$, $\epsilon > \epsilon' > 0$,

3. $\mathrm{Im}(S^\top) \subseteq \mathrm{Im}(R)$, *with* $S \triangleq -P_0(B_0+E_0G_0)+(C_0+F_0K_0)^\top - P_0(\Delta B+\Delta E G_0)+(\Delta C+\Delta F K_0)^\top$,

4. $Q \succcurlyeq SR^\dagger S^\top$.

Proof. Notice that Q and R are symmetric by construction. The proof follows from Lemma A.3.1. □

The tracking error ultimate boundedness can be shown as follows.

Proposition 2.4.5. *Assume that Proposition 2.4.4 holds, then the tracking error e is globally ultimately bounded as:*

$$||e|| \leq \sqrt{\frac{\lambda_{\max}(P_0)\eta_r}{\lambda^2_{\min}(P_0)\epsilon'}} \tag{2.65}$$

where η_r is the upper bound on the positive term $r(t)$, which is defined by the parametric uncertainties as detailed in the proof.

Proof. Under the proposition's assumptions, the rate of change of the Lyapunov function $V(e) = e^\top P_0 e$ where $P_0 = Q_0^{-1}$ is the solution of the strict state passivity LMI $M_{0_{lin}} \preccurlyeq \begin{pmatrix} -\epsilon Q_0 & 0 \\ 0 & 0 \end{pmatrix}$ where $M_{0_{lin}}$ is defined in (2.62) is:

$$\begin{aligned} \dot{V} &\leq -\begin{pmatrix} e \\ \Delta\lambda \end{pmatrix}^\top \left[-M_0 + \Delta M_0 - \begin{pmatrix} P_0\Lambda_1 P_0 & 0 \\ 0 & \Lambda_2 \end{pmatrix} \right] \begin{pmatrix} e \\ \Delta\lambda \end{pmatrix} + \underbrace{a^\top(t)\Lambda_1^{-1}a(t) + b^\top(t)\Lambda_2^{-1}b(t)}_{r(t)} \\ &\leq -\epsilon'\, e^\top P_0 e + r(t) \end{aligned}$$

where $\epsilon' > 0$ and $r(t)$ is a positive bounded term determined by the parametric uncertainties ΔA, ΔB, ΔC, ΔD, ΔE, and ΔF such that $||r(t)|| \leq \eta_r$. So,

$$\dot{V} \leq -\epsilon' \lambda_{\min}(P_0)||e||^2 + \eta_r$$

Hence, the rate of change of the storage function $\dot{V} < 0$ outside the ball $B_r(0) \subset I\!R^n$, with $r \triangleq \sqrt{\frac{\eta_r}{\epsilon'\lambda_{\min}(P_0)}}$. Therefore, the tracking error is GUUB [87, 60] and the expression of the ultimate bound is in (2.65). □

The difference between the case with strong passivity and the case with strict state passivity, is mainly that there is no $-||\Delta\lambda||^2$ that helps to accelerate the convergence in the second case (see (2.4.2)). Moreover, the strong passivity allows us to dispense with strict conditions on the structure of the uncertainties. In a sense, strict state passivity allows us to obtain a more fragile robustness.

It is of interest to analyze under which conditions on the plant's nominal model and on the uncertainties, the conditions in items 1–4 in Proposition 2.4.4 hold. For item 1, assume that $\Delta D = 0$, $\Delta F = 0$, $\Delta C = 0$ (the complementarity constraint has no uncertainty) then we may take $\Lambda_2 = 0$ (since $b(t) = 0$), so that $R \succcurlyeq 0$ by closed-loop strict-state passivity. For item 2, using the fact that $Q_0 \succ 0$, Corollary A.3.4

can be used to derive sufficient condition such that $Q \succ 0$: $\sigma_{\max}(Q_0) > \epsilon\lambda_{\max}(P_0) > 2\sigma_{\max}(P_0)(\sigma_{\max}(\Delta A) + \sigma_{\max}(\Delta E K_0)) + \sigma^2_{\max}(P_0)\sigma_{\max}(\Lambda_1)$, where we used [17, Fact 9.14.15, Corollary 9.6.5]. Let us focus on items 3 and 4. We have $-M_0 = \begin{pmatrix} Q_0 & S_0 \\ S_0^\top & R_0 \end{pmatrix}$, and $-M_0 + \Delta M_0 - \begin{pmatrix} P_0\Lambda_1 P_0 & 0 \\ 0 & \Lambda_2 \end{pmatrix} = \begin{pmatrix} Q_0 + \Delta Q & S_0 + \Delta S \\ S_0^\top + \Delta S^\top & R_0 + \Delta R \end{pmatrix}$, where the matrices stem from (2.56) and items 1, 2 and 3 in Proposition 2.4.4. Using Lemmas A.3.1 and A.3.2, the strict-state passivity LMI for the nominal system implies that $Q_0 \succ Q_0 - \epsilon P_0 \succcurlyeq S_0 R_0^\dagger S_0^\top$, and $\mathrm{Im}(S_0 R_0^\dagger S_0^\top) \subseteq \mathrm{Im}(Q_0 - \epsilon P_0)$ (we also have $\mathrm{Im}(S_0 R_0^\dagger S_0^\top) \subseteq \mathrm{Im}(Q_0) = \mathbb{R}^n$ since strict state passivity implies that $Q_0 \succ 0$), and $\mathrm{Im}(S_0^\top) \subseteq \mathrm{Im}(R_0) = \mathrm{Im}(R_0^\dagger)$ [18, Proposition 8.1.7]. Assume that $\mathrm{Im}(\Delta S^\top) \subseteq \mathrm{Im}(S_0^\top)$, then $\mathrm{Im}(S^\top) = \mathrm{Im}(S_0^\top + \Delta S^\top) \subseteq \mathrm{Im}(S_0^\top)$. Thus, item 3 is satisfied if $\mathrm{Im}(R) = \mathrm{Im}(R_0)$ (which holds if $\Delta D = 0$, $\Delta F = 0$, $\Delta C = 0$, since in this case $\Delta R = 0$). We can therefore state the following:

Lemma 2.4.6. *Let Assumption 2.1.4 hold for the nominal system. Assume that* $\mathrm{Im}(\Delta S^\top) \subseteq \mathrm{Im}(S_0^\top)$*, and that* $\mathrm{Im}(R) = \mathrm{Im}(R_0)$*, then* $\mathrm{Im}(S^\top) \subseteq \mathrm{Im}(R)$*.*

Notice that item 4 is $Q_0 + \Delta Q \succcurlyeq (S_0 + \Delta S)(R_0 + \Delta R)^\dagger(S_0^\top + \Delta S^\top)$. In the next proposition, we derive conditions on the uncertainty matrices that guarantee that the inequality in item 4 holds true when the nominal system is strictly state passive.

Proposition 2.4.7. *Let Assumption 2.1.4 hold for the quadruple* (A_0, B_0, C_0, D_0)*. Assume that: (i)* $R \succcurlyeq 0$*, (ii)* $\mathrm{Im}(\Delta R) \subseteq \mathrm{Im}(R_0)$*, (iii)* $\mathrm{rank}(R_0) = r$*,* $R_0 \neq 0$*,* $\sigma_{\max}(\Delta R) < \sigma_r(R_0)$*, (iv)* $\sigma_{\max}(OT) + \sigma_{\max}(\mathcal{O}((R_0^\dagger \Delta R)^2)) + \sigma_{\max}(\Delta Q) < \epsilon\lambda_{\max}(P_0)$*, where* OT *is in (2.66). Then,* $Q \succcurlyeq S R^\dagger S^\top$*.*

Proof. Since $\Delta R = \Delta R^\top$, using [18, Fact 8.4.3] and [18, Fact 8.4.38] and (ii), we have

$$(R_0 + \Delta R)^\dagger = (I_m + R_0^\dagger \Delta R)^\dagger (R_0^\dagger + R_0^\dagger \Delta R R_0^\dagger)(I_m + \Delta R R_0^\dagger)^\dagger$$

Using Corollary A.3.4, [18, Fact 8.3.33], [18, Corollary 11.6.5], it follows from (iii) that $I_m + R_0^\dagger \Delta R \succ 0$. Thus,

$$(I_m + R_0^\dagger \Delta R)^\dagger = (I_m + R_0^\dagger \Delta R)^{-1} = \sum_{k=0}^{\infty} (-R_0^\dagger \Delta R)^k = I_m - R_0^\dagger \Delta R + \mathcal{O}((R_0^\dagger \Delta R)^2)$$

[18, Proposition 11.3.10]. Therefore,

$$\begin{aligned} (R_0 + \Delta R)^\dagger &= (I_m - R_0^\dagger \Delta R)(R_0^\dagger + R_0^\dagger \Delta R R_0^\dagger)(I_m - \Delta R R_0^\dagger) + \mathcal{O}((R_0^\dagger \Delta R)^2) \\ &= R_0^\dagger - R_0^\dagger \Delta R R_0^\dagger + \mathcal{O}((R_0^\dagger \Delta R)^2) \end{aligned}$$

Consequently,

$$\begin{aligned} (S_0 + \Delta S)(R_0 + \Delta R)^\dagger (S_0^\top + \Delta S^\top) &= (S_0 + \Delta S)(R_0^\dagger - R_0^\dagger \Delta R R_0^\dagger + \mathcal{O}((R_0^\dagger \Delta R)^2))(S_0^\top + \Delta S^\top) \\ &= S_0 R_0^\dagger S_0^\top + OT + \mathcal{O}((R_0^\dagger \Delta R)^2) \end{aligned}$$

where OT stands for other terms defined as:

$$\begin{aligned} OT = \; & S_0R_0^\dagger\Delta S^\top - S_0R_0^\dagger\Delta RR_0^\dagger S_0^\top - S_0R_0^\dagger\Delta RR_0^\dagger\Delta S^\top + \Delta SR_0^\dagger S_0^\top + \Delta SR_0^\dagger\Delta S^\top \\ & -\Delta SR_0^\dagger\Delta RR_0^\dagger S_0^\top - \Delta SR_0^\dagger\Delta RR_0^\dagger\Delta S^\top. \end{aligned} \tag{2.66}$$

The result follows from $Q_0 - S_0R_0^\dagger S_0^\top \succcurlyeq \epsilon P_0$, (iv), Corollary A.3.4 and [18, Fact 11.16.18], which guarantee that $\epsilon P_0 \succ OT - \Delta Q + \mathcal{O}((R_0^\dagger\Delta R)^2)$, so that $Q_0 + \Delta Q \succ (S_0 + \Delta S)(R_0 + \Delta R)^\dagger(S_0^\top + \Delta S^\top)$. □

Item (iv) in Proposition 2.4.7 means that a class of nonzero, sufficiently small uncertainties are allowed. The matrix Λ_1 which appears in ΔQ can be chosen small if ΔA, ΔB, ΔE are small. As said above, ΔR can be made small if the uncertainties inside the complementarity constraints are small. In some cases, there are no uncertainties in the complementarity constraints, see Chapter 4 section 4.5.

Conclusion

This chapter focuses on the trajectory tracking of linear complementarity systems. Passification by feedback and maximal monotonicity are central tools for stability analysis. Systems with and without state jumps, as well as systems with and without parametric uncertainties, are analyzed. To illustrate stability analysis in the presence of state jumps, a simple example is provided. In addition, trajectory tracking in First-order Sweeping Process (FOSwP) is introduced, where LCS with matrix $D = 0$ is represented by a FOSwP under certain conditions.

Chapter 3

Numerical Applications and Simulations

This chapter is dedicated to study various numerical applications based on the theoretical results presented in Chapter 2. The main focus is on electrical circuits with ideal diodes (note that hydraulic circuits share same components where ideal diodes are replaced by check valves [88], hence all what applies to electrical circuits can be transposed to hydraulic circuits). These examples differ by the structure of the matrix D as well as the position and the type of the controller, affecting the passivity of the circuit and leading to possible state jumps. A detailed derivation of the dynamics of the electrical circuits is provided in Appendix D. In addition to the electrical circuits, the chapter also presents examples about networks with unilateral interactions and mechanical system with unilateral spring.

Each example includes numerical simulations which is performed using the INRIA software package SICONOS[1][3]. The algorithm begins with defining the the nominal system to optimize the controller gains by solving the BMI in (4.10) after being transformed into an LMI, according to Appendix A.1 using MOSEK 9.3.14 solver [9]. Then, these control gains are used to define the closed-loop system within SICONOS, more details about modeling and simulating the systems in SICONOS are provided in Appendix C.1.

3.1 Electrical Circuit with Parametric Uncertainties

Consider the circuit in Figure 3.1 with the states x_1: the charge on the capacitor **C** and x_2: the current passing through the inductor **L**. The dynamics of the electrical circuit in Figure 3.1 is given by the system in (3.1):

[1] https://nonsmooth.gricad-pages.univ-grenoble-alpes.fr/siconos/index.html

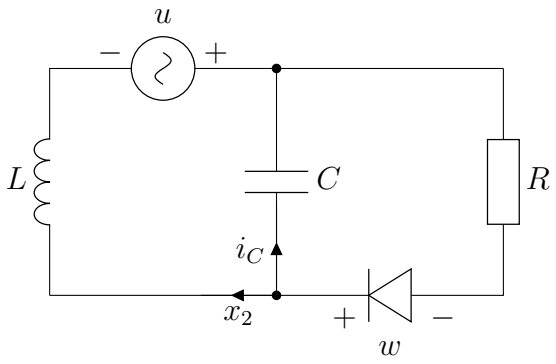

Figure 3.1: RLCD circuit with one ideal diode and voltage sources

$$\begin{cases} \dot{x}_1(t) = -x_2(t) + \lambda(t) \\ \dot{x}_2(t) = \frac{x_1(t)}{\mathbf{LC}} + \frac{u(t)}{\mathbf{L}} \\ 0 \leq \lambda(t) \perp w(t) = \frac{x_1(t)}{\mathbf{C}} + \mathbf{R}\lambda(t) \geq 0 \end{cases} \tag{3.1}$$

with $\mathbf{L} = 1$ H, $\mathbf{C} = 0.025$ F, $\mathbf{R} = 10\ \Omega$.

3.1.1 Open-loop Passivity

The energy stored in the circuit of Figure 3.1 with $u = 0$ is $V(x) = \frac{1}{2}\mathbf{C}\left(\frac{x_1}{\mathbf{C}}\right)^2 + \frac{1}{2}\mathbf{L}x_2^2$. The rate of change in stored energy is given by $\dot{V}(x) = \mathbf{C}\left(\frac{x_1}{\mathbf{C}}\right)\left(\frac{\dot{x}_1}{\mathbf{C}}\right) + \mathbf{L}x_2\dot{x}_2$. If the first two lines of (3.1) are substituted in the equation of $\dot{V}$, then

$$\dot{V}(x) = \mathbf{L}x_2\frac{x_1}{\mathbf{LC}} + \frac{x_1}{\mathbf{C}}(-x_2 + \lambda) = \frac{x_1\lambda}{\mathbf{C}}$$

Knowing that $x_1 = \mathbf{C}V_{\mathbf{C}} = \mathbf{C}(-V_{\mathbf{R}} - V_{\mathbf{D}})$ where $V_{\mathbf{R}}$ and $V_{\mathbf{D}}$ are the voltages across the resistor and the diode respectively, the rate of change of the storage function is represented as follows:

$$\dot{V}(x) = \frac{\lambda}{\mathbf{C}}(-R\lambda - w\lambda) = -\frac{R}{\mathbf{C}}\lambda^2$$

where $w\lambda = 0$ due to orthogonality. So, $\dot{V}(x) \leq 0$ (*i.e.,* the rate of change in stored energy is less than the power supplied to the system). Thus, the dynamical system in (3.1) with $u = 0$ is passive.

Let us check the passivity of (3.1) by proving that its open loop transfer function (*i.e.,* TF with $u = 0$) which is given by $H_0(s) = C(sI - A)^{-1}B + D$ is positive real (see Definition 8 for the relation between positive realness and passivity). Then,

$$H_0(s) = \frac{w(s)}{\lambda(s)} = \frac{\mathbf{RLC}s^2 + \mathbf{L}s + \mathbf{R}}{\mathbf{LC}s^2 + 1}$$

The transfer function H_0 is Hurwitz and $\mathbf{Re}(H_0(j\omega)) = \mathbf{R} > 0$. Then, the transfer function H_0 is strictly positive real [39, Theorem 2.45]. Therefore, the open loop system in (3.1) is strictly passive.

3.1.2 Passivity of the Closed-loop System without Uncertainties

Let $u = K(x - x_d) + G(\lambda - \lambda_d) + u_d$ with $K = \begin{pmatrix} k_1 & k_2 \end{pmatrix}$ and $G = g_1$. In the case of which the system (3.1) has no uncertainties, the control gains are calculated by solving the BMI in (2.7) after being transformed into LMI according to Appendix A.1; the solution is obtained as follows:

$$K = \begin{pmatrix} 493.079 & -42.075 \end{pmatrix}, \quad G = 40.650 \quad \text{and} \quad P = \begin{pmatrix} 40.121 & -3.143 \\ -3.143 & 0.323 \end{pmatrix}$$

If the BMI in (2.7) is solved with the minimum value of the control gain G, then the solution is given by the following:

$$K = \begin{pmatrix} 75.028 & -5.259 \end{pmatrix}, \quad G = -3.9 \times 10^{-13} \quad \text{and} \quad P = \begin{pmatrix} 26.063 & -0.992 \\ -0.992 & 0.257 \end{pmatrix} \tag{3.2}$$

It is observed that the control gain G has a negligible value and this indicates that the additional feedback from the complementarity variable λ is useless in this example. So, in the following, the value of G is neglected.

In order to decrease the magnitude of the control gain K, the steps below are followed knowing that $K = NQ^{-1}$:

- solve the LMI derived from the BMI in (2.7) (see Appendix A.1 for transformation) with $G = 0$ for the minimum Euclidean norm of the matrix N with fixed $Q = P^{-1}$ in (3.2).
- Now, fix the value of N obtained from the previous step and solve the LMI in (2.7) again for the maximum trace of the matrix Q.
- repeat the first two steps until there is no change in the values of N and Q obtained.

This methodology gives the following solution when followed:

$$K = \begin{pmatrix} 38.894 & -2.146 \end{pmatrix}, \quad P = \begin{pmatrix} 10.911 & -0.269 \\ -0.269 & 0.126 \end{pmatrix} \quad \text{and} \quad N = \begin{pmatrix} 3.32 & -9.946 \end{pmatrix}$$

The plots in Figures 3.2 and 3.3 show the numerical simulation for the desired and closed loop system with two different forms of controllers. The initial state vectors are $x(0) = (1, 0)^\top$ and $x_d(0) = (-1.5, 1)^\top$, the time step $h = 10^{-3}$ and the desired input is $u_d(t) = 30 \sin 5t$.

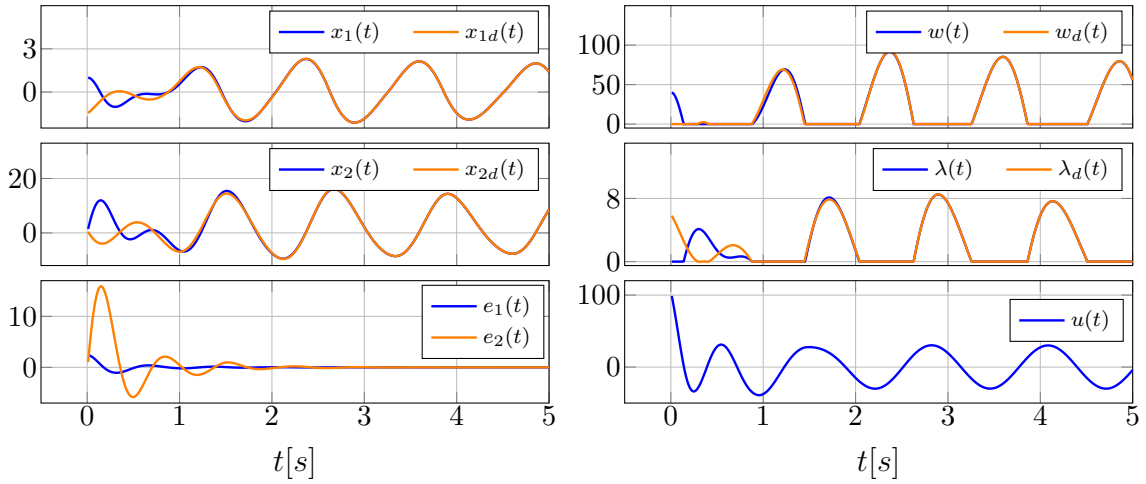

Figure 3.2: Numerical simulation showing the closed-loop system's trajectory x, the desired system's trajectory x_d and the error dynamics $e = x - x_d$ of the LCS in (3.1), without uncertainties. The simulation also presents the controller u with $G = 0$ and the complementarity variables λ and w.

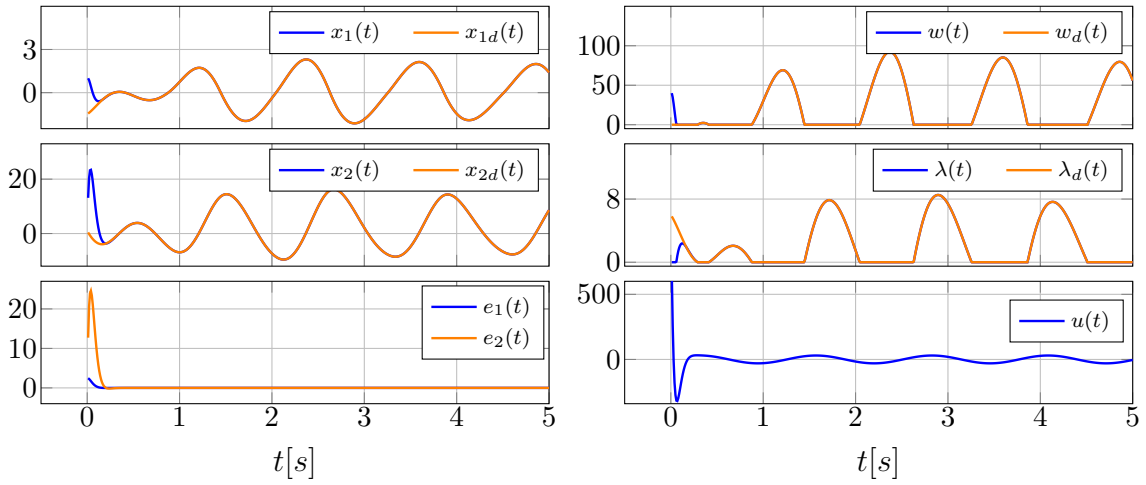

Figure 3.3: Numerical simulation showing the closed-loop system's trajectory x, the desired system's trajectory x_d and the error dynamics $e = x - x_d$ of the LCS in (3.1), without uncertainties. The simulation also presents the controller u with $G = 40.65$ and the complementarity variables λ and w.

In Figures 3.2 and 3.3, L_2 and L_∞ norms of the error between real and desired trajectories are observed at steady state. In Figure 3.2, $\|e_1\|_{[2,3],\infty} = 0.04$ and $\|e_2\|_{[2,3],\infty} = 0.23$ and both values decreases to zero as shown in Figure 3.3. This decrease shows that the transient response takes a shorter time when the controller has an additional feedback from the complementarity variable λ as observed in Figure 3.3 even if it is shown that this additional feedback is useless in the sense of tracking.

3.1.3 Passivity of the Closed-loop System in the Presence of Uncertainties

The uncertainties are introduced to the passive elements **R**, **L** and **C**. The plots below show the numerical simulation for the desired and closed-loop systems. It shows the

trajectories of the systems, the complementarity variables λ and w, and the controller u with different values of bounded uncertainties.
In Figure 3.4, the matrix D is perturbed by ΔD due to disturbance in the resistor $\mathbf{R}$. The perturbation is selected such that ΔD is bounded according to the value of Λ_D defined in (2.59), with $\Delta D = \Delta\mathbf{R}$. For this purpose, the following LMI

$$\left(\begin{array}{cc|cc} (M_{0_{lin}})_{11} & (M_{0_{lin}})_{12} & 0 & 0 \\ (M_{0_{lin}})_{21} & (M_{0_{lin}})_{22} & I_m & I_m \\ \hline 0 & I_m & \Lambda_2^{-1} & 0 \\ 0 & I_m & 0 & \tilde{\Lambda}_2^{-1} \end{array}\right) \succ 0 \tag{3.3}$$

which is a special case of the LMI in (2.63) is solved with $\tilde{\Lambda}_2^{-1} \leq 0.25$ and $\Lambda_2^{-1} \geq 10$; the solution is given as follows:

$$K_0 = \begin{pmatrix} 71.729 & -4.626 \end{pmatrix}, \quad P_0 = \begin{pmatrix} 26.648 & -0.891 \\ -0.891 & 0.257 \end{pmatrix}, \quad \Lambda_2^{-1} = 13.36\ , \quad \tilde{\Lambda}_2^{-1} = 0.15$$

The numerical simulations shown in Figures 3.4 and 3.5 with the initial vectors $x(0) = (1, 0)^\top$ and $x_d(0) = (-1.5, 1)^\top$, the time step $h = 10^{-3}$ and the desired input $u_d(t) = 30 \sin 5t$.

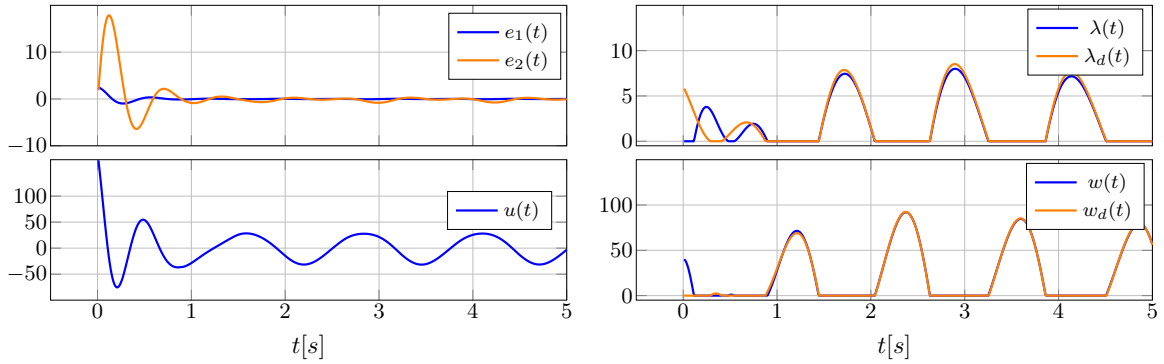

Figure 3.4: Numerical simulation showing the error dynamics $e = x - x_d$ of the LCS in (3.1), with the uncertainty $\Delta D = \Delta\mathbf{R} = \sin 5t$. The simulation also presents the controller u and the complementarity variables λ and w.

Then ΔD is selected such that $|\Delta D| \leq 2.38$ as in Figure 3.4. It is observed that $\|e_1\|_{[4,5],2} = 0.27$ and $\|e_2\|_{[4,5],2} = 3.64$. Also, $\|e_1\|_{[4,5],\infty} = 0.054$, $\|e_2\|_{[4,5],\infty} = 0.75$ and $\|u\|_{[4,5],\infty} = 31.74$. In order to increase the upper bound of ΔD, the constraint on $\tilde{\Lambda}_2^{-1}$ is modified such that $\tilde{\Lambda}_2^{-1} \leq 0.12$. The solutions of the LMI in (3.3) with a new constraint on $\tilde{\Lambda}_2^{-1}$ are given as follows:

$$K_0 = \begin{pmatrix} 83.9 & -4.51 \end{pmatrix}, \quad P_0 = \begin{pmatrix} 30.25 & -0.87 \\ -0.87 & 0.26 \end{pmatrix}, \quad \Lambda_2^{-1} = 13.4\ , \quad \tilde{\Lambda}_2^{-1} = 0.09.$$

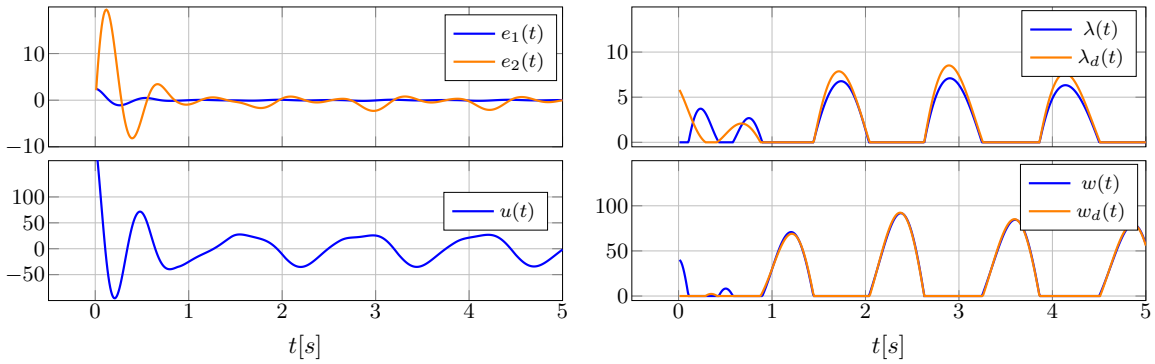

Figure 3.5: Numerical simulation showing the error dynamics $e = x - x_d$ of the LCS in (3.1), with increasing value of uncertainty such that $\Delta D = \Delta\mathbf{R} = 3\sin 5t$. The simulation also presents the controller u and the complementarity variables λ and w.

Then, it is possible to choose ΔD such that $|\Delta D| \leq 3.17$. It is noticeable that a higher control gain K_0 is obtained when the bound of the uncertainty is increased. As the value of ΔD increases, it is noticed in Figure 3.5 that L_2 and L_∞ norms of the error function increase such that $\|e_1\|_{[4,5],2} = 0.67$, $\|e_2\|_{[4,5],2} = 10$, $\|e_1\|_{[4,5],\infty} = 0.13$ and $\|e_2\|_{[4,5],\infty} = 2.08$ with $\|u\|_{[2,3],\infty} = 34.2$.

Let us introduce disturbances in the resistor, the inductor, and the capacitor as $\Delta\mathbf{R}$, $\Delta\mathbf{L}$, and $\Delta\mathbf{C}$ respectively. Thus, the uncertainties are present in the matrices $A = A_0 + \Delta A$, $C = C_0 + \Delta C$, $D = D_0 + \Delta D$ and $E = E_0 + \Delta E$. The controller is designed by calculating K_0 and G_0 such that the quadruple $(A_0 + E_0K_0, B_0 + E_0G_0, C_0, D_0)$ is strongly passive where the control gains are given by the solution of the LMI in (2.63):

$$K_0 = \begin{pmatrix} 34.88 & -10.52 \end{pmatrix}, \; G_0 = 2.686, \; P_0 = \begin{pmatrix} 58.187 & -4.671 \\ -4.671 & 1.374 \end{pmatrix}, \; \tilde{\Lambda}_1^{-1} = \begin{pmatrix} 18 & 0.195 \\ 0.195 & 7.74 \end{pmatrix}$$

$$\tilde{\Lambda}_2^{-1} = 0.101, \quad \Lambda_1^{-1} = \begin{pmatrix} 15.635 & 0.16 \\ 0.16 & 7.2 \end{pmatrix} \quad \text{and} \quad \Lambda_2^{-1} = 15.54$$

and the bounds of the uncertainties are calculated according to the values of $\tilde{\Lambda}_1^{-1}$ and $\tilde{\Lambda}_2^{-1}$.

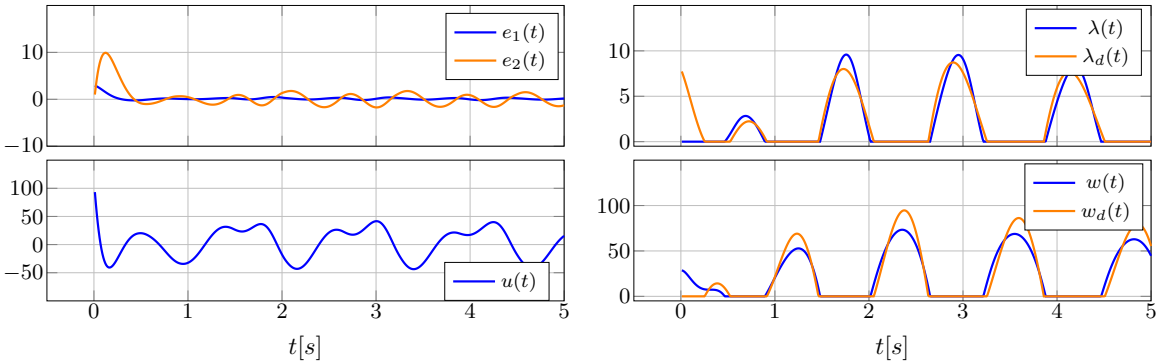

Figure 3.6: Numerical simulation showing the error dynamics $e = x - x_d$ of the LCS in (3.1), with the parametric uncertainties $\Delta\mathbf{R} = 2\sin 5t$, $\Delta\mathbf{L} = 0.02$, and $\Delta\mathbf{C} = 0.01\cos 5t$. The simulation also presents the controller u and the complementarity variables λ and w.

The plot in Figure 3.6 shows the numerical simulation of the error $e(t) = x(t) - x_d(t)$, and the complementarity variables. The initial state vectors are $x(0) = (1, 0)^\top$ and $x_d(0) = (-2, 1)^\top$, the time step $h = 10^{-3}$ and the desired input is $u_d(t) = 30 \sin 5t$. The values of L_2 norm of the error function are $\|e_1\|_{[4,5],2} = 1.65$ and $\|e_2\|_{[4,5],2} = 10.7$ and that of L_∞ norm are $\|e_1\|_{[4,5],\infty} = 0.34$ and $\|e_2\|_{[4,5],\infty} = 1.6$.

In this section, strong passivity, which is a crucial property to prove stability in the presence of uncertainties, is achieved without the need of additional feedback from λ (*i.e.*, $G = 0$). The results presented confirm that of Proposition 2.4.3. It is noticeable that adding uncertainties in more matrices complicates the LMI to be solved and that the bound of the error increases with larger values of uncertainties or when it is presented in more matrices.

3.2 Enhancing Electrical Circuit Passivity through Current Source Integration

In this section, we explore how changing the type of the controller in electrical circuits (current source or voltage source) can affect the passivity of the circuit, with detailed examination for each approach.

3.2.1 Passivity Analysis with Voltage Sources: Motivation

Consider the circuit depicted in Figure 3.7, with the states x_1 which is the charge on capacitor $\mathbf{C}$ and x_2 is the current passing through the inductor $\mathbf{L}$.

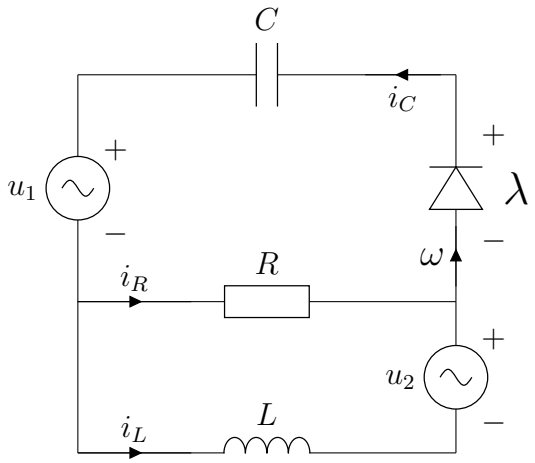

Figure 3.7: RLCD circuit with one ideal diode and voltage sources

$$\begin{cases} \dot{x}_1(t) = -\frac{x_1(t)}{\mathbf{RC}} + x_2(t) + \frac{1}{\mathbf{R}}\lambda(t) - \frac{1}{\mathbf{R}}u_1(t) \\ \dot{x}_2(t) = -\frac{x_1(t)}{\mathbf{LC}} + \frac{1}{\mathbf{L}}\lambda(t) - \frac{1}{\mathbf{L}}u_1(t) - \frac{1}{\mathbf{L}}u_2(t) \\ 0 \leq \lambda(t) \perp w(t) = -\frac{x_1(t)}{\mathbf{RC}} + x_2(t) + \frac{1}{\mathbf{R}}\lambda(t) - \frac{1}{\mathbf{R}}u_1(t) \geq 0 \end{cases} \tag{3.4}$$

Take $\mathbf{L} = 1H$, $\mathbf{C} = 0.025F$ and $\mathbf{R} = 10\Omega$. Let us begin with studying the passivity of the open loop system. So, it is required to check passivity of the quadruple (A, B, C, D) with $u_1 = u_2 = 0$ by checking the positive realness of the transfer function (see Definition 8 for the relation between positive realness and passivity):

$$H_0(s) = \frac{w(s)}{\lambda(s)} = \frac{s^2 + \frac{\mathbf{R}}{\mathbf{L}}s}{\mathbf{R}s^2 + \frac{1}{\mathbf{C}}s + \frac{\mathbf{R}}{\mathbf{LC}}}$$

where $H(s) = C(sI - A)^{-1}B + D$. The Nyquist plot of $H(s)$ lies in the closed right-half plane (see Figure 3.8), which is consistent with positive-real systems theory.

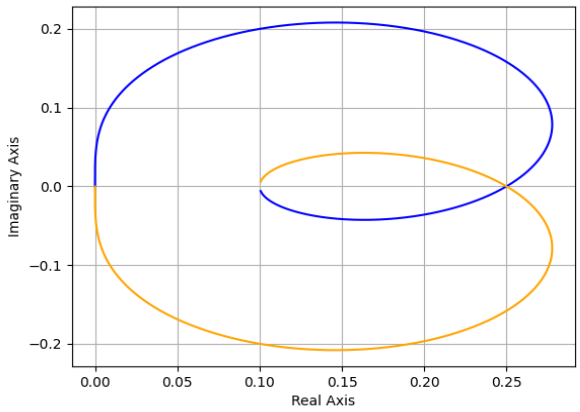

Figure 3.8: Nyquist Diagram

Then, from minimality and the KYP Lemma [39], the quadruple (A, B, C, D) is passive. The storage function of the circuit of Figure 3.7 with $u = 0$ is: $V(x) = \frac{1}{2}\mathbf{C}\left(\frac{x_1}{\mathbf{C}}\right)^2 + \frac{1}{2}\mathbf{L}x_2^2$. It follows that:

$$\dot{V}(x) = -\frac{x_1^2}{\mathbf{RC}^2} + \lambda\left(x_2 + \frac{x_1}{\mathbf{RC}}\right)$$

Due to complementarity conditions between λ and w, we have:

- If $\lambda = 0$, then $\dot{V}(x) = -\frac{x_1^2}{\mathbf{RC}^2} \leq 0$.
- If $\lambda > 0$, then $w = 0$ and $\lambda = \frac{x_1}{\mathbf{C}} - \mathbf{R}x_2$. Hence, $\dot{V}(x) = -\mathbf{R}x_2^2 \leq 0$.

Thus, the storage function of the circuit of Figure 3.7 with $u = 0$ is nonincreasing. Take $u = u_1$ and $u_2 = 0$, then the transfer function of the closed-loop system is: $H_1(s) = [C + FK][sI - (A + EK)]^{-1}[B + EG] + D + FG$. Knowing that $u = K[x - x_d] + G[\lambda - \lambda_d] + u_d$ with $K = \begin{pmatrix} k_1 & k_2 \end{pmatrix}$ and $G = g$, the following is obtained:

$$H_1(s) = \frac{w(s)}{\lambda(s)} = (1 - g)\frac{\mathbf{LC}s^2 + \mathbf{RC}s}{\mathbf{RLC}s^2 + (\mathbf{L} + k_1\mathbf{LC} + k_2\mathbf{RC})s + k_1\mathbf{RC} + \mathbf{R}} \tag{3.5}$$

Let us consider $u_1 = 0$ and $u = u_2$. The transfer function of the systems is represented as follows:

$$H_2(s) = \frac{w(s)}{\lambda(s)} = \frac{\mathbf{LC}s^2 + (k_2\mathbf{C} + \mathbf{RC} - g\mathbf{RC})s}{\mathbf{RLC}s^2 + (k_2\mathbf{RC} + \mathbf{L})s + k_2 + k_1\mathbf{RC} + \mathbf{R}} \tag{3.6}$$

If $u = (u_1, u_2)^\top$ with $K = \begin{pmatrix} k_1 & k_2 \\ k_3 & k_4 \end{pmatrix}$ and $G = \begin{pmatrix} g_1 \\ g_2 \end{pmatrix}$, then the transfer function of the system is represented as follows:

$$H_3(s) = \frac{w(s)}{\lambda(s)} = \frac{(1-g_1)(\mathbf{LC}s^2 + [(k_2+k_4)\mathbf{C} - g_2(\mathbf{RC}+k_2\mathbf{C})]s)}{\mathbf{RLC}s^2 + [\mathbf{RC}(k_2+k_4) + \mathbf{L} + k_1\mathbf{LC}]s + \mathbf{RC}(k_1+k_3) + \mathbf{C}(k_1k_4+k_2k_3) + \mathbf{R} + k_4} \tag{3.7}$$

We can see from (3.5), (3.6) and (3.7) that the transfer functions of the closed loop system cannot be made strictly positive real, thus the circuit shown in Figure 3.7 cannot be made strictly passive with u_1 and u_2 of the general form $u = K[x - x_d] + G[\lambda - \lambda_d] + u_d$. In terms of zero dynamics of the closed-loop system, when $w = 0$, there is always one zero at zero (i.e $\dot{x}_1 = 0$).

3.2.2 Passivity Analysis with Current Source

The problem that appeared in section 3.2.1, which states that the system in (3.4) cannot be made strictly state passive even with $u = (u_1, u_2)^\top$ motivates us to change the type and the connection of the controller for the circuit of Figure 3.7. If the controller is implemented as a current source connected in parallel with the capacitor, then the following is obtained:

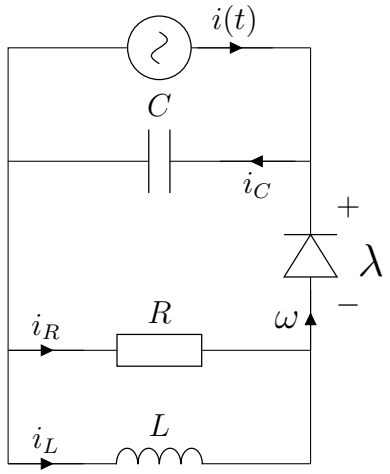

Figure 3.9: RLCD circuit with current source

Let $i(t) \triangleq u(t)$ and $i_d(t) \triangleq u_d(t)$ be the controller and the desired controller respectively. The dynamics are represented as follows:

$$\begin{cases} \dot{x}_1(t) = -\frac{x_1(t)}{\mathbf{RC}} + x_2(t) + \frac{1}{\mathbf{R}}\lambda(t) + u(t) \\ \dot{x}_2(t) = -\frac{x_1(t)}{\mathbf{LC}} + \frac{1}{\mathbf{L}}\lambda(t) \\ 0 \le \lambda(t) \perp w(t) = -\frac{x_1(t)}{\mathbf{RC}} + x_2(t) + \frac{1}{\mathbf{R}}\lambda(t) \ge 0 \end{cases} \tag{3.8}$$

If $u(t) = K[x - x_d] + u_d(t)$, then the transfer function of the closed loop system is: $H_4(s) = C[sI - (A + EK)]^{-1}B + D$ and represented as follows:

$$H_4(s) = \frac{\mathbf{LC}s^2 + (\mathbf{RC} - k_1\mathbf{LC})s - k_1\mathbf{RC}}{\mathbf{RLC}s^2 + (\mathbf{L} - k_1\mathbf{RLC})s + \mathbf{R} + k_2\mathbf{R}} \tag{3.9}$$

It is noticeable that the zeros of the transfer function are replaced by the feedback controller designed and implemented in the RLCD circuit as shown in Figure 3.9. This is observed through the zero dynamics of the system presented in (3.8). If $w = 0$, then $\dot{x}_1 = u$ which means that the zero dynamics is set in the desired place using the feedback controller.

Proposition 3.2.1. *The transfer function in (3.9) is strongly strictly positive real (SSPR) if and only if there exists* $K = \begin{pmatrix} k_1 & k_2 \end{pmatrix}$ *such that*

- $k_1 < 0$
- $k_2 \in \Big]-1,\ k_1(k_1\boldsymbol{LC} - \frac{\boldsymbol{L}}{\boldsymbol{R}} - 2\boldsymbol{RC}) + 2\sqrt{-k_1^3\boldsymbol{RLC}^2 + k_1^2\boldsymbol{LC} - k_1\boldsymbol{R}^2\boldsymbol{C} - k_1\boldsymbol{R}}\Big[$

Proof. In order to check the strong strict positive realness of the transfer function $H_4(s)$, it is required to present the transfer function in its frequency domain as $H_4(j\omega) = \mathbf{Re}[H_4(j\omega)] + \mathbf{Im}[H_4(j\omega)]$ such that:

$$\mathbf{Re}[H_4(j\omega)] = \frac{\mathbf{RL}^2\mathbf{C}^2\omega^4 + (-k_2\mathbf{RLC} + k_1^2\mathbf{RL}^2\mathbf{C}^2 - k_1\mathbf{L}^2\mathbf{C})\omega^2 - k_1\mathbf{R}^2\mathbf{C}(1+k_2)}{(-\mathbf{RLC}\omega^2 + \mathbf{R} + k_2\mathbf{R})^2 + (\mathbf{L} - k_1\mathbf{RLC})^2\omega^2} \tag{3.10}$$

$$\mathbf{Im}[H_4(j\omega)] = j\frac{(\mathbf{L}^2\mathbf{C} - \mathbf{R}^2\mathbf{LC}^2)\omega^3 + (\mathbf{R}^2\mathbf{C} + k_2\mathbf{R}^2\mathbf{C} - k_1^2\mathbf{R}^2\mathbf{LC}^2 - k_1k_2\mathbf{RLC})\omega}{(-\mathbf{RLC}\omega^2 + \mathbf{R} + k_2\mathbf{R})^2 + (\mathbf{L} - k_1\mathbf{RLC})^2\omega^2} \tag{3.11}$$

The transfer function $H_4(s)$ is strongly strictly positive real if and only if the following conditions are satisfied [39, Definition 2.78]:

- $H_4(s)$ is Hurwitz,
- $\mathbf{Re}[H_4(j\omega)] \geq \delta > 0 \quad$ for all $\omega \in [-\infty, \infty]$ and some $\delta \in \mathbb{R}$.

The transfer function $H_4(s)$ is Hurwitz if the poles of H_4 have real part in the open left half-plane (LHP). The quadratic function: $\mathbf{RLC}s^2 + (\mathbf{L} - k_1\mathbf{RLC})s + \mathbf{R} + k_2\mathbf{R}$ has roots with negative real part if and only if k_1 and k_2 satisfy:

- $1 + k_2 > 0$
- $\mathbf{L} - k_1\mathbf{RLC} > 0$

The function $\mathbf{Re}[H_4(jw)] \geq \delta > 0$ if and only if the function $g(\omega) \triangleq \mathbf{RL}^2\mathbf{C}^2\omega^4 + (-k_2\mathbf{RLC} + k_1^2\mathbf{RL}^2\mathbf{C}^2 - k_1\mathbf{L}^2\mathbf{C})\omega^2 - k_1\mathbf{R}^2\mathbf{C}(1+k_2)$ has a global minimum at $\omega = \omega_0$ such that $g(\omega_0) > 0$. Knowing that $1 + k_2 > 0$, it is necessary to have:

$$-k_1\mathbf{R}^2\mathbf{C}(1+k_2) > 0 \quad \Rightarrow \quad k_1 < 0 \tag{3.12}$$

so that the function $g(0) > 0$. The minimum of $g(\omega)$ is studied as follows:

$$\frac{\partial g}{\partial \omega}(\omega) = 4\mathbf{RL}^2\mathbf{C}^2\omega^3 + 2(-k_2\mathbf{RLC} + k_1^2\mathbf{RL}^2\mathbf{C}^2 - k_1\mathbf{L}^2\mathbf{C})\omega$$

At this step, there are two cases:

First case: If

$$-k_2\mathbf{RLC} + k_1^2\mathbf{RL}^2\mathbf{C}^2 - k_1\mathbf{L}^2\mathbf{C} > 0 \quad \Leftrightarrow \quad k_2 < k_1\frac{\mathbf{L}}{\mathbf{R}}\left(k_1\mathbf{RC} - 1\right)$$

then the function $g(\omega)$ is convex and has a global minimum at $\omega = 0$ where $\frac{\partial g}{\partial \omega}(0) = 0$. The function $g(\omega) > 0\ \forall \omega \in [-\infty, +\infty]$ if and only if the following holds:

$$g(0) = -k_1\mathbf{R}^2\mathbf{C}(1 + k_2) > 0 \quad \Leftrightarrow \quad k_1 < 0$$

Second case: If

$$-k_2\mathbf{RLC} + k_1^2\mathbf{RL}^2\mathbf{C}^2 - k_1\mathbf{L}^2\mathbf{C} < 0 \quad \Leftrightarrow \quad k_2 > k_1\frac{\mathbf{L}}{\mathbf{R}}\left(k_1\mathbf{RC} - 1\right) \tag{3.13}$$

then the roots of $\frac{\partial g}{\partial \omega}(\omega)$ are: $\omega_1 = 0$ and $\omega_{2,3} = \pm\sqrt{-\frac{-k_2\mathbf{RLC} + k_1^2\mathbf{RL}^2\mathbf{C}^2 - k_1\mathbf{L}^2\mathbf{C}}{2\mathbf{RL}^2\mathbf{C}^2}}$. The second derivative of $g(\omega)$ is:

$$\frac{\partial^2 g}{\partial \omega^2}(\omega) = 12\mathbf{RL}^2\mathbf{C}^2\omega^2 + 2(-k_2\mathbf{RLC} + k_1^2\mathbf{RL}^2\mathbf{C}^2 - k_1\mathbf{L}^2\mathbf{C})$$

The value of $\frac{\partial^2 g}{\partial \omega^2}(\omega_{2,3}) = -4(-k_2\mathbf{RLC} + k_1^2\mathbf{RL}^2\mathbf{C}^2 - k_1\mathbf{L}^2\mathbf{C}) > 0$. So, the function $g(\omega)$ has global minima at $\omega = \pm\sqrt{-\frac{-k_2\mathbf{RLC} + k_1^2\mathbf{RL}^2\mathbf{C}^2 - k_1\mathbf{L}^2\mathbf{C}}{2\mathbf{RL}^2\mathbf{C}^2}}$. The value of $g(\omega_{2,3})$ must be positive. It follows that:

$$g(\omega_{2,3}) = \frac{-(-k_2\mathbf{RLC} + k_1^2\mathbf{RL}^2\mathbf{C}^2 - k_1\mathbf{L}^2\mathbf{C})^2 + 4\mathbf{RL}^2\mathbf{C}^2(-k_1\mathbf{R}^2\mathbf{C}(1 + k_2))}{4\mathbf{RL}^2\mathbf{C}^2} > 0 \tag{3.14}$$

Then,

$$-\frac{\mathbf{R}}{4}k_2^2 + k_2\left(k_1^2\frac{\mathbf{RLC}}{2} - k_1\frac{\mathbf{L}}{2} - k_1\mathbf{R}^2\mathbf{C}\right) - k_1^4\frac{\mathbf{RL}^2\mathbf{C}^2}{4} + k_1^3\frac{\mathbf{L}^2\mathbf{C}}{2} - k_1^2\frac{\mathbf{L}^2}{4\mathbf{R}} - k_1\mathbf{R}^2\mathbf{C} > 0 \tag{3.15}$$

The function $g(\omega_{2,3})$ in (3.15) is a concave function in k_2 with the discriminant:

$$\Delta = 16\mathbf{R}^4\mathbf{C}(-k_1^3\mathbf{RLC} + k_1^2\mathbf{L} + k_1^2\mathbf{R}^2\mathbf{C} - k_1\mathbf{R}) > 0 \ \text{ since } \ k_1 < 0$$

The roots of the quadratic function $h(k_2)$ are:

$$k_{2_1} = k_1^2\mathbf{LC} - k_1(\frac{\mathbf{L}}{\mathbf{R}} + 2\mathbf{RC}) + 2\sqrt{-k_1^3\mathbf{RLC}^2 + k_1^2\mathbf{LC} - k_1\mathbf{R}^2\mathbf{C} - k_1\mathbf{R}}$$

or

$$k_{2_2} = k_1^2\mathbf{LC} - k_1(\frac{\mathbf{L}}{\mathbf{R}} + 2\mathbf{RC}) - 2\sqrt{-k_1^3\mathbf{RLC}^2 + k_1^2\mathbf{LC} - k_1\mathbf{R}^2\mathbf{C} - k_1\mathbf{R}}$$

So, the function $h(k_2)$ is positive if and only if $k_{2_2} < k_2 < k_{2_1}$. Hence, the function $g(\omega)$, in this case, is positive, if and only if the conditions (3.12),(3.13) and (3.14) are satisfied.

It is noteworthy that if $k_2 = k_1\frac{\mathbf{L}}{\mathbf{R}}\left(k_1\mathbf{RC} - 1\right)$, then:

$$\mathbf{RL}^2\mathbf{C}^2\omega^4 - k_1\mathbf{R}^2\mathbf{C}\left(1 + k_1^2\mathbf{LC} - k_1\frac{\mathbf{L}}{\mathbf{R}}\right) > 0 \ \ \forall \omega \in [-\infty, +\infty]$$

□

If the transfer function in (3.9) is SSPR for k_1 and k_2 satisfying Proposition 3.2.1, then the BMI in (2.7) always has a solution. Thus, the system is strongly passive.
Let us check strong passivity by solving the LMI derived from the BMI in (2.7) (see Appendix A.1). Take $\mathbf{L} = 1$ H, $\mathbf{C} = 0.025$ F, and $\mathbf{R} = 10\ \Omega$. The solution is shown below:

$$K = \begin{pmatrix} -11.7802 & 0.5488 \end{pmatrix} \quad \text{and} \quad P = \begin{pmatrix} 27.6522 & -0.2693 \\ -0.2693 & 0.9959 \end{pmatrix}$$

Using the given values of $\mathbf{L}$, $\mathbf{R}$, $\mathbf{C}$ and K parameters, the plot of $\mathbf{Re}[H_4(j\omega)]$ in (3.10) is depicted in the following figure:

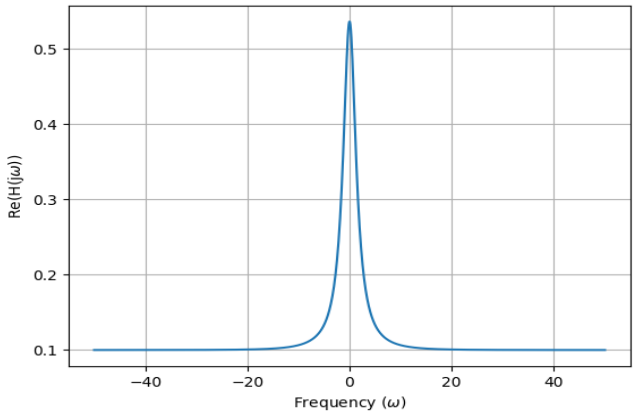

Figure 3.10: Graphical representation of (3.10) with given parameters

which shows that $\mathbf{Re}[H_4(j\omega)] \geq \delta > 0$ with $\delta = \mathbf{Re}[H_4(j\infty)] = \frac{1}{\mathbf{R}} = 0.1$. After designing the controller, the simulation of the system is performed with the desired current source $u_d = 30 \sin 5t$ and the initial state vectors are $x(0) = \begin{pmatrix} -5 & 1 \end{pmatrix}^\top$ and $x_d(0) = \begin{pmatrix} -3 & -1 \end{pmatrix}^\top$ with the time step $h = 10^{-2}$.

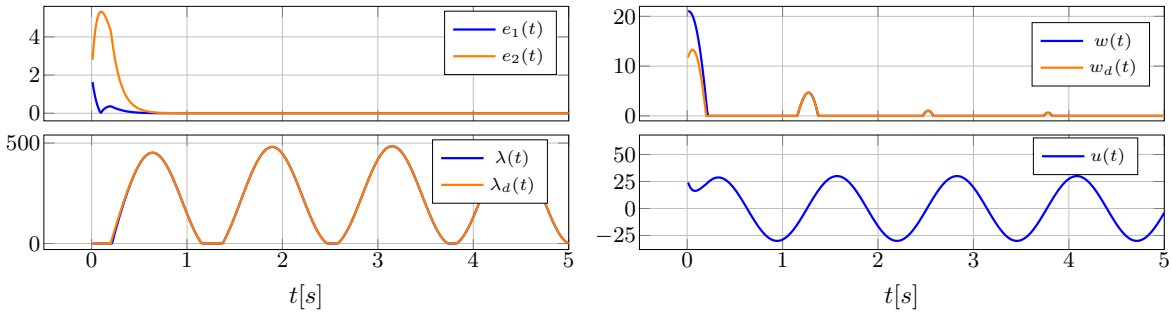

Figure 3.11: Numerical simulation showing the error dynamics $e = x - x_d$ of the LCS in (3.8). The simulation also presents the controller u and the complementarity variables λ and w.

It is shown in Figure 3.11 that the error converges to zero quickly. Consequently, the controller $u = K(x - x_d) + u_d$ converges to the sinusoidal function $u_d(t)$. Additionally, the error between the real and the desired complementarity variables converges to zero as well.

In this section, simply having more controllers (*i.e.*, two voltage sources) as in the circuit of Figure 3.7 didn't ensure the strict state passivity of the system. However, by changing the type of the controller (*i.e.*, one current source) as in the circuit of Figure 3.9, strict state passivity is achieved.

3.3 Electrical Circuits with Possible State Jumps

In this section, some electrical circuits that may possess state jumps ($D = 0$ or $D \succeq 0$) are introduced. The main property in order to be able to analyse state jumps is strict state passivity which is studied for each circuit introduced.

3.3.1 Building Strictly State Passive Circuit

The circuits of the foregoing section have the matrix $D = D^\top \succeq 0$ which gives the possibility of having state jumps according to section 2.1.3. Let x_1, x_2, x_3 and x_4 be the voltages across the capacitors $\mathbf{C}_1$, $\mathbf{C}_2$, $\mathbf{C}_3$ and $\mathbf{C}_4$ respectively. Take $\mathbf{C}_1 = \mathbf{C}_2 = \mathbf{C}_3 = \mathbf{C}_4 = \mathbf{C}$ and $\mathbf{C} = 0.025$ F, $\mathbf{R} = 10\ \Omega$. Consider the circuit of Figure 3.12 with its dynamics in (3.16)

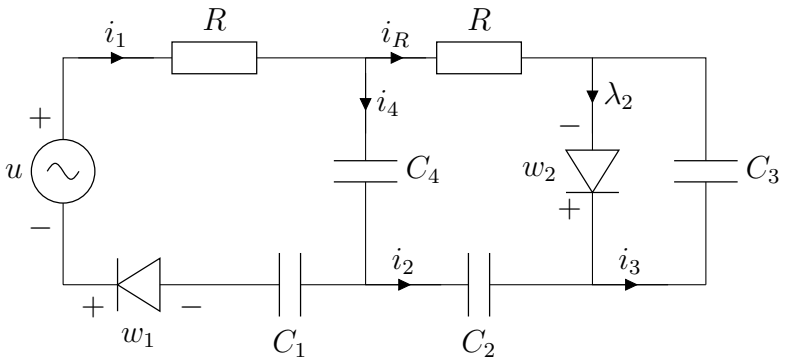

Figure 3.12: RC circuit with two ideal diodes

$$
\begin{cases}
\begin{pmatrix}\dot{x}_1(t)\\ \dot{x}_2(t)\\ \dot{x}_3(t)\\ \dot{x}_4(t)\end{pmatrix} = \underbrace{\begin{pmatrix}0 & 0 & 0 & 0\\ 0 & -\frac{1}{\mathbf{RC}} & -\frac{1}{\mathbf{RC}} & -\frac{1}{\mathbf{RC}}\\ 0 & -\frac{1}{\mathbf{RC}} & -\frac{1}{\mathbf{RC}} & -\frac{1}{\mathbf{RC}}\\ 0 & -\frac{1}{\mathbf{RC}} & -\frac{1}{\mathbf{RC}} & -\frac{1}{\mathbf{RC}}\end{pmatrix}}_{\triangleq A}\begin{pmatrix}x_1(t)\\ x_2(t)\\ x_3(t)\\ x_4(t)\end{pmatrix} + \underbrace{\begin{pmatrix}\frac{1}{\mathbf{C}} & 0\\ 0 & 0\\ 0 & \frac{1}{\mathbf{C}}\\ \frac{1}{\mathbf{C}} & 0\end{pmatrix}}_{\triangleq B}\begin{pmatrix}\lambda_1(t)\\ \lambda_2(t)\end{pmatrix}\\
0 \leq \begin{pmatrix}\lambda_1(t)\\ \lambda_2(t)\end{pmatrix} \perp \begin{pmatrix}w_1(t)\\ w_2(t)\end{pmatrix} = \underbrace{\begin{pmatrix}1 & 0 & 0 & 1\\ 0 & 0 & 1 & 0\end{pmatrix}}_{\triangleq C}\begin{pmatrix}x_1(t)\\ x_2(t)\\ x_3(t)\\ x_4(t)\end{pmatrix} + \underbrace{\begin{pmatrix}\mathbf{R} & 0\\ 0 & 0\end{pmatrix}}_{\triangleq D}\begin{pmatrix}\lambda_1(t)\\ \lambda_2(t)\end{pmatrix}\\
\qquad + \begin{pmatrix}-1\\ 0\end{pmatrix} u \geq 0
\end{cases}
\tag{3.16}
$$

Motivation

In order to study the trajectory tracking in the presence of state jumps, it is required to have strict state passivity of the closed-loop LCS according to section 2.1.3. Note that there exists $P \succeq 0$ such that the open-loop system's quadruple (A, B, C, D) of (3.16) is passive (i.e the LMI in (1.8) has a solution).

In order to check the strict state passivity of the closed-loop system's quadruple $(A, B, C + FK, D)$ with the controller $u = K(x - x_d) + u_d$, let us observe the strict positive realness (SPR) of the transfer function matrix (see Definition 8 for the relation between positive realness and passivity). Given that $K = \begin{pmatrix}k_1 & k_2 & k_3 & k_4\end{pmatrix}$, then

$$
G(s) = \begin{pmatrix}
\frac{\mathbf{R}^2\mathbf{C}s^4 + s^3(5\mathbf{R} - k_1\mathbf{R} - k_4\mathbf{R}) + \frac{s^2}{\mathbf{C}}(-3k_1 + k_2 + k_3 - 2k_4 + 5)}{\mathbf{RC}s^4 + 3s^3} & \frac{k_3\mathbf{RC}s^3 + s^2(k_2 + 2k_3 + k_4 - 1)}{\mathbf{RC}^2s^4 + 3\mathbf{C}s^3}\\
\frac{-s^2}{\mathbf{RC}^2s^4 + 3\mathbf{C}s^3} & \frac{\mathbf{R}s^3 + \frac{2s^2}{\mathbf{C}}}{\mathbf{RC}s^4 + 3s^3}
\end{pmatrix}
\tag{3.17}
$$

where $G(s) \triangleq \begin{pmatrix}G_{11}(s) & G_{12}(s)\\ G_{21}(s) & G_{22}(s)\end{pmatrix} \triangleq \begin{pmatrix}\frac{w_1}{\lambda_1} & \frac{w_1}{\lambda_2}\\ \frac{w_2}{\lambda_1} & \frac{w_2}{\lambda_2}\end{pmatrix}$.

In view of the matrix of the transfer functions in (3.17), it is noticeable that the transfer function is not Hurwitz, hence not strictly positive real due to the pole at zero of multiplicity 3. This pole at zero persists even if the controller is extended by considering another feedback from λ such that $u = K(x - x_d) + G(\lambda - \lambda_d) + u_d$ where $G = \begin{pmatrix}g_1 & g_2\end{pmatrix}$.

Remark 3.3.1. *According to [39, Definition 2.70], all the principal sub-matrices of the transfer function matrix G_{11}, G_{22} and $|G_{11} * G_{22} - G_{21} * G_{12}|$ are of index $= 1$ (i.e all the principal sub-matrices are proper). So, the transfer matrix $G(s)$ is totally index 1. As well, according to [39, Proposition 2.71], the transfer matrix G(s) (3.17) is totally*

of index 1 *knowing that* (A, B, C, D) *is passive,* (A, B) *is controllable and the matrix* $\begin{pmatrix} B \\ D + D^\top \end{pmatrix}$ *has full column rank.*

Thus, the electrical circuit of Figure 3.12 is not strictly state passive (SSP) under the control input $u(t)$ and we cannot analyze the stability of the error dynamics $e = x - x_d$ in the presence of state jumps. This result motivates us to build a strictly state passive electrical circuit from that in Figure 3.12 using two different approaches as discussed in the following sections.

First approach: adding resistors for passivity

In the case of state jumps, strict state passivity is sufficient condition for stability analysis. The aim is to find a strictly state passive circuit with a matrix $D \succeq 0$. One approach would be adding proper resistors, (*i.e.*, adding dissipativity into the circuit) to ensure that the circuit of Figure 3.12 becomes strictly state passive. Consider the circuit in Figure 3.13 where three resistor are connected in parallel with the capacitors $\mathbf{C}_1$, $\mathbf{C}_2$ and $\mathbf{C}_4$ to enhance passivity. This connection allows each capacitor to dissipate its stored energy through the resistor, rather than being returned to the circuit when it discharges.

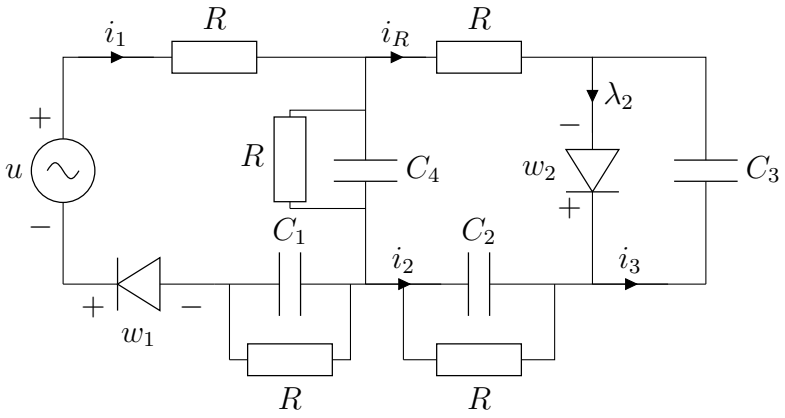

Figure 3.13: Strictly state passive RC circuit with two ideal diodes

Recall that the states x_1, x_2, x_3 and x_4 are the voltages across the capacitors $\mathbf{C}_1$, $\mathbf{C}_2$, $\mathbf{C}_3$ and $\mathbf{C}_4$ respectively and that $\mathbf{C}_1 = \mathbf{C}_2 = \mathbf{C}_3 = \mathbf{C}_4 = \mathbf{C}$. The dynamical system is

given by:

$$\begin{cases} \begin{pmatrix} \dot{x}_1(t) \\ \dot{x}_2(t) \\ \dot{x}_3(t) \\ \dot{x}_4(t) \end{pmatrix} = \begin{pmatrix} -\frac{1}{\mathbf{RC}} & 0 & 0 & 0 \\ 0 & -\frac{2}{\mathbf{RC}} & -\frac{1}{\mathbf{RC}} & -\frac{1}{\mathbf{RC}} \\ 0 & -\frac{1}{\mathbf{RC}} & -\frac{1}{\mathbf{RC}} & -\frac{1}{\mathbf{RC}} \\ 0 & -\frac{1}{\mathbf{RC}} & -\frac{1}{\mathbf{RC}} & -\frac{2}{\mathbf{RC}} \end{pmatrix} \begin{pmatrix} x_1(t) \\ x_2(t) \\ x_3(t) \\ x_4(t) \end{pmatrix} + \begin{pmatrix} \frac{1}{\mathbf{C}} & 0 \\ 0 & 0 \\ 0 & \frac{1}{\mathbf{C}} \\ \frac{1}{\mathbf{C}} & 0 \end{pmatrix} \begin{pmatrix} \lambda_1(t) \\ \lambda_2(t) \end{pmatrix} \\ 0 \leq \begin{pmatrix} \lambda_1(t) \\ \lambda_2(t) \end{pmatrix} \perp \begin{pmatrix} w_1(t) \\ w_2(t) \end{pmatrix} = \begin{pmatrix} 1 & 0 & 0 & 1 \\ 0 & 0 & 1 & 0 \end{pmatrix} \begin{pmatrix} x_1(t) \\ x_2(t) \\ x_3(t) \\ x_4(t) \end{pmatrix} + \begin{pmatrix} \mathbf{R} & 0 \\ 0 & 0 \end{pmatrix} \begin{pmatrix} \lambda_1(t) \\ \lambda_2(t) \end{pmatrix} \\ \qquad + \begin{pmatrix} -1 \\ 0 \end{pmatrix} u \geq 0 \end{cases} \tag{3.18}$$

Remark 3.3.2. *The connection of a resistor across the capacitor $\boldsymbol{C}_3$ cancels the property of positive semi-definiteness (PSD) for the matrix D which is a necessary condition for the existence of state jumps. The matrix D becomes positive definite such that* $D = \begin{pmatrix} \boldsymbol{R} & 0 \\ 0 & \boldsymbol{R} \end{pmatrix}$.

Let us define $H(s)$ as the matrix of the transfer function of the closed-loop system of the LCS in (3.18) with $u = K(x - x_d) + u_d$ and $K = \begin{pmatrix} k_1 & k_2 & k_3 & k_4 \end{pmatrix}$. Then,

$$H(s) \triangleq \begin{pmatrix} \frac{w_1}{\lambda_1} & \frac{w_1}{\lambda_2} \\ \frac{w_2}{\lambda_1} & \frac{w_2}{\lambda_2} \end{pmatrix} \triangleq \begin{pmatrix} H_{11}(s) & H_{12}(s) \\ H_{21}(s) & H_{22}(s) \end{pmatrix}$$

where

$$H_{11}(s) = \frac{\mathbf{R}^4\mathbf{C}^3(k_1+k_2+2)s^3+\mathbf{R}^3\mathbf{C}^2(5k_1-k_2-k_3+4k_4+9)s^2+\mathbf{R}^2\mathbf{C}(5k_1-k_2-2k_3+4k_4+9)s}{\mathbf{R}^4\mathbf{C}^4s^4+6\mathbf{R}^3\mathbf{C}^3s^3+10\mathbf{R}^2\mathbf{C}^2s^2+6\mathbf{RC}s+1}$$

$$+\frac{\mathbf{R}(k_1-k_3+k_4+2)}{\mathbf{R}^4\mathbf{C}^4s^4+6\mathbf{R}^3\mathbf{C}^3s^3+10\mathbf{R}^2\mathbf{C}^2s^2+6\mathbf{RC}s+1} + \mathbf{R}$$

$$H_{12}(s) = \frac{\mathbf{R}^4\mathbf{C}^3k_3s^3 + \mathbf{R}^3\mathbf{C}^2(-k_2+5k_3-k_4-1)s^2 + \mathbf{R}^2\mathbf{C}(-2k_2+4k_3-2k_4-2)s + \mathbf{R}(-k_2+3k_3-k_4-1)}{\mathbf{R}^4\mathbf{C}^4s^4 + 6\mathbf{R}^3\mathbf{C}^3s^3 + 10\mathbf{R}^2\mathbf{C}^2s^2 + 6\mathbf{RC}s + 1}$$

$$H_{21}(s) = \frac{-\mathbf{R}^3\mathbf{C}^2s^2 - 2\mathbf{R}^2\mathbf{C}s - \mathbf{R}}{\mathbf{R}^4\mathbf{C}^4s^4 + 6\mathbf{R}^3\mathbf{C}^3s^3 + 10\mathbf{R}^2\mathbf{C}^2s^2 + 6\mathbf{RC}s + 1}$$

$$H_{22}(s) = \frac{\mathbf{R}^4\mathbf{C}^3s^3 + 5\mathbf{R}^3\mathbf{C}^2s^2 + 4\mathbf{R}^2\mathbf{C}s + 3\mathbf{R}}{\mathbf{R}^4\mathbf{C}^4s^4 + 6\mathbf{R}^3\mathbf{C}^3s^3 + 10\mathbf{R}^2\mathbf{C}^2s^2 + 6\mathbf{RC}s + 1}$$

The poles are the roots of the characteristic equation:

$$\mathbf{R}^4\mathbf{C}^4s^4 + 6\mathbf{R}^3\mathbf{C}^3s^3 + 10\mathbf{R}^2\mathbf{C}^2s^2 + 6\mathbf{RC}s + 1$$

and they are represented as follows:

- $s = -\frac{1}{\mathbf{RC}}$ (double root),

- $s = -\frac{2}{\mathbf{RC}} + \sqrt{\frac{3}{\mathbf{R^2C^2}}}$, and
- $s = -\frac{2}{\mathbf{RC}} - \sqrt{\frac{3}{\mathbf{R^2C^2}}}$.

Hence, the problem of the pole at zero with multiplicity 3 which appears in the LCS represented by the circuit in Figure 3.12 is solved in the LCS represented by the circuit in Figure 3.13 since all the poles have a negative real part.

In order to check if there exist K and P such that the quadruple $(A, B, C + FK, D)$ of the closed loop system of the LCS in (3.18) is strictly state passive, the BMI in (4.10) is transformed to LMI as shown in Appendix A.1 and it is solved. The solution is:

$$K = \begin{pmatrix} -0.304 & -0.658 & 0 & -0.962 \end{pmatrix} \text{ and } P = \begin{pmatrix} 0.0032 & 0 & 0 & 0 \\ 0 & 0.005 & 0 & 0.002 \\ 0 & 0 & 0.0025 & 0 \\ 0 & 0.002 & 0 & 0.005 \end{pmatrix}$$

with $\epsilon = 0.1$. The variable ϵ is chosen arbitrarily by the user such that the system is strictly state passive with a desired degree of strict passivity (as ϵ increases, the degree of strict passitvity increases). The value of ϵ can be increased until it reaches a critical value, at which the LMI becomes infeasible again. If $F = 0$, then the open loop system of (3.18) is strictly passive as well. So, in our case, the open loop system is strictly passive and the role of ϵ is to increase the degree of strict passivity by pushing the eigenvalues of the matrix $A + EK$ to be more negative. But, $E = 0$ in this system, thus varying the value of ϵ does not have an interesting effect on the control gain. It is noteworthy that the critical value of ϵ (the last value at which the system is strictly passive) is $\epsilon = 2$ in the closed-loop system of the LCS represented by (3.18).

Remark 3.3.3. *It is necessary to connect three resistors in parallel across* $\boldsymbol{C}_1$, $\boldsymbol{C}_2$, *and* $\boldsymbol{C}_3$ *to get strict state passivity. If one of the resistor is removed, then a pole at zero appears when evaluating the transfer function.*

Second approach: adding controllers for passivity

Let us now add controllers (current sources) to the circuit in Figure 3.12 in order to study strict state passivity of the closed-loop system.

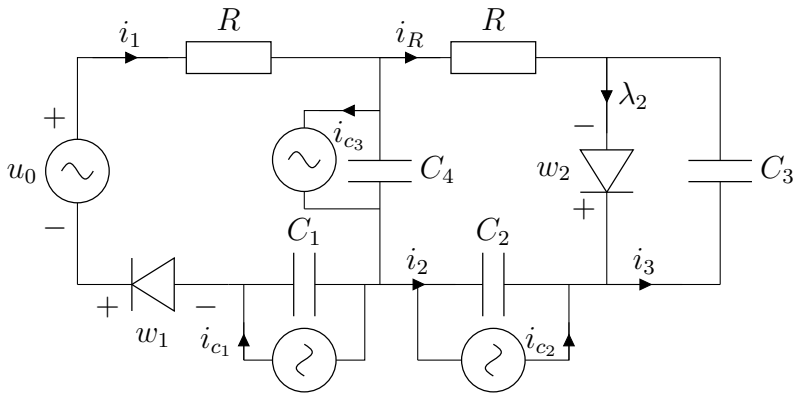

Figure 3.14: Strictly state passive RC circuit with current and voltage sources

The dynamics are given by the following LCS:

$$\begin{cases} \dot{x}(t) = \begin{pmatrix} 0 & 0 & 0 & 0 \\ 0 & -\frac{1}{\mathbf{RC}} & -\frac{1}{\mathbf{RC}} & -\frac{1}{\mathbf{RC}} \\ 0 & -\frac{1}{\mathbf{RC}} & -\frac{1}{\mathbf{RC}} & -\frac{1}{\mathbf{RC}} \\ 0 & -\frac{1}{\mathbf{RC}} & -\frac{1}{\mathbf{RC}} & -\frac{1}{\mathbf{RC}} \end{pmatrix} x(t) + \begin{pmatrix} \frac{1}{\mathbf{C}} & 0 \\ 0 & 0 \\ 0 & \frac{1}{\mathbf{C}} \\ \frac{1}{\mathbf{C}} & 0 \end{pmatrix} \lambda(t) + \begin{pmatrix} 0 & -\frac{1}{\mathbf{C}} & 0 & 0 \\ 0 & 0 & -\frac{1}{\mathbf{C}} & 0 \\ 0 & 0 & 0 & 0 \\ 0 & 0 & 0 & -\frac{1}{\mathbf{C}} \end{pmatrix} u(t) \\ 0 \leq \lambda(t) \perp w(t) = \begin{pmatrix} 1 & 0 & 0 & 1 \\ 0 & 0 & 1 & 0 \end{pmatrix} x(t) + \begin{pmatrix} \mathbf{R} & 0 \\ 0 & 0 \end{pmatrix} \lambda(t) + \begin{pmatrix} -1 & 0 & 0 & 0 \\ 0 & 0 & 0 & 0 \end{pmatrix} u(t) \geq 0 \end{cases} \tag{3.19}$$

where $u = (u_0, i_{c1}, i_{c2}, i_{c3})^\top$. If $E = 0$ and $F = 0$, then the BMI in (4.10) has no solution and the open loop system (A, B, C, D) for the circuit in Figure 3.14 is not strictly passive. In order to avoid Dirac measure in the presence of state jumps, let us take $G = 0$ in the following study (so that **(C1)** is satisfied). The BMI in (4.10) for strict state passivity has a solution when solved after being transformed to LMI (see Appendix A.1) for the closed loop system $(A + EK, B, C + FK, D)$ represented by (3.19). The solution is:

$$K = \begin{pmatrix} 0.52 & -0.01 & 0 & 0.504 \\ 0.014 & -0.00001 & 0 & -0.0006 \\ 0 & -0.088 & -0.302 & -0.025 \\ -0.0006 & 0.18 & 0.302 & 0.09 \end{pmatrix}, \; P = \begin{pmatrix} 0.012 & 0 & 0 & 0 \\ 0 & 0.012 & 0 & 0.00025 \\ 0 & 0 & 0.025 & 0 \\ 0 & 0.00025 & 0 & 0.012 \end{pmatrix} \tag{3.20}$$

with $\epsilon = 0.1$. Thus, the closed-loop system with controller $u = (u_0, i_{c1}, i_{c2}, i_{c3})^\top$ is strictly state passive and stability of the error dynamics can be analyzed in the presence of state jumps.

Let us decrease the number of controllers (current sources) as shown in Figure 3.15 below.

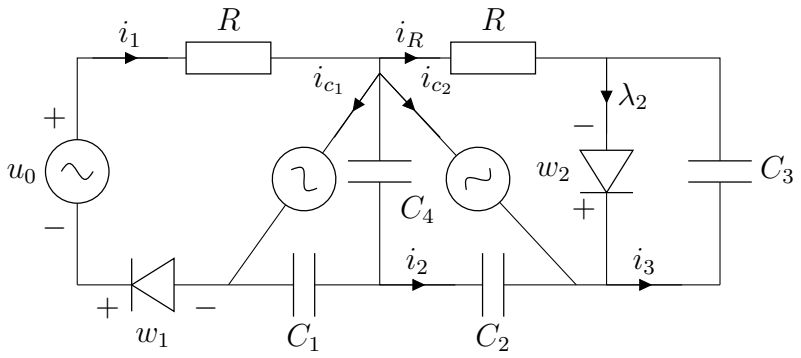

Figure 3.15: RC circuit with a voltage source and two current sources

The dynamics are given by the following LCS:

$$\begin{cases} \dot{x}(t) = \begin{pmatrix} 0 & 0 & 0 & 0 \\ 0 & -\frac{1}{\mathbf{RC}} & -\frac{1}{\mathbf{RC}} & -\frac{1}{\mathbf{RC}} \\ 0 & -\frac{1}{\mathbf{RC}} & -\frac{1}{\mathbf{RC}} & -\frac{1}{\mathbf{RC}} \\ 0 & -\frac{1}{\mathbf{RC}} & -\frac{1}{\mathbf{RC}} & -\frac{1}{\mathbf{RC}} \end{pmatrix} x(t) + \begin{pmatrix} \frac{1}{\mathbf{C}} & 0 \\ 0 & 0 \\ 0 & \frac{1}{\mathbf{C}} \\ \frac{1}{\mathbf{C}} & 0 \end{pmatrix} \lambda(t) + \begin{pmatrix} 0 & -\frac{1}{\mathbf{C}} & 0 \\ 0 & 0 & -\frac{1}{\mathbf{C}} \\ 0 & 0 & 0 \\ 0 & -\frac{1}{\mathbf{C}} & -\frac{1}{\mathbf{C}} \end{pmatrix} u(t) \\ 0 \leq \lambda(t) \perp w(t) = \begin{pmatrix} 1 & 0 & 0 & 1 \\ 0 & 0 & 1 & 0 \end{pmatrix} x(t) + \begin{pmatrix} \mathbf{R} & 0 \\ 0 & 0 \end{pmatrix} \lambda(t) + \begin{pmatrix} -1 & 0 & 0 \\ 0 & 0 & 0 \end{pmatrix} u(t) \geq 0 \end{cases} \tag{3.21}$$

where $u = (u_0, i_{c1}, i_{c2})^\top$. In order to check if the closed-loop system's quadruple $(A + EK, B, FK, D)$, is strictly passive, let us check if there exist matrices P and K such that the BMI in (4.10) has a solution. This is done by transforming the BMI into an LMI and solve it using MOSEK 9.3.14 solver. The result indicates that the problem is infeasible, thus, the closed-loop system with $u = (u_0, i_{c1}, i_{c2})^\top$ is not strictly state passive.

3.3.2 Analysis of State Jumps

This section analyzes the state jumps of the desired system, the closed-loop system and the error $e = x - x_d$. It explains that the state jumps can occur at the initial time if the states are initialized such that the complementarity constraints are not satisfied, and at $t = t_c$ if there is a discontinuous controller u_d at $t = t_c$ (see section 2.1.3). The following analysis is followed by numerical simulation for each case. Recall that the simulation is performed with the INRIA software package SICONOS[2], and the LMIs are solved with MOSEK 9.3.14 solver.

At the initial time $t = 0$

Let us consider the circuit of Figure 3.14 with the dynamics in (3.19). The state jumps are analysed for the desired system and the closed-loop system. The desired system $x_d = (x_{1d}, x_{2d}, x_{3d}, x_{4d})^\top$ is defined by the following LCS:

$$\begin{cases} \dot{x}_d(t) = \begin{pmatrix} 0 & 0 & 0 & 0 \\ 0 & -\frac{1}{\mathbf{RC}} & -\frac{1}{\mathbf{RC}} & -\frac{1}{\mathbf{RC}} \\ 0 & -\frac{1}{\mathbf{RC}} & -\frac{1}{\mathbf{RC}} & -\frac{1}{\mathbf{RC}} \\ 0 & -\frac{1}{\mathbf{RC}} & -\frac{1}{\mathbf{RC}} & -\frac{1}{\mathbf{RC}} \end{pmatrix} x_d(t) + \begin{pmatrix} \frac{1}{\mathbf{C}} & 0 \\ 0 & 0 \\ 0 & \frac{1}{\mathbf{C}} \\ \frac{1}{\mathbf{C}} & 0 \end{pmatrix} \lambda_d(t) + \begin{pmatrix} 0 & -\frac{1}{\mathbf{C}} & 0 & 0 \\ 0 & 0 & -\frac{1}{\mathbf{C}} & 0 \\ 0 & 0 & 0 & 0 \\ 0 & 0 & 0 & -\frac{1}{\mathbf{C}} \end{pmatrix} u_d(t) \\ 0 \leq \lambda_d(t) \perp w_d(t) = \begin{pmatrix} 1 & 0 & 0 & 1 \\ 0 & 0 & 1 & 0 \end{pmatrix} x_d(t) + \begin{pmatrix} \mathbf{R} & 0 \\ 0 & 0 \end{pmatrix} \lambda_d(t) + \begin{pmatrix} -1 & 0 & 0 & 0 \\ 0 & 0 & 0 & 0 \end{pmatrix} u_d(t) \geq 0 \end{cases} \tag{3.22}$$

with $u_d(t) = (u_{0d}, i_{c1d}, i_{c2d}, i_{c3d})^\top$. In order to study the state jumps in the desired system represented by the LCS in (3.22), let us define the corresponding sets which are

[2] https://nonsmooth.gricad-pages.univ-grenoble-alpes.fr/siconos/index.html

defined and explained in paragraph State Jumps in section 1.2.2 and in section 2.1.3:

$$Q_{d,D} = \{\lambda_d \in I\!R^2 \mid 0 \leq \lambda_d \perp D\lambda_d \geq 0\} = \{\lambda_d \in I\!R^2 \mid \lambda_{1d} = 0 \text{ and } \lambda_{2d} \in I\!R_+\}$$

The dual cone of $Q_{d,D}$ is given by:

$$Q^\star_{d,D} = \{w_d \in I\!R^2 \mid \langle w_d, \lambda_d \rangle \geq 0\} = \{w_d \in I\!R^2 \mid w_{1d} \in I\!R \text{ and } w_{2d} \in I\!R_+\}$$

and

$$\mathcal{K}_d = \{x_d \in I\!R^4 \mid Cx_d + Fu_d(t^+) \in Q^\star_{d,D}\} = \{x_d \in I\!R^4 \mid x_{1d},\ x_{2d},\ x_{4d} \in I\!R \text{ and } x_{3d} \geq 0\}$$

Notice that the post-jump $x_d^+ \in \mathcal{K}_d$. According to the conditions stated in the set $\mathcal{K}_d$, a state jump exists only at the initial time in the desired system trajectory x_{3d}. This jumps occurs if and only if $x_{3d}(0^-) < 0$. Notably, by solving the minimization problem in (1.11), if $x_{3d}(0^-) < 0$, then $x_{3d}(0^+) = 0$. Otherwise, if $x_{3d}(0^-) \geq 0$, then $x_{3d}(0^+) = x_{3d}(0^-)$.

The closed loop system with $u = \begin{pmatrix} u_0 & i_{c1} & i_{c2} & i_{c3} \end{pmatrix}^\top = K(x - x_d) + u_d$ where $K = \begin{pmatrix} k_{11} & k_{12} & k_{13} & k_{14} \\ k_{21} & k_{22} & k_{23} & k_{24} \\ k_{31} & k_{32} & k_{33} & k_{34} \\ k_{41} & k_{42} & k_{43} & k_{44} \end{pmatrix}$ is represented as follows:

$$\begin{cases} \dot{x}(t) = \begin{pmatrix} \frac{-k_{21}}{\mathbf{C}} & \frac{-k_{22}}{\mathbf{C}} & \frac{-k_{23}}{\mathbf{C}} & \frac{-k_{24}}{\mathbf{C}} \\ \frac{-k_{31}}{\mathbf{C}} & -\frac{1}{\mathbf{C}}(\frac{1}{\mathbf{R}} + k_{32}) & -\frac{1}{\mathbf{C}}(\frac{1}{\mathbf{R}} + k_{33}) & -\frac{1}{\mathbf{C}}(\frac{1}{\mathbf{R}} + k_{34}) \\ 0 & -\frac{1}{\mathbf{RC}} & -\frac{1}{\mathbf{RC}} & -\frac{1}{\mathbf{RC}} \\ -\frac{k_{41}}{\mathbf{C}} & -\frac{1}{\mathbf{C}}(\frac{1}{\mathbf{R}} + k_{42}) & -\frac{1}{\mathbf{C}}(\frac{1}{\mathbf{R}} + k_{43}) & -\frac{1}{\mathbf{C}}(\frac{1}{\mathbf{R}} + k_{44}) \end{pmatrix} x(t) + \begin{pmatrix} \frac{1}{\mathbf{C}} & 0 \\ 0 & 0 \\ 0 & \frac{1}{\mathbf{C}} \\ \frac{1}{\mathbf{C}} & 0 \end{pmatrix} \lambda(t) \\ \qquad - \begin{pmatrix} -\frac{k_{21}}{\mathbf{C}} & -\frac{k_{22}}{\mathbf{C}} & -\frac{k_{23}}{\mathbf{C}} & -\frac{k_{24}}{\mathbf{C}} \\ -\frac{k_{31}}{\mathbf{C}} & -\frac{k_{32}}{\mathbf{C}} & -\frac{k_{33}}{\mathbf{C}} & -\frac{k_{34}}{\mathbf{C}} \\ 0 & 0 & 0 & 0 \\ -\frac{k_{41}}{\mathbf{C}} & -\frac{k_{42}}{\mathbf{C}} & -\frac{k_{43}}{\mathbf{C}} & -\frac{k_{44}}{\mathbf{C}} \end{pmatrix} x_d(t) + \begin{pmatrix} 0 & -\frac{1}{\mathbf{C}} & 0 & 0 \\ 0 & 0 & -\frac{1}{\mathbf{C}} & 0 \\ 0 & 0 & 0 & 0 \\ 0 & 0 & 0 & -\frac{1}{\mathbf{C}} \end{pmatrix} u_d(t) \\ 0 \le w(t) = \begin{pmatrix} 1 - k_{11} & -k_{12} & -k_{13} & 1 - k_{14} \\ 0 & 0 & 1 & 0 \end{pmatrix} x(t) + \begin{pmatrix} \mathbf{R} & 0 \\ 0 & 0 \end{pmatrix} \lambda(t) \\ \qquad - \begin{pmatrix} -k_{11} & -k_{12} & -k_{13} & -k_{14} \\ 0 & 0 & 0 & 0 \end{pmatrix} x_d(t) + \begin{pmatrix} -1 & 0 & 0 & 0 \\ 0 & 0 & 0 & 0 \end{pmatrix} u_d(t) \perp \lambda(t) \ge 0 \end{cases} \tag{3.23}$$

For the closed-loop system (3.23), the state jumps are analysed by considering the following sets:

$$Q_D = \{\lambda \in I\!R^2 \mid 0 \le \lambda \perp D\lambda \ge 0\} = \{\lambda \in I\!R^2 \mid \lambda_1 = 0 \text{ and } \lambda_2 \in I\!R_+\}$$

with a dual cone:

$$Q_D^\star = \{w \in I\!R^2 \mid \langle w, \lambda \rangle \ge 0\} = \{w \in I\!R^2 \mid w_1 \in I\!R \text{ and } w_2 \in I\!R_+\}$$

and the set:

$$\begin{aligned} \mathcal{K} &= \{x \in I\!R^4 \mid (C + FK)x - FKx_d + Fu_d(t) \in Q_D^\star\} \\ &= \{x \in I\!R^4 \mid x_3 \ge 0 \text{ and } x_1,\ x_2 \text{ and } x_4 \in I\!R\} \end{aligned}$$

In the closed-loop system, it is observed from the set $\mathcal{K}$ and the state jump rule in (1.11) that a state jump occurs in the state x_3 only at $t = 0$, and it occurs if and only if $x_3(0^-) < 0$ so that $x_3(0^+) = 0$.

The error dynamics $e = x - x_d$ is written in the form of (2.5) as follows:

$$\begin{cases} \dot{e}(t) = \begin{pmatrix} \frac{-k_{21}}{\mathbf{C}} & \frac{-k_{22}}{\mathbf{C}} & \frac{-k_{23}}{\mathbf{C}} & \frac{-k_{24}}{\mathbf{C}} \\ \frac{-k_{31}}{\mathbf{C}} & -\frac{1}{\mathbf{C}}(\frac{1}{\mathbf{R}}+k_{32}) & -\frac{1}{\mathbf{C}}(\frac{1}{\mathbf{R}}+k_{33}) & -\frac{1}{\mathbf{C}}(\frac{1}{\mathbf{R}}+k_{34}) \\ 0 & -\frac{1}{\mathbf{RC}} & -\frac{1}{\mathbf{RC}} & -\frac{1}{\mathbf{RC}} \\ -\frac{k_{41}}{\mathbf{C}} & -\frac{1}{\mathbf{C}}(\frac{1}{\mathbf{R}}+k_{42}) & -\frac{1}{\mathbf{C}}(\frac{1}{\mathbf{R}}+k_{43}) & -\frac{1}{\mathbf{C}}(\frac{1}{\mathbf{R}}+k_{44}) \end{pmatrix} e(t) + \begin{pmatrix} \frac{1}{\mathbf{C}} & 0 \\ 0 & 0 \\ 0 & \frac{1}{\mathbf{C}} \\ \frac{1}{\mathbf{C}} & 0 \end{pmatrix} \begin{pmatrix} \lambda_1 - \lambda_{1d} \\ \lambda_2 - \lambda_{2d} \end{pmatrix} \\ 0 \leq \begin{pmatrix} w_1(t) \\ w_2(t) \\ w_{1d}(t) \\ w_{2d}(t) \end{pmatrix} = \begin{pmatrix} 1-k_{11} & -k_{12} & -k_{13} & 1-k_{14} \\ 0 & 0 & 1 & 0 \\ k_{11}-1 & k_{12} & k_{13} & k_{14}-1 \\ 0 & 0 & -1 & 0 \end{pmatrix} e(t) + \begin{pmatrix} \mathbf{R} & 0 & 0 & 0 \\ 0 & 0 & 0 & 0 \\ 0 & 0 & \mathbf{R} & 0 \\ 0 & 0 & 0 & 0 \end{pmatrix} \begin{pmatrix} \lambda_1(t) \\ \lambda_2(t) \\ \lambda_{1d}(t) \\ \lambda_{2d}(t) \end{pmatrix} \\ + \begin{pmatrix} 0 & 0 & 0 & 0 & 1 & 0 & 0 & 1 \\ 0 & 0 & 0 & 0 & 0 & 0 & 1 & 0 \\ 1-k_{11} & -k_{12} & -k_{13} & 1-k_{14} & k_{11} & k_{12} & k_{13} & k_{14} \\ 0 & 0 & 1 & 0 & 0 & 0 & 0 & 0 \end{pmatrix} \begin{pmatrix} x_1 \\ x_2 \\ x_3 \\ x_4 \\ x_{1d} \\ x_{2d} \\ x_{3d} \\ x_{4d} \end{pmatrix} + \begin{pmatrix} -u_{0d} \\ 0 \\ -u_{0d} \\ 0 \end{pmatrix} \\ \perp \begin{pmatrix} \lambda_1(t) \\ \lambda_2(t) \\ \lambda_{1d}(t) \\ \lambda_{2d}(t) \end{pmatrix} \geq 0 \end{cases} \tag{3.24}$$

The sets for the state jumps in the error dynamics in (3.24) are:

$$\begin{aligned} Q_{e,D} &= \left\{ \lambda \in I\!R^4 \mid 0 \leq \begin{pmatrix} \lambda_1 \\ \lambda_2 \\ \lambda_{1d} \\ \lambda_{2d} \end{pmatrix} \perp \begin{pmatrix} \mathbf{R} & 0 & 0 & 0 \\ 0 & 0 & 0 & 0 \\ 0 & 0 & \mathbf{R} & 0 \\ 0 & 0 & 0 & 0 \end{pmatrix} \begin{pmatrix} \lambda_1 \\ \lambda_2 \\ \lambda_{1d} \\ \lambda_{2d} \end{pmatrix} \geq 0 \right\} \\ &= \left\{ \lambda \in I\!R^4 \mid \lambda_1 = 0,\ \lambda_{1d} = 0,\ \lambda_2 \text{ and } \lambda_{2d} \in I\!R_+ \right\} \end{aligned}$$

with the dual cone given by:

$$Q^\star_{e,D} = \{ w \in I\!R^4 \mid \langle w, \lambda \rangle \geq 0 \} = \{ w \in I\!R^4 \mid w_1 \in I\!R, w_2 \in I\!R_+, w_{1d} \in I\!R \text{ and } w_{2d} \in I\!R_+ \}$$

and the set

$$\begin{aligned} \mathcal{K}_e &= \left\{ e \in I\!R^4 \mid \begin{pmatrix} C+FK \\ -C-FK \end{pmatrix} e + \begin{pmatrix} 0 & C \\ C+FK & -FK \end{pmatrix} \begin{pmatrix} x \\ x_d \end{pmatrix} + \begin{pmatrix} Fu_d \\ Fu_d \end{pmatrix} \in Q^\star_{e,D} \right\} \\ &= \{ e \in I\!R^4 \mid e_1,\ e_2,\ e_4 \in I\!R,\ e_3 + x_{3d}(0^+) \geq 0 \text{ and } -e_3 + x_3(0^+) \geq 0 \} \\ &= \{ e \in I\!R^4 \mid e_1,\ e_2,\ e_4 \in I\!R \text{ and } e_3 \in \left[-x_{3d}(0^+),\ x_3(0^+) \right] \} \end{aligned}$$

Knowing that the minimization problem in (1.11) is the same at initial time for the states x_3 and x_{3d}, the jump in e_3 vanishes when $x_3(0^-) = x_{3d}(0^-)$. A jump occurs at

$t = 0$, in the error dynamics in e_3 if and only if $e_3(0^-) < -x_{3d}(0^-)$ or $e_3(0^-) > x_3(0^-)$. If x_{3d} and x_3 have state jumps at $t = 0$ and if $x_3(0^-) \neq x_{3d}(0^-)$, then e_3 jumps.

Consider the following numerical simulation with the initial state $x(0^-) = (-1,\ 1,\ -2,\ 2)$ and $x_d(0^-) = (1,\ 0,\ 1,\ -2)$ and with a time step $h = 0.001$. Take $u_{0d} = 5\sin 10t$, $i_{c1d} = \sin 5t$, $i_{c2d} = 3\sin 5t$ and $i_{c3d} = 2\sin 3t$.

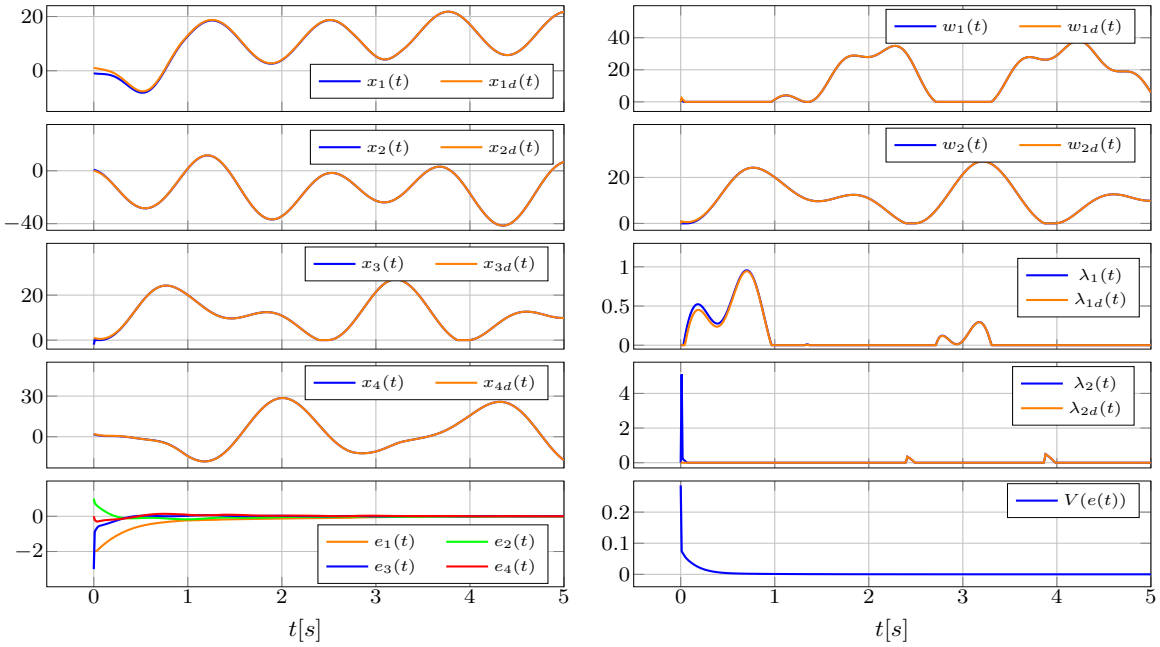

Figure 3.16: Numerical Simulation of desired, closed-loop and error dynamics of LCS in (3.19). The numerical simulation show the complementarity variables λ and w, as well as the storage function of the error system $V(e(t))$.

It is observed from the numerical simulation in Figure 3.16 that the state x_3 of the closed-loop system performs a state jump from $x_3(0^-) = -2$ to $x_3(0^+) = 0$. This numerical result confirms the jump rule given by the minimization problem in (1.11).

In the plots of the complementarity variables λ and w, a synchronization is noticed between the desired and the real systems. The reason of this result is the fact that the term $\lambda - \lambda_d$ in (3.24) converges to $\mathrm{Ker}(B + EG)$ which is zero in this example.

It is also observable in Figure 3.16 that the storage function of the error $V = e^\top Pe$ jumps at initial time such that $V(0^+) - V(0^-) < 0$. By applying Lemma 2.1.10, it is given in our example that $u_{0d}(0)$ is time continuous, x_d is continuous at $t = 0$ and $FKx_d(0) - Fu_d(0) \geq 0 \Leftrightarrow 0 \in \{x \in \mathbb{R}^4 \mid (C + FK)x + FKx_d(0) - Fu_d(0) \geq 0\}$, then at an initial state jump we have $V(0^+) - V(0^-) \leq 0$ where $P = P^\top \succ 0$ given in (3.20).

Further jump at $t = t_c \geq 0$

In this section, the goal is to create a jump at $t = t_c > 0$ when u_d is discontinuous at time t_c. For this purpose, let us move the voltage controller u_0 in the circuit of Figure 3.14 and connect it in series with the capacitor $\mathbf{C}_3$ as shown in the figure below:

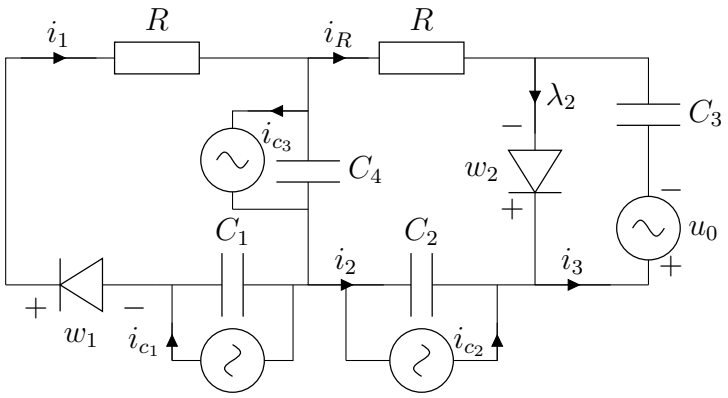

Figure 3.17: RC circuit with two ideal diodes

The dynamics are given by the following LCS:

$$\begin{cases} \dot{x}(t) = \begin{pmatrix} 0 & 0 & 0 & 0 \\ 0 & -\frac{1}{\mathbf{RC}} & -\frac{1}{\mathbf{RC}} & -\frac{1}{\mathbf{RC}} \\ 0 & -\frac{1}{\mathbf{RC}} & -\frac{1}{\mathbf{RC}} & -\frac{1}{\mathbf{RC}} \\ 0 & -\frac{1}{\mathbf{RC}} & -\frac{1}{\mathbf{RC}} & -\frac{1}{\mathbf{RC}} \end{pmatrix} x(t) + \begin{pmatrix} \frac{1}{\mathbf{C}} & 0 \\ 0 & 0 \\ 0 & \frac{1}{\mathbf{C}} \\ \frac{1}{\mathbf{C}} & 0 \end{pmatrix} \lambda(t) + \begin{pmatrix} 0 & -\frac{1}{\mathbf{C}} & 0 & 0 \\ -\frac{1}{\mathbf{RC}} & 0 & -\frac{1}{\mathbf{C}} & 0 \\ -\frac{1}{\mathbf{RC}} & 0 & 0 & 0 \\ -\frac{1}{\mathbf{RC}} & 0 & 0 & -\frac{1}{\mathbf{C}} \end{pmatrix} u(t) \\ 0 \leq \lambda(t) \perp w(t) = \begin{pmatrix} 1 & 0 & 0 & 1 \\ 0 & 0 & 1 & 0 \end{pmatrix} x(t) + \begin{pmatrix} \mathbf{R} & 0 \\ 0 & 0 \end{pmatrix} \lambda(t) + \begin{pmatrix} 0 & 0 & 0 & 0 \\ 1 & 0 & 0 & 0 \end{pmatrix} u(t) \geq 0 \end{cases} \tag{3.25}$$

where $u = (u_0, i_{c1}, i_{c2}, i_{c3})^\top$.

The open loop quadruple (A, B, C, D) (*i.e.*, $E = 0$ and $F = 0$) of the circuit in Figure 3.17 is not strictly passive. But, while checking if there exist matrices K and P such that the closed loop quadruple $(A + EK, B, C + FK, D)$ is strictly passive, the BMI which is transformed to LMI according to Appendix A.1 in (4.10) has a solution such that:

$$K = \begin{pmatrix} -0.238 & 0.625 & 0.298 & 0.389 \\ 0.009 & 0.006 & 0.009 & 0.003 \\ 0.042 & -0.22 & -0.25 & -0.109 \\ 0.045 & -0.31 & -0.303 & -0.17 \end{pmatrix}, \; P = \begin{pmatrix} 0.029 & 0.001 & -0.006 & -0.004 \\ 0.001 & 0.033 & 0.016 & 0.001 \\ -0.006 & 0.016 & 0.032 & 0.01 \\ -0.004 & 0.001 & 0.01 & 0.0304 \end{pmatrix} \tag{3.26}$$

with $\epsilon = 0.01$.

The desired dynamics of (3.25) is given as follows:

$$\begin{cases} \dot{x}_d(t) = \begin{pmatrix} 0 & 0 & 0 & 0 \\ 0 & -\frac{1}{\mathbf{RC}} & -\frac{1}{\mathbf{RC}} & -\frac{1}{\mathbf{RC}} \\ 0 & -\frac{1}{\mathbf{RC}} & -\frac{1}{\mathbf{RC}} & -\frac{1}{\mathbf{RC}} \\ 0 & -\frac{1}{\mathbf{RC}} & -\frac{1}{\mathbf{RC}} & -\frac{1}{\mathbf{RC}} \end{pmatrix} x_d(t) + \begin{pmatrix} \frac{1}{\mathbf{C}} & 0 \\ 0 & 0 \\ 0 & \frac{1}{\mathbf{C}} \\ \frac{1}{\mathbf{C}} & 0 \end{pmatrix} \lambda_d(t) + \begin{pmatrix} 0 & -\frac{1}{\mathbf{C}} & 0 & 0 \\ -\frac{1}{\mathbf{RC}} & 0 & -\frac{1}{\mathbf{C}} & 0 \\ -\frac{1}{\mathbf{RC}} & 0 & 0 & 0 \\ -\frac{1}{\mathbf{RC}} & 0 & 0 & -\frac{1}{\mathbf{C}} \end{pmatrix} u_d(t) \\ 0 \leq \begin{pmatrix} \lambda_{1d}(t) \\ \lambda_{2d}(t) \end{pmatrix} \perp w_d(t) = \begin{pmatrix} 1 & 0 & 0 & 1 \\ 0 & 0 & 1 & 0 \end{pmatrix} x_d(t) + \begin{pmatrix} \mathbf{R} & 0 \\ 0 & 0 \end{pmatrix} \lambda_d(t) + \begin{pmatrix} 0 & 0 & 0 & 0 \\ 1 & 0 & 0 & 0 \end{pmatrix} u_d(t) \geq 0 \end{cases} \tag{3.27}$$

In order to study the state jumps in the desired system represented by the LCS in (3.27), let us define the corresponding sets:

$$Q_{d,D} = \{\lambda_d \in I\!R^2 \mid 0 \leq \lambda_d \perp D\lambda_d \geq 0\} = \{\lambda_d \in I\!R^2 \mid \lambda_{1d} = 0 \text{ and } \lambda_{2d} \in I\!R_+\}$$

The dual cone of $Q_{d,D}$ is

$$Q^\star_{d,D} = \{w_d \in I\!R^2 \mid \langle w_d, \lambda_d\rangle \geq 0\} = \{w_d \in I\!R^2 \mid w_{1d} \in I\!R \text{ and } w_{2d} \in I\!R_+\}$$

and the set

$$\begin{aligned}\mathcal{K}_d &= \{x_d \in I\!R^4 \mid Cx_d + Fu_d(t^+) \in Q^\star_{d,D}\}\\ &= \{x_d \in I\!R^4 \mid x_{1d},\ x_{2d},\ x_{4d} \in I\!R \text{ and } x_{3d} + u_{1d}(t^+) \geq 0\}\end{aligned}$$

Thus, the desired state x_{3d} jumps at $t = t_c \geq 0$ if and only if $x_{3d}(t^-) < -u_{1d}(t^+)$. Let $u = \begin{pmatrix} u_1 & i_{c1} & i_{c2} & i_{c3}\end{pmatrix}^\top = K(x - x_d) + u_d$ with $K = \begin{pmatrix} k_{11} & k_{12} & k_{13} & k_{14}\\ k_{21} & k_{22} & k_{23} & k_{24}\\ k_{31} & k_{32} & k_{33} & k_{34}\\ k_{41} & k_{42} & k_{43} & k_{44}\end{pmatrix}$. The closed-loop system is represented as follows:

$$\begin{cases} \dot{x}(t) = \begin{pmatrix} \frac{-k_{21}}{\mathbf{C}} & \frac{-k_{22}}{\mathbf{C}} & \frac{-k_{23}}{\mathbf{C}} & \frac{-k_{24}}{\mathbf{C}}\\ \frac{-k_{11}}{\mathbf{RC}} - \frac{k_{31}}{\mathbf{C}} & -\frac{1}{\mathbf{RC}}(1+k_{12}) - \frac{k_{32}}{\mathbf{C}} & -\frac{1}{\mathbf{RC}}(1+k_{13}) - \frac{k_{33}}{\mathbf{C}} & -\frac{1}{\mathbf{RC}}(1+k_{14}) - \frac{k_{34}}{\mathbf{C}}\\ -\frac{k_{11}}{\mathbf{RC}} & -\frac{1}{\mathbf{RC}}(1+k_{12}) & -\frac{1}{\mathbf{RC}}(1+k_{13}) & -\frac{1}{\mathbf{RC}}(1+k_{14})\\ -\frac{k_{11}}{\mathbf{RC}} - \frac{k_{41}}{\mathbf{C}} & -\frac{1}{\mathbf{RC}} - \frac{k_{12}}{\mathbf{RC}} - \frac{k_{42}}{\mathbf{C}} & -\frac{1}{\mathbf{RC}} - \frac{k_{13}}{\mathbf{RC}} - \frac{k_{43}}{\mathbf{C}} & -\frac{1}{\mathbf{RC}} - \frac{k_{14}}{\mathbf{RC}} - \frac{k_{44}}{\mathbf{C}}\end{pmatrix} x(t)\\ \qquad + \begin{pmatrix} \frac{1}{\mathbf{C}} & 0\\ 0 & 0\\ 0 & \frac{1}{\mathbf{C}}\\ \frac{1}{\mathbf{C}} & 0\end{pmatrix} \lambda(t) - \begin{pmatrix} -\frac{k_{21}}{\mathbf{C}} & -\frac{k_{22}}{\mathbf{C}} & -\frac{k_{23}}{\mathbf{C}} & -\frac{k_{24}}{\mathbf{C}}\\ \frac{-k_{11}}{\mathbf{RC}} - \frac{k_{31}}{\mathbf{C}} & \frac{-k_{12}}{\mathbf{RC}} - \frac{k_{32}}{\mathbf{C}} & \frac{-k_{13}}{\mathbf{RC}} - \frac{k_{33}}{\mathbf{C}} & \frac{-k_{14}}{\mathbf{RC}} - \frac{k_{34}}{\mathbf{C}}\\ \frac{-k_{11}}{\mathbf{RC}} & \frac{-k_{12}}{\mathbf{RC}} & \frac{-k_{13}}{\mathbf{RC}} & \frac{-k_{14}}{\mathbf{RC}}\\ \frac{-k_{11}}{\mathbf{RC}} - \frac{k_{41}}{\mathbf{C}} & \frac{-k_{12}}{\mathbf{RC}} - \frac{k_{42}}{\mathbf{C}} & \frac{-k_{13}}{\mathbf{RC}} - \frac{k_{43}}{\mathbf{C}} & \frac{-k_{14}}{\mathbf{RC}} - \frac{k_{44}}{\mathbf{C}}\end{pmatrix} x_d(t)\\ \qquad + \begin{pmatrix} 0 & -\frac{1}{\mathbf{C}} & 0 & 0\\ -\frac{1}{\mathbf{RC}} & 0 & -\frac{1}{\mathbf{C}} & 0\\ -\frac{1}{\mathbf{RC}} & 0 & 0 & 0\\ -\frac{1}{\mathbf{RC}} & 0 & 0 & -\frac{1}{\mathbf{C}}\end{pmatrix} u_d(t)\\ 0 \leq w(t) = \begin{pmatrix} 1 & 0 & 0 & 1\\ k_{11} & k_{12} & 1+k_{13} & k_{14}\end{pmatrix} x(t) + \begin{pmatrix} \mathbf{R} & 0\\ 0 & 0\end{pmatrix} \lambda(t) - \begin{pmatrix} 0 & 0 & 0 & 0\\ k_{11} & k_{12} & k_{13} & k_{14}\end{pmatrix} x_d(t)\\ \qquad + \begin{pmatrix} 0 & 0 & 0 & 0\\ 1 & 0 & 0 & 0\end{pmatrix} u_d(t) \perp \lambda(t) \geq 0 \end{cases} \tag{3.28}$$

For the closed-loop system whose dynamics is in (3.28), the sets are calculated as :

$$Q_D = \{\lambda \in I\!R^2 \mid 0 \leq \lambda \perp D\lambda \geq 0\} = \{\lambda \in I\!R^2 \mid \lambda_1 = 0 \text{ and } \lambda_2 \in I\!R_+\}$$

with a dual cone:

$$Q^\star_D = \{w \in I\!R^2 \mid \langle w, \lambda\rangle \geq 0\} = \{w \in I\!R^2 \mid w_1 \in I\!R \text{ and } w_2 \in I\!R_+\}$$

and the set:

$$\begin{aligned}\mathcal{K} &= \{x \in I\!R^4 \mid (C+FK)x - FKx_d + Fu_d(t) \in Q_D^\star\} \\ &= \{x \in I\!R^4 \mid x_1 + x_4 \in I\!R \text{ and } k_{11}(x_1 - x_{1d}) + k_{12}(x_2 - x_{2d}) + k_{13}(x_3 - x_{3d}) \\ &\qquad + k_{14}(x_4 - x_{4d}) + x_3 + u_{1d}(t^+) \geq 0\}\end{aligned}$$

Let t_c be the time of discontinuity of the controller $u_{1d}(\cdot)$. Given that the states x^- and x_d^- are known, it is possible to determine which state jumps at t_c. However, this is not trivial in the closed-loop system during the transient response due to the coupled conditions in the set $\mathcal{K}$. In the interval $[t^\star, \infty]$ where $e = 0$ for all $t \geq t^\star$ (*i.e.*, the steady state response), the set $\mathcal{K}$ simplifies to $\mathcal{K} = \{x \in I\!R^4 \;\; x_1 + x_4 \in I\!R \;\text{ and }\; x_3 + u_{1d}(t^+) \geq 0\}$. If the controller is discontinuous at time $t_c \in [t^\star, \infty]$ and the states $x_3(t_c^-) = x_{3d}(t_c^-) < -u_{1d}(t_c^+)$, then the states x_{3d} and x_3 jump simultaneously at t_c to the same value $-u_{1d}(t_c^+)$. In this example, a numerical simulation is performed to show which state in the closed-loop system jumps when u_{1d} is discontinuous.

The error dynamics is written in the form of the dynamics in (2.12) as follows:

$$\begin{cases} \dot{e}(t) = \begin{pmatrix} \frac{-k_{21}}{\mathbf{C}} & \frac{-k_{22}}{\mathbf{C}} & \frac{-k_{23}}{\mathbf{C}} & \frac{-k_{24}}{\mathbf{C}} \\ \frac{-k_{11}}{\mathbf{RC}} - \frac{k_{31}}{\mathbf{C}} & -\frac{1}{\mathbf{RC}}(1+k_{12}) - \frac{k_{32}}{\mathbf{C}} & -\frac{1}{\mathbf{RC}}(1+k_{13}) - \frac{k_{33}}{\mathbf{C}} & -\frac{1}{\mathbf{RC}}(1+k_{14}) - \frac{k_{34}}{\mathbf{C}} \\ -\frac{k_{11}}{\mathbf{RC}} & -\frac{1}{\mathbf{RC}}(1+k_{12}) & -\frac{1}{\mathbf{RC}}(1+k_{13}) & -\frac{1}{\mathbf{RC}}(1+k_{14}) \\ -\frac{k_{11}}{\mathbf{RC}} - \frac{k_{41}}{\mathbf{C}} & -\frac{1}{\mathbf{RC}} - \frac{k_{12}}{\mathbf{RC}} - \frac{k_{42}}{\mathbf{C}} & -\frac{1}{\mathbf{RC}} - \frac{k_{13}}{\mathbf{RC}} - \frac{k_{43}}{\mathbf{C}} & -\frac{1}{\mathbf{RC}} - \frac{k_{14}}{\mathbf{RC}} - \frac{k_{44}}{\mathbf{C}} \end{pmatrix} e(t) \\ \qquad + \begin{pmatrix} \frac{1}{\mathbf{C}} & 0 & -\frac{1}{\mathbf{C}} & 0 \\ 0 & 0 & 0 & 0 \\ 0 & \frac{1}{\mathbf{C}} & 0 & -\frac{1}{\mathbf{C}} \\ \frac{1}{\mathbf{C}} & 0 & -\frac{1}{\mathbf{C}} & 0 \end{pmatrix} \begin{pmatrix} \lambda_1(t) \\ \lambda_2(t) \\ \lambda_{1d}(t) \\ \lambda_{2d}(t) \end{pmatrix} \\ 0 \leq \begin{pmatrix} w_1(t) \\ w_2(t) \\ w_{1d}(t) \\ w_{2d}(t) \end{pmatrix} = \begin{pmatrix} 1 & 0 & 0 & 1 \\ k_{11} & k_{12} & 1+k_{13} & k_{14} \\ 0 & 0 & 0 & 0 \\ 0 & 0 & 0 & 0 \end{pmatrix} \begin{pmatrix} e_1(t) \\ e_2(t) \\ e_3(t) \\ e_4(t) \end{pmatrix} + \begin{pmatrix} \mathbf{R} & 0 & 0 & 0 \\ 0 & 0 & 0 & 0 \\ 0 & 0 & \mathbf{R} & 0 \\ 0 & 0 & 0 & 0 \end{pmatrix} \begin{pmatrix} \lambda_1(t) \\ \lambda_2(t) \\ \lambda_{1d}(t) \\ \lambda_{2d}(t) \end{pmatrix} \\ \qquad + \begin{pmatrix} x_{1d}(t) + x_{4d}(t) \\ x_{3d}(t) + u_{1d}(t) \\ x_{1d}(t) + x_{4d}(t) \\ x_{3d}(t) + u_{1d}(t) \end{pmatrix} \perp \begin{pmatrix} \lambda_1(t) \\ \lambda_2(t) \\ \lambda_{1d}(t) \\ \lambda_{2d}(t) \end{pmatrix} \geq 0 \end{cases} \tag{3.29}$$

Consider the following numerical simulation with the initial state $x(0^-) = (1,\ 3,\ -3,\ 1)$ and $x_d(0^-) = (1,\ 1,\ -3,\ 0)$ and with a time step $h = 0.01$. The value of the control gain K is given in (3.26). Take $i_{c1d}(t) = \sin 5t$, $i_{c2d} = 0.5 \sin 5t$, $i_{c3d}(t) = 0.2 \sin 3t$ and $u_{1d}(t) = \begin{cases} 1 & \text{if } t \leq 1 \\ -10 & \text{if } t \geq 1 \end{cases}$

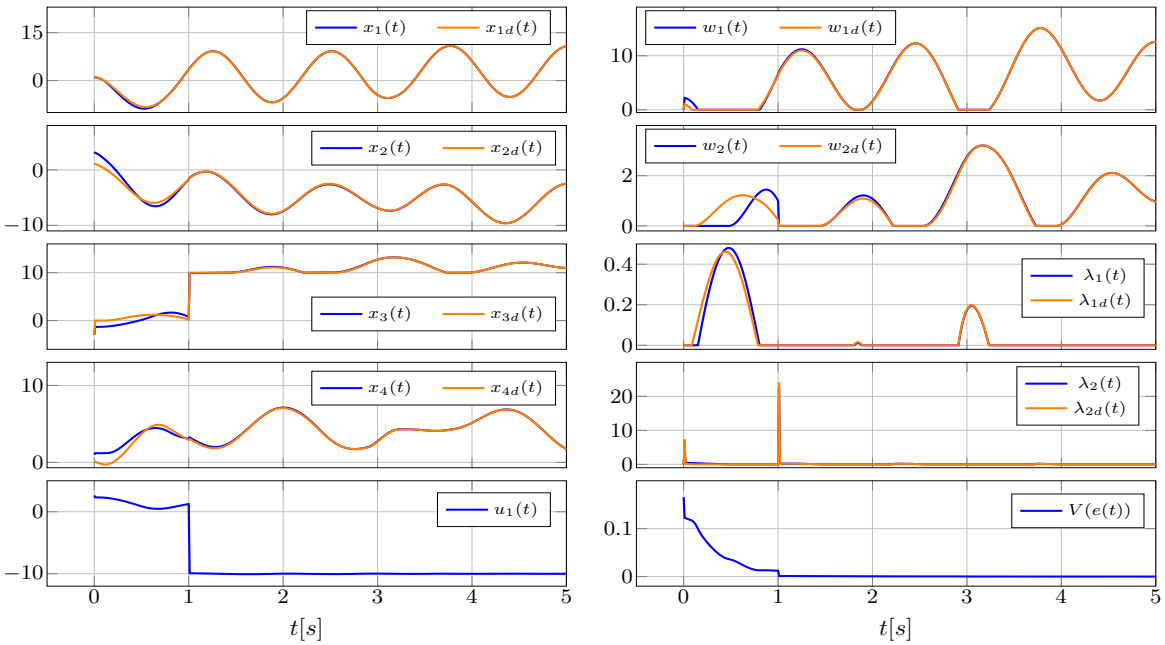

Figure 3.18: Numerical Simulation of the desired, the closed-loop and the error dynamics of LCS in (3.19). The numerical simulation show the complementarity variables λ and w, as well as the storage function of the error system $V(e(t))$.

The numerical simulation in Figure 3.18 shows two state jumps at $t = 0$ and $t = 1$s. At the initial time, the states x_3 and x_{3d} jump, but not to the same value, according to the conditions stated in sets $\mathcal{K}$ and $\mathcal{K}_d$ at $t = 0$, respectively. Another jump is observed in x_3 and x_{3d} at $t = 1$s due to the discontinuity in the controller u_1 at the same time $t = 1$s.

In the plot of the storage function of the error $V(e(t))$, it is noticeable that the variation of the storage function is negative during these jumps where $V(0^+) - V(0^-) < 0$ and $V(1^+) - V(1^-) < 0$. In addition, the complementarity variables λ_2 and λ_{2d} exhibit a Dirac measure at the times of the jumps (*i.e.*, at $t = 0$ and $t = 1$s).

3.4 Diode Bridge Example

Consider the diode bridge rectifier circuit in Figure 3.19. Let x_1 be the current passing through the inductor $\mathbf{L}$, x_2 be the voltage across the capacitor $\mathbf{C}_1$, and x_3 be the voltage across the capacitor $\mathbf{C}_2$. The dynamics are written as a linear complementarity system LCS and are given in (3.30), where $\lambda(t) \triangleq \left(i_{DF1},\ i_{DR1},\ -v_{DF2},\ i_{DR2}\right)^\top$ and $w(t) \triangleq \left(-v_{DF1},\ -v_{DR1},\ i_{DF2},\ -v_{DR2}\right)^\top$.

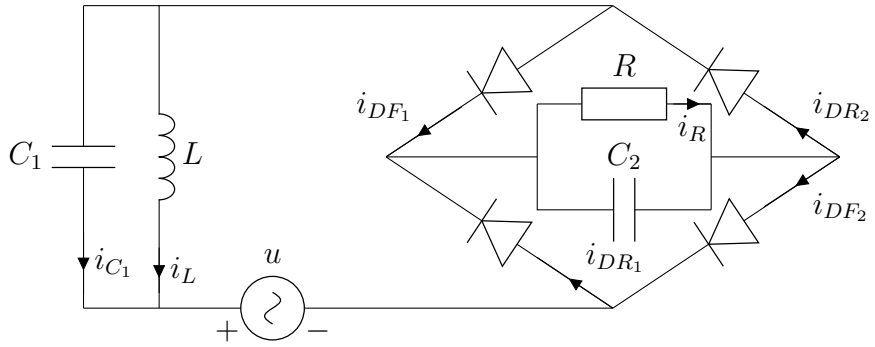

Figure 3.19: Diode Bridge with one controller

$$\begin{cases} \dot{x}(t) = \begin{pmatrix} 0 & \frac{1}{\mathbf{L}} & 0 \\ -\frac{1}{\mathbf{C}_1} & 0 & 0 \\ 0 & 0 & -\frac{1}{\mathbf{RC}_2} \end{pmatrix} x(t) + \begin{pmatrix} 0 & 0 & 0 & 0 \\ -\frac{1}{\mathbf{C}_1} & 0 & 0 & \frac{1}{\mathbf{C}_1} \\ \frac{1}{\mathbf{C}_2} & \frac{1}{\mathbf{C}_2} & 0 & 0 \end{pmatrix} \lambda(t) \\ 0 \leq \lambda(t) \perp w(t) = \begin{pmatrix} 0 & -1 & 1 \\ 0 & 0 & 1 \\ 0 & 0 & 0 \\ 0 & 1 & 0 \end{pmatrix} x(t) + \begin{pmatrix} 0 & 0 & -1 & 0 \\ 0 & 0 & -1 & 0 \\ 1 & 1 & 0 & -1 \\ 0 & 0 & 1 & 0 \end{pmatrix} \lambda(t) + \begin{pmatrix} -1 \\ 0 \\ 0 \\ 1 \end{pmatrix} u(t) \geq 0 \end{cases} \tag{3.30}$$

Clearly $PB = C^\top$ with $P = \mathbf{C}I_3$ when $\mathbf{C}_1 = \mathbf{C}_2 = \mathbf{C}$, and $D + D^\top = 0$ (*i.e.,* D is a skew-symmetric matrix). Numerical analysis shows that the BMI in (4.10) transformed to LMI for the closed-loop system's quadruple $(A, B, C+FK, D)$ has no solution. Thus, the closed-loop system with $u = K(x - x_d) + u_d$ is not strictly state passive, and the results from section 2.1 cannot be applied.

Let us add another controller (*i.e.,* voltage source) as shown in the circuit in Figure 3.20

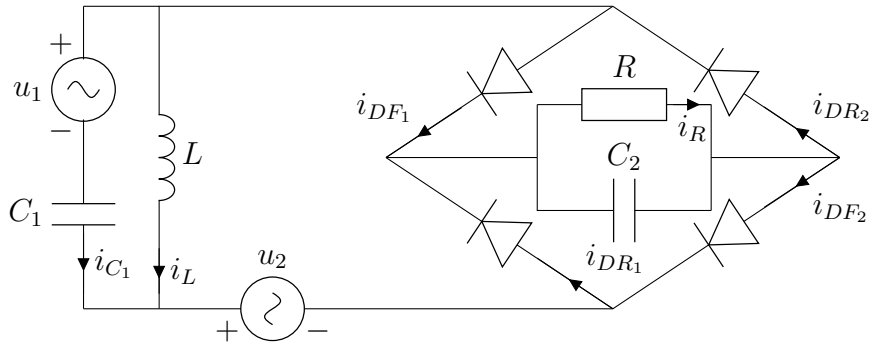

Figure 3.20: Diode Bridge with two controllers

The dynamics are given by the following LCS:

$$\begin{cases} \dot{x}(t) = \begin{pmatrix} 0 & \frac{1}{\mathbf{L}} & 0 \\ -\frac{1}{\mathbf{C}_1} & 0 & 0 \\ 0 & 0 & -\frac{1}{\mathbf{R}\mathbf{C}_2} \end{pmatrix} x(t) + \begin{pmatrix} 0 & 0 & 0 & 0 \\ -\frac{1}{\mathbf{C}_1} & 0 & 0 & \frac{1}{\mathbf{C}_1} \\ \frac{1}{\mathbf{C}_2} & \frac{1}{\mathbf{C}_2} & 0 & 0 \end{pmatrix} \lambda(t) + \begin{pmatrix} \frac{1}{\mathbf{L}} & 0 \\ 0 & 0 \\ 0 & 0 \end{pmatrix} u(t) \\ 0 \leq \lambda(t) \perp w(t) = \begin{pmatrix} 0 & -1 & 1 \\ 0 & 0 & 1 \\ 0 & 0 & 0 \\ 0 & 1 & 0 \end{pmatrix} x(t) + \begin{pmatrix} 0 & 0 & -1 & 0 \\ 0 & 0 & -1 & 0 \\ 1 & 1 & 0 & -1 \\ 0 & 0 & 1 & 0 \end{pmatrix} \lambda(t) + \begin{pmatrix} -1 & -1 \\ 0 & 0 \\ 0 & 0 \\ 1 & 1 \end{pmatrix} u(t) \geq 0 \end{cases} \tag{3.31}$$

The closed-loop system of the LCS with the external input $u = (u_1, u_2)^\top = K(x - x_d) + u_d$ where $K = \begin{pmatrix} k_{11} & k_{12} & k_{13} \\ k_{21} & k_{22} & k_{23} \end{pmatrix}$ is given by:

$$\begin{cases} \dot{x} = \begin{pmatrix} \frac{k_{11}}{\mathbf{L}} & \frac{1}{\mathbf{L}} + \frac{k_{12}}{\mathbf{L}} & \frac{k_{13}}{\mathbf{L}} \\ -\frac{1}{\mathbf{C}_1} & 0 & 0 \\ 0 & 0 & -\frac{1}{\mathbf{R}\mathbf{C}_2} \end{pmatrix} x(t) + \begin{pmatrix} 0 & 0 & 0 & 0 \\ -\frac{1}{\mathbf{C}_1} & 0 & 0 & \frac{1}{\mathbf{C}_1} \\ \frac{1}{\mathbf{C}_2} & \frac{1}{\mathbf{C}_2} & 0 & 0 \end{pmatrix} \lambda(t) - \begin{pmatrix} \frac{k_{11}}{\mathbf{L}} & \frac{k_{12}}{\mathbf{L}} & \frac{k_{13}}{\mathbf{L}} \\ 0 & 0 & 0 \\ 0 & 0 & 0 \end{pmatrix} x_d(t) \\ \qquad + \begin{pmatrix} \frac{1}{\mathbf{L}} & 0 \\ 0 & 0 \\ 0 & 0 \end{pmatrix} u_d(t) \\ 0 \leq \lambda(t) \perp w(t) = \begin{pmatrix} -k_{11} - k_{21} & -1 - k_{12} - k_{22} & 1 - k_{13} - k_{23} \\ 0 & 0 & 1 \\ 0 & 0 & 0 \\ k_{11} + k_{21} & 1 + k_{12} + k_{22} & k_{13} + k_{23} \end{pmatrix} x(t) \\ \qquad + \begin{pmatrix} 0 & 0 & -1 & 0 \\ 0 & 0 & -1 & 0 \\ 1 & 1 & 0 & -1 \\ 0 & 0 & 1 & 0 \end{pmatrix} \lambda(t) - \begin{pmatrix} -k_{11} - k_{21} & -k_{12} - k_{22} & -k_{13} - k_{23} \\ 0 & 0 & 0 \\ 0 & 0 & 0 \\ k_{11} + k_{21} & k_{12} + k_{22} & k_{13} + k_{23} \end{pmatrix} x_d(t) \\ \qquad + \begin{pmatrix} -1 & -1 \\ 0 & 0 \\ 0 & 0 \\ 1 & 1 \end{pmatrix} u(t) \geq 0 \end{cases} \tag{3.32}$$

The BMI of the closed-loop system's quadruple $(A+EK, B, C+FK, D)$ is transformed into an LMI according to Appendix A.1 and solved using MOSEK. Take $\mathbf{L} = 0.5$ H, $\mathbf{C}_1 = 0.25$ F, $\mathbf{R} = 1$ ohms, and $\mathbf{C}_2 = 0.025$ F, the solution is given by:

$$P = \begin{pmatrix} 0.0008 & -0.0001 & 0 \\ -0.0001 & 0.0008 & 0 \\ 0 & 0 & 0.024 \end{pmatrix} \quad \text{and} \quad K = \begin{pmatrix} -0.54 & 1.07 & -0.003 \\ 0.54 & -2.068 & 0.003 \end{pmatrix} \tag{3.33}$$

with $\epsilon = 0.1$ and where $PB = (C + FK)^\top$ holds. Thus, the closed-loop system in (3.32) with $u = (u_1, u_2)^\top$ is strictly state passive.

Consider the following numerical simulation with the initial states $x(0) = (3, \ , -1 \ , -5)^\top$ and $x_d(0) = (-2, \ , 2 \ , -3)^\top$ and with a time step $h = 0.01$. Take the desired external inputs as $u_{1d}(t) = 5 \sin 3t$ and $u_{2d}(t) = \sin 2t$.

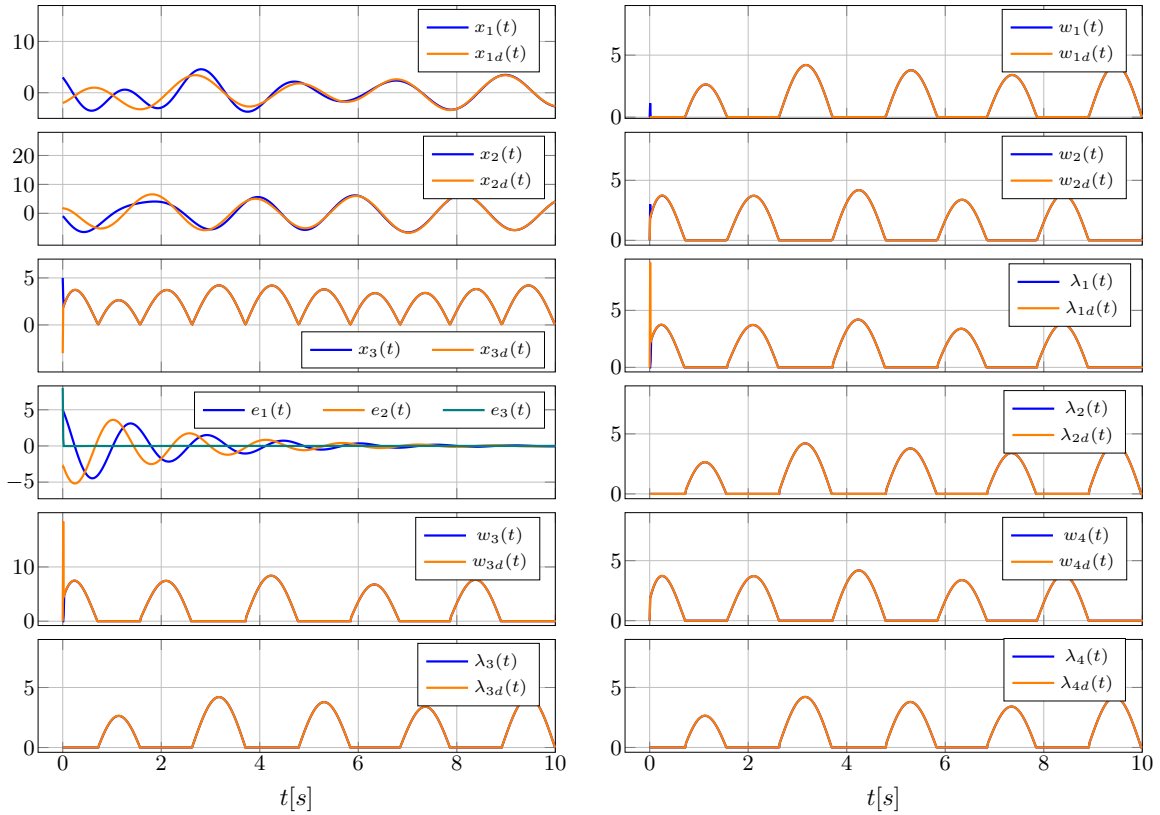

Figure 3.21: Numerical Simulation of the desired, the closed-loop and the error dynamics of LCS in (3.31). The numerical simulation show the complementarity variables λ and w.

The numerical simulation in Figure 3.21 shows that the error $e = x - x_d$ converges to zero, confirming the result stated in Proposition 2.1.8 for a strictly state passive system without uncertainties. The plot of the state x_3 (*i.e.*, the voltage across the capacitor C_2) represents the output of the diode bridge and displays a full-wave rectified voltage. An interesting observation from the plot is that both states x_3 and x_{3d} jumps at $t = 0$, resulting in a jump in the error $e_3 = x_3 - x_{3d}$ at $t = 0$, which converges promptly to zero. This jump occurs due to the initial values assigned to the states x_3 and x_{3d} such that the complementarity constraints are not satisfied at the initial time. As a result of the coupling between the states and the complementarity variables in the LCS (3.31), it is noticeable that some of the complementarity variables such as w_3, λ_1 exhibit a Dirac measure at $t = 0$ (the jump time of x_3).

3.5 Networks with Unilateral Interactions

This example focuses on the study of trajectory tracking for a system of networks with unilateral interactions with inputs. Let us present an example of a network with

unilateral interactions [110]. These systems can be treated as LCS [37], and by adding exogenous signals, they can be formulated as LCS with external inputs as in (1.1). They find applications in various fields such as sensor network, robotics, and game theory. Let us consider the following dynamics:

$$\begin{cases} \dot{x}_1(t) = \max(0, x_3(t) - x_1(t) - u_1(t)) + u_2(t) \\ \dot{x}_2(t) = x_1(t) - x_2(t) + \min(0, x_3(t) - x_2(t) + u_3(t)) + u_4(t) \\ \dot{x}_3(t) = \max(0, x_1(t) - x_3(t) - u_5(t)) + u_6(t) \end{cases} \tag{3.34}$$

which is written in the form of the LCS in (1.1) with [37, Equation (3.16)]:

$$A = \begin{pmatrix} 0 & 0 & 0 \\ 1 & -1 & 0 \\ 0 & 0 & 0 \end{pmatrix}, \quad B = \begin{pmatrix} 1 & 0 & 0 \\ 0 & -1 & 0 \\ 0 & 0 & 1 \end{pmatrix}, \quad C = \begin{pmatrix} 1 & 0 & -1 \\ 0 & -1 & 1 \\ -1 & 0 & 1 \end{pmatrix}, \quad D = \begin{pmatrix} 1 & 0 & 0 \\ 0 & 1 & 0 \\ 0 & 0 & 1 \end{pmatrix},$$

$$E = \begin{pmatrix} 0 & 1 & 0 & 0 & 0 & 0 \\ 0 & 0 & 0 & 1 & 0 & 0 \\ 0 & 0 & 0 & 0 & 0 & 1 \end{pmatrix} \quad \text{and} \quad F = \begin{pmatrix} 1 & 0 & 0 & 0 & 0 & 0 \\ 0 & 0 & 1 & 0 & 0 & 0 \\ 0 & 0 & 0 & 0 & 1 & 0 \end{pmatrix} \tag{3.35}$$

The desired system is defined by the LCS in (2.1) with the same plant matrices in (3.35).

Remark 3.5.1. *In this analysis, the most general form of inputs is chosen (they appear in both the linear and the nonsmooth parts of the dynamics). It is out of the scope of this analysis to justify the feasibility of such inputs. The well-posedness of this LCS easily follows from section 1.2.2 item 1.*

First case: Complete controller

Let $u = \begin{pmatrix} u_1 & u_2 & u_3 & u_4 & u_5 & u_6 \end{pmatrix}^\top$. The closed-loop system with $u(t) = K[x(t) - x_d(t)] + u_d(t)$ where $K = \begin{pmatrix} k_{11} & k_{21} & k_{31} & k_{41} & k_{51} & k_{61} \\ k_{12} & k_{22} & k_{32} & k_{42} & k_{52} & k_{62} \\ k_{13} & k_{23} & k_{33} & k_{43} & k_{53} & k_{63} \end{pmatrix}^\top$ is written in the form of the LCS in (2.3) with

$$\begin{cases} \dot{x}(t) = \begin{pmatrix} k_{21} & k_{22} & k_{23} \\ 1 + k_{41} & -1 + k_{42} & k_{43} \\ k_{61} & k_{62} & k_{63} \end{pmatrix} x(t) + \begin{pmatrix} 1 & 0 & 0 \\ 0 & -1 & 0 \\ 0 & 0 & 1 \end{pmatrix} \lambda(t) - \begin{pmatrix} k_{21} & k_{22} & k_{23} \\ k_{41} & k_{42} & k_{43} \\ k_{61} & k_{62} & k_{63} \end{pmatrix} x_d(t) + \begin{pmatrix} u_{2d}(t) \\ u_{4d}(t) \\ u_{6d}(t) \end{pmatrix} \\ 0 \le \lambda(t) \perp w(t) = \begin{pmatrix} 1 + k_{11} & k_{12} & -1 + k_{13} \\ k_{31} & -1 + k_{32} & 1 + k_{33} \\ -1 + k_{51} & k_{52} & 1 + k_{53} \end{pmatrix} x(t) + \begin{pmatrix} 1 & 0 & 0 \\ 0 & 1 & 0 \\ 0 & 0 & 1 \end{pmatrix} \lambda(t) \\ \qquad - \begin{pmatrix} k_{11} & k_{12} & k_{13} \\ k_{31} & k_{32} & k_{33} \\ k_{51} & k_{51} & k_{53} \end{pmatrix} x_d(t) + \begin{pmatrix} u_{1d}(t) \\ u_{3d}(t) \\ u_{5d}(t) \end{pmatrix} \ge 0 \end{cases} \tag{3.36}$$

The solution of the BMI in (4.10) which is transformed to LMI (see Appendix A.1) with $\epsilon = 0.001$ for the closed-loop system in (3.36)

$$K = \begin{pmatrix} -0.43 & -0.003 & 0.996 \\ -0.497 & -0.017 & 0.0029 \\ 0.003 & 0.431 & -0.996 \\ -0.97 & 0.5 & -0.003 \\ 0.996 & -0.003 & -0.43 \\ 0.002 & 0.009 & -0.497 \end{pmatrix} \quad \text{and} \quad P = \begin{pmatrix} 0.57 & -0.003 & -0.003 \\ -0.0032 & 0.57 & -0.003 \\ -0.003 & -0.003 & 0.57 \end{pmatrix}$$

Hence, the closed-loop system's quadruple $(A + EK, B, C + FK, D)$ is strictly state passive. Take $x(0) = (-1, 1, 0)^\top$, $x_d(0) = (1, 2, -1)^\top$ and $u_d = \begin{pmatrix} \sin t & \cos t & \sin 2t & \cos 2t & \sin 3t & \cos 3t \end{pmatrix}^\top$. The numerical simulation is shown below with time step $h = 0.01$s (see Figure 3.22).

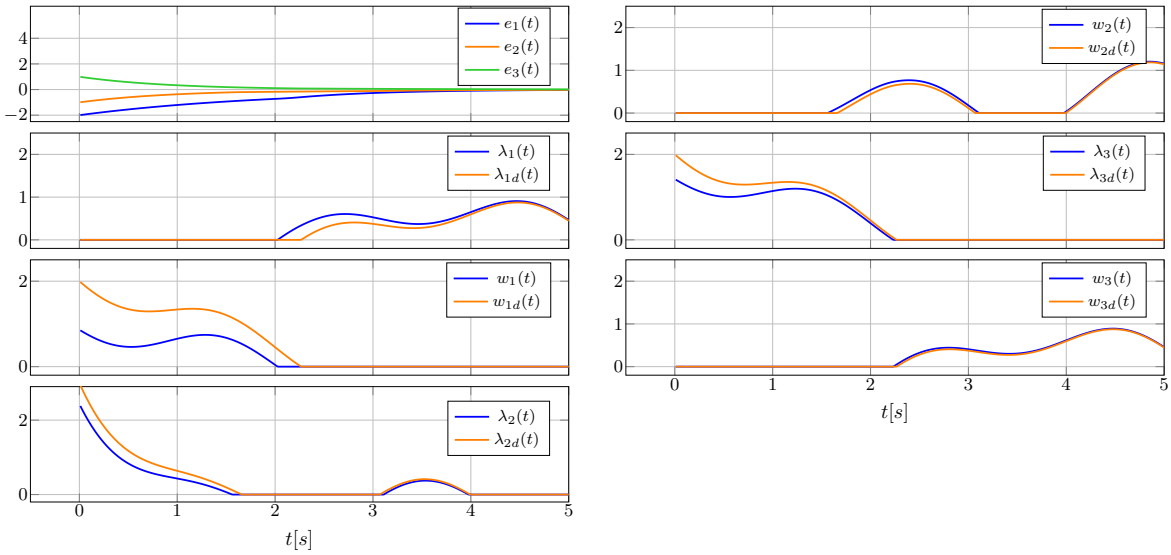

Figure 3.22: Numerical simulation showing the tracking error $e = x - x_d$ of the Network dynamics in (3.34) controlled by the complete controller u. The simulation also shows the behaviour of the complementarity variables λ and w.

In this case, the closed-loop quadruple $(A+EK, B, C+FK, D)$ is strongly passive. Thus, the system can be studied within the framework of section 2.4 which allows the consideration of uncertainties.

Second case: $u = \begin{pmatrix} u_2 & u_4 & u_6 \end{pmatrix}^\top$

The solution is:

$$K = \begin{pmatrix} 0 & -0.87 & 0 & -0.16 & 0 & 0.26 \\ 0 & -0.42 & 0 & 0.327 & 0 & 0.233 \\ 0 & 0.18 & 0 & -0.0001 & 0 & -1.27 \end{pmatrix}^\top \quad \text{and} \quad P = \begin{pmatrix} 0.99 & -0.085 & -0.26 \\ -0.085 & 0.72 & -0.2 \\ -0.26 & -0.2 & 1.18 \end{pmatrix}$$

Hence, the closed-loop system $(A+EK, B, C, D)$ is strictly state passive. Take $x(0) = (-2, 1, 1)^\top$, $x_d(0) = (2, -5, -1)^\top$ and $u_d = \begin{pmatrix} \sin t & \cos t & \sin 2t & \cos 2t & \sin 3t & \cos 3t \end{pmatrix}^\top$. The numerical simulation is shown below with time step $h = 0.01$s (see Figure 3.23).

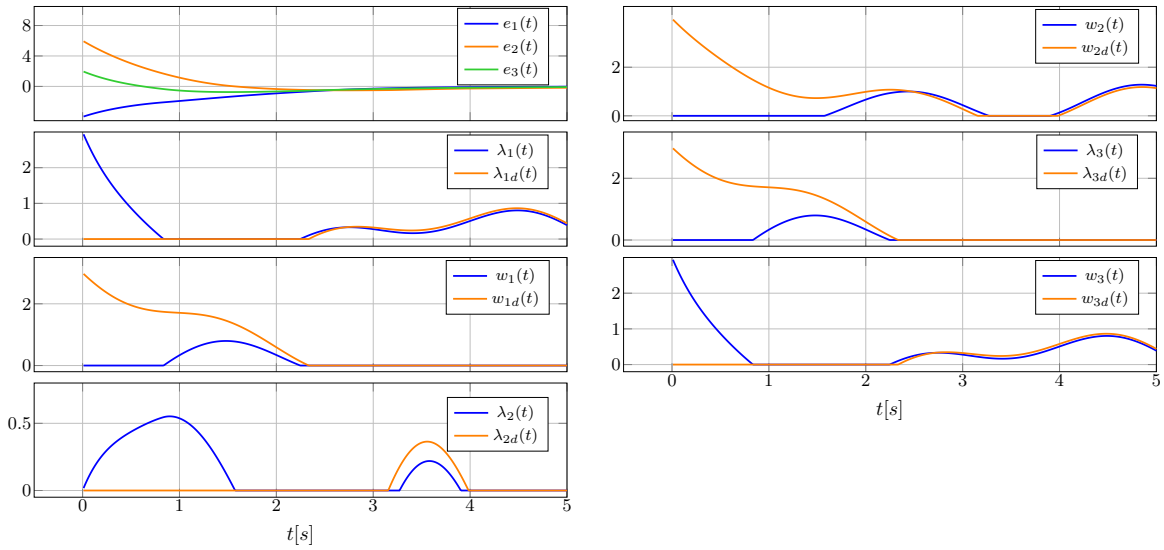

Figure 3.23: Numerical simulation showing the tracking error $e = x - x_d$ of the Network dynamics in (3.34) with the active controller $u = (u_2, u_4, u_6)^\top$ included in the linear part of the LCS in (3.34). The simulation also shows the behaviour of the complementarity variables λ and w.

It is important to note that, in this case, the closed-loop quadruple $(A+EK, B, C, D)$ is strongly passive. This property allows us to analyse the problem of trajectory tracking in the presence of uncertainties (see section 2.4). However, whether or not considering such uncertainties in networks with unilateral interactions makes sense, is out of the scope of this thesis.

Third case: $u = \begin{pmatrix} u_1 & u_3 & u_5 \end{pmatrix}^\top$

The BMI in (4.10) has no solution. Hence, the quadruple of the closed-loop system $(A, B, C + FK, D)$ cannot be made strictly state passive with such a set of inputs and the chosen feedback, and the framework developed in the foregoing sections does not apply. It is noteworthy that the conclusions are still valid even if we consider $G \neq 0$.

3.6 Nonsmooth Mechanical Systems with Unilateral Springs

It is known that unilateral spring/dashpot contact/impact models, can be written in a complementarity framework [26, 37, 27, 11]. This class of contact/impact models significantly differs from unilateral constraints which yield complementarity constraints and impact models as in Remark 3.6.1

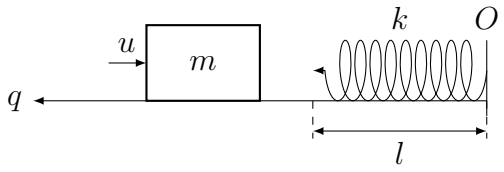

Figure 3.24: Mechanical system with unilateral spring.

Consider the mechanical system in Figure 3.24 which possesses the following dynamics:

$$\begin{cases} m\ddot{q}(t) = u(t) + \lambda(t) \\ 0 \leq \lambda(t) \perp w(t) = \lambda(t) + k(q(t) - l) \geq 0 \end{cases} \tag{3.37}$$

where $q - l$ is the deformation of the spring, $k > 0$ is the stiffness of the spring. The complementarity constraint is written between the contact force and the signed distance between the spring and the mass. Clearly the dynamics (3.37) fits with our general framework. Let $x = (x_1, x_2)^\top = (q - l, \dot{q})^\top$, (3.37) is rewritten equivalently as the LCS:

$$\begin{cases} \dot{x}(t) = \begin{pmatrix} 0 & 1 \\ 0 & 0 \end{pmatrix} x(t) + \begin{pmatrix} 0 \\ \frac{1}{m} \end{pmatrix} \lambda(t) + \begin{pmatrix} 0 \\ \frac{1}{m} \end{pmatrix} u(t) \\ 0 \leq \lambda(t) \perp w(t) = \lambda(t) + kx_1(t) \geq 0 \end{cases} \tag{3.38}$$

Here $A = \begin{pmatrix} 0 & 1 \\ 0 & 0 \end{pmatrix}$, $B = E = \begin{pmatrix} 0 \\ \frac{1}{m} \end{pmatrix}$, $C = (k, 0)$, $D = 1$, $F = 0$, and the system has AC solutions with uniqueness, see section 1.2.2 item 1. The quadruple (A, B, C, D) can be made strongly passive with state feedback $u = Kx = k_1x_1 + k_2x_2$. This means that there exists a control gain $K = (k_1, k_2)$ such that the quadruple $(A + EK, B, C, D)$ of the closed-loop system is strongly passive. Equivalently, the BMI in (2.7) has a solution after being transformed into an LMI, as detailed in Appendix A.1 and the solution is given by:

$$P = \begin{pmatrix} 7.863 & 0.538 \\ 0.538 & 0.337 \end{pmatrix} \quad \text{and} \quad K = \begin{pmatrix} -21.38 & -2.148 \end{pmatrix}$$

with $m = 1\text{kg}$ and $k = 5\text{N/m}$. Thus, the results in section 2.4.2 apply to this example. As the stiffness of the spring k increases, the control gain gives very large numerical values like $k_1 = -1.2 \times 10^7$ for $k = 100\text{N/m}$. This is explained analytically by explicitly writing the matrix inequality in (2.7) and verifying the positive definiteness conditions. Following the matrix M in (4.10), the matrix inequality is written as:

$$\begin{pmatrix} -\frac{2p_{12}k_1}{m} & -p_{11} - \frac{p_{12}k_2}{m} - \frac{p_{22}k_1}{m} & -\frac{p_{12}}{m} + k \\ -p_{11} - \frac{p_{12}k_2}{m} - \frac{p_{22}k_1}{m} & -2p_{12} - \frac{2p_{22}k_2}{m} & -\frac{p_{22}}{m} \\ -\frac{p_{12}}{m} + k & -\frac{p_{22}}{m} & 2 \end{pmatrix} \succ 0$$

with $P = \begin{pmatrix} p_{11} & p_{12} \\ p_{12} & p_{22} \end{pmatrix} \succ 0$. One of the necessary conditions to be satisfied is:

$$2 \times \begin{pmatrix} -\frac{2p_{12}k_1}{m} & -p_{11} - \frac{p_{12}k_2}{m} - \frac{p_{22}k_1}{m} \\ -p_{11} - \frac{p_{12}k_2}{m} - \frac{p_{22}k_1}{m} & -2p_{12} - \frac{2p_{22}k_2}{m} \end{pmatrix} - \begin{pmatrix} \left(-\frac{2p_{12}}{m} + k\right)^2 & 0 \\ 0 & 0 \end{pmatrix} \succ 0$$

Given that $-\frac{p_{12}k_1}{m} > 0$ which is a necessary condition for positive definiteness, thus for strong passivity of the quadruple $(A+EK, B, C, D)$, it is required to prove that: $-\frac{4p_{12}k_1}{m} - \left(-\frac{2p_{12}}{m} + k\right)^2 > 0$. This condition implies that if $k \to +\infty$, then $k_1 \to +\infty$. This conclusion is similar to the result in [26, section 7.6] [34] which deals with quadratic stabilization of the same system. It demonstrates the limitation of the stabilization approach which certainly provides conservative sufficient conditions.

It is seen that, in a certain sense, this class of mechanical systems (with $D > 0$ and $F = 0$) lies in-between the unilaterally constrained mechanical systems (with always $D = 0$ and $F = 0$), and LCS (with possibly both D and F nonzero).

Remark 3.6.1 (Linear Complementarity Lagrangian Systems)**.** *Linear Lagrangian systems with unilateral constraints have the nonlinear nonsmooth dynamics:*

$$\begin{cases} M\ddot{q}(t) + R\dot{q}(t) + Sq(t) = u(t) + C_q^\top \lambda(t) \\ 0 \le \lambda(t) \perp w(t) = C_q q(t) + F_q \ge 0 \\ C_q\dot{q}(t^+) = -e_{\mathrm{n}} C_q \dot{q}(t) \text{ if } C_q q(t) = 0 \text{ and } C_q\dot{q}(t^-) \le 0, \end{cases} \tag{3.39}$$

where $q(t) \in \mathbb{R}^n$, $M = M^\top \succ 0$, the restitution coefficient $e_{\mathrm{n}} \in [0,1]$, $R \succcurlyeq 0$ is a Rayleigh dissipation matrix [39, Definition 6.12], $S \succcurlyeq 0$ is a stiffness matrix, and it is assumed that $\dot{q}$ has left and right limits. For simplicity, we also assume that there is a unique unilateral constraint, i.e., *$C_q \in \mathbb{R}^{1\times n}$, $\lambda \in \mathbb{R}$ and $F_q \in \mathbb{R}$ is a constant (the system's admissible domain in the configuration space, is a convex polyhedral set, assumed to be nonempty). Denoting $x = (q^\top, \dot{q}^\top)^\top$, $x_1 = q$, $x_2 = \dot{q}$, we obtain:*

$$\begin{cases} \dot{x}(t) = \begin{pmatrix} 0 & I_n \\ -M^{-1}S & -M^{-1}R \end{pmatrix} x(t) + \begin{pmatrix} 0 \\ M^{-1} \end{pmatrix} u(t) + \begin{pmatrix} 0 \\ M^{-1}C_q^\top \end{pmatrix} \lambda(t) \\ 0 \le \lambda(t) \perp w(t) = Cx(t) + F_q = (C_q, 0)x(t) + F_q \ge 0 \\ C\dot{x}(t^+) = -e_{\mathrm{n}} C\dot{x}(t^-) \text{ if } Cx(t) = 0 \text{ and } C\dot{x}(t^-) \le 0. \end{cases} \tag{3.40}$$

Therefore, $A = \begin{pmatrix} 0 & I_n \\ -M^{-1}S & -M^{-1}R \end{pmatrix}$, $B = \begin{pmatrix} 0 \\ M^{-1}C_q^\top \end{pmatrix}$, $E = \begin{pmatrix} 0 \\ M^{-1} \end{pmatrix}$, $F = 0$, $C = (C_q, 0)$, $D = 0$. Since $D = 0$ and no control acts in the complementarity constraint, passivity implies that $PB = C^\top$ whatever the controller $u(x) = Kx$. It can be checked that this is not possible with $P \succ 0$. Adding a multiplier feedback $u(x,\lambda) = Kx + G\lambda$ does not change the conclusion. Fundamentally, systems as (3.40) have a relative degree 2 when λ is seen as the input and w is seen as the output [26] (hence hampering passivity [39]), while systems as in (3.38) have a relative degree 0 between the same input/output variables.

Conclusion

This chapter studies various numerical applications on electrical circuits, networks with unilateral interactions and mechanical systems with unilateral springs, which illustrate the theoretical developments in Chapter 2. The controller gains are computed using MOSEK 9.3.14 solver, and numerical simulations are performed using the software package SICONOS. The analysis of electrical circuits in this chapter shows how the

structure of the circuit affects its passivity properties. So, different approaches are proposed, such as changing the type of the controller to enhance the passivity of the circuit.

Chapter 4

Trajectory Tracking in Frictional Oscillators

This chapter addresses the problem of trajectory tracking control in frictional oscillators. First, the dynamics of frictional oscillators are represented within the framework of complementarity systems, which is followed by analysis of the stick/slip behaviour of the desired system. Then, the stability analysis of the error dynamics in nominal case is investigated based on theoretical results derived in Chapter 2. These results are extended to tackle the case with parametric uncertainties. In this case, strong passivity assumption is relaxed to strict state passivity for the stability analysis of the error dynamics in the presence of uncertainties. In addition, this chapter introduces a new approach for the control design, based on passifying the friction model when Stribeck effect is considered, along with analyzing the stability of the error dynamics. Theoretical findings in this chapter are supported by numerical simulations made with SICONOS.

4.1 Friction Modeling

There is a plethora of friction models, and the analysis and the control of systems with friction has witnessed a huge number of articles in the past thirty years both in the Automatic Control and in the Nonlinear Dynamics scientific communities. Roughly speaking, friction models of interest for Control may be classified as follows: static models (which may be set-valued or single-valued, with constant or with varying friction coefficient), and dynamic models which aim at incorporating pre-sliding effects, bristle effects, hysteretic behaviours, *etc.* Static models comprise Coulomb's friction with constant coefficient or varying coefficient (*e.g.*, Stribeck [12, 105], Dieterich-Ruina [41, Equation (21)]), which are set-valued at zero relative tangential velocity, as well as regularized models (mainly applied to planar friction where the signum function is replaced by a saturation, or a sigmoid function). Set-valuedness at zero tangential velocity allows to correctly handle sticking modes (contrarily to regularized models) and is thus essential in multibody applications. Dynamic models with internal state are numerous (LuGre, Leuven, Bliman-Sorine, Dahl, elastoplastic *etc* [105]). Dynamic models are better for modeling micro stick-slip effects, though Coulomb with Stribeck

coefficient of friction also provides good results in this respect [105]. However, dynamic models also present severe drawbacks [133, 137]. Coulomb friction (with constant coefficient) has limitations [41], but it can also provide quite good results in many instances, see, *e.g.*, [111, 102, 59]. It is sometimes not easy task to choose between a regularized (around zero tangential velocity) model and the set-valued model, see, *e.g.*, [149]. It is inferred that conducting preliminary research work using the set-valued Coulomb's model (with constant coefficient of friction) is a reasonable path for trajectory traking, keeping in mind that Stribeck effects, which render the system nonlinear, can be included in the analysis: this will be done in this work, within a robustness analysis. Finally see [15] for a survey on friction models.

4.2 Controlled Frictional Oscillators

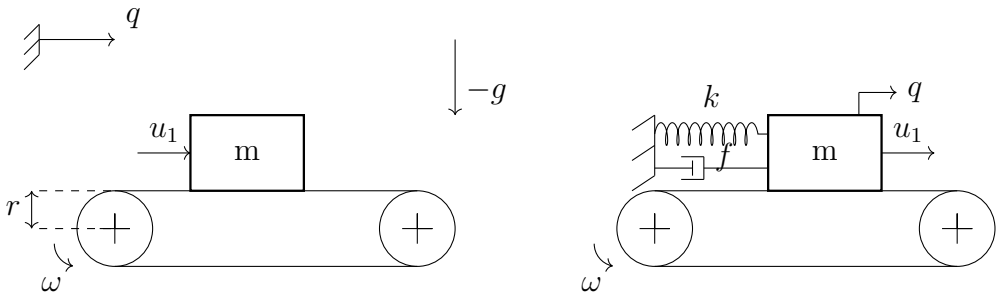

(a) (b)

Figure 4.1: Simple frictional oscillators with Coulomb's friction

Consider the simple frictional oscillator system depicted in Figure 4.1a. The objective is to perform trajectory tracking for the mass m. Two main steps will be tackled: first, we assume that the pulleys can be given arbitrary angular velocity in this Chapter, second, the pulley-belt system dynamics is taken into account in Chapter 5. Assuming that the belt can be given arbitrary velocity, its dynamics are given by:

$$\ddot{q}(t) \in \frac{1}{m} u_1(t) - \mu g \, \mathrm{sgn}(\dot{q}(t) - u_2(t)) \tag{4.1}$$

with $u = (u_1, u_2)^\top$, $u_2 = r\omega$ is considered as a control input, $\mu > 0$ is the friction coefficient, ω rad/s is the pulleys' angular velocity, r is their radius, g is the gravity acceleration, m in kg is the mass weight. Notice that the dynamics (4.1) can be rewritten as $\ddot{q}(t) = \frac{1}{m} u_1(t) - \mu g \lambda_t(t)$, with $\lambda_t(t) \in \mathrm{sgn}(\dot{q}(t) - u_2(t))$. If $u_1 \equiv 0$ or if $u_1 = u_1(q, \dot{q}, t)$, then the dynamics (4.1) fit within the robot-object class of systems [25] where the robot's dynamics (the pulley-belt system) is neglected: the mass m is the object which can be controlled only through the contact force multiplier $\lambda_t(\cdot)$. Neglecting the friction effects on the belt dynamics so that the pulleys-belt's velocity can be considered not influenced by the friction with the mass, is a common assumption in the Nonlinear Dynamics literature [99, 96, 95, 63, 65, 139, 103], see also references therein. The system in Figure 4.1a represents a one-degree-of-freedom oscillator. In

this setting we may link the mass to a rigid wall with a linear spring-dashpot model as shown in Figure 4.1b, yielding the dynamics:

$$\ddot{q}(t) \in \frac{1}{m}u_1(t) - \frac{k}{m}(q(t) - l) - \frac{f}{m}\dot{q}(t) - \mu g \,\mathrm{sgn}(\dot{q}(t) - u_2(t)) \tag{4.2}$$

where $k > 0$ is the stiffness, $f > 0$ is the viscous friction coefficient, and l is the natural length of the spring. Under these conditions, the analysis made in the sequel shows that u_1 can be chosen as a feedforward controller that depends only on exogenous signals. It is also noteworthy that u_1 could be chosen as the displacement imposed to one tip of the spring, changing $k(q - l)$ to $k(q + u_1 - l)$ in (4.2). Provided that k is known, this does not modify the analysis made in the next sections.

Remark 4.2.1. *The system in (4.1) is fully actuated (if we consider both u_1 and u_2, then it is even overactuated with two independent inputs and one degree of freedom q). The system in (4.2) is fully actuated. As we shall see next, the passivity-based control strategy that is chosen uses the monotonicity of the set-valued part.*

4.2.1 The Complementarity System Framework

The dynamics (4.1) are equivalently rewritten in a complementarity systems framework as:

$$\begin{cases} \dot{x}(t) = \underbrace{\begin{pmatrix} 0 & 1 \\ 0 & 0 \end{pmatrix}}_{\triangleq A} x(t) + \underbrace{\begin{pmatrix} 0 & 0 \\ \frac{1}{m} & 0 \end{pmatrix}}_{\triangleq E} u(t) + \underbrace{\begin{pmatrix} 0 \\ \mu g \end{pmatrix}}_{\triangleq E'} + \underbrace{\begin{pmatrix} 0 & 0 \\ -2\mu g & 0 \end{pmatrix}}_{\triangleq B} \lambda(t) \\ 0 \leq \lambda(t) \perp w(t) = \underbrace{\begin{pmatrix} 0 & 1 \\ 0 & 0 \end{pmatrix}}_{\triangleq F} u(t) + \begin{pmatrix} 0 \\ 1 \end{pmatrix} + \underbrace{\begin{pmatrix} 0 & 1 \\ -1 & 0 \end{pmatrix}}_{\triangleq D} \lambda(t) + \underbrace{\begin{pmatrix} 0 & -1 \\ 0 & 0 \end{pmatrix}}_{\triangleq C} x(t) \geq 0, \end{cases} \tag{4.3}$$

with $x = (q, \dot{q})^\top$, $\lambda = (\lambda_1, \lambda_2)^\top$, $u = (u_1, u_2)^\top$. The complementarity conditions in (4.3) stem from the representation of the set-valued signum function [42]. It is verified that the quadruple (A, B, C, D) is passive with storage matrix $P = \begin{pmatrix} p_{11} & 0 \\ 0 & \frac{1}{2g} \end{pmatrix}$. There are two peculiarities to system (4.3): a) $D \succcurlyeq 0$ and $D + D^\top = 0$, b) there are constant terms $\begin{pmatrix} 0 \\ 1 \end{pmatrix} \notin \mathrm{Im}(F)$ and $E' = \begin{pmatrix} 0 \\ -\mu g \end{pmatrix} \in \mathrm{Im}(E)$, hence it does not fit with (1.1). Solutions to (4.3) are AC under some conditions on the control input, as discussed below. The first step is the computation of fixed points of (1.1) in the closed-loop, in order to determine whether or not a feedback controller of the form:

$$u(x, \lambda, t) = K[x - x_d(t)] + G[\lambda - \lambda_d(t)] + u_d(t). \tag{4.4}$$

with feedback gains $K \in \mathbb{R}^{2\times 2}$ and $G \in \mathbb{R}^{2\times 2}$, is able to modify the set of equilibria. Notice that $\lambda_1 = \frac{\lambda_t + 1}{2}$ where $\mu m g \lambda_t$ is the tangent interaction force between the mass and the belt, *i.e.*, $\lambda_t \in \mathrm{sgn}(\dot{q} - u_2)$. However, the multiplier λ_2 is a slack variable that has no clear mechanical meaning and may be assumed as non-measurable. It is

inferred that only λ_1 is available for feedback. Moreover, we avoid the use of λ_1 in u_1, for otherwise the tangential force could be compensated for directly: this is not a desirable control strategy. *Most importantly, our analysis applies to the case when the mass is attached to a rigid wall by a linear spring-dashpot system as in Figure 4.1b, while u_1 is to be interpreted as a feedforward controller, that depends only on $x_d(t)$ and $u_d(t)$. In such a setting, the tracking control problem is that of a mass+spring-dashpot system, with feedforward control and feedback control through the tangential contact force.* These observations constrain the input matrix G to satisfy $G = \begin{pmatrix} 0 & 0 \\ g_{21} & 0 \end{pmatrix}$. It is also noticed that a feedback using λ_2 is useless as it is unable to modify the matrix D_{cl} to get strong passivity ($\Rightarrow D_{cl} \succ 0$) instead of strict state passivity, because of the structure of the matrix F. In general, it is even better to assume $G = 0$. However, the subsequent analysis in section 4.5 shows that $g_{21} > 0$ allows to regularize the set-valued friction and to get robustness that is otherwise impossible to obtain. Thus, it is worth presenting it even if its implementation may remain questionable. Inserting (4.4) to (4.3), with the above restrictions on G, gives the closed-loop system dynamics:

$$\begin{cases} (a)\ \ \dot{x}(t) = \underbrace{\begin{pmatrix} 0 & 1 \\ \frac{k_{11}}{m} & \frac{k_{12}}{m} \end{pmatrix}}_{\triangleq A_{cl}} x(t) + \underbrace{\begin{pmatrix} 0 & 0 \\ -2\mu g & 0 \end{pmatrix}}_{\triangleq B_{cl}} \lambda(t) - \begin{pmatrix} 0 & 0 \\ \frac{k_{11}}{m} & \frac{k_{12}}{m} \end{pmatrix} x_d(t) + \begin{pmatrix} 0 \\ \mu g \end{pmatrix} \\ \qquad\qquad + \begin{pmatrix} 0 & 0 \\ \frac{1}{m} & 0 \end{pmatrix} u_d(t) \\ (b)\ \ 0 \le \lambda(t) \perp w(t) = \overbrace{\begin{pmatrix} k_{21} & -1+k_{22} \\ 0 & 0 \end{pmatrix}}^{\triangleq C_{cl}} x(t) + \overbrace{\begin{pmatrix} g_{21} & 1 \\ -1 & 0 \end{pmatrix}}^{\triangleq D_{cl}} \lambda(t) - \begin{pmatrix} k_{21} & k_{22} \\ 0 & 0 \end{pmatrix} x_d(t) \\ \qquad\qquad - \begin{pmatrix} g_{21} & 0 \\ 0 & 0 \end{pmatrix} \lambda_d(t) + \begin{pmatrix} u_{2d}(t) \\ 1 \end{pmatrix} \ge 0 \end{cases} \tag{4.5}$$

Remark 4.2.2. *No physical parameters appear in the complementarity conditions in (4.3) or (4.5), because the complementarity merely represents the set-valued signum function. This will have consequences on the robustness analysis (see section 4.5). It is noteworthy that even a feedback from λ_1 cannot guarantee strong passivity of the closed-loop, because at best $D_{cl} \succcurlyeq 0$. One question which arises is how much $g_{21} \neq 0$ can improve the robustness with respect to uncertainties in μ.*

The desired system is:

$$\begin{cases} \dot{x}_d(t) = \begin{pmatrix} 0 & 1 \\ 0 & 0 \end{pmatrix} x_d(t) + \begin{pmatrix} 0 & 0 \\ \frac{1}{m} & 0 \end{pmatrix} u_d(t) + \begin{pmatrix} 0 \\ \mu g \end{pmatrix} + \begin{pmatrix} 0 & 0 \\ -2\mu g & 0 \end{pmatrix} \lambda_d(t) \\ 0 \le \lambda_d(t) \perp w_d(t) = \begin{pmatrix} 0 & 1 \\ 0 & 0 \end{pmatrix} u_d(t) + \begin{pmatrix} 0 \\ 1 \end{pmatrix} + \begin{pmatrix} 0 & 1 \\ -1 & 0 \end{pmatrix} \lambda_d(t) + \begin{pmatrix} 0 & -1 \\ 0 & 0 \end{pmatrix} x_d(t) \ge 0, \end{cases} \tag{4.6}$$

where $x_d = (q_d, \dot{q}_d)^\top = (x_{1d}, x_{2d})^\top$. This is equivalent to its differential inclusion form:

$$\ddot{q}_d(t) \in \frac{1}{m} u_{1d}(t) - \mu g \lambda_{t,d}(t), \quad \lambda_{t,d}(t) \in \operatorname{sgn}(\dot{q}_d(t) - u_{2d}(t)) \tag{4.7}$$

The closed-loop error dynamics $e = x - x_d$ is:

$$\begin{cases} \dot{e}(t) = \left(\begin{pmatrix} 0 & 1 \\ 0 & 0 \end{pmatrix} + \begin{pmatrix} 0 & 0 \\ \frac{1}{m} & 0 \end{pmatrix} K \right) e(t) + \left(\begin{pmatrix} 0 & 0 \\ -2\mu g & 0 \end{pmatrix} + \begin{pmatrix} 0 & 0 \\ \frac{1}{m} & 0 \end{pmatrix} G \right) (\lambda(t) - \lambda_d(t)) \\ 0 \leq \lambda_d(t) \perp w_d(t) = \begin{pmatrix} 0 & 1 \\ 0 & 0 \end{pmatrix} u_d(t) + \begin{pmatrix} 0 \\ 1 \end{pmatrix} + \begin{pmatrix} 0 & 1 \\ -1 & 0 \end{pmatrix} \lambda_d(t) + \begin{pmatrix} 0 & -1 \\ 0 & 0 \end{pmatrix} x_d(t) \geq 0 \\ 0 \leq \lambda(t) \perp w(t) = \left(\begin{pmatrix} 0 & 1 \\ 0 & 0 \end{pmatrix} K + \begin{pmatrix} 0 & -1 \\ 0 & 0 \end{pmatrix} \right) e(t) - \begin{pmatrix} 0 & 1 \\ 0 & 0 \end{pmatrix} G \lambda_d(t) + \begin{pmatrix} 0 & 1 \\ 0 & 0 \end{pmatrix} u_d(t) \\ \qquad + \left(\begin{pmatrix} 0 & 1 \\ -1 & 0 \end{pmatrix} + \begin{pmatrix} 0 & 1 \\ 0 & 0 \end{pmatrix} G \right) \lambda(t) + \begin{pmatrix} 0 & -1 \\ 0 & 0 \end{pmatrix} x_d(t) + \begin{pmatrix} 0 \\ 1 \end{pmatrix} \geq 0, \end{cases} \tag{4.8}$$

which is equivalent to:

$$\begin{cases} \dot{e}(t) = \overbrace{\begin{pmatrix} 0 & 1 \\ \frac{k_{11}}{m} & \frac{k_{12}}{m} \end{pmatrix}}^{A_{cl}} e(t) + \overbrace{\begin{pmatrix} 0 & 0 \\ -2\mu g & 0 \end{pmatrix}}^{B_{cl}} (\lambda(t) - \lambda_d(t)) \\ 0 \leq \lambda_d(t) \perp w_d(t) = \begin{pmatrix} 0 & 1 \\ 0 & 0 \end{pmatrix} u_d(t) + \begin{pmatrix} 0 \\ 1 \end{pmatrix} + \begin{pmatrix} 0 & 1 \\ -1 & 0 \end{pmatrix} \lambda_d(t) + \begin{pmatrix} 0 & -1 \\ 0 & 0 \end{pmatrix} x_d(t) \geq 0 \\ 0 \leq \lambda(t) \perp w(t) = \underbrace{\begin{pmatrix} k_{21} & k_{22} - 1 \\ 0 & 0 \end{pmatrix}}_{C_{cl}} e(t) - \begin{pmatrix} g_{21} & 0 \\ 0 & 0 \end{pmatrix} \lambda_d(t) + \begin{pmatrix} 0 \\ 1 \end{pmatrix} + \underbrace{\begin{pmatrix} g_{21} & 1 \\ -1 & 0 \end{pmatrix}}_{D_{cl}} \lambda(t) \\ \qquad + \begin{pmatrix} 0 & -1 \\ 0 & 0 \end{pmatrix} x_d(t) + \begin{pmatrix} 0 & 1 \\ 0 & 0 \end{pmatrix} u_d(t) \geq 0 \end{cases} \tag{4.9}$$

with $G = \begin{pmatrix} 0 & 0 \\ g_{21} & 0 \end{pmatrix}$. The closed-loop LCP matrix is D_{cl}.

Remark 4.2.3. *It is important to note that* $\operatorname{rank}(B) = \operatorname{rank}(B_{cl}) = 1$. *So, the passification conditions on the rank of the input matrix [39, Theorem 3.61] are not met in this context.*

4.2.2 Well-posedness issues

The well-posedness of (4.5) and (4.6) has to be guaranteed as a prerequisite to stability analysis. Similarly to Assumption 2.1.4, we are led to assume the following:

Assumption 4.2.4. *The quadruple* $(A_{cl}, B_{cl}, C_{cl}, D_{cl})$ *in* (4.5) *is strictly state passive.*

This means that there exist gain matrices K and G such that the following nonlinear matrix inequality with unknowns P, K and G:

$$M \triangleq \begin{pmatrix} (A + EK)^\top P + P(A + EK) & P(B + EG) - (C + FK)^\top \\ (B + EG)^\top P - (C + FK) & -(D + FG) - (D + FG)^\top \end{pmatrix} \preccurlyeq \begin{pmatrix} -\epsilon P & 0 \\ 0 & 0 \end{pmatrix}, \tag{4.10}$$

has a solution $P = P^\top \succ 0$. This implies that $g_{21} \geq 0$. As examples will show, strict state passivity can hold with $g_{21} = 0$ in certain cases, which may be interesting in practice. Let us examine the well-posedness of the closed-loop system in (4.5) and of the desired dynamics in (4.6). First, let us verify that no state jump can occur in the closed-loop system. Indeed, let us consider (1.11), we obtain: $Q_{D_{cl}} = \begin{pmatrix} 0 \\ I\!R_+ \end{pmatrix}$, $Q^\star_{D_{cl}} = \begin{pmatrix} I\!R \\ I\!R_+ \end{pmatrix}$, and $\mathcal{K}_{cl} = I\!R^2$. Thus, $x(t^+) = x(t^-)$ and there is no state jump in (4.5), even at times where $\lambda_d(\cdot)$ may be discontinuous. Therefore, solutions to (4.5), if they exist, must be continuous. Let us deal with the well-posedness of (4.6), equivalently of (4.7). Assume that $u_d(\cdot)$ is AC, then posing $z = \dot{q}_d - u_{2d}$ it follows that $\dot{z} = \ddot{q}_d - \dot{u}_{2d}$ where $\dot{u}_{2d}$ is the almost-everywhere derivative of u_{2d}. This gives the DI:

$$\dot{z}(t) \in -\dot{u}_{2d}(t) + \frac{u_{1d}(t)}{m} - \mu g \, \mathrm{sgn}(z(t)). \tag{4.11}$$

Using for instance [13], it is deduced that the DI in (4.11) has a unique Lipschitz continuous solution on $[0, T)$ for any $T > 0$, for any $z(0) = z_0 \in I\!R$ and any $u_d(\cdot)$ with $\dot{u}_{1d}(\cdot)$ and $\ddot{u}_{2d}(\cdot)$ bounded in the extended (or local) $\mathcal{L}_2$ norm. Thus, $\dot{q}_d(\cdot)$ is AC (Lipschitzness implies AC), $\ddot{q}_d(\cdot)$ is defined almost everywhere, and $q_d(t) = q_d(0) + \int_0^t \dot{q}_d(s)ds$ is continuously differentiable. However, the multiplier $\lambda_d(\cdot)$ can undergo jumps at some junction times. Therefore, the closed-loop plant (4.5) is an LCS with exogenous signal $F_{cl}(t) \triangleq -\begin{pmatrix} k_{21} & k_{22} \\ 0 & 0 \end{pmatrix} x_d(t) - \begin{pmatrix} g_{21} & 0 \\ 0 & 0 \end{pmatrix} \lambda_d(t) + \begin{pmatrix} u_{2d}(t) \\ 1 \end{pmatrix}$ entering the complementarity constraints, where no state jump can occur.

Remark 4.2.5. *Let us consider the DI in (4.1). There is in principle no problem in introducing a kind of contact force feedback inside the signum set-valued function. Let $u_2 = u_2(q, \dot{q}, \lambda_t)$, then $\lambda_t \in \mathrm{sgn}(\dot{q} - u_2(q, \dot{q}, \lambda_t)) \Leftrightarrow \dot{q} - u_2(q, \dot{q}, \lambda_t) \in \mathcal{N}_{[-1,1]}(\lambda_t)$, where the inversion of maximal monotone set-valued mapping is used. This is a generalized equation with unknown λ_t, whose well-posedness can be characterized. Indeed, $u_2(q, \dot{q}, \lambda_t) = k_{21}(q - q_d) + k_{22}(\dot{q} - \dot{q}_d) + g_{21}(\lambda_1 - \lambda_{1d}) + u_{2d}$, with $\lambda_1(q, \dot{q}) = \frac{\lambda_t(q,\dot{q})+1}{2}$. This yields when $g_{21} > 0$:*

$$\begin{array}{c} -\dot{q} + k_{21}(q - q_d) + k_{22}(\dot{q} - \dot{q}_d) + g_{21}(\frac{\lambda_t+1}{2} - \lambda_{1d}) + u_{2d} \in -\mathcal{N}_{[-1,1]}(\lambda_t) \\ \Updownarrow \\ \lambda_t(q, \dot{q}) = \mathrm{proj}\left([-1, 1];\ 2\frac{\dot{q} - k_{21}(q-q_d) - k_{22}(\dot{q}-\dot{q}_d) + g_{21}\lambda_{1d} - \frac{g_{21}}{2} - u_{2d}}{g_{21}}\right), \end{array} \tag{4.12}$$

see Fact A.3.5. Therefore, the force feedback regularizes the set-valued signum function, as is known in other contexts [26, Remark 2.8] [89]. It is also possible to prove that the LCP in (4.5) (b) has a unique solution $\lambda(t)$ for any $C_{cl}x(t) + F_{cl}(t)$ and $g_{21} > 0$. In spite of the fact that $D_{cl} \succcurlyeq 0$, the result holds due to the special structure of the LCP (especially the second line) and $\mathrm{rank}(D_{cl}) = 2$. Also, the result concerns only $\lambda_1 = \frac{\lambda_t+1}{2}$, not λ_2. It is noteworthy that the multiplier λ_t in (4.12) depends only on known control parameters, mass state, and desired signals.This is expected since the LCP in (4.5) does not involve mechanical parameters. Taking $g_{21} > 0$ means that the multiplier λ_1, solution to the LCP in (4.5) (b), can be explicitly calculated. So there is

no need for a contact force measurement in this case, measurement of x is sufficient to solve the LCP in (4.5) (b). Note that λ_1 does not depend on μ nor on the normal contact force.

Let us continue the well-posedness study. When $g_{21} = 0$, it follows from [44, Theorems 11 and 26] that the closed-loop system (4.5) has unique AC solutions. This can be shown using passivity of the quadruple $(A_{cl}, B_{cl}, C_{cl}, D_{cl})$ in Assumption 4.2.4, the fact that $\mathrm{Im}(D_{cl} + \mathcal{N}_{\mathbb{R}^2_+}) - F_{cl}(t)) = \mathrm{Im}(D_{cl}) + \mathbb{R}^2_- - F_{cl}(t) = \mathbb{R}^2$ (here a result from [128] is used with the fact that $\mathcal{N}_{\mathbb{R}^2_+}(\cdot) = \mathcal{N}^{-1}_{\mathbb{R}^2_-}(\cdot)$). This together with the fact that $F_{cl}(\cdot)$ is AC allows us to guarantee that [44, Theorem 26 (ii)] holds true. When $g_{21} > 0$ (which will be imposed in some cases), then it follows from (4.12) that $\lambda_1(\cdot)$ (which is the only component of $\lambda(\cdot)$ that intervenes in (4.5) (a)) is a Lipschitz continuous function of the state and exogenous terms. Therefore (4.5) (a) boils down to an ordinary differential equation with Lipschitz continuous right-hand side, existence and uniqueness of locally AC solutions follows from general results [143, Proposition C. 3.8].

The conclusion of this section is that imposing mild conditions on $u_d(\cdot)$ together with passivity as in Assumption 4.2.4, guarantees the well-posedness of the closed-loop, the desired, and the error dynamics, with AC states $x(\cdot)$ and $x_d(\cdot)$ (hence the error dynamics (4.9) is well-posed also).

4.2.3 Equilibrium Points of the Error System

Let us assume that the closed-loop system in (4.5) is strictly state-passive (*i.e.*, Assumption 2.1.4 holds). Recall that from passivity of $(A_{cl}, B_{cl}, C_{cl}, D_{cl})$, it follows that $g_{21} \geq 0$. The equilibria of the LCS (4.8) are characterized as follows:

Proposition 4.2.6. *Consider the error dynamics in (4.8) or (4.9). Assume that the quadruple $(A_{cl}, B_{cl}C_{cl}, D_{cl})$ is strictly state passive. Then, the unique equilibrium point is $e^\star = (0, 0)$.*

Proof. In order to find the equilibrium points of the error dynamics, the LCS in (4.8) is written as follows:

$$\begin{cases} 0 = e_2^\star \\ 0 = \frac{k_{11}}{m} e_1^\star - 2\mu g(\lambda_1^\star(t) - \lambda_{1d}(t)) \\ 0 \leq \lambda_d(t) \perp w_d(t) = \begin{pmatrix} 0 & 1 \\ 0 & 0 \end{pmatrix} u_d(t) + \begin{pmatrix} 0 \\ 1 \end{pmatrix} + \begin{pmatrix} 0 & 1 \\ -1 & 0 \end{pmatrix} \lambda_d(t) + \begin{pmatrix} 0 & -1 \\ 0 & 0 \end{pmatrix} x_d(t) \geq 0 \\ 0 \leq \lambda^\star(t) \perp w^\star(t) = \begin{pmatrix} k_{21} & k_{22} - 1 \\ 0 & 0 \end{pmatrix} e^\star(t) + \begin{pmatrix} g_{21} & 1 \\ -1 & 0 \end{pmatrix} \lambda^\star(t) - \begin{pmatrix} g_{21} & 0 \\ 0 & 0 \end{pmatrix} \lambda_d(t) \\ \qquad\qquad + \begin{pmatrix} 0 & 1 \\ 0 & 0 \end{pmatrix} u_d(t) \geq 0 \end{cases} \tag{4.13}$$

The problem in (4.13) is a mixed LCP with unknown $e_1^\star$, $e_2^\star$, $\lambda_1^\star$, $\lambda_2^\star$. The equilibrium point of the error dynamics is given by $e_1^\star(t) = \frac{2m\mu g}{k_{11}}(\lambda_1^\star(t) - \lambda_{1d}(t))$. It is dependent on the complementarity variables λ_{1d} and $\lambda_1^\star$. In the above analysis, the LCP of the

desired system is solved which gives the values of λ_d and x_d. Now, it is required to solve the LCP of the closed-loop system (*i.e.,* $0 \leq \lambda^\star \perp w^\star \geq 0$) in order to find $\lambda^\star$ and then calculate the equilibrium point $e_1^\star$. Let us substitute $e^\star$ in terms of $\lambda^\star$ and λ_d, then the LCP to be solved is:

$$0 \leq \begin{pmatrix} \lambda_1^\star(t) \\ \lambda_2^\star(t) \end{pmatrix} \perp \begin{pmatrix} w_1^\star(t) \\ w_2^\star(t) \end{pmatrix} = \begin{pmatrix} 2m\mu g\frac{k_{21}}{k_{11}} + g_{21} & 1 \\ -1 & 0 \end{pmatrix} \begin{pmatrix} \lambda_1^\star(t) \\ \lambda_2^\star(t) \end{pmatrix} + \begin{pmatrix} u_{2d}(t) - x_{2d}(t) \\ 1 \end{pmatrix} + \begin{pmatrix} -2m\mu g\frac{k_{21}}{k_{11}} - g_{21} & 0 \\ 0 & 0 \end{pmatrix} \begin{pmatrix} \lambda_{1d}(t) \\ \lambda_{2d}(t) \end{pmatrix} \geq 0 \tag{4.14}$$

It is important to note that the system can be at equilibrium, while the multipliers are time-varying. We can observe the new term $2m\mu g\frac{k_{21}}{k_{11}} + g_{21}$ that appears in the matrix of the multiplier $\lambda^\star(t)$ in (4.14). This term plays a significant role in the subsequent analysis of the equilibrium point, so let us study the sign of this term. Let Assumption 4.2.4 holds for the closed-loop system in (4.8), then it is necessary to ensure that the following holds:

$$-A_{cl}^\top P - PA_{cl} - \epsilon P \succeq 0 \tag{4.15}$$

where $P = P^\top = \begin{pmatrix} p_{11} & p_{12} \\ p_{12} & p_{22} \end{pmatrix} \succ 0$ and $\epsilon > 0$. Then, the matrix inequality in (4.15) is written as:

$$\begin{pmatrix} -\frac{2k_{11}}{m}p_{12} & -p_{11} - \frac{k_{11}}{m}p_{22} - \frac{k_{12}}{m}p_{12} \\ -p_{11} - \frac{k_{11}}{m}p_{22} - \frac{k_{12}}{m}p_{12} & -2p_{12} - \frac{2k_{12}}{m}p_{22} \end{pmatrix} - \epsilon \begin{pmatrix} p_{11} & p_{12} \\ p_{12} & p_{22} \end{pmatrix} \succeq 0 \tag{4.16}$$

According to the equality implied by passivity, $PB_{cl} = C_{cl}^\top$ since $D_{cl} + D_{cl}^\top = 0$, we have $-2p_{12}\mu g = k_{21}$ and $-2p_{22}\mu g = k_{22} - 1$. Let us substitute the value of p_{12} in (4.16), then

$$-\frac{2k_{11}}{m}p_{12} - \epsilon p_{11} \geq 0 \Leftrightarrow \frac{k_{11}k_{21}}{m\mu g} - \epsilon p_{11} \geq 0$$

Given that $p_{11} > 0$, then $\frac{k_{11}k_{21}}{m\mu g}$ must be positive. This means that k_{11} and k_{21} have same signs. So, the term $2m\mu g\frac{k_{21}}{k_{11}}$ and according to Assumption 4.2.4 that imposes strict passivity on the closed-loop system is nonnegative (*i.e.,* $2m\mu g\frac{k_{21}}{k_{11}} \geq 0$). Hence, the term $2m\mu g\frac{k_{21}}{k_{11}} + g_{21}$ which is multiplied by $\lambda_1^\star(t)$ is non-negative. In order to study the well-posedness of the closed-loop system's LCP in (4.14), let us consider different cases as above:

case 1: $\lambda_1^\star \in]0, 1[$ In this case, $w_1^\star = (2m\mu g\frac{k_{21}}{k_{11}} + g_{21})(\lambda_1^\star - \lambda_{1d}) = 0$. Hence, $\lambda_1^\star = \lambda_{1d}$. The solutions are given by: $\begin{cases} \lambda^\star = (\lambda_{1d}, 0)^\top \\ w^\star = (0, 1 - \lambda_{1d})^\top \end{cases}$.

case 2: $\lambda_1^\star = 0$ In this case, $w_1^\star = -(2m\mu g\frac{k_{21}}{k_{11}} + g_{21})\lambda_{1d} + u_{2d} - x_{2d} \geq 0$ which holds only if $u_{2d} - x_{2d} \geq 0$. If $u_{2d} - x_{2d} > 0$, then the solution of the desired LCP in (4.13) is:

$$\begin{cases} \lambda_d = (0, 0)^\top \\ w_d = (u_{2d} - x_{2d}, 1)^\top \end{cases}$$

If $u_{2d} - x_{2d} = 0$, then the solution is $\lambda_{1d} = 0$. Thus, in this case, $\lambda_1^\star = \lambda_{1d} = 0$. The unique solution is given by: $\begin{cases} \lambda^\star = (0,0)^\top \\ w^\star = (u_{2d} - x_{2d}, 1)^\top \end{cases}$.

case 3: $\lambda_1^\star = 1$ In this case, $w_1^\star = (2m\mu g\frac{k_{21}}{k_{11}} + g_{21})(1 - \lambda_{1d}) + \lambda_2^\star + u_{2d} - x_{2d} = 0 \Rightarrow \lambda_2^\star = -(2m\mu g\frac{k_{21}}{k_{11}} + g_{21})(1 - \lambda_{1d}) + x_{2d} - u_{2d} \geq 0$ which holds only if $x_{2d} - u_{2d} \geq 0$. If $x_{2d} - u_{2d} > 0$, then the solution of the desired system's LCP in (4.13) is:

$$\begin{cases} \lambda_d = (1, x_{2d} - u_{2d})^\top \\ w_d = (0,0)^\top \end{cases}$$

If $x_{2d} - u_{2d} = 0$, then the inequality $-(2m\mu g\frac{k_{21}}{k_{11}} + g_{21})(1 - \lambda_{1d}) \geq 0$ holds if and only if $\lambda_{1d} = 0$. So, $\lambda_1^\star = \lambda_{1d} = 1$. The solution is unique and it is given by: $\begin{cases} \lambda^\star = (1, x_{2d} - u_{2d})^\top \\ w^\star = (0,0)^\top \end{cases}$

Therefore, in all the possible cases of $\lambda_1^\star$, it is observed that $\lambda_1^\star = \lambda_{1d}$. It is noteworthy that in all cases, we have $\lambda^\star = \lambda_d$ and $w^\star = w_d$. Given that $e_1^\star = \frac{2m\mu g}{k_{11}}(\lambda_1^\star(t) - \lambda_{1d}(t))$ and $\lambda^\star(t) = \lambda_d(t)$, then $e^\star = (e_1^\star, e_2^\star)^\top = (0,0)^\top$. This is in accordance with the fact that Proposition 4.4.2 guarantees global exponential stability (hence uniqueness of the origin of the error dynamics). □

4.3 Analysis of the Desired Trajectories

This section focuses on the analysis of the desired trajectories of the LCS in (4.6) by studying the stick/slip behaviour. Furthermore, it shows the impact of external forces $u_{1d}(t)$ and $u_{2d}(t)$ on the behaviour of the system through numerical simulation.

4.3.1 Properties of the Desired Trajectories

The desired dynamics are given in our work in the form of a dynamical system that produces some trajectories. In practice it is certainly interesting to understand which desired trajectories can be designed. To that aim it is of interest to understand the properties of the desired trajectory represented by (4.6) to be tracked. In the study of harmonically forced dry frictional oscillators, there are results on the construction of periodic solutions of such systems. The physical system considered in [65, 139, 63] is a simple mass-spring dashpot system with dry friction which is different from the system considered in Figure 4.1a. When addressing the non-sticking behaviour, the solution relies on solving a second-order differential equation which represents the equation of motion.

Denhartog [65] provided an exact symmetric and periodic solution for non-sticking motion with $\mu = 1$. His approach starts by assuming that the external force exerted has the form of $F_{ext} = Pcos(\omega t + \phi)$ and that the solution is symmetric (*i.e.,* the period

T is divided into two equal half cycles each of length π/ω). The boundary conditions of the steady-state solution were established as follows:

$$\begin{cases} t = 0, \;\; x(0) = x_0, \;\; \dot{x}(0) = 0 \\ t = \frac{\pi}{\omega}, \;\; x(\frac{\pi}{\omega}) = -x_0, \;\; \dot{x}(\frac{\pi}{\omega}) = 0 \end{cases} \tag{4.17}$$

Shaw [139] extended this work to the case where $\mu \neq 1$. He followed the same boundary conditions in (4.17) for non-sticking motion, then analyzed the stability of the periodic motion. By following the same approach as before (*i.e.,* two turnarounds per cycle and boundary conditions in (4.17)), the authors in [63] prove mathematically that the $\frac{2\pi}{\omega}$-periodic solutions, where ω is the excitation frequency, are symmetric. This property was previously assumed but not proven yet.

Following up from the system studied in [139, 65, 63] where there is no moving belt (*i.e.,* $u_{2d} = 0$), let us analyse, in the following, the stick/slip behaviour of these trajectories based on the desired input $u_{1d}(t)$, which represents the external force applied on the mass m and $u_{2d}(t) = 0$. According to the complementarity problem in (4.6), the multiplier $\lambda_{1d} \in [0, 1]$. Let us determine the value of u_{1d} for each behavior by considering the following analysis of the desired system in (4.6):

- If $\lambda_{1d} \in]0, 1[\Rightarrow x_{2d} = 0 \Rightarrow \dot{x}_{2d} = 0 \Rightarrow u_{1d} \in]-m\mu g, m\mu g[$. The system is in sticking mode as shown in Figure 4.2a.

- If $\lambda_{1d} = 0 \Rightarrow x_{2d} \leq 0$. When $u_{1d} = -m\mu g$, then $x_{2d} = 0$ and the system is in sticking mode as shown in Figure 4.2b. But, when $u_{1d}(t) < -m\mu g \;\; \forall t$, then the solution $x_{2d} < 0$ (*i.e.,* sliding mode) and it diverges.

- If $\lambda_{1d} = 1 \Rightarrow x_{2d} = \lambda_{2d} \geq 0$. When $u_{1d} = m\mu g$, then $x_{2d} = 0$ and the system behaves in sticking mode. When u_{1d} is chosen such that $u_{1d}(t) > m\mu g \;\; \forall t$, then the solution $x_{2d} > 0$, it behaves in sliding mode and it is unbounded.

  It is noteworthy that, in the cases when $\lambda_{1d} = 1$ or $\lambda_{1d} = 0$ (*i.e.,* $u_{1d} = m\mu g$ or $u_{1d} = -m\mu g$ respectively), and the initial velocity of the mass $x_{2d}(0)$ is chosen such that it is in the direction of the external force u_{1d} (*i.e.,* $u_{1d} < 0$ and $x_{2d}(0) < 0$). Then the trajectory x_{1d} diverges and it is sliding mode at a constant velocity as illustrated in Figure 4.2c.

  If $u_{1d}(t)$ is chosen as a periodic, time-varying, and bounded signal in the form of $u_{1d} = Acos(wt)$ where $|A| > m\mu g$, then the system will behave in both sticking and sliding modes as shown in Figure 4.2d or non-sticking mode depending on the amplitude A.

  The following numerical simulation is carried out at $m = 1kg$, $\mu = 0.5$, and $h = 0.01$ using SICONOS.

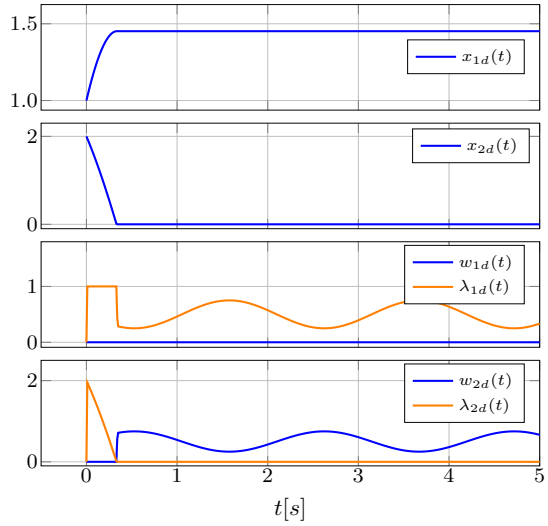

(a) $u_{1d} = -0.5m\mu g \sin 3t$ and $x_{2d}(0) = 2$

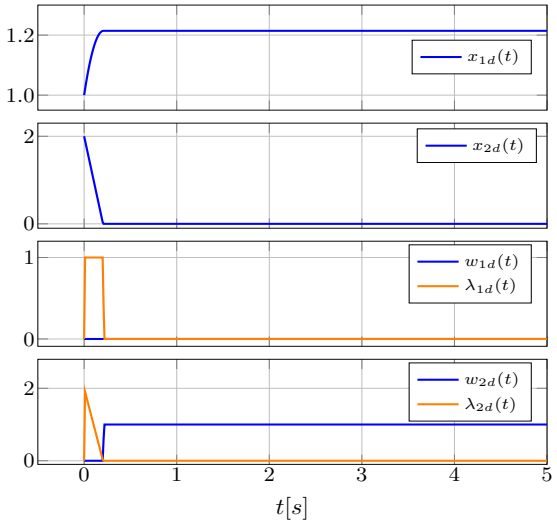

(b) $u_{1d} = -m\mu g$ and $x_{2d}(0) = 2$

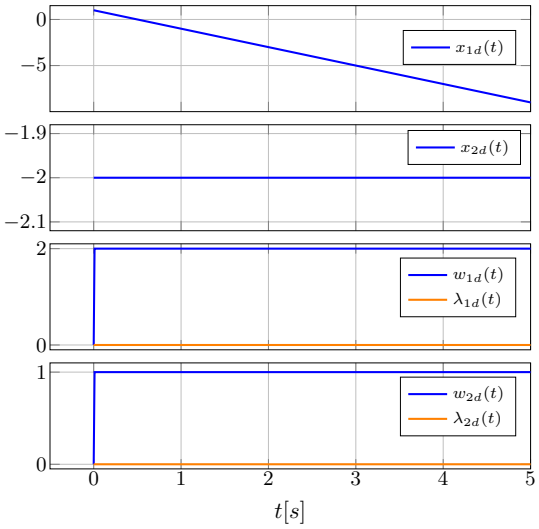

(c) $u_{1d} = -m\mu g$ and $x_{2d}(0) = -2$

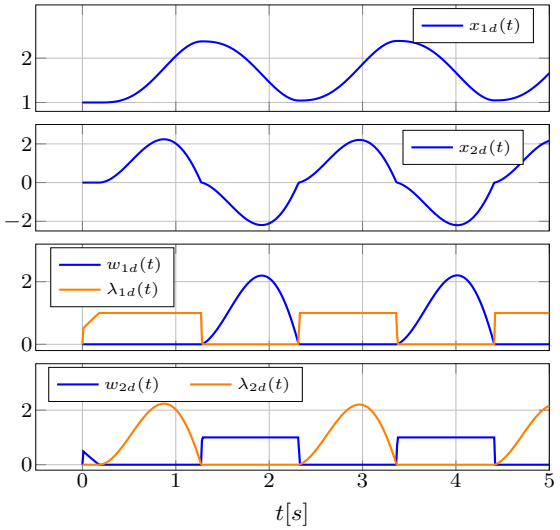

(d) $u_{1d} = 2m\mu g \sin 3t$ and $x_{2d}(0) = 0$

Figure 4.2: Numerical simulation of (4.6) with $u_{2d} = 0$ for different values of $u_{1d}(t)$

In the above numerical simulation, a periodic solution with a periodic external input $u_{1d}(t)$ is depicted in Figure 4.2d. It represents a periodic and bounded solution $x(t)$ and it has the same period T as the input $u_{1d}(t)$. The existence of periodic solution confirms the results presented in [65, 99, 63].

However, note that not every bounded periodic input leads to a bounded periodic solution. In order to achieve both periodicity and boundedness, it is important to follow the general conditions in (4.17). Let us consider the case when $u_{2d} \neq 0$ which is studied in [99, 96, 95, 7] when u_{2d} is constant and [108] when $u_{2d}(t)$ is time-varying. The stick-slip mechanical system considered in [99, 96, 95] is a simple mass-spring system on a moving belt with constant speed. But, our system presented in Figure 4.1a differs because it includes an external force $u_{1d}(t)$ acting on the mass and allows for time-varying belt speed $u_{2d}(t)$. In [99], the authors introduce the shooting method as a periodic solution finder to address the computational challenges of solving stiff

differential equations. To tackle this issue, the authors present the switch model as an alternate friction model to simulate stick-slip vibrations by solving a set of non-stiff differential equations. Furthermore, a time-dependent friction model is studied. The authors in [95] study bifurcations of periodic solutions in mechanical systems with dry friction and discuss the existence of infinitely unstable periodic solutions through repulsion sliding mode in stick/slip mechanical systems.

The paper [82] proposes two numerical methods for the computation of periodic solution in maximal monotone dynamical systems, including linear complementarity systems and systems with dry friction. It provides formal justifications to ensure the consistency of the proposed numerical schemes. The results of [82] could be applied to our frictional oscillator system, which is represented as an LCS in (4.6) and, equivalently, as a differential inclusion with maximal monotonicity properties in (4.7). A recent paper [94] introduces a new method for computing periodic solutions of systems with frictional occurrences. The approach formulates all equations, including friction, as equalities and allows for an exact Coulomb's friction law without regularizing the friction force. This equality-based approach is implemented through a highly compact weighted residual formulation and it represents accurately multiple sticking and sliding phases that converges to the solution in few iterations. Given that the Coulomb friction in our system is represented within the the complementarity framework in (4.3) and without any approximation of the friction force, the method developed in [94] is applicable to design periodic desired trajectories.

4.3.2 Numerical Simulation of the Desired Trajectories

In this section, a numerical simulation of the desired trajectory represented by the LCS in (4.6) is performed. This simulation involves implementing a suitable desired input u_d and observe the resulting desired trajectory. The simulation is done with the INRIA software package SICONOS[1][3].

The following Figures 4.3-4.6 show the numerical simulations of the desired system in (4.6) with different values of $u_{1d}(t)$ and $u_{2d}(t)$ leading to different interesting results. For some Figures, the phase portrait of the desired system in (4.6) is presented as a 3-dimensional plot, depicting the two states x_{1d} and x_{2d} and the time axis t as the system is non-autonomous.

In order to design a periodic desired trajectory x_d, the frictional oscillator is excited by periodic desired input $u_d = (u_{1d}, u_{2d})^\top$ where u_{1d} and u_{2d} have the same period T but different amplitudes, as shown in Figure 4.3. Take $x_d(0) = (1, 0)^\top$ and the time step $h = 0.01$s.

[1] https://nonsmooth.gricad-pages.univ-grenoble-alpes.fr/siconos/index.html

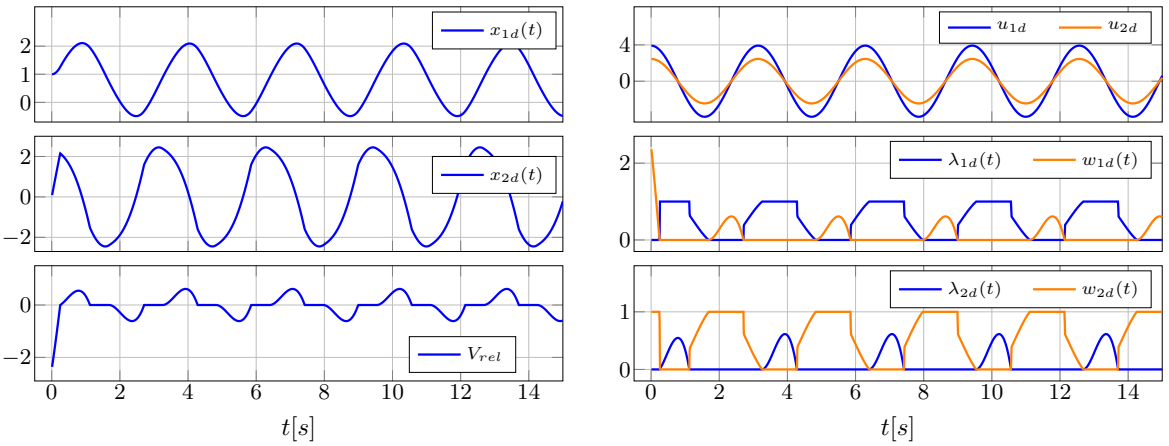

Figure 4.3: Numerical simulation of (4.6) with $u_{1d} = 0.8m\mu g \cos 2t$, $u_{2d} = 0.5m\mu g \cos 2t$

The simulation depicted in Figure 4.3 shows a periodic desired trajectory with period $T = \frac{2\pi}{2}$s which is the same period as that of the desired input u_d. Also, it can be observed that the frictional oscillator exhibits both sticking and slipping behaviours, as depicted in the plot of the relative velocity $V_{rel} = x_{2d} - u_{2d}$.

Let us consider the desired inputs u_{1d} and u_{2d} with different periods.

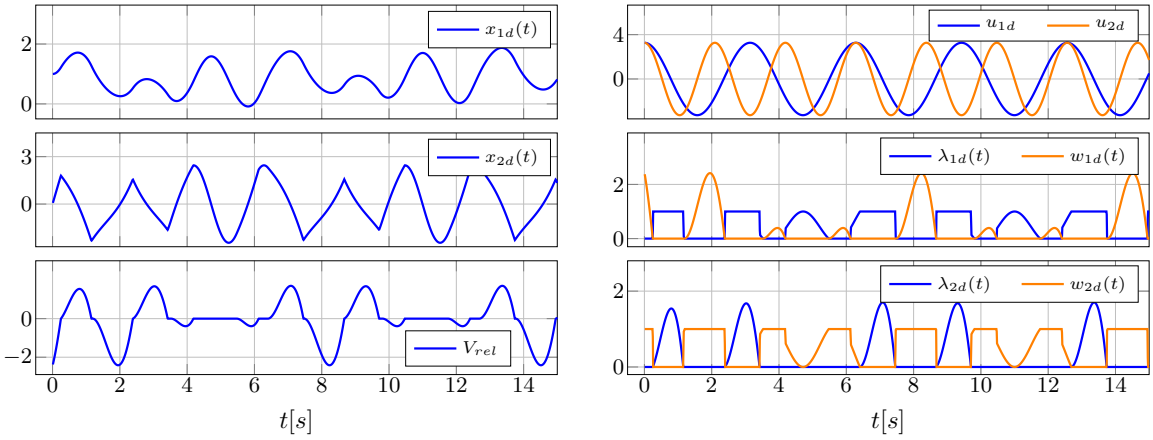

Figure 4.4: Numerical simulation of (4.6) with $u_{1d} = 0.5m\mu g \cos 2t$, $u_{2d} = 0.5m\mu g \cos 3t$

In Figure 4.4, the external inputs are chosen to be periodic with the same amplitude but with different periods $T_{u_{1d}} = \frac{2\pi}{2}$s and $T_{u_{2d}} = \frac{2\pi}{3}$s. It is noticeable that the desired trajectories doesn't exhibit a periodic behaviour. This can be further illustrated by the phase portrait given by Figure 4.5:

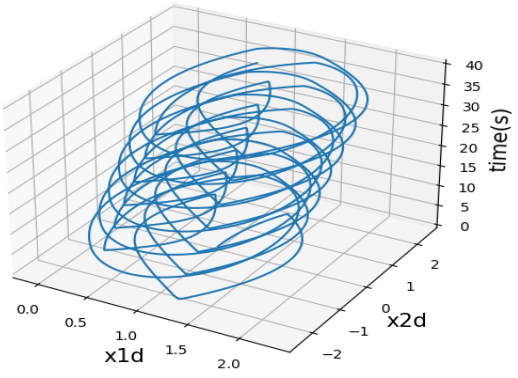

Figure 4.5: Phase portrait of simulated system in Figure 4.4

The novelty of the simulation in Figure 4.6 is the selection of the desired inputs, which impacts the solution of the desired system (4.6). The inputs u_{1d} and u_{2d} are periodic with non-rational periods $T_{u_{1d}} = \frac{2\pi}{\sqrt{2}}$ and $T_{u_{2d}} = \frac{2\pi}{\sqrt{5}}$ while having the same amplitude.

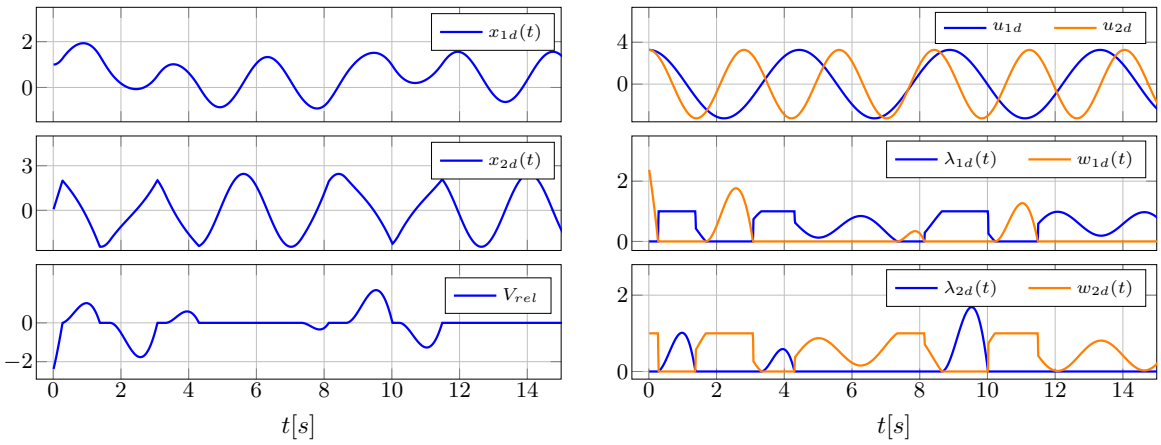

Figure 4.6: Numerical simulation of (4.6) with $u_{1d} = 0.5mg\cos\sqrt{2}$, $u_{2d} = 0.5mg\cos\sqrt{5}$

The desired trajectories depicted in Figure 4.6 are not periodic. It is interesting to observe from the plot of $V_{rel} = x_{2d} - u_{2d}$ in Figure 4.6 that the mass has a larger sticking period which shows a different stick/slip behaviour from the previous Figures. Consider the phase portrait of this system in Figure 4.7.

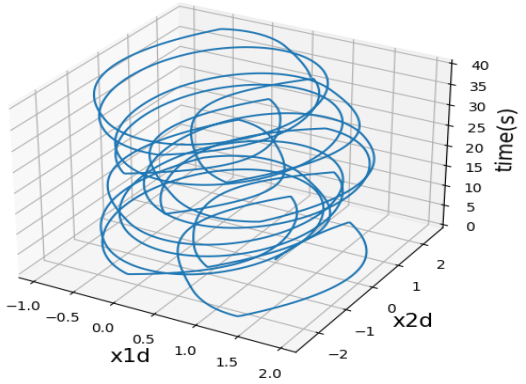

Figure 4.7: Phase portrait ofnthe system simulated in Figure 4.6

The behaviour of the system shown in the phase portrait in Figure 4.7 is obviously not periodic. However, it is out of the scope of this thesis to determine whether this system is chaotic.

The purpose of this section is to highlight the possibility to generate various desired trajectories to be tracked later, particularly periodic ones. As it is possible to track any desired trajectory generated by the LCS in (4.6), even in the cases where the behavior depicted appears unusual as in Figure 4.6.

Comments on passivity: By considering incremental passivity, let us recall the dynamics of the desired system in (4.7) as follows:

$$\begin{cases} m\ddot{x}_{1d}(t) = -mg\mu\lambda_t + u_{1d}(t) \\ \lambda_t \in \operatorname{sgn}(\dot{x}_{1d}(t) - u_{2d}(t)) \end{cases} \tag{4.18}$$

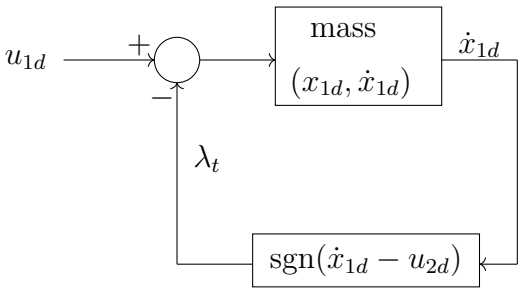

Figure 4.8: Feedback interconnection of an incrementally passive system and a maximal monotone mapping.

This approach is valid when u_{2d} is constant, in order to keep the property of maximal monotonicity of the signum multifunction (for otherwise it would be monotone for each $t \geq 0$ only). The system as represented in Figure 4.8 is an interconnection of the

plant (*i.e.,* integrator), which is passive between the input $v_1 \triangleq -\mu g \lambda_t + u_{1d}$ and the output $\dot{x}_{1d}$. The storage function corresponding to the output is given by $V = \frac{1}{2} m \dot{x}_{1d}^2$. Then, the feedback nonlinearity is maximal monotone if we are considering λ_t and the relative velocity $\dot{x}_{1d} - u_{2d}$, ensuring the incremental passivity of the system (4.18) [127] (the fact that the graph of the mapping in the feedback does not contain in general the point $(0, 0)$ because of constant but nonzero u_{2d}, prevents the interconnection to be passive). The papers [142] and [8, Proposition 4.4] present a result about the existence of T-periodic solution for incrementally stable system forced with T-periodic input. However, it is important to note that this result is established in the context of smooth systems, and extending this result to a non-smooth system requires technical work and is out of the scope of this study. In [80], the authors focus on the numerical computation of periodic solutions for a class of set-valued dynamical systems with maximal monotonicity properties when subjected to periodic excitation. They introduce two numerical time-stepping methods: the Asymptotic Simulation (AS) and the Two-Point Boundary Value (2PBV) as it highlights their theoretical guarantee such as convergence properties.

4.4 Trajectory Tracking of Frictional Oscillator in Nominal Case

In this section, the trajectory tracking of the frictional oscillator is solved without uncertainties. The stability analysis of the error dynamics is shown using two approaches: one using LCS formulation and the other one based on the maximal monotonicity of the signum function.

4.4.1 Passivity-based Control Framework

In the subsequent analysis, consider that $g_{21} = 0$. Then, the closed-loop plant is the DI:

$$\begin{aligned} \ddot{q}(t) \in \; & \tfrac{1}{m} \left(k_{11}(q(t) - x_{1d}(t)) + k_{12}(\dot{q}(t) - x_{2d}(t)) + u_{1d}(t) \right) \\ & -\mu g \, \mathrm{sgn} \left(\dot{q}(t) - k_{21}(q(t) - x_{1d}(t)) - k_{22}(\dot{q}(t) - x_{2d}(t)) - u_{2d}(t) \right). \end{aligned} \tag{4.19}$$

Remark 4.4.1. *It is noteworthy that due to the matrix F structure, it is impossible to get strong passivity of the closed-loop system quadruple $(A_{cl}, B_{cl}, C_{cl}, D_{cl})$, because even a feedback with nonzero G in (4.3) cannot make D_{cl} full rank in (4.5) (b).*

Using (4.7) and (4.19) , the error dynamics are equal to:

$$\begin{aligned}\ddot{\tilde{q}}(t) \in \;& \mu g\,\mathrm{sgn}(\dot{q}_d(t)-u_{2d}(t)) + \tfrac{1}{m}\left(k_{11}(q(t)-x_{1d}(t)) + k_{12}(\dot{q}(t)-x_{2d}(t)) + u_{1d}(t)\right)\\ & -\mu g\,\mathrm{sgn}\left(\dot{q}(t) - k_{21}(q(t)-x_{1d}(t)) - k_{22}(\dot{q}(t)-x_{2d}(t)) - u_{2d}(t)\right) - \tfrac{1}{m}u_{1d}(t)\\ & = \tfrac{1}{m}\left(k_{11}\tilde{q}(t) + k_{12}\dot{\tilde{q}}(t)\right) + \mu g[\mathrm{sgn}(\dot{q}_d(t)-u_{2d}(t))\\ & -\mathrm{sgn}\left(\dot{\tilde{q}}(t) - k_{21}\tilde{q}(t) - k_{22}\dot{\tilde{q}}(t) + \dot{q}_d(t) - u_{2d}(t)\right)]\\ & = \tfrac{1}{m}\left(k_{11}\tilde{q}(t) + k_{12}\dot{\tilde{q}}(t)\right) + \mu g[\lambda_{t,d}(t) - \lambda_t(t)].\end{aligned} \tag{4.20}$$

which is equivalent, when $g_{21}=0$, to its complementarity system counterpart (4.8) and (4.9), with $e=(\tilde{q},\dot{\tilde{q}})^\top$. Finally, recalling that $\lambda_1 = \frac{\lambda_t+1}{2}$, we can rewrite equivalently (4.20) as:

$$\begin{aligned}\dot{e}(t) \in \;& A_{cl}e(t) + \begin{pmatrix}0\\ \mu g\end{pmatrix}\mathrm{sgn}(\dot{q}_d(t)-u_{2d}(t)) - \begin{pmatrix}0\\ \mu g\end{pmatrix}\mathrm{sgn}(-(C_{cl})_{1,\bullet}e(t) + \dot{q}_d(t) - u_{2d}(t))\\ & = A_{cl}e(t) - B_{cl}\begin{pmatrix}\lambda_{1d}(t)-\lambda_1(t)\\ \lambda_{2d}(t)-\lambda_2(t)\end{pmatrix}\end{aligned} \tag{4.21}$$

where $\lambda_{1d}(t)\in\mathrm{sgn}(\dot{q}_d(t)-u_{2d}(t))$, $\lambda_1(t)\in\mathrm{sgn}(-(C_{cl})_{1,\bullet}e(t)+\dot{q}_d(t)-u_{2d}(t))$. Notice that since $D_{cl} = -D_{cl}^\top$ (when $g_{21}=0$), it follows that the strict state passivity of $(A_{cl},B_{cl},C_{cl},D_{cl})$ is equivalent to the strict state passivity of $(A_{cl},B_{cl},C_{cl},0)$.

4.4.2 Closed-loop Error Stability Analysis

The stability analysis from section 2.1.2 based on the LCS formulations is repeated in this section. Furthermore, an alternative analysis method is presented (see Remark 4.4.3). Assume that all the trajectories are AC.

Proposition 4.4.2. *Consider the error dynamics (4.21) with bounded initial conditions, and assume that $(A_{cl},B_{cl},C_{cl},D_{cl})$ is strictly state passive with constant $\epsilon>0$. Then, **(i)**: $e(\cdot)$ converges globally exponentially fast to zero; **(ii)**: when $g_{21}>0$, the multiplier error $(\lambda_1-\lambda_{1d})(\cdot)$ converges globally exponentially fast to zero.*

Proof. **(i)**: Consider the Lyapunov candidate function $V(e(t)) = e^\top Pe$, with $P = P^\top \succ 0$ the solution of the closed-loop passivity matrix inequality. Then, along the closed-loop error dynamics trajectories:

$$\dot{V}(e(t)) = e^\top(A_{cl}^\top P + PA_{cl})e(t) + 2e(t)^\top PB_{cl}(\lambda(t)-\lambda_d(t))$$

Starting from (4.3) and (4.6) the following is obtained:

$$\begin{cases} w(t) = C_{cl}x(t) + D_{cl}\lambda(t) + Cx_d(t) + Fu_d(t) + \begin{pmatrix}0\\1\end{pmatrix} - C_{cl}x_d(t)\\ w_d(t) = C_{cl}x_d(t) + D_{cl}\lambda_d(t) + Cx_d(t) + Fu_d(t) + \begin{pmatrix}0\\1\end{pmatrix} - C_{cl}x_d(t).\end{cases}$$

Therefore, it is inferred that:

$$\begin{cases} \lambda(t) \in \mathcal{N}_{S(t)}(C_{cl}x(t) + D_{cl}\lambda(t)) \\ \\ \lambda_d(t) \in \mathcal{N}_{S(t)}(C_{cl}x_d(t) + D_{cl}\lambda_d(t)), \end{cases} \tag{4.22}$$

with $S(t) \triangleq \{\xi \in I\!R^m \mid \xi + Cx_d(t) + Fu_d(t) + \begin{pmatrix} 0 \\ 1 \end{pmatrix} - C_{cl}x_d(t) \geq 0\}$. From the monotonicity of the normal cone, it follows that:

$$(w(t) - w_d(t))^\top (\lambda(t) - \lambda_d(t)) \leq 0$$

Given that $w(t) - w_d(t) = C_{cl}e(t) + D_{cl}(\lambda(t) - \lambda_d(t))$, $\dot{V}(e(t))$ is written in the matrix form as:

$$\begin{aligned} \dot{V}(t) &= \begin{pmatrix} e \\ \Delta\lambda \end{pmatrix}^\top M \begin{pmatrix} e \\ \Delta\lambda \end{pmatrix} + \begin{pmatrix} e \\ \Delta\lambda \end{pmatrix}^\top \begin{pmatrix} 0 & (C+FK)^\top \\ C+FK & D+FG+(D+FG)^\top \end{pmatrix} \begin{pmatrix} e \\ \Delta\lambda \end{pmatrix} \\ &= \begin{pmatrix} e \\ \Delta\lambda \end{pmatrix}^\top M \begin{pmatrix} e \\ \Delta\lambda \end{pmatrix} + 2\Delta\lambda^\top \Delta w \leq \begin{pmatrix} e \\ \Delta\lambda \end{pmatrix}^\top M \begin{pmatrix} e \\ \Delta\lambda \end{pmatrix} \leq -\epsilon\, e(t)^\top P e(t), \end{aligned}$$

where M is the matrix defined in (4.10) and satisfying the strict state passivity LMI. Hence, $e^\star = 0$ is globally exponentially stable.

(ii): follows from the projection form of λ_t in (4.12) which can be represented as:

$$\lambda_t(q, \dot{q}) = \text{proj}\left([-1,1];\ \frac{2}{g_{21}}\left((\dot{q} - \dot{q}_d) - k_{21}(q - q_d) - k_{22}(\dot{q} - \dot{q}_d) + g_{21}\lambda_{1d} - \frac{g_{21}}{2} + \dot{q}_d - u_{2d}\right)\right)$$

Similarly, $\lambda_{t,d}$ is written as follows

$$\lambda_{t,d} \in \text{sgn}(\dot{q} - u_{2d}) = \text{sgn}\left(\frac{2}{g_{21}}(\dot{q}_d - u_{2d})\right) \quad \Leftrightarrow \quad \lambda_{t,d} = \text{proj}\left([-1,1]; \frac{2}{g_{21}}(\dot{q}_d - u_{2d}) + \lambda_{t,d}\right)$$

Recall that $x \triangleq (q, \dot{q})^\top$ and $x_d \triangleq (q_d, \dot{q}_d)^\top$. Given that $\lambda_t = 2\lambda_1 - 1$ and $\lambda_{t,d} = 2\lambda_{1,d} - 1$, then:

$$\begin{aligned} |\lambda_1 - \lambda_{1d}| &= \frac{1}{2}|\lambda_t - \lambda_{t,d}| \\ &= \frac{1}{2}\left|\text{proj}\left([-1,1]; \frac{2}{g_{21}}(-[C_{cl}]_{1,\bullet}e + \lambda_{t,d} + x_{2d} - u_{2d})\right) - \text{proj}\left([-1,1]; \frac{2}{g_{21}}(\lambda_{t,d} + x_{2d} - u_{2d})\right)\right| \\ &\leq \frac{1}{g_{21}}\|C_{cl}e\|, \end{aligned}$$

where we have used the Lipschitz continuity property of the projection operator ([14, Proposition 4.8]) to obtain the last inequality.
Hence, $\lim_{t\to\infty}|\lambda_1(t) - \lambda_{1d}(t)| \leq \frac{1}{g_{21}}\lim_{t\to\infty}\|C_{cl}e(t)\| = 0$. □

Remark 4.4.3. *The stability analysis of part (i) of Proposition 4.4.2 can be established directly through the maximal monotonicity of the signum function when $g_{21} = 0$ without relying on the LCS interpretation (*i.e.*, the normal cone approach as in (4.22)). This*

will be useful later when we deal with Stribeck effects. Let us consider again the closed-loop error dynamics in (4.21) as:

$$\dot{e}(t) \in A_{cl}e(t) + \begin{pmatrix} 0 \\ \mu g \end{pmatrix} sgn(\dot{q}_d(t) - u_{2d}(t)) - \begin{pmatrix} 0 \\ \mu g \end{pmatrix} sgn(\dot{q}(t) - u_2(t))$$

By taking $V(e) = e^\top Pe$, with $P = P^\top \succ 0$ as before, then:

$$\dot{V}(e(t)) = e^\top (A_{cl}^\top P + PA_{cl})e + 2e^\top P \begin{pmatrix} 0 \\ \mu g \end{pmatrix} [sgn(\dot{q}_d(t) - u_{2d}(t)) - sgn(\dot{q}(t) - u_2(t))]$$

Take $P = \begin{pmatrix} p_{11} & p_{12} \\ p_{12} & p_{22} \end{pmatrix}$, then: $P \begin{pmatrix} 0 \\ \mu g \end{pmatrix} = \begin{pmatrix} p_{12}\mu g \\ p_{22}\mu g \end{pmatrix}$ and $PB_{cl} = \begin{pmatrix} -2p_{12}\mu g & 0 \\ -2p_{22}\mu g & 0 \end{pmatrix}$. Hence, $P \begin{pmatrix} 0 \\ \mu g \end{pmatrix} = -\frac{1}{2}(PB_{cl})_{\bullet,1} = -\frac{1}{2}(C_{cl}^\top)_{\bullet,1}$. From the fact that $(C_{cl})_{1,\bullet}e(t) = u_2(t) - \dot{q}(t) - u_{2d}(t) + \dot{q}_d(t)$ (see (4.5)), and that the mapping $x \mapsto sgn(x)$ is maximal monotone, the rate of change of the storage function is calculated as:

$$\begin{aligned}
\dot{V}(e(t)) &= e^\top (A_{cl}^\top P + PA_{cl})e - e^\top (PB_{cl})_{\bullet,1} [sgn(\dot{q}_d(t) - u_{2d}(t)) - sgn(\dot{q}(t) - u_2(t))] \\
&= e^\top (A_{cl}^\top P + PA_{cl})e - e^\top (C_{cl}^\top)_{\bullet,1} [sgn(\dot{q}_d(t) - u_{2d}(t)) - sgn(\dot{q}(t) - u_2(t))] \\
&= [\dot{q}(t) - u_2(t) - \dot{q}_d(t) + u_{2d}(t)]^\top [sgn(\dot{q}_d(t) - u_{2d}(t)) - sgn(\dot{q}(t) - u_2(t))] \\
&\quad + e^\top (A_{cl}^\top P + PA_{cl})e \\
&= -[\dot{q}(t) - u_2(t) - (\dot{q}_d(t) - u_{2d}(t))]^\top [sgn(\dot{q}(t) - u_2(t)) - sgn(\dot{q}_d(t) - u_{2d}(t))] \\
&\quad + e^\top (A_{cl}^\top P + PA_{cl})e \\
&\leq e^\top (A_{cl}^\top P + PA_{cl})e \leq -\epsilon\, e(t)^\top Pe(t)
\end{aligned} \tag{4.23}$$

Thus, $e(\cdot)$ converges globally exponentially to zero.

Remark 4.4.4. *Proposition 4.4.2 shows that a linear feedback $u_1(q, \dot{q}, t)$ is sufficient to guarantee exponential stability. Another approach is to design a sliding-mode controller to compensate for the friction force as if it was a disturbance. This is however a quite different approach which does not use u_2 as an input. The goal here is to investigate how the combination of u_1 and u_2 allows to achieve tracking.*

4.4.3 Numerical Simulation

Take $m = 1$ kg, $g = 9.8m/s^2$, and $\mu = 0.5$. Let us check if there exist matrices K, G and P such that the closed-loop system's quadruple $(A_{cl} = A + EK, B_{cl} = B + EG, C_{cl} = C + FK, D_{cl} = D + FG)$ is strictly state passive. This means that the BMI in (4.10) has a solution which is given by the following:

$$K = \begin{pmatrix} -1.49 & -1.18 \\ -5.463 & -12.09 \end{pmatrix}, \quad G = \begin{pmatrix} 0 & 0 \\ 0.5 & 0 \end{pmatrix} \quad \text{and} \quad P = \begin{pmatrix} 1.3367 & 0.56 \\ 0.56 & 1.3361 \end{pmatrix} \succ 0$$

with $\epsilon = 0.01$. Let us take $G = 0$ and check if there exist K and P such that the closed-loop system's quadruple $(A_{cl} = A + EK, B_{cl} = B, C_{cl} = C + FK, D_{cl} = D)$ is strictly state passive which means that the BMI in (4.10) has a solution given by:

$$K = \begin{pmatrix} -1.49 & -1.17 \\ -5.46 & -12.1 \end{pmatrix} \quad \text{and} \quad P = \begin{pmatrix} 1.34 & 0.557 \\ 0.557 & 1.34 \end{pmatrix}$$

with $\epsilon = 0.01$. Notice that when $G = 0$ the passivity LMI implies that $PB_{cl} = C_{cl}^{\top}$ since $D + D^{\top} = 0$, which yields $-2p_{12}\mu g = k_{21}$ and $-2p_{22}\mu g = k_{22} - 1 < 0$.

The plots in Figures 4.9 and 4.10 show the numerical simulation of the desired system in (4.6), the closed-loop system in (4.5), and the error dynamics in (4.9) with external input $u = (u_1, u_2)^{\top} = K(x - x_d) + u_d$. The desired system which is subject to tracking is analyzed in section 4.3. Take $x(0) = (0, -1)^{\top}$, $x_d(0) = (1, 0)^{\top}$ and the time step $h = 0.01$.

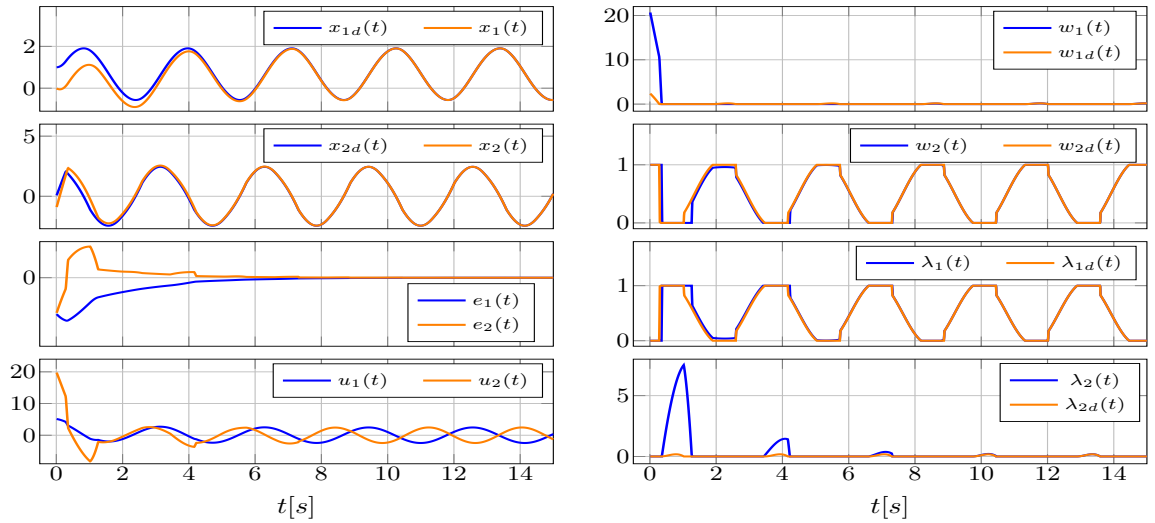

Figure 4.9: Numerical simulation of the desired, closed-loop and error systems of the LCS in (4.3) showing the controller $u(t)$ with $u_{1d} = u_{2d} = 0.5m\mu g \cos 2t$ and $G = 0$. The simulation also presents the complementarity variables λ and w.

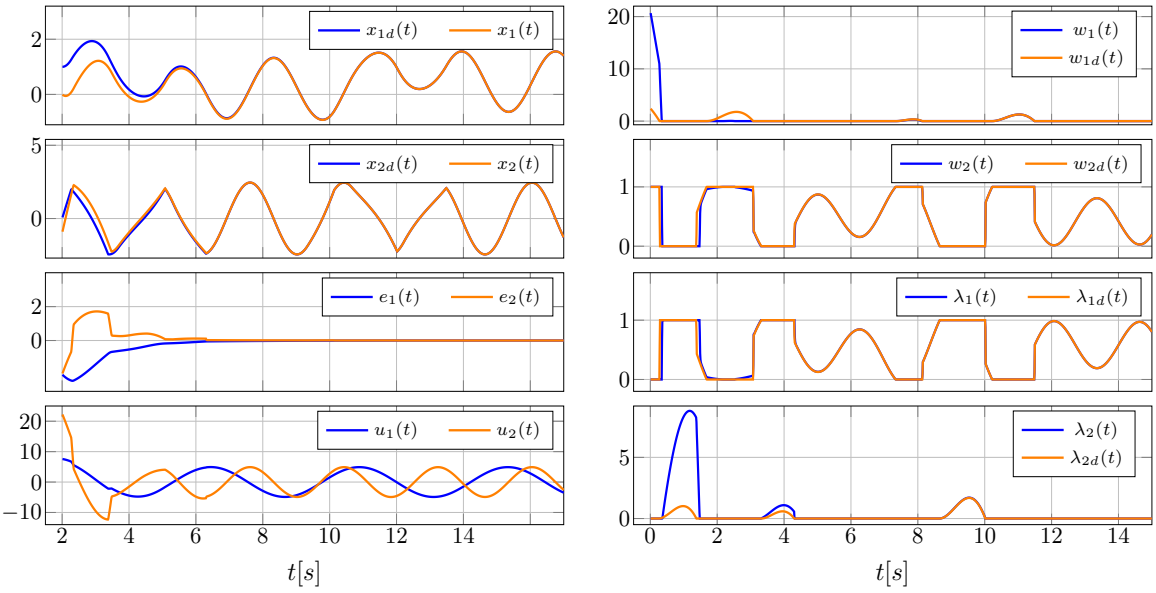

Figure 4.10: Numerical simulation of the desired, closed-loop and error systems of the LCS in (4.3) with $u_{1d} = 0.5m\mu g \cos\sqrt{2}t$, $u_{2d} = 0.5m\mu g \cos\sqrt{5}t$ and $G \neq 0$. The simulation also presents the complementarity variables λ and w.

The numerical simulation depicted in Figure 4.9 shows that tracking of the desired trajectory x_d is achieved without the requirement of an additional feedback from λ (*i.e.*, $G = 0$) which aligns with the result presented in Remark 4.4.3. An additional feedback from λ results in faster convergence for the system simulated in Figure 4.10 with different external desired inputs. Furthermore, it is interesting to observe that the complementarity variables of the closed-loop system (λ and w) converge to the complementarity variables of the desired system (λ_d and w_d) in both Figures 4.9 and 4.10. The plots of the controller u in the two figures exhibit a periodic behaviour in the steady state response (*i.e.*, $e = x - x_d = 0$), where u converges to the periodic desired input u_d.

4.5 Parametric Robustness Analysis

This section is dedicated to analyse the robustness of the above scheme (which is designed assuming the strict state passivity of the closed-loop system, not its strong passivity) when uncertainties $\Delta\mu$ are present in the friction coefficient, which is supposed to be known only with a nominal value $\mu_0 > 0$. Then, it is crucial that a kind of contact force feedback is made (using the multiplier λ_1 and the gain g_{21}), for otherwise the robustness is lost. Propositions 2.4.4, 2.4.7 and Lemma 2.4.6 are used in this setting.

4.5.1 Robustness Analysis with Bounded and Time-varying Uncertainties $\Delta\mu(\dot{q}_{rel})$

Let us recall that with $\dot{q}_{rel} = \dot{q} - u_2$. Here, we consider that the nominal friction coefficient μ_0 (used in the desired dynamics and the nominal model of the plant) and the "real" plant's friction coefficient μ, are not the same. It could even be that μ_0 is chosen constant while $\mu = \mu(t, \dot{q})$, then $\Delta\mu(\dot{q}_{rel}) = \mu(\dot{q}_{rel}) - \mu_0$. It is noteworthy from (4.3) that uncertainties satisfy:

$$\Delta A = 0, \Delta C = 0, \Delta D = 0, \Delta E = 0, \Delta F = 0, \Delta B = \begin{pmatrix} 0 & 0 \\ -2g\Delta\mu & 0 \end{pmatrix}, \Delta E' = \begin{pmatrix} 0 \\ g\Delta\mu \end{pmatrix}.$$

According to Remark 4.4.1, the closed-loop system in (4.5) cannot be made strongly passive. Thus, it is not possible to apply directly the results from section 2.4.2. Instead, let us try to relax the conditions of strong passivity by referring to the material in section 2.4.3. Recall the dynamics of the desired system in (4.6) as:

$$\begin{cases} \dot{x}_d(t) = \underbrace{\begin{pmatrix} 0 & 1 \\ 0 & 0 \end{pmatrix}}_{A_0} x_d(t) + \underbrace{\begin{pmatrix} 0 & 0 \\ -2\mu_0 g & 0 \end{pmatrix}}_{B_0} \lambda_d(t) + \underbrace{\begin{pmatrix} 0 & 0 \\ \frac{1}{m} & 0 \end{pmatrix}}_{E_0} u_d(t) + \underbrace{\begin{pmatrix} 0 \\ \mu_0 g \end{pmatrix}}_{E_0'} \\ 0 \leq \lambda_d(t) \perp w_d(t) = \underbrace{\begin{pmatrix} 0 & -1 \\ 0 & 0 \end{pmatrix}}_{C_0} x_d(t) + \underbrace{\begin{pmatrix} 0 & 1 \\ -1 & 0 \end{pmatrix}}_{D_0} \lambda_d(t) + \underbrace{\begin{pmatrix} 0 & 1 \\ 0 & 0 \end{pmatrix}}_{F_0} u_d(t) + \underbrace{\begin{pmatrix} 0 \\ 1 \end{pmatrix}}_{F_0'} \geq 0 \end{cases}$$

The dynamics of the closed-loop system in (4.5) with parametric uncertainties is written as:

$$\begin{cases} \dot{x}(t) = (A_0 + E_0K_0)x(t) + (B_0 + \Delta B)\lambda(t) - E_0K_0x_d(t) + E_0u_d(t) + E_0' + \Delta E' \\ 0 \leq \lambda(t) \perp w(t) = (C_0 + F_0K_0)x(t) + (D_0 + F_0G_0)\lambda(t) - F_0K_0x_d(t) - F_0G_0\lambda_d(t) \\ \qquad\qquad +F_0u_d(t) + F_0' \geq 0 \end{cases} \tag{4.24}$$

The closed-loop error dynamics $e = x - x_d$ is:

$$\begin{cases} \dot{e}(t) = A_{cl}e(t) + B_{cl}\Delta\lambda(t) + \Delta B\lambda(t) + \Delta E' \\ \Delta w(t) = C_{cl}e(t) + D_{cl}\Delta\lambda(t) \\ 0 \leq \lambda(t) \perp w(t) \geq 0 \quad \text{and} \quad 0 \leq \lambda_d(t) \perp w_d(t) \geq 0 \end{cases} \tag{4.25}$$

where $\Delta\lambda(t) = \lambda(t) - \lambda_d(t)$ and $A_{cl} = A_0 + E_0K_0, B_{cl} = B_0, C_{cl} = C_0 + F_0K_0$ and $D_{cl} = D_0 + F_0G_0$. The stability result is stated as follows.

Proposition 4.5.1. *Consider the error dynamics in (4.25). Assume that:*

- *(i) The uncertainties are bounded such that* $\Delta B^\top \hat{\Lambda}_B^{-1} \Delta B \preccurlyeq \begin{pmatrix} 1 & 0 \\ 0 & 0 \end{pmatrix}$ *and* $\Delta E'^\top \hat{\Lambda}_1^{-1} \Delta E' \preccurlyeq I_m$, *given the matrices* $\hat{\Lambda}_k = \hat{\Lambda}_k^\top \succ 0$ *where* $k \in \{1, B\}$.

- *(ii) There exists a matrix* $P_0 = P_0^\top \succ 0$ *such that the quadruple* $(A_{cl}, B_0, C_{cl}, D_{cl})$, *corresponding to the nominal closed-loop system in* (4.5) *with* $\mu = \mu_0$, *is strictly state passive with* $\epsilon > 0$.
- *(iii) The control gain* $G = \begin{pmatrix} 0 & 0 \\ g_{21} & 0 \end{pmatrix}$ *is chosen such that* $g_{21} > \frac{1}{2}$.
- *(iv) The following inequality holds:*

$$\sigma_{\max}\left(-P_0(\hat{\Lambda}_1 + \hat{\Lambda}_B)P_0\right) + \sigma_{\max}\left(\left(-P_0B_0 + C_{cl}^\top\right)\left(-B_0^\top P_0 + C_{cl}\right)\right) \leq \epsilon\lambda_{\max}(P_0)$$

for $P_0 = P_0^\top \succ 0$ *and* $\epsilon > 0$.

Then, the solution of the error dynamics in (4.25) *is globally uniformly ultimately bounded (GUUB), satisfying:* $\|e\| \leq \sqrt{\frac{\lambda_{\max}(P_0)\lambda_{\min}^{-1}(\hat{\Lambda}_1)\rho}{\lambda_{\min}^2(P_0)\epsilon'}}$, *where* $\rho = \frac{det(\hat{\Lambda}_B)}{\hat{\Lambda}_{B_{11}}}$ *defines the bound on* ΔE.

For the sake of notation simplicity, the matrices M_0 and ΔM_0 are not explicitly stated in the theorem. These matrices are defined in the following proof.

Proof. The proof is divided into two main parts. In the first part, a suitable storage is derived for the error dynamics in (4.25) to serve as a Lyapunov function. Then, the second part presents explicitly the conditions to prove that the Lyapunov function decreases over time.

Construction of Lyapunov function. The storage function $V(t) = e^\top P_0 e$ where P_0 is the solution of the strict passivity BMI transformed into LMI (see Appendix A.1) given by: $M_0 \preccurlyeq \begin{pmatrix} -\epsilon P_0 & 0 \\ 0 & 0 \end{pmatrix}$ where M_0 is defined as:

$$M_0 \triangleq \begin{pmatrix} A_{cl}^\top P_0 + P_0 A_{cl} & P_0 B_{cl} - C_{cl}^\top \\ B_{cl}^\top P_0 - C_{cl} & -D_{cl} - D_{cl}^\top \end{pmatrix} \tag{4.26}$$

Let us define $p(t, \lambda) \triangleq \Delta B\lambda(t) + \Delta E'$. The rate of change of the storage function is:

$$\dot{V} = e^\top(A_{cl}^\top P_0 + P_0 A_{cl})e + 2e^\top P_0 B_{cl}\Delta\lambda + 2e^\top P_0 p(t, \lambda) \pm 2\Delta\lambda^\top \Delta w$$

The added and subtracted term is to recover the matrix M_0 in (4.26). In matrix form, it is represented as:

$$2\Delta\lambda^\top \Delta w = \begin{pmatrix} e \\ \Delta\lambda \end{pmatrix}^\top \begin{pmatrix} 0 & C_{cl}^\top \\ C_{cl} & D_{cl} + D_{cl}^\top \end{pmatrix} \begin{pmatrix} e \\ \Delta\lambda \end{pmatrix}$$

Then,

$$\dot{V} = \begin{pmatrix} e \\ \Delta\lambda \end{pmatrix}^\top M_0 \begin{pmatrix} e \\ \Delta\lambda \end{pmatrix} + 2e^\top P_0 p(t, \lambda) + 2\Delta\lambda^\top \Delta w \tag{4.27}$$

Let us substitute the expression of $p(t,\lambda)$ in (4.27), then:

$$\dot{V} = \begin{pmatrix} e \\ \Delta\lambda \end{pmatrix}^\top M_0 \begin{pmatrix} e \\ \Delta\lambda \end{pmatrix} + \begin{pmatrix} e \\ \Delta\lambda \end{pmatrix}^\top \begin{pmatrix} 0 & P_0\Delta B \\ \Delta B^\top P_0 & 0 \end{pmatrix} \begin{pmatrix} e \\ \Delta\lambda \end{pmatrix} + 2e^\top P_0 \Delta E' + 2\Delta\lambda^\top \Delta w$$

By considering monotonicity of the mapping $-\lambda \mapsto w$ (or $-\lambda_d \mapsto w_d$) in (4.25), the following inequality is obtained:

$$\dot{V} \leq -\begin{pmatrix} e \\ \Delta\lambda \end{pmatrix}^\top (-M_0 + \Delta M_0) \begin{pmatrix} e \\ \Delta\lambda \end{pmatrix} + 2e^\top P_0 \Delta E'$$

with $\Delta M_0 \triangleq \begin{pmatrix} 0 & -P_0\Delta B \\ -\Delta B^\top P_0 & 0 \end{pmatrix}$. For any $\hat{\Lambda}_1^\top = \hat{\Lambda}_1 \succ 0$, the following holds:

$$|2e^\top P_0 \Delta E'| \leq e^\top P_0 \hat{\Lambda}_1 P_0 e + \Delta E'^\top \hat{\Lambda}_1^{-1} \Delta E'$$

Thus,

$$\dot{V} \leq -\begin{pmatrix} e \\ \Delta\lambda \end{pmatrix}^\top \left(-M_0 + \Delta M_0 - \begin{pmatrix} P_0\hat{\Lambda}_1 P_0 & 0 \\ 0 & 0 \end{pmatrix}\right) \begin{pmatrix} e \\ \Delta\lambda \end{pmatrix} + \Delta E'^\top \hat{\Lambda}_1^{-1} \Delta E' \tag{4.28}$$

The expression $\begin{pmatrix} e \\ \Delta\lambda \end{pmatrix}^\top \Delta M_0 \begin{pmatrix} e \\ \Delta\lambda \end{pmatrix}$ is equivalently written as: $-2e^\top P_0 \Delta B \Delta\lambda$. Assume that $\Delta B^\top \hat{\Lambda}_B^{-1} \Delta B \preccurlyeq I_m$ for $\hat{\Lambda}_B^\top = \hat{\Lambda}_B \succ 0$, then:

$$2\Delta\lambda^\top \Delta B^\top P_0 e \geq -e^\top P_0 \hat{\Lambda}_B P_0 e - \Delta\lambda^\top \Delta B^\top \hat{\Lambda}_B^{-1} \Delta B \Delta\lambda$$

Let $z \triangleq \begin{pmatrix} e \\ \Delta\lambda \end{pmatrix}$, thus:

$$z^\top \left[-M_0 + \Delta M_0 - \begin{pmatrix} P_0\hat{\Lambda}_1 P_0 & 0 \\ 0 & 0 \end{pmatrix}\right] z \geq z^\top \begin{pmatrix} -(M_0)_{11} - P_0(\hat{\Lambda}_1 + \hat{\Lambda}_B)P_0 & -(M_0)_{12} \\ -(M_0)_{21} & -(M_0)_{22} - I_m \end{pmatrix} z \tag{4.29}$$

It is impossible to prove that the matrix inequality $-M_0 + \Delta M_0 - \begin{pmatrix} P_0\hat{\Lambda}_1 P_0 - \epsilon' P_0 & 0 \\ 0 & 0 \end{pmatrix} \succcurlyeq 0$ holds because, according to the conditions for positive semi-definiteness in Lemma A.3.1, the bottom-right diagonal term: $-(M_0)_{22} - I_m = D_{cl} + D_{cl}^\top - I_m = \begin{pmatrix} 2g_{21} - 1 & 0 \\ 0 & -1 \end{pmatrix}$ is not positive semidefinite.

This result motivates us to change the assumption $\Delta B^\top \hat{\Lambda}_B^{-1} \Delta B \preccurlyeq I_m$ which is similar to the assumptions in (2.59) stated in Proposition 2.4.3. Now, let us take $\hat{\Lambda}_B = \begin{pmatrix} d & e \\ e & f \end{pmatrix} \succ 0$ for some $d, e, f \in \mathbb{R}$. Assume that:

$$\Delta B^\top \hat{\Lambda}_B^{-1} \Delta B = \frac{1}{df - e^2} \begin{pmatrix} 4g^2\Delta\mu^2 d & 0 \\ 0 & 0 \end{pmatrix} \preccurlyeq \begin{pmatrix} 1 & 0 \\ 0 & 0 \end{pmatrix} \tag{4.30}$$

According to the new assumption in (4.30), the inequality in (4.29) is written as:

$$z^\top \left[-M_0 + \Delta M_0 - \begin{pmatrix} P_0\hat{\Lambda}_1 P_0 & 0 \\ 0 & 0 \end{pmatrix}\right] z \geq z^\top \begin{pmatrix} -(M_0)_{11} - P_0(\hat{\Lambda}_1 + \hat{\Lambda}_B)P_0 & -(M_0)_{12} \\ -(M_0)_{21} & -(M_0)_{22} - \hat{I} \end{pmatrix} z$$

where $\hat{I} \triangleq \begin{pmatrix} 1 & 0 \\ 0 & 0 \end{pmatrix}$. Let us define

$$\begin{aligned} \hat{L} &\triangleq -M_0 + \Delta M_0 - \begin{pmatrix} P_0\hat{\Lambda}_1 P_0 & 0 \\ 0 & 0 \end{pmatrix} - \begin{pmatrix} \epsilon' P_0 & 0 \\ 0 & 0 \end{pmatrix} \\ &\triangleq \begin{pmatrix} -A_{cl}^\top P_0 - P_0 A_{cl} - P_0(\hat{\Lambda}_1 + \hat{\Lambda}_B)P_0 - \epsilon' P_0 & -P_0 B_{cl} + C_{cl}^\top \\ -B_{cl}^\top P_0 + C_{cl} & D_{cl} + D_{cl}^\top - \hat{I} \end{pmatrix} \succcurlyeq 0 \end{aligned} \tag{4.31}$$

The term $\epsilon' P_0$ is introduced for bounding the error as will be shown later. For stability analysis, it is required to prove that $\dot{V} \leq 0$ holds in a certain domain to be defined. This means that it is necessary to show that the matrix inequality $\hat{L} \succcurlyeq 0$ holds for $\epsilon' > 0$, as detailed below.

Conditions for $\hat{L} \succcurlyeq 0$ in (4.31) to hold true. The goal is to prove that the matrix inequality $\hat{L} \succcurlyeq 0$ holds. The conditions presented below are derived from proving positive semi-definite matrix and relaxing strong passivity into strict state passivity which is explained in section 2.4.3.

Take $\hat{Q} \triangleq \underbrace{-A_{cl}^\top P_0 - P_0 A_{cl} - \epsilon' P_0}_{\hat{Q}_0} + \underbrace{(-P_0(\hat{\Lambda}_1 + \hat{\Lambda}_B)P_0)}_{\Delta\hat{Q}}$, $\hat{S} \triangleq \underbrace{-P_0 B_{cl} + C_{cl}^\top}_{\hat{S}_0}$ and $\hat{R} \triangleq \underbrace{D_{cl} + D_{cl}^\top}_{\hat{R}_0} + \underbrace{(-\hat{I})}_{\Delta\hat{R}}$ where $P_0 = \begin{pmatrix} p_{11} & p_{12} \\ p_{12} & p_{22} \end{pmatrix}$ such that $P_0 = P_0^\top \succ 0$, which is the solution of $M_0 \preccurlyeq \begin{pmatrix} -\epsilon P_0 & 0 \\ 0 & 0 \end{pmatrix}$ with M_0 defined in (4.26).

Consider that $\hat{\Lambda}_1 = \begin{pmatrix} a & b \\ b & c \end{pmatrix} \succ 0$ for some $a, b, c \in \mathbb{R}$. The matrices A_{cl}, B_{cl}, C_{cl} and D_{cl} are defined in (4.5). Let us explicitly write the matrices $\hat{Q} = \hat{Q}_0 + \Delta\hat{Q}$, $\hat{R} = \hat{R}_0 + \Delta\hat{R}$ and $\hat{S} = \hat{S}_0$:

$$\hat{Q}_0 = \begin{pmatrix} -2p_{12}\frac{k_{11}}{m} - \epsilon' p_{11} & -p_{11} - \frac{k_{12}}{m}p_{12} - \frac{k_{11}}{m}p_{22} - \epsilon' p_{12} \\ -p_{11} - \frac{k_{12}}{m}p_{12} - \frac{k_{11}}{m}p_{22} - \epsilon' p_{12} & -2p_{12} - 2\frac{k_{12}}{m}p_{22} - \epsilon' p_{22} \end{pmatrix},$$

$$-\Delta\hat{Q} = \begin{pmatrix} p_{11}^2(a+d) + p_{12}^2(c+f) + 2p_{11}p_{12}(b+e) & (p_{12}^2 + p_{11}p_{22})(b+e) + p_{11}p_{12}(a+d) + p_{12}p_{22}(c+f) \\ (p_{12}^2 + p_{11}p_{22})(b+e) + p_{11}p_{12}(a+d) + p_{12}p_{22}(c+f) & p_{12}^2(a+d) + p_{22}^2(c+f) + 2p_{12}p_{22}(b+e) \end{pmatrix}$$

$$\hat{S} = \hat{S}_0 = \begin{pmatrix} 2p_{12}\mu g + k_{21} & 0 \\ 2p_{22}\mu g - 1 + k_{22} & 0 \end{pmatrix}, \quad \hat{R}_0 = \begin{pmatrix} 2g_{21} & 0 \\ 0 & 0 \end{pmatrix}, \text{ and } \Delta\hat{R} = \begin{pmatrix} -1 & 0 \\ 0 & 0 \end{pmatrix}$$

By considering the conditions for positive semi-definiteness in Appendix A.3, and following Lemma A.3.1, the matrix $\hat{L} \triangleq \begin{pmatrix} \hat{Q}_0 + \Delta\hat{Q} & \hat{S}_0 \\ \hat{S}_0^\top & \hat{R}_0 + \Delta\hat{R} \end{pmatrix} \succcurlyeq 0$ if and only if:

1. $\hat{R} \succcurlyeq 0 \Leftrightarrow \begin{pmatrix} 2g_{21}-1 & 0 \\ 0 & 0 \end{pmatrix} \succcurlyeq 0$ which is satisfied for all g_{21} such that $g_{21} \geq \frac{1}{2}$.

2. $\mathrm{Im}(\hat{S}^\top) \subseteq \mathrm{Im}(\hat{R})$ and this condition holds as a consequence of the following:

$$\begin{aligned}
&\mathrm{Im}(\hat{S}_0^\top) = \mathrm{Im}(\hat{S}^\top) \\
&= \left\{ w \in \mathbb{R}^2 \mid w = \begin{pmatrix} (2\mu g p_{12} + k_{12})x + (2\mu g p_{22} - 1 + k_{22})y \\ 0 \end{pmatrix} \text{ for some } x,\ y \in \mathbb{R} \right\} \\
&\subseteq \mathrm{Im}(\hat{R}) = \left\{ w \in \mathbb{R}^2 \mid w = \begin{pmatrix} (2g_{21}-1)t \\ 0 \end{pmatrix} \text{ for some } t \in \mathbb{R} \right\}
\end{aligned}$$

3. $\hat{Q} \succeq \hat{S}\hat{R}^\dagger\hat{S}^\top$. Let us follow the conditions presented in Proposition 2.4.7 in order to check the validity of this item (*i.e.,* $Q \succeq SR^\dagger S^\top$), then:
(i) $\hat{R} \succcurlyeq 0$ for $g_{21} \geq \frac{1}{2}$,

(ii) $\mathrm{Im}(\Delta R) = \left\{ w \in \mathbb{R}^2 \mid w = \begin{pmatrix} -y \\ 0 \end{pmatrix} \text{ for some } y \in \mathbb{R} \right\}$
$\subseteq \mathrm{Im}(R_0) = \left\{ w \in \mathbb{R}^2 \mid w = \begin{pmatrix} 2g_{21}x \\ 0 \end{pmatrix} \text{ for some } x \in \mathbb{R} \right\}$,

(iii) $\mathrm{rank}(R_0) = 1$, $\sigma_{\max}(\Delta R) = 1 < \sigma_1(R_0) = 2g_{21}$ which holds for $g_{21} > \frac{1}{2}$,

(iv) $\sigma_{\max}(OT) + \sigma_{\max}(\Delta\hat{Q}) < \epsilon\lambda_{\max}(P_0)$ where OT is defined in (2.66) and in this case, where $\Delta\hat{S} = 0$, it is written as:

$$OT = -\hat{S}_0\hat{R}_0^\dagger\Delta\hat{R}\hat{R}_0^\dagger\hat{S}_0^\top$$

with $\hat{R}^\dagger = \begin{pmatrix} \frac{1}{2g_{21}} & 0 \\ 0 & 0 \end{pmatrix}$. After performing calculations, the matrix OT is explicitly written as:

$$\begin{aligned}
OT &= \tfrac{1}{4g_{21}^2} \begin{pmatrix} (2p_{12}\mu g + k_{21})^2 & (2p_{12}\mu g + k_{21})(2p_{22}\mu g - 1 + k_{22}) \\ (2p_{22}\mu g - 1 + k_{22})(2p_{12}\mu g + k_{21}) & (2p_{22}\mu g - 1 + k_{22})^2 \end{pmatrix} \\
&= \tfrac{1}{4g_{21}^2}\hat{S}_0\hat{S}_0^\top
\end{aligned}$$

According to [17, Fact 5.11.5] and given that OT is positive semi-definite, $\sigma_i(OT) = \lambda_i(OT)$ for $i \in 1, 2$. Then,
$\sigma_{\max}(OT) = \frac{1}{4g_{21}^2}\left((2p_{12}\mu g + k_{21})^2 + (2p_{22}\mu g - 1 + k_{22})^2\right) > 0$. Given that $P_0 = P_0^\top \succ 0$, then $\lambda_{\max}(P_0) > 0$. Note that the matrices $\Delta\hat{Q}$ and $-(\hat{\Lambda}_1 + \hat{\Lambda}_B)$ are congruent, so they have the same number and signs of eigenvalues [85, Theroem 4.5.8]. This means that $\lambda_i(\Delta\hat{Q}) < 0$ for $i \in \{1, 2\}$. Assume that $\hat{\Lambda}_1 = \alpha I_2$ and $\hat{\Lambda}_B = \beta I_2$, $\alpha > 0$, $\beta > 0$, then $\Delta\hat{Q} = -(\alpha + \beta)P_0^2$ which is symmetric (*i.e.,* $\Delta\hat{Q} = \Delta\hat{Q}^\top$). As $P_0 = P_0^\top \succ 0$, it follows that $\sigma_i(P_0) = \lambda_i(P_0)$. Thus, $\sigma_{\max}(\Delta\hat{Q}) = (\alpha + \beta)\lambda_{\max}^2(P_0)$. Hence, item (iv) is written as: $(\alpha + \beta)\lambda_{\max}(P_0)^2 - \epsilon\lambda_{\max}(P_0) + \sigma_{max}(OT) < 0$. In order to find the conditions

such that item (iv) in Proposition 2.4.7 is satisfied, let us solve the inequality with the variable $\hat{\theta}$ as follows:

$$(\alpha+\beta)\hat{\theta}^2 - \epsilon\hat{\theta} + \sigma_{\max}(OT) < 0 \tag{4.32}$$

The roots are

$$\hat{\theta}_1 = \frac{1}{2(\alpha+\beta)}\left(\epsilon - \sqrt{\epsilon^2 - 4(\alpha+\beta)\sigma_{\max}(OT)}\right)$$

$$\hat{\theta}_2 = \frac{1}{2(\alpha+\beta)}\left(\epsilon + \sqrt{\epsilon^2 - 4(\alpha+\beta)\sigma_{\max}(OT)}\right)$$

Based on the solution of the quadratic inequality (4.32), and following the condition of item (iv) in Proposition 2.4.7, $\lambda_{\max}(P_0)$ must satisfy the condition

$$\hat{\theta}_1 < \lambda_{\max}(P_0) < \hat{\theta}_2 \tag{4.33}$$

where the roots $\hat{\theta}_1$ and $\hat{\theta}_2$ are real and positive if the discriminant: $\epsilon^2 - 4(\alpha+\beta)\sigma_{\max}(OT) \geq 0$, given that $\alpha+\beta > 0$. It is possible to find $\lambda_{\max}(P_0)$ satisfying (4.33) by properly constraining α and β, consequently constraining the uncertainty $\Delta\mu$. Additionally, ϵ can be chosen to determine the control gain K_0, which determines $\sigma_{\max}(OT)$.

Thus, this item (*i.e.*, $\hat{Q} \succcurlyeq \hat{S}\hat{R}^{\dagger}\hat{S}^{\top}$) is satisfied such that all the conditions in Proposition 2.4.7 holds as explained above.

Therefore, the matrix inequality $\hat{L} \succcurlyeq 0$ in (4.31) holds. Given that $\frac{4\Delta\mu^2 g^2 d}{df-e^2} \leq 1$ derived from the bound on ΔB in (4.30) where $\hat{\Lambda}_B = \begin{pmatrix} d & e \\ e & f \end{pmatrix} \succ 0$, let us assume that $||\Delta E'||^2 \leq \rho$ where $\rho = \frac{df-e^2}{4d}$. Thus, the inequality in (4.28) is written as:

$$\begin{aligned}
\dot{V} &\leq -\begin{pmatrix} e \\ \Delta\lambda \end{pmatrix}^{\top} \left(-M_0 + \Delta M_0 - \begin{pmatrix} P_0\hat{\Lambda}_1 P_0 & 0 \\ 0 & 0 \end{pmatrix}\right)\begin{pmatrix} e \\ \Delta\lambda \end{pmatrix} + \Delta E'^{\top}\hat{\Lambda}_1^{-1}\Delta E' \\
&\leq -\epsilon' e^{\top}P_0 e + E'^{\top}\hat{\Lambda}_1^{-1}\Delta E' \\
&\leq -\epsilon'\lambda_{\min}(P_0)||e||^2 + \lambda_{\min}^{-1}(\hat{\Lambda}_1)||\Delta E'||^2 \\
&\leq -\epsilon'\lambda_{\min}(P_0)||e||^2 + \lambda_{\min}^{-1}(\hat{\Lambda}_1)\rho
\end{aligned} \tag{4.34}$$

So, $\dot{V} < 0$ in (4.34) outside the ball $B_r(0) \subset \mathbb{R}^n$, with $r \triangleq \sqrt{\frac{\lambda_{\min}^{-1}(\hat{\Lambda}_1)\rho}{\lambda_{\min}(P_0)\epsilon'}}$. Thus, the solution of (4.25) is GUUB [87] by relaxing strong passivity and, according to Proposition 2.4.5, the ultimate bound is given by:

$$||e|| \leq \sqrt{\frac{\lambda_{\max}(P_0)\lambda_{\min}^{-1}(\hat{\Lambda}_1)\rho}{\lambda_{\min}^2(P_0)\epsilon'}} \tag{4.35}$$

□

Remark 4.5.2. *It is important to note that taking $g_{21} = 0$ within the framework of bounded uncertainties in this section is not feasible. This is due to the necessary condition in item 1 ($\hat{R} \succcurlyeq 0$) to ensure that the matrix inequality $\hat{L} \succcurlyeq 0$ in (4.31) holds. Furthermore, it is necessary to select $g_{21} \geq \frac{1}{2}$ as imposed by item 1 in the above analysis. It is also worth noting that nowhere is used the fact that the set-valued part in right-hand side of (4.1) or (4.2) (equivalently, the multiplier λ_1) is bounded.*

4.5.2 Robustness Analysis with Constant Bounded Uncertainties $\Delta\mu = \mu - \mu_0$

In this setting, it is possible to incorporate ΔB directly as an unknown of the matrix inequality, the techniques used in Proposition 2.4.3 have to be used. Let us recall the inequality of the storage function $\dot{V}(e)$ in (4.28):

$$\dot{V} \leq -\begin{pmatrix} e \\ \Delta\lambda \end{pmatrix}^\top \left(-M_0 + \Delta M_0 - \begin{pmatrix} P_0\hat{\Lambda}_1 P_0 & 0 \\ 0 & 0 \end{pmatrix} \right) \begin{pmatrix} e \\ \Delta\lambda \end{pmatrix} + \Delta E'^\top \hat{\Lambda}_1^{-1} \Delta E'$$

where M_0 is defined in (4.26), $\Delta M_0 \triangleq \begin{pmatrix} 0 & -P_0\Delta B \\ -\Delta B^\top P_0 & 0 \end{pmatrix}$, and $\hat{\Lambda}_1^\top = \hat{\Lambda}_1 \succ 0$.

It is required to prove that $-M_0 + \Delta M_0 - \begin{pmatrix} P_0\hat{\Lambda}_1 P_0 & 0 \\ 0 & 0 \end{pmatrix} \succcurlyeq \begin{pmatrix} \epsilon' P_0 & 0 \\ 0 & 0 \end{pmatrix}$ for $\epsilon' > 0$. Let us explicitly represent the matrix to be proven positive semi-definite as follows:

$$\begin{aligned} L \;&\triangleq -M_0 + \Delta M_0 - \begin{pmatrix} P_0\hat{\Lambda}_1 P_0 & 0 \\ 0 & 0 \end{pmatrix} - \begin{pmatrix} \epsilon' P_0 & 0 \\ 0 & 0 \end{pmatrix} \\ &= \begin{pmatrix} -A_{cl}^\top P_0 - P_0 A_{cl} - P_0\hat{\Lambda}_1 P_0 - \epsilon' P_0 & -P_0(B_{cl} + \Delta B) + C_{cl}^\top \\ -(B_{cl} + \Delta B)^\top P_0 + C_{cl} & D_{cl} + D_{cl}^\top \end{pmatrix} \end{aligned} \tag{4.36}$$

Take $Q \triangleq \underbrace{-A_{cl}^\top P_0 - P_0 A_{cl} - \epsilon' P_0}_{Q_0} + \underbrace{(-P_0\hat{\Lambda}_1 P_0)}_{\Delta Q}$, $S \triangleq \underbrace{-P_0 B_{cl} + C_{cl}^\top}_{S_0} + \underbrace{(-P_0\Delta B)}_{\Delta S}$ and $R \triangleq \underbrace{D_{cl} + D_{cl}^\top}_{R_0}$ as defined in section 2.4.3 where $P_0 = \begin{pmatrix} p_{11} & p_{12} \\ p_{12} & p_{22} \end{pmatrix}$ such that $P_0 = P_0^\top \succ 0$.

Recall that $\hat{\Lambda}_1 = \begin{pmatrix} a & b \\ b & c \end{pmatrix} \succ 0$ for some $a, b, c \in \mathbb{R}$ and the matrices B_{cl}, C_{cl} and D_{cl} are defined in (4.5). Let us write explicitly the matrices Q, S and R.

$$Q_0 = \begin{pmatrix} -2p_{12}\frac{k_{11}}{m} - \epsilon' p_{11} & -p_{11} - \frac{k_{12}}{m}p_{12} - \frac{k_{11}}{m}p_{22} - \epsilon' p_{12} \\ -p_{11} - \frac{k_{12}}{m}p_{12} - \frac{k_{11}}{m}p_{22} - \epsilon' p_{12} & -2p_{12} - 2\frac{k_{12}}{m}p_{22} - \epsilon' p_{22} \end{pmatrix},$$

$$-\Delta Q = \begin{pmatrix} p_{11}^2 a + p_{12}^2 c + 2p_{11}p_{12}b & p_{12}^2 b + p_{11}p_{12}a + p_{11}p_{22}b + p_{12}p_{22}c \\ p_{12}^2 b + p_{11}p_{12}a + p_{11}p_{22}b + p_{12}p_{22}c & p_{12}^2 a + p_{22}^2 c + 2p_{12}p_{22}b \end{pmatrix},$$

$$S_0 = \begin{pmatrix} 2p_{12}\mu g + k_{21} & 0 \\ 2p_{22}\mu g - 1 + k_{22} & 0 \end{pmatrix}, \quad \Delta S = \begin{pmatrix} 2p_{12}\Delta\mu\, g & 0 \\ 2p_{22}\Delta\mu\, g & 0 \end{pmatrix}, \quad R = R_0 = \begin{pmatrix} 2g_{21} & 0 \\ 0 & 0 \end{pmatrix}$$

By considering the conditions for positive semi-definiteness in Appendix A.3 and by following Lemma A.3.1, the matrix $L \triangleq \begin{pmatrix} Q_0 + \Delta Q & S_0 + \Delta S \\ S_0^\top + \Delta S^\top & R_0 \end{pmatrix} \succcurlyeq 0$ if and only if:

1. $R_0 \succcurlyeq 0$ which is satisfied by the assumption of strict passivity of the closed-loop system in (4.5).

2. $\mathrm{Im}\left(S_0^\top + \Delta S^\top\right) \subseteq \mathrm{Im}(R_0)$ and this condition is satisfied according to Lemma 2.4.6 because the following conditions hold:
   (i) $\mathrm{Im}(\Delta S^\top) = \left\{ w \in I\!R^2 \mid w = \begin{pmatrix} 2g\Delta\mu(p_{12}x + p_{22}y) \\ 0 \end{pmatrix} \text{ for some } x, y \in I\!R \right\} \subseteq$
   $\mathrm{Im}(S_0^\top) = \left\{ w \in I\!R^2 \mid \begin{pmatrix} (2\mu g p_{12} + k_{12})t + (2\mu g p_{22} - 1 + k_{22})z \\ 0 \end{pmatrix} \text{ for some } t, z \in I\!R \right\}$,
   (ii) $\mathrm{Im}(R) = \mathrm{Im}(R_0)$ since $R = R_0$ in the system (4.25) studied in this section.

3. $Q \succeq SR^\dagger S^\top$. Let us follow the conditions presented in Proposition 2.4.7 in order to check the validity of this item (*i.e.,* $Q \succeq SR^\dagger S^\top$), then:
   (i) $R = R_0 \succeq 0$,

   (ii) $\mathrm{Im}(\Delta R) = 0 \subseteq \mathrm{Im}(R_0) = \left\{ w \in I\!R^2 \mid w = \begin{pmatrix} 2g_{21}x \\ 0 \end{pmatrix} \text{ for some } x \in I\!R \right\}$,

   (iii) $\mathrm{rank}(R_0) = 1$, $\sigma_{\max}(\Delta R) = 0 < \sigma_1(R_0) = 2g_{21}$ where $g_{21} > 0$ from the strict passivity of the quadruple $(A_{cl}, B_{cl}, C_{cl}, D_{cl})$,

   (iv) $\sigma_{\max}(OT) + \sigma_{\max}(\Delta Q) < \epsilon\lambda_{\max}(P_0)$ where OT is defined in (2.66) and in this case, where $\Delta R = 0$, it is written as:

$$OT = S_0 R^\dagger \Delta S^\top + \Delta S R^\dagger S_0^\top + \Delta S R^\dagger \Delta S^\top$$

   with $R^\dagger = \begin{pmatrix} \frac{1}{2g_{21}} & 0 \\ 0 & 0 \end{pmatrix}$. After performing calculations, the matrix OT is explicitly written as:

$$OT = \frac{2g^2\Delta\mu^2}{g_{21}} \begin{pmatrix} p_{12}^2 & p_{12}p_{22} \\ p_{12}p_{22} & p_{22}^2 \end{pmatrix}$$

   Note that $\frac{2g^2\Delta\mu^2}{g_{21}} \geq 0$, then the matrix OT is positive semi-definite (*i.e.,* $OT \succcurlyeq 0$) since $p_{12}^2 > 0, p_{22}^2 > 0$ and $p_{12}^2 p_{22}^2 - (p_{12}p_{22})(p_{12}p_{22}) = 0$. According to [17, Fact 5.11.19], given that OT is positive semi-definite, $\sigma_i(OT) = \lambda_i(OT)$ for $i \in \{1, 2\}$. Also, by referring to [17, Definition 5.6.1], $\sigma_i(OT) = \frac{2g^2\Delta\mu^2}{g_{21}} \sigma_i \begin{pmatrix} p_{12}^2 & p_{12}p_{22} \\ p_{12}p_{22} & p_{22}^2 \end{pmatrix}$ for $i \in \{1, 2\}$. Thus, $\sigma_{\max}(OT) = \frac{2g^2\Delta\mu^2}{g_{21}}(p_{12}^2 + p_{22}^2) > 0$. Knowing that $P_0 \succ 0$, then $\lambda_{\max}(P_0) > 0$ such that $\lambda_{\max}(P_0) = \frac{1}{2}\left(p_{11} + p_{22} + \sqrt{(p_{11} + p_{22})^2 - 4p_{12}^2}\right)$. It is noteworthy that ΔQ and $-\hat{\Lambda}_1$ are congruent matrices, so the two matrices have the same number and signs of eigenvalues [85, Theroem 4.5.8]. This means that $\lambda_i(\Delta Q) < 0$ for $i \in \{1, 2\}$. Let us assume that $\hat{\Lambda}_1 = \alpha I_2$, then $\Delta Q = -\alpha P_0^2$ which

is symmetric (*i.e.*, $\Delta Q = \Delta Q^\top$). As $P_0 = P_0^\top \succ 0$, it follows that $\sigma_i(P_0) = \lambda_i(P_0)$. Thus, $\sigma_{\max}(\Delta Q) = \alpha\lambda^2_{\max}(P_0)$. Hence, item (iv) is written as follows:

$$\frac{2g^2\Delta\mu^2}{g_{21}}(p_{12}^2 + p_{22}^2) + \alpha\lambda^2_{\max}(P_0) - \epsilon\lambda_{\max}(P_0) < 0 \tag{4.37}$$

In order to determine the conditions on $\lambda_{\max}(P_0)$ that satisfy item (iv) in Proposition 2.4.7, let us solve the following quadratic inequality for the variable θ:

$$\alpha\theta^2 - \epsilon\theta + \frac{2g^2\Delta\mu^2}{g_{21}}(p_{12}^2 + p_{22}^2) < 0$$

Then, the solution is:

$$\theta_1 = \tfrac{1}{2\alpha}\left(\epsilon - \sqrt{\epsilon^2 - \tfrac{8\alpha g^2\Delta\mu^2(p_{12}^2+p_{22}^2)}{g_{21}}}\right),$$

$$\theta_2 = \tfrac{1}{2\alpha}\left(\epsilon + \sqrt{\epsilon^2 - \tfrac{8\alpha g^2\Delta\mu^2(p_{12}^2+p_{22}^2)}{g_{21}}}\right)$$

where $\theta_1 > 0$ and $\theta_2 > 0$. For the inequality in (4.37) to be valid (*i.e.*, item (iv) in Proposition 2.4.7 holds), the following condition must be satisfied:

$$-\sqrt{\epsilon^2 - \frac{8\alpha g^2\Delta\mu^2(p_{12}^2 + p_{22}^2)}{g_{21}}} < 2\alpha\lambda_{\max}(P_0) - \epsilon < \sqrt{\epsilon^2 - \frac{8\alpha g^2\Delta\mu^2(p_{12}^2 + p_{22}^2)}{g_{21}}} \tag{4.38}$$

Given the flexibility to choose or constrain the parameter α, consequently constraining $\Delta\mu$ and the parameter ϵ, it is possible to choose these parameters within the bounds in (4.38). Then, item (iv) in Proposition 2.4.7 is satisfied. In other words, by analyzing the inequality (4.37), choosing a sufficiently large ϵ guarantees the validity of item (iv) (*i.e.*, inequality (4.37)).

Therefore, the matrix L in (4.36) is positive semi-definite (*i.e.*, $L \succcurlyeq 0$) and the inequality in (4.28) is written as follows:

$$\begin{aligned}
\dot{V} &\leq -\begin{pmatrix} e \\ \Delta\lambda \end{pmatrix}^\top \left(-M_0 + \Delta M_0 - \begin{pmatrix} P_0\hat{\Lambda}_1 P_0 & 0 \\ 0 & 0 \end{pmatrix}\right)\begin{pmatrix} e \\ \Delta\lambda \end{pmatrix} + \Delta E'^\top \hat{\Lambda}_1^{-1}\Delta E' \\
&\leq -\epsilon' e^\top P_0 e + \Delta E'^\top \hat{\Lambda}_1^{-1}\Delta E' \\
&\leq -\epsilon'\lambda_{\min}(P_0)||e||^2 + \lambda^{-1}_{\min}(\hat{\Lambda}_1)||\Delta E'||^2
\end{aligned}$$

Thus, the solution of the error dynamics in (4.25) is GUUB [87, 60]. According to Proposition 2.4.5, the global ultimate bound is given by

$$||e|| \leq \sqrt{\frac{\lambda_{\max}(P_0)\lambda^{-1}_{\min}(\hat{\Lambda}_1)||\Delta E'||^2}{\lambda^2_{\min}(P_0)\epsilon'}}$$

Remark 4.5.3. *It is clear from (4.38) that it is necessary to have $g_{21} > 0$. What happens when $g_{21} = 0$, which means that there is no multiplier λ_1 feedback? In that case, that $R = 0$, thus $R^\dagger = 0$. So, $L \succcurlyeq 0$ if and only if $S_0 + \Delta S = 0$, which implies $\Delta B = 0$ which implies $\Delta\mu = 0$. It is inferred that the above analysis of robustness against uncertainties in the friction coefficient (which is sufficient only) implies $g_{21} \neq 0$. This is in agreement with Proposition 2.4.7 item (iv).*

4.5.3 Numerical simulations

In the presence of uncertainties, it is useful to enhance the dissipativity of the closed-loop system in (4.5). This involves increasing the parameter ϵ of the strict passivity that appears in (2.56). However, the limitations of this method is the potential for high overshoot and extremely large control gains. Let us check if there exists P_0, K_0 and G_0 such that the BMI:

$$M_0 \preccurlyeq \begin{pmatrix} -\epsilon P_0 & 0 \\ 0 & 0 \end{pmatrix}, \tag{4.39}$$

holds where M_0 is defined in (4.26). For numerical purposes the BMI in (4.39) is transformed into an LMI (see Appendix A.1). Take $\mu_0 = 0.5, m = 1$ and $g = 9.8$. For $\epsilon = 10$, the solution is:

$$K_0 = \begin{pmatrix} -70.79 & -11.95 \\ -29.89 & -4.22 \end{pmatrix}, \quad G_0 = \begin{pmatrix} 0 & 0 \\ 0.67 & 0 \end{pmatrix} \quad \text{and} \quad P_0 = \begin{pmatrix} 31.8 & 3.05 \\ 3.05 & 0.53 \end{pmatrix} \tag{4.40}$$

In order to find the admissible $\Delta\mu$, let us solve the LMI of uncertainties $\hat{L} \succcurlyeq 0$ in (4.31) with the unknowns $\hat{\Lambda}_1$ and $\hat{\Lambda}_B$ given the values of K_0, P_0 and G_0 from the strict passivity of the nominal system $(A_0 + E_0K_0, B_0, C_0 + F_0K_0, D_0 + F_0G_0)$. The solution is:

$$\hat{\Lambda}_1 = \begin{pmatrix} 0.16 & 0 \\ 0 & 9.2 \end{pmatrix} \quad \text{and} \quad \hat{\Lambda}_B = \begin{pmatrix} 0.14 & 0 \\ 0 & 0.567 \end{pmatrix}$$

with the constraint $tr(\hat{\Lambda}_1) \leq 10$ and without constraining $\hat{\Lambda}_B$. The admissible value of the upperbound on the uncertainty is $\Delta\mu \leq 0.038$. It is possible to increase the admissible $\Delta\mu$ for the same ϵ by increasing the values of $\hat{\Lambda}_1$ or $\hat{\Lambda}_B$ (*i.e.*, increasing the trace of the matrices $\hat{\Lambda}_1$ and $\hat{\Lambda}_B$), maintaining the BMI $\hat{L} \succcurlyeq 0$. Let us increase the value of $\hat{\Lambda}_B$ consequently $\Delta\mu$ such that $tr(\hat{\Lambda}_B) = 20$, the numerical solution is:

$$\hat{\Lambda}_1 = \begin{pmatrix} 0.032 & 0 \\ 0 & 0.86 \end{pmatrix} \quad \text{and} \quad \hat{\Lambda}_B = \begin{pmatrix} 0.023 & 0 \\ 0 & 19.9 \end{pmatrix}$$

The admissible value of the uncertainty is bounded such that $\Delta\mu \leq 0.22$. The following figures illustrate the robustness of the closed-loop error system (4.9) through simulations, considering perturbation on the parameter μ_0 by constant, and bounded time-varying uncertainties $\Delta\mu$. The system depicted in Figure 4.6 is the desired system used in the numerical simulations for trajectory tracking in the presence of constant uncertainties in Figures 4.11 and 4.12. Take $x_d(0) = (1, 0)^\top$, $x(0) = (0, -1)^\top$, and the time step $h = 0.01$s.

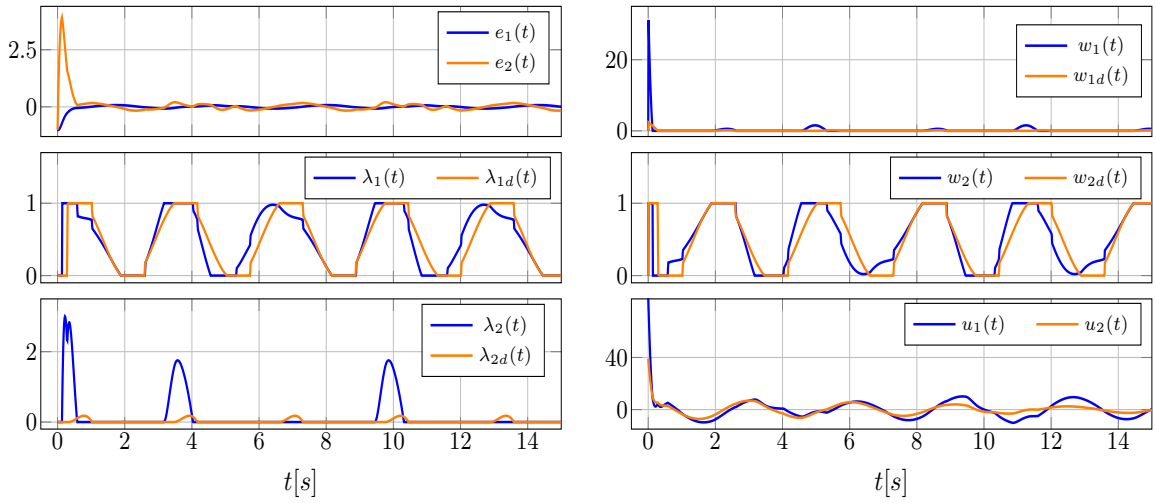

Figure 4.11: Numerical simulation of the closed-loop error system with control gains from (4.40) and the uncertainty value $\Delta\mu = 0.1$

In Figure 4.11, it is observed that the error $e(t) = x(t) - x_d(t)$, in the presence of uncertainties on the coefficient of friction in the closed-loop system in (4.25) (*i.e.*, $\Delta\mu$), has the following L_∞ norms: $\|e_1\|_{[5,15],\infty} = 0.07$ and $\|e_2\|_{[5,15],\infty} = 0.202$. It is noteworthy that these norms increase as the value of $\Delta\mu$ increases (see Figure 4.12).

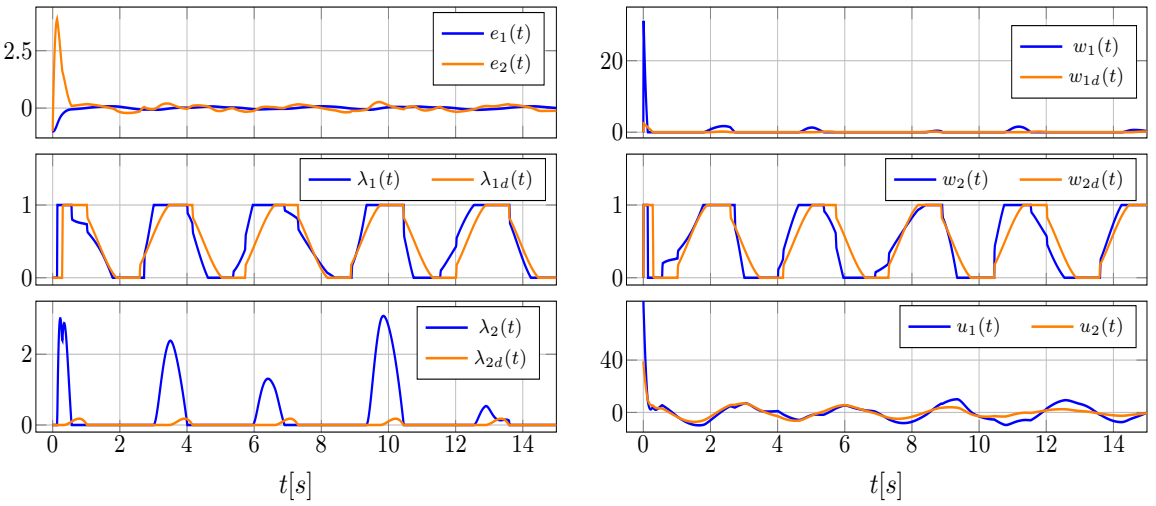

Figure 4.12: Numerical simulation of the closed-loop error system with control gains from (4.40) and the uncertainty value $\Delta\mu = 0.2 \sin \sqrt{3}t$.

In Figure 4.12, the value of the uncertainty $\Delta\mu$ is bounded such that $\Delta\mu < 0.22$. The numerical simulation observed shows that the L_∞ norms of the error $e = x - x_d$ are $||e_1||_{[5,15],\infty} = 0.08$ and $||e_2||_{[5,15],\infty} = 0.26$. It is also noticeable that in both Figures 4.11 and 4.12, the synchronization between the complementarity variables λ and λ_d, as well as between w and w_d is lost in the presence of uncertainties.

4.6 Controller Design and Stability Analysis with Stribeck Effect

As usual in control theory, it is interesting to analyse whether or not refining the model yields better results than designing a robust feedback controller. The foregoing study guarantees some robustness w.r.t. time-varying bounded uncertainties in the friction coefficient. Now let us assume that the Coulomb's model is enhanced to include Stribeck effects. The reason of this assumption is that on one hand, Stribeck effects often represent in an acceptable way the frictional effects, on the other hand it will allow us to propose different control approach, using its hypomonotonicity (actually, any other modification of Coulomb's set-valued model which satisfies a hypomonotonicity constraint, would fit with the control framework in this section). This new approach consists of passifying (or "monotonifying") a hypomonotone friction model. As noted in the introduction of this chapter, Stribeck effects often play a major role in practice.

4.6.1 The Stribeck Model and its Properties

One example of a physical model that may be considered as a bounded uncertainty, is the Stribeck model of sliding friction [12], which states that $\mu = \mu(\dot{q}_{rel})$, where $\dot{q}_{rel} \triangleq \dot{q} - u_2$ is the relative tangential velocity, which can be expressed as [23, Equation (17)]:

$$F_{\text{str}}(\dot{q}_{rel}(t)) = \underbrace{-F_{\text{n}}(\mu_s - \mu_c)\left(\exp\left(-\frac{\dot{q}_{rel}^2(t)}{v_s^2}\right) - 1\right)\text{sgn}(\dot{q}_{rel}(t))}_{F_{diff}(\dot{q}_{rel})} \underbrace{-\mu_s F_{\text{n}}\text{sgn}(\dot{q}_{rel}(t))}_{F_{sv}(\dot{q}_{rel}(t))}, \tag{4.41}$$

where $\mu_s > \mu_c > 0$, v_s are parameters, $F_{\text{n}} = mg > 0$ is the constant normal contact force. The total force is therefore the sum of a continuously differentiable, Lipschitz continuous, hypomonotone decreasing term $F_{diff}(\dot{x})$, and a set-valued maximal monotone term $F_{sv}(\dot{x})$.

Figure 4.13 shows the graphical representations of different frictional forces, including Coulomb friction as F_{sv} and Stribeck friction F_{str} in (4.41) with respect to relative velocity $\dot{q}_{rel}$. The behaviour of the function F_{diff} is depicted with variations in its parameter v_s. Take $F_n = mg = 9.8$, $\mu_s = 0.5$ and $\mu_c = 0.4$.

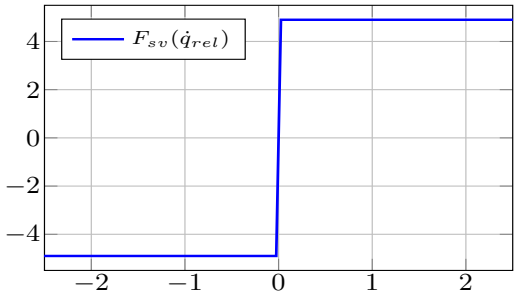

(a) Coulomb friction function

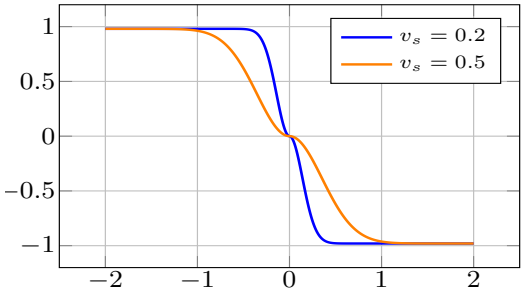

(b) Frictional force $F_{diff}(\dot{q}_{rel})$

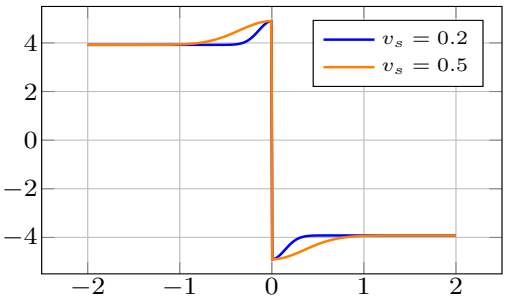

(c) Stribeck without viscous friction $F_{str}(\dot{q}_{rel})$

Figure 4.13: Different frictional forces as a function of relative velocity $\dot{q}_{rel}$

The plot in Figure 4.13a shows the Coulomb friction force with respect to the relative velocity $\dot{q}_{rel}$ and it varies inside an interval such that $F_{sv} \in [-F_n\mu_s, F_n\mu_s]$. In Figure 4.13b, the function F_{diff} shows a smoother non-linearity when a smaller value of the parameter v_s is observed and $F_{diff} \in [-F_n(\mu_s - \mu_c), F_n(\mu_s - \mu_c)]$. The plot in Figure 4.13c displays the friction force F_{str} without viscous friction represented in (4.41) for two different values of the parameter v_s which causes faster decay towards the value $F_n(\mu_s - \mu_c)$ as it increases.

Let us analyze the behaviour of the function $F_{diff}(\dot{q}_{rel})$ by finding its derivative. Denote $\dot{q}_{rel}$ as x for simplicity, then the function $F_{diff}(x)$ is expressed as follows:

$$F_{diff}(x(t)) = F_n(\mu_s - \mu_c)\left(\exp\left(-\frac{x^2(t)}{v_s^2}\right) - 1\right)\operatorname{sgn}(x(t))$$

The derivative of $F_{diff}(x)$ with respect to x is given for $x \neq 0$ by:

$$\frac{d}{dx}F_{diff}(x) = F_n(\mu_s - \mu_c)\left(-\frac{2x}{v_s^2}\exp\left(-\frac{x^2}{v_s^2}\right)\right)\operatorname{sgn}(x)$$

For $x > 0$: $\frac{d}{dx}F_{diff}(x) = -F_n(\mu_s - \mu_c)\frac{2x}{v_s^2}\exp\left(-\frac{x^2}{v_s^2}\right)$. For $x < 0$: $\frac{d}{dx}F_{diff}(x) = F_n(\mu_s - \mu_c)\frac{2x}{v_s^2}\exp\left(-\frac{x^2}{v_s^2}\right)$. Then, $\lim_{x\to 0^-}\frac{d}{dx}F_{diff}(x) = \lim_{x\to 0^+}\frac{d}{dx}F_{diff}(x) = 0$.

Thus, the function $\frac{d}{dx}F_{diff}(\cdot)$ is continuous at 0, and the function $F_{diff}(\cdot)$ is continuously differentiable everywhere, with bounded derivatives (bounded in absolute value).

It follows that it is a hypomonotone single-valued mapping. Let us write the dynamics in (4.1) with Stribeck friction presented in (4.41), then:

$$\ddot{q}(t) \in \frac{1}{m}u_1(t) - \mu g \, \mathrm{sgn}(\dot{q}_{rel}(t)) - F_{diff}(\dot{q}_{rel}(t)) \pm \alpha \dot{q}_{rel}(t) \tag{4.42}$$

where the linear term $\alpha\dot{q}_{rel}$ is added and subtracted for compensation. Thus, the dynamics in (4.42) is written as follows:

$$\ddot{q}(t) \in \frac{1}{m}u_1'(t) - \mu g \, \mathrm{sgn}(\dot{q}_{rel}(t)) - (F_{diff} + \alpha \mathrm{I_d})(\dot{q}_{rel}(t)) \tag{4.43}$$

where $u_1 = u_1' - m\alpha\dot{q}_{rel}$. It is required to find the suitable gain $\alpha > 0$ such that the mapping $\dot{q}_{rel} \mapsto (F_{diff} + \alpha \mathrm{I_d})(\dot{q}_{rel})$ is monotone (it is automatically maximal since it is single-valued). For this purpose, it is required to find the maximum slope of the function $F_{diff}(.)$. The second derivative of $F_{diff}(x)$ is:

$$\frac{d^2}{dx^2}F_{diff}(x) = \frac{2}{v_s^4}F_n(\mu_s - \mu_c)\left((2x^2 - v_s^2)\exp\left(\frac{-x^2}{v_s^2}\right)\right)\mathrm{sgn}(x)$$

Let $m_{\max}$ be the maximum slope of $F_{diff}(x)$ which is the absolute value of $\frac{d}{dx}F_{diff}(x)$ at $x = \frac{v_s}{\sqrt{2}}$ and it is given by:

$$m_{\max} = \frac{2}{v_s\sqrt{2}}F_n(\mu_s - \mu_c)\exp\left(-\frac{1}{2}\right) \tag{4.44}$$

Thus, the monotonicity of the mapping $\dot{q}_{rel} \mapsto (F_{diff} + \alpha \mathrm{I_d})(\dot{q}_{rel})$ is guaranteed by choosing the gain α such that $\alpha > m_{\max}$. Take

$$\alpha = \sqrt{2}\exp(\frac{1}{2})m_{\max} = \frac{2}{v_s}F_n(\mu_s - \mu_c) \tag{4.45}$$

in the following.

Remark 4.6.1. *If the viscous friction is included in the force of friction given in (4.41), then the dynamics in (4.43) is rewritten as:*

$$\ddot{q}(t) \in \frac{1}{m}u_1'(t) - \mu g \; sgn(\dot{q}_{rel}(t)) - (F_{diff} + k_v + \alpha \mathrm{I_d})(\dot{q}_{rel}(t))$$

where k_v is the coefficient of viscous friction. Given that $k_v > 0$, the term $k_v\dot{q}_{rel}$ increases the overall damping by k_v, thus enhancing the dissipativity of the system which is crucial for our analysis. The main effect of adding viscous friction is that the value of the compensating term α changes such that $\alpha > \frac{2}{v_s\sqrt{2}}F_n(\mu_s - \mu_c)\exp\left(-\frac{1}{2}\right) + k_v$. Therefore, it is important to note that the following analytical approach applies to the Stribeck effect in (4.41) with viscous friction.

4.6.2 Controller Calculation

Let a suitable α be calculated. The next step consists of applying the foregoing passivity-based (or monotonicity-based) technique to calculate $u = (u_1', u_2)^\top = K(x - x_d) + u_d$ with $x \triangleq (q, \dot{q})^\top$ as independent input, then we have $u_1 = u_1' - m\alpha(\dot{q} - u_2)$.

Let us write the dynamics in (4.43) according to the expression of F_{diff} in (4.41) as:

$$\begin{aligned}\ddot{q}(t) &\in \tfrac{1}{m}u_1'(t) - g\lambda_t\left(\mu_s + (\mu_s - \mu_c)\left(\exp\left(\tfrac{-(\dot{q}(t)-u_2(t))^2}{v_s^2}\right) - 1\right)\right) - \alpha(\dot{q}(t) - u_2(t)) \\ &= \tfrac{1}{m}u_1'(t) - g\mu_s\lambda_t - F_{diff,\alpha}(\dot{q} - u_2),\end{aligned}$$

where $\lambda_t \in \operatorname{sgn}(\dot{q} - u_2)$ and

$$\begin{aligned}F_{diff,\alpha}(\dot{q}_{rel}(t)) &\triangleq (F_{diff} + \alpha \mathrm{I_d})(\dot{q}_{rel}(t)) \\ &= F_n(\mu_s - \mu_c)\left(\left(\exp\left(\tfrac{-(\dot{q}_{rel})^2}{v_s^2}\right) - 1\right) + \tfrac{2}{v_s}\right)(\dot{q}_{rel}(t))\end{aligned}$$

is maximal monotone given that $\dot{q}_{rel}(t) \triangleq \dot{q}(t) - u_2(t)$ and α is given in (4.45).

Let us keep the plant dynamics as in (4.43) and write the desired dynamics in (4.7) with Stribeck friction in (4.41) as:

$$\begin{aligned}\ddot{q}_d(t) &\in \tfrac{1}{m}u_{1d}(t) - \mu_s g\operatorname{sgn}(\dot{q}_{rel,d}(t)) - F_{diff}(\dot{q}_{rel,d}(t)) \pm \alpha\dot{q}_{rel,d} \\ &\in \tfrac{1}{m}u_{1d}'(t) - \mu_s g\operatorname{sgn}(\dot{q}_{rel,d}(t)) - (F_{diff} + \alpha I_d)(\dot{q}_{rel,d}(t))\end{aligned} \tag{4.46}$$

where $u_{1d} = u_{1d}' - m\alpha(\dot{q}_{rel,d})$ and $F_{diff,\alpha}(\dot{q}_{rel,d}(t)) \triangleq (F_{diff} + \alpha \mathrm{I_d})(\dot{q}_{rel,d}(t))$ is maximal monotone.

Therefore, the Stribeck model is incorporated into the desired dynamics. In view of the philosophy followed in this work, this is a logical step.

4.6.3 Error Dynamics Stability Analysis

Using (4.46) and (4.43), the error $\ddot{\tilde{q}} = \ddot{q} - \ddot{q}_d$ is written as:

$$\begin{aligned}\ddot{\tilde{q}}(t) &\in \tfrac{1}{m}(u_1(t) - u_{1d}(t)) - \mu_s g\operatorname{sgn}(\dot{q}_{rel}(t)) + \mu_s g\operatorname{sgn}(\dot{q}_{rel,d}(t)) \pm F_{diff,\alpha}(\dot{q}_{rel}(t)) \\ &\quad + F_{diff,\alpha}(\dot{q}_{rel,d}(t)) \\ &\in \tfrac{1}{m}(u_1'(t) - m\alpha(\dot{q}_{rel}(t) - \dot{q}_{rel,d}(t)) - u_{1d}'(t)) - \mu_s g(\operatorname{sgn}(\dot{q}_{rel}(t)) - \operatorname{sgn}(\dot{q}_{rel,d}(t))) \\ &\quad - (F_{diff,\alpha}(\dot{q}_{rel}(t)) - F_{diff,\alpha}(\dot{q}_{rel,d}(t))) \\ &\in \tfrac{1}{m}\left(k_{11}(q(t) - q_d(t)) + k_{12}(\dot{q}(t) - \dot{q}_d(t))\right) - \mu_s g(\operatorname{sgn}(\dot{q}_{rel}(t)) - \operatorname{sgn}(\dot{q}_{rel,d}(t))) \\ &\quad - \alpha\left(\dot{q}(t) - k_{21}(q(t) - q_d(t)) - k_{22}(\dot{q}(t) - \dot{q}_d(t)) - \dot{q}_d(t)\right) \\ &\quad - (F_{diff,\alpha}(\dot{q}_{rel}(t)) - F_{diff,\alpha}(\dot{q}_{rel,d}(t)))\end{aligned} \tag{4.47}$$

with $\tilde{q} = q - q_d$ and $e = (\tilde{q}, \dot{\tilde{q}})^\top$. The error dynamics in (4.47) is equivalently written as:

$$\begin{aligned}\dot{e}(t) \quad \in & \underbrace{\left(A_{cl} + \begin{pmatrix}0\\ \alpha\end{pmatrix}(C_{cl})_{1,\bullet}\right)}_{\triangleq \hat{A}_{cl}} e(t) - \begin{pmatrix}0\\ \mu_s g\end{pmatrix}\left(\operatorname{sgn}(\dot{q}_{rel}(t)) - \operatorname{sgn}(\dot{q}_{rel,d}(t))\right) \\ & - \begin{pmatrix}0\\ F_{diff,\alpha}(\dot{q}_{rel}(t)) - F_{diff,\alpha}(\dot{q}_{rel,d}(t))\end{pmatrix}\end{aligned} \tag{4.48}$$

where $\lambda_{1d}(t) \in \operatorname{sgn}(\dot{q}_d(t) - u_{2d}(t))$, $\lambda_1(t) \in \operatorname{sgn}(-(C_{cl})_{1,\bullet}e(t) + \dot{q}_d(t) - u_{2d}(t))$.

Proposition 4.6.2. *Consider the error dynamics in (4.48) with bounded initial conditions, and assume that the quadruple $(\hat{A}_{cl}, B_{cl}, C_{cl}, D_{cl})$ of the closed loop system is strictly state passive with $\epsilon > 0$. Then, the equilibrium point $e^\star = 0$ is globally exponentially stable.*

Proof. Consider the error dynamics in (4.48). Let us define

$$\hat{A}_{cl} \triangleq A_{cl} + \begin{pmatrix}0\\ \alpha\end{pmatrix}(C_{cl})_{1,\bullet} = \begin{pmatrix}0 & 1\\ \frac{k_{11}}{m} + \alpha k_{21} & \frac{k_{12}}{m} + \alpha(-1 + k_{22})\end{pmatrix}$$

Assume that the new closed-loop quadruple $(\hat{A}_{cl}, B_{cl}, C_{cl}, D_{cl})$ is strictly state passive. This means that the following matrix inequality:

$$\begin{pmatrix}\hat{A}_{cl}^\top \hat{P} + \hat{P}\hat{A}_{cl} & \hat{P}B_{cl} - C_{cl}^\top\\ B_{cl}^\top \hat{P} - C_{cl} & -D_{cl} - D_{cl}^\top\end{pmatrix} \preccurlyeq \begin{pmatrix}-\epsilon\hat{P} & 0\\ 0 & 0\end{pmatrix}$$

has a solution with $\hat{P} = \hat{P}^\top \succ 0$. Note that this BMI is transformed into a LMI (see Appendix A.1) to be solved numerically. Consider the storage function $V(e(t)) = e^\top(t)\hat{P}e(t)$. The rate of change of the storage function is:

$$\begin{aligned}\dot{V}(e(t)) \quad = & e^\top(\hat{A}_{cl}^\top \hat{P} + \hat{P}\hat{A}_{cl})e + 2e^\top \hat{P}\begin{pmatrix}0\\ \mu_s g\end{pmatrix}\left[\operatorname{sgn}(\dot{q}_{rel,d}(t)) - \operatorname{sgn}(\dot{q}_{rel}(t))\right] \\ & -2e^\top \hat{P}\begin{pmatrix}0\\ F_{diff,\alpha}(\dot{q}_{rel,d}) - F_{diff,\alpha}(\dot{q}_{rel})\end{pmatrix}\end{aligned}$$

Take $\hat{P} = \begin{pmatrix}\hat{p}_{11} & \hat{p}_{12}\\ \hat{p}_{21} & \hat{p}_{22}\end{pmatrix}$. Given that $\hat{P}B_{cl} = C_{cl}$ holds and that $(C_{cl})_{1,\bullet}e(t) = u_2(t) -$

$\dot{q}(t) - u_{2d}(t) + \dot{q}_d(t)$, then the rate of change of the storage function is written as follows:

$$\begin{aligned}
\dot{V}(e) &= e^\top(\hat{A}_{cl}^\top \hat{P} + \hat{P}\hat{A}_{cl})e - e^\top(\hat{P}B_{cl})_{\bullet,1}\left[\operatorname{sgn}(\dot{q}_{rel,d}(t)) - \operatorname{sgn}(\dot{q}_{rel}(t))\right] \\
&\quad -\tfrac{1}{\mu_s g} e^\top(\hat{P}B_{cl})_{\bullet,1}\left[F_{diff,\alpha}(\dot{q}_{rel,d}) - F_{diff,\alpha}(\dot{q}_{rel})\right] \\
&= e^\top(\hat{A}_{cl}^\top \hat{P} + \hat{P}\hat{A}_{cl})e + e^\top(C_{cl}^\top)_{\bullet,1}\left[\operatorname{sgn}(\dot{q}_{rel}(t)) - \operatorname{sgn}(\dot{q}_{rel,d}(t))\right] \\
&\quad +\tfrac{1}{\mu_s g} e^\top(C_{cl}^\top)_{\bullet,1}\left[F_{diff,\alpha}(\dot{q}_{rel}) - F_{diff,\alpha}(\dot{q}_{rel,d})\right] \\
&= e^\top(\hat{A}_{cl}^\top \hat{P} + \hat{P}\hat{A}_{cl})e - \left[\dot{q}_{rel}(t) - \dot{q}_{rel,d}(t)\right]^\top \left[\operatorname{sgn}(\dot{q}_{rel}(t)) - \operatorname{sgn}(\dot{q}_{rel,d}(t))\right] \\
&\quad - \left[\dot{q}_{rel}(t) - \dot{q}_{rel,d}(t)\right]^\top \left[F_{diff,\alpha}(\dot{q}_{rel}) - F_{diff,\alpha}(\dot{q}_{rel,d})\right] \\
&\leq e^\top(\hat{A}_{cl}^\top \hat{P} + \hat{P}\hat{A}_{cl})e \leq -\epsilon e(t)^\top \hat{P} e(t)
\end{aligned} \tag{4.49}$$

Therefore, the equilibrium point pf the error dynamics in (4.48), $e^\star = 0$, is globally exponentially stable due to the fact: $\|e(t)\|^2 \leq \frac{V(0)}{\lambda_{\min}(\hat{P})} \exp(-\epsilon t)$. □

4.6.4 Numerical simulation

Recall that $x \triangleq (q, \dot{q})$, $x_d \triangleq (q_d, \dot{q}_d)$, and $e \triangleq (\tilde{q}, \dot{\tilde{q}})$. The desired dynamics in (4.46), the closed-loop dynamics in (4.43) and the error dynamics in (4.48) can be equivalently expressed in the form of LCS as explained in section 4.2.1. The following numerical simulation is obtained using the LCS time-stepping scheme available in SICONOS [3, 1]. Take $m = 1\text{kg}$, $F_n = mg = 9.8\text{m/s}^2, v_s = 0.2, \mu_s = 0.5$ and $\mu_c = 0.4$. Let us check if there exists a control gain K such that the closed-loop system's quadruple $(A + EK, B, C + FK, D)$ is strictly state passive. The LMI derived from the BMI of strict state passivity in (4.10) has a solution which is given by:

$$K = \begin{pmatrix} -70.79 & -11.95 \\ -23.91 & -3.18 \end{pmatrix} \quad \text{and} \quad P = \begin{pmatrix} 31.8 & 3.05 \\ 3.05 & 0.53 \end{pmatrix}$$

Consider the value of the linear term α in (4.45), and the controller $u_1 = k_{11}(x_1 - x_{1d}) + k_{12}(x_2 - x_{2d}) + u_{1d} - m\alpha(x_2 - u_2)$ and $u_2 = k_{21}(x_1 - x_{1d}) + k_{22}(x_2 - x_{2d}) + u_{2d}$. The initial conditions are $x_d(0) = (-1, -2)^\top$ and $x(0) = (1, 3)^\top$, with desired inputs $u_{1d} = 0.7m\mu g \cos 5t$ and $u_{2d} = 0.5m\mu g \sin 3t$, and a time step $h = 0.01\text{s}$.

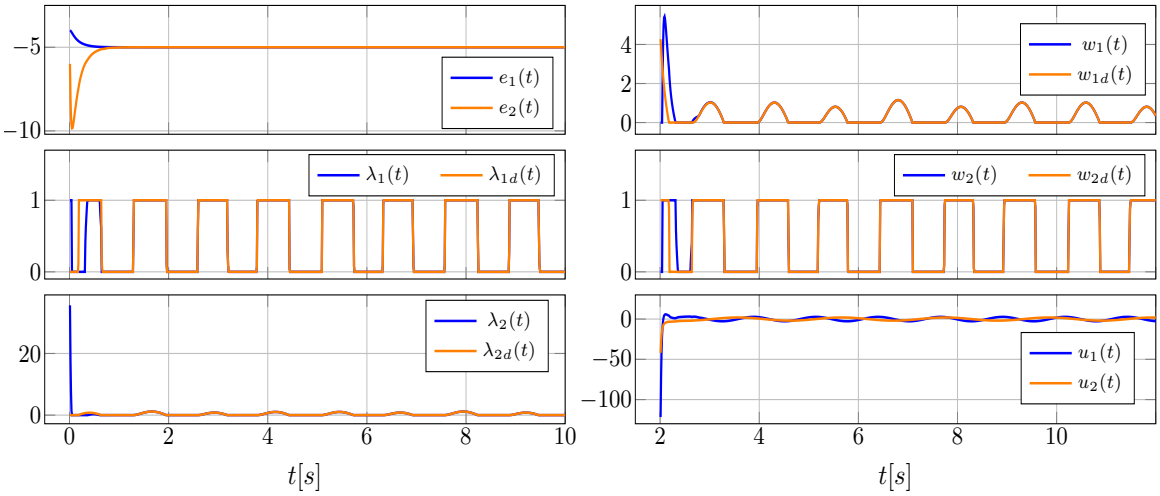

Figure 4.14: The desired, closed-loop and error systems of the LCS in (4.43), complementarity variables (λ, w) and input $u = (u_1, u_2)^\top$.

The numerical simulation in Figure 4.14 is performed using a different methodology from the previous simulations, which enables addressing the nonlinear Stribeck effect (more details are available in Appendix C.1). It is observed that the the error converges exponentially to zero when the friction model is improved by including Stribeck effect, as stated in Proposition 4.6.2. Moreover, it can be observed that the plant's complementarity variables (λ, w) converge to the desired complementarity variables (λ_d, w_d).

Conclusion

This chapter gives a solution for the trajectory tracking problem in frictional oscillators for several cases. In the nominal case, the passivity-based controller is designed to achieve exponential stability of the error dynamics. Then, the case with parametric uncertainties is investigated under a relaxed assumption of passivity, showing that the tracking error remains bounded. Moreover, the model of friction is refined to include Stribeck effect. In this case, the controller is designed based on the approach of passifying the friction model, which ensures that the tracking error converges exponentially to zero. Numerical simulations are presented to illustrate the theoretical results developed.

Chapter 5

Backstepping Tracking Control of Frictional Oscillators with Pulley-Belt Dynamics

Tracking control of frictional oscillators poses a complex control problem when incorporating pulley-belt dynamics. To address this problem, a backstepping strategy is proposed in this chapter for the controller design. This strategy requires stabilizing the pulley-belt dynamics by considering λ_t as a fictitious input. This chapter begins with introducing the framework of the controller design based on the backstepping strategy. Then, the stability of the error dynamics is analyzed and the convergence of the pulley's error dynamics is investigated. Numerical simulations are presented for the nominal case and for the case when parametric uncertainties are added, in order to ensure some robustness for the proposed approach. The last part of the chapter focuses on studying the controller design in discrete time using the Backward-Euler method, ensuring well-posedness and stability analysis in discrete time.

5.1 Frictional Oscillator with Pulley-Belt Dynamics

Recall the frictional oscillator depicted in Figure 4.1a.

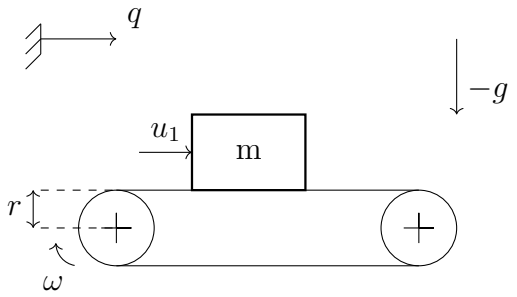

Figure 5.1: Simple Frictional Oscillator

If the pulley-belt dynamics are not neglected, meaning that the assumption $\frac{r\mu mg}{I} \ll 1$ does not hold, then the following dynamical system is obtained:

$$\begin{cases} (a) & m\ddot{q}(t) = u_1(t) - \mu mg\lambda_t(t) \\ (b) & I\ddot{\theta}(t) = \tau(t) + r\mu mg\lambda_t(t) \\ (c) & \lambda_t(t) \in \operatorname{sgn}(\dot{q}(t) - r\dot{\theta}(t)) \end{cases} \tag{5.1}$$

where τ is the control torque applied on one of the pulleys I is the inertia momentum of each pulley, $\dot{\theta} = \omega$. Once again we wee that the system in (5.1) possesses the robot-object structure when $u_1 \equiv 0$ or if $u_1 = u_1(q, \dot{q})$.

The link between the two dynamics (5.1) (a) and (b) is made through the potential function in (c) (recall that $\operatorname{sgn}(\dot{q} - r\dot{\theta}) = \partial|\dot{q} - r\dot{\theta}|$, where the subdifferential is with respect to the whole argument (*i.e.*, $\partial|x| = \operatorname{sgn}(x)$ for all reals x). Hence, the interconnection is made with a superpotential in Moreau's terminology [121], so that the system has the triangular structure that is suitable for backstepping control (originally backstepping has been applied to flexible-joint manipulators where the potential term derives from the joint elastic potential energy [106, 35] and is a quadratic smooth function of the state).

Remark 5.1.1. *The passage from (5.1) to the simpler system in (4.1) is achieved by assuming that* $\frac{r\mu mg}{I} \ll 1$*, keeping in mind that* $|\lambda_t| \leq 1$*. In other words, the belt dynamics is unaffected by the contact force, and the biggest assumption is that* $\dot{\theta}$ *can be given arbitrary values.*

Remark 5.1.2. *The system in (5.1) has two degrees of freedom and (considering that* u_1 *has been fixed as* $u_1(q, \dot{q}, t)$*) it has one input* $\tau(\cdot)$*: it is underactuated with underactuation degree one.*

5.2 First Control Approach: Motivation for Backstepping Strategy

This section proposes an approach to control the system in (5.1), which aims at considering the mass-belt-pulley dynamics as a whole. In this approach, the theoretical results developed in Chapter 4 can be directly applied to the system with pulley-belt dynamics.

Let us denote $z = (q, \dot{q}, \theta, \dot{\theta})^\top$, then (5.1) is rewritten equivalently as the relay system [42]:

$$\dot{z}(t) \in Az(t) + Eu(t) - B\operatorname{sgn}(Cz(t)),$$

with $A = \begin{pmatrix} 0 & 1 & 0 & 0 \\ 0 & 0 & 0 & 0 \\ 0 & 0 & 1 & 0 \\ 0 & 0 & 0 & 0 \end{pmatrix}$, $B = \begin{pmatrix} 0 \\ \mu g \\ 0 \\ \frac{-r\mu mg}{I} \end{pmatrix}$, $C = (0, 1, 0, -r)$, $E = \begin{pmatrix} 0 & 0 \\ \frac{1}{m} & 0 \\ 0 & 0 \\ 0 & \frac{1}{I} \end{pmatrix}$, $u = (u_1, \tau)^\top$.

It is observed that $PB = C^\top$ with $P = \operatorname{diag}\left(1, \frac{1}{\mu g}, 1, \frac{I}{\mu mg}\right)$. This relation can be seen as a consequence of the principle of virtual work, or of the coordinate invariance principle

[26, Section 5.8]. Let us use the state space change introduced in [22] (see also [37, section 3.4]). Let $\zeta = Rz$, $R^2 = P$, to obtain:

$$\dot{\zeta}(t) \in RAR^{-1}\zeta(t) + REu(t) - R^{-1}C^{\top}\,\mathrm{sgn}(CR^{-1}\zeta(t)), \tag{5.2}$$

By applying the chain rule of Convex Analysis, let us define $f \triangleq |\cdot| \circ CR^{-1}$. Then, (5.2) is rewritten equivalently as:

$$\dot{\zeta}(t) \in RAR^{-1}\zeta(t) + REu(t) - \partial f(\zeta(t)),$$

where $\partial f(\cdot)$ is the subdifferential of the convex proper continuous function $f(\cdot)$. The difference with respect to foregoing sections is that no controller acts inside the set-valued term (*i.e.*, $F = 0$). The desired dynamics are:

$$\dot{\zeta}_d(t) \in RAR^{-1}\zeta_d(t) + REu_d(t) - \partial f(\zeta_d(t)),$$

Let $\tilde{\zeta} = \zeta - \zeta_d$. The error dynamics are given by:

$$\dot{\tilde{\zeta}}(t) \in RAR^{-1}\tilde{\zeta}(t) + RE(u(t) - u_d(t)) - \partial f(\zeta(t)) + \partial f(\zeta_d(t)).$$

It is required to check if there exists a matrix K such that the controller $u = K(\zeta - \zeta_d) + u_d$ makes the triple $(RAR^{-1} + REK, I, I)$ strictly state passive, which is equivalent to $RAR^{-1} + REK + (RAR^{-1} + REK)^{\top} \preccurlyeq -\epsilon I$ for some $\epsilon > 0$. Then, the exponential stability of the error dynamics $\dot{\tilde{\zeta}}(t) \in (RAR^{-1} + REK)\tilde{\zeta}(t) - \partial f(\zeta(t)) + \partial f(\zeta_d(t))$ is analysed with the storage function $V(\tilde{\zeta}) = \frac{1}{2}\tilde{\zeta}^{\top}\tilde{\zeta}$.
Let us check the inequality: $RAR^{-1} + REK + (RAR^{-1} + REK)^{\top} \preccurlyeq -\epsilon I$ for some $\epsilon > 0$ analytically. For this purpose, assume that the matrices P, R, and K are defined as:

$$K = \begin{pmatrix} k_{11} & k_{12} & k_{13} & k_{14} \\ k_{21} & k_{22} & k_{23} & k_{24} \end{pmatrix}, \quad P = \begin{pmatrix} 1 & 0 & 0 & 0 \\ 0 & \frac{1}{\mu g} & 0 & 0 \\ 0 & 0 & 1 & 0 \\ 0 & 0 & 0 & \frac{1}{\mu m g} \end{pmatrix}, \quad R = P^{\frac{1}{2}} = \begin{pmatrix} 1 & 0 & 0 & 0 \\ 0 & \frac{1}{\sqrt{\mu g}} & 0 & 0 \\ 0 & 0 & 1 & 0 \\ 0 & 0 & 0 & \frac{1}{\sqrt{\mu m g}} \end{pmatrix}$$

Then, the expression: $RAR^{-1} + REK + (RAR^{-1} + REK)^{\top}$ is given by the following matrix:

$$\begin{pmatrix} 0 & \sqrt{\mu g} + \frac{k_{11}}{m\sqrt{\mu g}} & 0 & \frac{k_{21}}{I\sqrt{\mu m g}} \\ \sqrt{\mu g} + \frac{k_{11}}{m\sqrt{\mu g}} & \frac{2k_{12}}{m\sqrt{\mu g}} & \frac{k_{13}}{m\sqrt{\mu g}} & \frac{k_{14}}{m\sqrt{\mu g}} + \frac{k_{22}}{I\sqrt{\mu m g}} \\ 0 & \frac{k_{13}}{m\sqrt{\mu g}} & 2 & \frac{k_{23}}{I\sqrt{\mu m g}} \\ \frac{k_{21}}{I\sqrt{\mu m g}} & \frac{k_{14}}{m\sqrt{\mu g}} + \frac{k_{22}}{I\sqrt{\mu m g}} & \frac{k_{23}}{I\sqrt{\mu m g}} & \frac{2k_{24}}{I\sqrt{\mu m g}} \end{pmatrix} \tag{5.3}$$

According to the structure of the matrix in (5.3), it is infeasible to find a control gain K such that $RAR^{-1} + REK + (RAR^{-1} + REK)^{\top} \preccurlyeq -\epsilon I$. This limitation is due to the zero value in the first diagonal element and the positive value of 2 in the third diagonal element, which makes it impossible to have a strictly state passive closed-loop system

even with a full controller when $P = \text{diag}(1, \frac{1}{\mu g}, 1, \frac{I}{\mu m g})$. However, it is important to note that the matrix P is not unique. So, let us consider a more general matrix P that satisfies the passivity condition $PB = C^\top$ given that $D = 0$.

Take $P = \begin{pmatrix} p_{11} & p_{12} & p_{13} & p_{14} \\ p_{12} & p_{22} & p_{23} & p_{24} \\ p_{13} & p_{23} & p_{33} & p_{34} \\ p_{14} & p_{24} & p_{34} & p_{44} \end{pmatrix} \succ 0$ such that $PB = C^\top$. This implies that:

$$\begin{cases} p_{12} = p_{14}\frac{rm}{I} \\ p_{22}\mu g = 1 + p_{24}\frac{r\mu mg}{I} \\ p_{23} = p_{34}\frac{rm}{I} \\ p_{24} = p_{44}\frac{r\mu mg}{I} + r \end{cases}$$

It is quite cumbersome to check analytically if $RAR^{-1} + REK + (RAR^{-1} + REK)^\top \preccurlyeq -\epsilon I$. Thus, our approach focuses on finding numerically R and K such that $(RAR^{-1} + REK, I, I)$ is strictly state passive. This is equivalent to check if there exist K and P such that the BMI of strict state passivity in (4.10) for the closed-loop system $(A + EK, B, C)$, after being transformed into an LMI (see Appendix A.1), has a solution. This numerical verification is performed using MOSEK 9.3.14 solver for various sets of parameters such as $m = 1, 3, 10$ kg, $r = 0.02, 0.2, 0.7$ m, $I = 0.01, 0.001, 0.1$ kgm^2, and $\mu = 0.5, 0.3, 0.06$. However, the solver fails to find a solution.

Thus, this approach fails to verify that the closed-loop system is strictly state passive for all the parameters, which is a critical property for the stability analysis of the error. Additionally, this approach requires tracking both the mass $(q, \dot{q})$ and the pulley $(\theta, \dot{\theta})$, however our primary focus is on tracking the mass only. This motivates us us to consider a second approach outlined in the following section.

5.3 Backstepping-Based Control Approach

The dynamical system presented in (5.1) is of the robot-object type when $u_1 = u_1(q, \dot{q}, q_d, \dot{q}_d, u_{1d}, t)$. The goal of this section is to design a controller for (5.1) based on a backstepping strategy, as advocated in [25] for the class of robot-object systems. The stability of the error dynamics $e = (q - q_d, \dot{q} - \dot{q}_d)$ is analyzed, and the convergence of the pulley's error dynamics is studied. The results are followed by numerical simulations to validate the proposed control approach.

5.3.1 Controller Design and Stability Analysis

The goal is to control (5.1) (a), not (5.1) (b). Given that the dynamics in (5.1) is of the robot-object type, then it can be controlled only through the action of λ_t. The signum set-valued function can be seen as the derivative of a Moreau's superpotential (*i.e.*, as the subdifferential of a nonsmooth, convex function [121]). Hence, provided that u_1 has been assigned a value (see (5.5) below), the system can be considered as the cascade of two subsystems: the first one with state $(q, \dot{q})$ in (5.1) (a), the second

one with state $(\theta, \dot{\theta})$ in (5.1) (b). Both are related through the superpotential contact force λ_t in (5.1) (c).

Roughly speaking, the first step consists of stabilizing the object dynamics (5.1) (a) using λ_t as a "fictitious" input. Thus, the results concerning the control of (4.1) with input $u_2(\cdot)$ are important. The second step is to propagate the fictitious controller to the robot dynamics in order to get $\tau(\cdot)$.

From this point of view, once $u_1 = u_1(q, \dot{q}, t)$ is designed, the system in (5.1) has the triangular structure, which is suitable for the backstepping method. The friction superpotential plays the same role as the role played by the elasticity potential in flexible-joint manipulators [144]. Backstepping was introduced in [106, 35] for solving trajectory tracking control in flexible-joint manipulators. Thus, this approach extends backstepping from the quadratic elastic potential function $\frac{1}{2}(q_1 - q_2)^\top K(q_1 - q_2)$, $K = K^\top \succ 0$, to the set-valued superpotential $|\dot{q} - r\dot{\theta}|$.

In the following, two main cases are considered: $g_{21} = 0$ and $g_{21} > 0$. However, it will become evident that backstepping does not accommodate the feedback of the multiplier λ_1 because it is not guaranteed to be differentiable. Below, the last two steps of the backstepping strategy are described, with the first step being the design of the controller $u_2(\cdot)$ as done in sections 4.2.1–4.4.

Case $g_{21} = 0$

Consider the mass dynamics in (5.1)(a). Let us define $u_2^d \triangleq k_{21}(q - q_d) + k_{22}(\dot{q} - \dot{q}_d) + u_{2d}$, then (5.1) (a) is equivalently rewritten as:

$$\ddot{q}(t) \in \frac{u_1(t)}{m} - \mu g \, \mathrm{sgn}(\dot{q}(t) - u_2^d(t) - \tilde{u}_2(t)) \tag{5.4}$$

with $\tilde{u}_2 \triangleq r\dot{\theta} - u_2^d$. Here, u_2^d plays the role of u_2 in (4.1) and should not be confused with u_{2d}, which is a purely exogenous, time-varying signal. Let us write the closed-loop dynamics of the mass $(q, \dot{q})$ with $u_1(t) = k_{11}(q - q_d) + k_{12}(\dot{q} - \dot{q}_d) + u_{1d}$, then (5.4) is written as:

$$\begin{aligned} \ddot{q}(t) \in \; & \tfrac{k_{11}}{m}(q(t) - q_d(t)) + \tfrac{k_{12}}{m}(\dot{q}(t) - \dot{q}_d(t)) + \tfrac{u_{1d}(t)}{m} \\ & -\mu g \mathrm{sgn}\left(\dot{q}(t) - k_{21}(q(t) - q_d(t)) - k_{22}(\dot{q}(t) - \dot{q}_d(t)) - u_{2d}(t) - \tilde{u}_2(t)\right) \end{aligned} \tag{5.5}$$

Recall the desired dynamics in (4.7):

$$\ddot{q}_d(t) \in \frac{u_{1d}(t)}{m} - \mu g \mathrm{sgn}(\dot{q}_d(t) - u_{2d}(t))$$

Using the dynamics in (4.7) and (5.5), the error dynamics $\tilde{q} = q - q_d$ is

$$\begin{aligned} \ddot{\tilde{q}}(t) \; & \in \tfrac{k_{11}}{m}\tilde{q}(t) + \tfrac{k_{12}}{m}\dot{\tilde{q}}(t) - \mu g \mathrm{sgn}(\dot{q}(t) - k_{21}\tilde{q}(t) - k_{22}\dot{\tilde{q}}(t) - u_{2d}(t) - \tilde{u}_2(t)) \\ & \quad + \mu g \mathrm{sgn}(\dot{q}_d(t) - u_{2d}(t)) \\ & = \tfrac{1}{m}(k_{11}\tilde{q}(t) + k_{12}\dot{\tilde{q}}(t)) + \mu g \left[\lambda_{t,d} - \lambda_t(t)\right] \end{aligned} \tag{5.6}$$

where $\lambda_{t,d}(t) \in \text{sgn}(\dot{q}_d(t) - u_{2d}(t))$ and $\lambda_t(t) \in \text{sgn}(\dot{q}(t) - u_2^d(t) - \tilde{u}_2(t))$.

The objective is to design the controller $\tau(\cdot)$ such that $\tilde{u}_2 \to 0$. Thus $\dot{\tilde{u}}_2 = r\ddot{\theta} - \dot{u}_2^d$, *i.e.*:

$$\dot{\tilde{u}}_2(t) \in \frac{r}{I}\tau(t) + \frac{r^2\mu mg}{I}\text{sgn}(\dot{q}(t) - u_2^d(t) - \tilde{u}_2(t)) - k_{21}(\dot{q}(t) - \dot{q}_d(t)) - k_{22}(\ddot{q}(t) - \ddot{q}_d(t)) - \dot{u}_{2d}(t), \tag{5.7}$$

where $u_{2d}(\cdot)$ is assumed to be differentiable almost everywhere. Inserting (5.5) into (5.7) yields:

$$\begin{aligned}\dot{\tilde{u}}_2(t) \quad &\in \tfrac{r}{I}\tau(t) + \tfrac{r^2\mu mg}{I}\text{sgn}(\dot{q}(t) - u_2^d(t) - \tilde{u}_2(t)) - k_{21}(\dot{q}(t) - \dot{q}_d(t)) - \dot{u}_{2d}(t) \\ &-k_{22}\left(\tfrac{k_{11}}{m}(q(t) - q_d(t)) + \tfrac{k_{12}}{m}(\dot{q}(t) - \dot{q}_d(t)) + \tfrac{u_{1d}(t)}{m} - \mu g\ \text{sgn}(\dot{q}(t) - u_2^d(t) - \tilde{u}_2(t)) - \ddot{q}_d(t)\right)\end{aligned} \tag{5.8}$$

Consequently, it is possible to rewrite (5.8) as:

$$\begin{aligned}\dot{\tilde{u}}_2(t) \quad &\in \tfrac{r}{I}\tau(t) + \left(\tfrac{r^2\mu mg}{I} + k_{22}\mu g\right)\text{sgn}(\dot{q}(t) - u_2^d(t) - \tilde{u}_2(t)) \\ &-g(q(t), \dot{q}(t), q_d(t), \dot{q}_d(t), u_{1d}(t), u_{2d}(t), \dot{u}_{2d}(t)),\end{aligned} \tag{5.9}$$

where

$$g(q, \dot{q}, q_d, \dot{q}_d, t) = k_{21}(\dot{q}(t) - \dot{q}_d(t)) + k_{22}\frac{u_1(t)}{m} - k_{22}\ddot{q}_d(t) + \dot{u}_{2d}(t), \tag{5.10}$$

with $u_1 = k_{11}(q - q_d) + k_{12}(\dot{q} - \dot{q}_d) + u_{1d}$.

The next step is to design an input $\tau(\cdot)$ such that $\tilde{u}_2$ converges to zero, at least asymptotically. For this purpose, let us choose $\tau(t)$ such that:

$$\frac{r}{I}\tau(t) = g(q(t), \dot{q}(t), x_{1d}(t), x_{2d}(t), u_{1d}(t), u_{2d}(t), \dot{u}_{2d}(t)) + \tau_s(t), \tag{5.11}$$

with

$$\tau_s \in -k_{sl}\text{sgn}(\tilde{u}_2), \tag{5.12}$$

and $k_{sl} > \mu g|\frac{r^2 m}{I} + k_{22}|$. The closed-loop dynamics for $\tilde{u}_2$ is the differential inclusion:

$$\dot{\tilde{u}}_2(t) \in -k_{sl}\ \text{sgn}(\tilde{u}_2(t)) + \mu g\left(\frac{r^2 m}{I} + k_{22}\right)\lambda_t(t), \quad \lambda_t(t) \in \text{sgn}(\dot{q}(t) - u_2^d(t) - \tilde{u}_2(t)). \tag{5.13}$$

Thus, in this context of sliding mode control, λ_t which is a selection of the set-valued signum function, is considered as a bounded disturbance. Under the stated assumptions, there exists $t^\star < +\infty$ such that $\tilde{u}_2(t) = 0$ for all $t \geq t^\star$. Therefore, $\ddot{q}(t) \in \frac{u_1(t)}{m} - \mu g\ \text{sgn}(\dot{q}(t) - u_2^d(t))$ on $[t^\star, +\infty)$, and we are back to the analysis made in sections 4.2.1 to 4.4.

Remark 5.3.1. *The two-stage backstepping strategy allows us to define the desired dynamics as in (4.7), specifically for the "object" part in (5.1) (a). Consequently, it is the extension of the material in sections 4.2.1 to 4.4 to the case when the belt-pulleys dynamics are no longer neglected, which is significant in practice.*

The following stability result is stated.

Proposition 5.3.2. *Consider the dynamics in (5.1) with bounded initial data and bounded time-varying functions $q_d(\cdot)$, $\dot{q}_d(\cdot)$, $\ddot{q}_d(\cdot)$, $u_{1d}(\cdot)$, $u_{2d}(\cdot)$, $\dot{u}_{2d}(\cdot)$, and let $g_{21} = 0$. The controller defined in (5.11)-(5.12) with $u_1(q, \dot{q}, t) = k_{11}(q - q_d) + k_{12}(\dot{q} - \dot{q}_d) + u_{1d}$, where K is given such that $(A_{cl}, B_{cl}, C_{cl}, D_{cl})$ is strictly state passive. Therefore, the error $e = (\tilde{q}, \dot{\tilde{q}})$, where $\tilde{q} = q - q_d$ and $\dot{\tilde{q}} = \dot{q} - \dot{q}_d$, is bounded and converges exponentially fast to zero. Moreover, the variables $\dot{\theta}$ and $\ddot{\theta}$ remain bounded.*

The proof uses material from section 5.3.2 on the pulley's angle error dynamics.

Proof. The proof is performed in three steps. First, the focus is on demonstrating the finite time convergence of $\tilde{u}_2$ in (5.13) to zero (*i.e.*, proving that (5.13) has finite time stable equilibrium point $\tilde{u}_2^\star = 0$). Then, the stability of (5.6) is analysed when $\tilde{u}_2 = 0$. The third step demonstrates the boundedness of the variables.

First step: Consider the dynamics of $\dot{\tilde{u}}_2(t)$ in (5.13). The objective is to show that $\tilde{u}_2 = 0$ for all $t \geq t^\star$ where $t^\star < \infty$, under the sliding mode control $\tau_s = -k_{sl}\text{sgn}(\tilde{u}_2)$ in (5.12), with the sliding surface $\tilde{u}_2 = 0$. The input $\tau(t)$ in (5.8) is recovered using (5.11). Let us take the Lyapunov function $V(\tilde{u}_2(t)) = \frac{1}{2}\tilde{u}_2^2(t)$, then the rate of change of the storage function is:

$$\begin{aligned}
\dot{V} &= \tilde{u}_2 \dot{\tilde{u}}_2 \\
&= \tilde{u}_2 \left(\tau_s + \left(\tfrac{r^2 \mu m g}{I} + k_{22} \mu g \right) \lambda_t \right) \\
&= -k_{sl} \tilde{u}_2 \, \text{sgn}(\tilde{u}_2) + \tilde{u}_2 \left(\tfrac{r^2 \mu m g}{I} + k_{22} \mu g \right) \lambda_t
\end{aligned}$$

Given that λ_t is bounded such that $\lambda_t \in [-1, 1]$ and that $\tilde{u}_2 \text{sgn}(\tilde{u}_2) = |\tilde{u}_2|$, hence:

$$\begin{aligned}
\dot{V} &= -k_{sl}|\tilde{u}_2| + \tilde{u}_2 \left(\tfrac{r^2 \mu m g}{I} + k_{22} \mu g \right) \lambda_t \\
&\leq -k_{sl}|\tilde{u}_2| + |\tilde{u}_2| \left| \tfrac{r^2 \mu m g}{I} + k_{22} \mu g \right| \\
&\leq |\tilde{u}_2| \left(\left| \tfrac{r^2 \mu m g}{I} + k_{22} \mu g \right| - k_{sl} \right)
\end{aligned}$$

Considering that $k_{sl} > \left| \frac{r^2 \mu m g}{I} + k_{22} \mu g \right|$, let us define $-a \triangleq \left| \frac{r^2 \mu m g}{I} + k_{22} \mu g \right| - k_{sl} < 0$ with $a > 0$. Then, the rate of change of the storage function is:

$$\dot{V} \leq -a|\tilde{u}_2| \leq -a\sqrt{2} V^{\frac{1}{2}}$$

Thus, according to [19, Theorem 4.2], the equilibrium point $\tilde{u}_2^\star = 0$ of the dynamics in (5.13) is globally finite-time-stable. Let $t^\star$ to be the finite time required for $\tilde{u}_2$ to reach zero (*i.e.*, the solution $\tilde{u}_2(t)$ of (5.13) is defined on $[0, t^\star]$ and $\lim_{t \to t^\star} \tilde{u}_2(t) = 0$). In order to calculate the time $t^\star$, let us write the following:

$$\begin{aligned}
\tfrac{dV(\tilde{u}_2(t))}{dt} \leq -a\sqrt{2} V^{\frac{1}{2}}(\tilde{u}_2(t)) \quad &\Leftrightarrow \int_{V(\tilde{u}_2(0))}^{V(\tilde{u}_2(t^\star))} \tfrac{dV(\tilde{u}_2(t))}{V^{\frac{1}{2}}(\tilde{u}_2(t))} \leq -a\sqrt{2} \int_0^{t^\star} dt \\
&\Leftrightarrow 2 \left(V^{\frac{1}{2}}(\tilde{u}_2(t^\star)) - V^{\frac{1}{2}}(\tilde{u}_2(0)) \right) \leq -a\sqrt{2} t^\star
\end{aligned}$$

Given that $V(\tilde{u}_2(t^\star)) = 0$ (*i.e.*, $\tilde{u}_2(t^\star) = 0$), the finite time $t^\star$ is chosen such that $t^\star = \frac{2V^{\frac{1}{2}}(\tilde{u}_2(0))}{a\sqrt{2}}$. This result aligns with the function of the settling-time given by [19, Theorem 4.2], which could be directly applied to compute $t^\star$. It is important to note that the duration of the transient period $[0, t^\star]$ decreases as the value of k_{sl} and, consequently, as the value of a increases.
The expression of the controller $\tau(t)$ such that the dynamics in (5.8) converges to zero as $t \to t^\star$ is given by:

$$\begin{aligned}\tau(t) &= \tfrac{I}{r}\left(\tau_s(t) + \dot{u}_2^d + k_{22}\mu g\,\mathrm{sgn}(\dot{q}(t) - u_2^d(t) - \tilde{u}_2(t))\right)\\ &= \tfrac{I}{r}\left(-k_{sl}\mathrm{sgn}(\tilde{u}_2(t)) + \tfrac{k_{22}k_{11}}{m}(q(t) - q_d(t)) + \left(k_{21} + \tfrac{k_{12}k_{22}}{m}\right)(\dot{q}(t) - \dot{q}_d(t))\right)\\ &\quad + \tfrac{I}{r}\left(k_{22}\mu g\lambda_{t,d} + \dot{u}_{2d}(t)\right)\end{aligned} \tag{5.14}$$

which confirms the expression given in (5.11).

Second step: In this step, the stability of (5.6) is analysed for all $t \in [t^\star, \infty)$ when $\tilde{u}_2(t) = 0$. The closed-loop system in (5.5) is reduced to the following on the interval $[t^\star, \infty)$:

$$\begin{aligned}\ddot{q}(t) \in\ & \tfrac{k_{11}}{m}(q(t) - q_d(t)) + \tfrac{k_{12}}{m}(\dot{q}(t) - \dot{q}_d(t)) + \tfrac{u_{1d}(t)}{m}\\ & -\mu g\ \mathrm{sgn}\left(\dot{q}(t) - k_{21}(q(t) - q_d(t)) - k_{22}(\dot{q}(t) - \dot{q}_d(t)) - u_{2d}(t)\right)\end{aligned} \tag{5.15}$$

The reduced dynamics in (5.15) are equivalent to those in (4.19). Consequently, the error dynamics $\tilde{q} = q - q_d$ in (5.6) is reduced on the interval $[t^\star, \infty)$ and is written as:

$$\ddot{\tilde{q}}(t) = \frac{1}{m}(k_{11}\tilde{q}(t) + k_{12}\dot{\tilde{q}}(t)) + \mu g\left[\lambda_{t,d}(t) - \lambda_t(t)\right] \tag{5.16}$$

where $\lambda_{t,d}(t) \in \mathrm{sgn}(\dot{q}_d(t) - u_{2d}(t))$ and $\lambda_t(t) \in \mathrm{sgn}(\dot{q}(t) - u_2^d(t))$. Given that $u_2^d(t) = k_{21}(q(t) - q_d(t)) + k_{22}(\dot{q}(t) - \dot{q}_d(t)) + u_{2d}(t)$, the error dynamics in (5.16) are equivalent to the error dynamics in (4.20). Hence, the same analysis in section 4.4 is applied in this step. Recall the LCS of the error dynamics in (4.21) with $e = (\tilde{q}, \dot{\tilde{q}})$:

$$\begin{aligned}\dot{e}(t) \in\ & A_{cl}e(t) + \begin{pmatrix}0\\ \mu g\end{pmatrix}\mathrm{sgn}(\dot{q}_d(t) - u_{2d}(t)) - \begin{pmatrix}0\\ \mu g\end{pmatrix}\mathrm{sgn}(-(C_{cl})_{1,\bullet}e(t) + \dot{q}_d(t) - u_{2d}(t))\\ &= A_{cl}e(t) - B_{cl}\begin{pmatrix}\lambda_{1d}(t) - \lambda_1(t)\\ \lambda_{2d}(t) - \lambda_2(t)\end{pmatrix}\end{aligned}$$

where $\lambda_1 = \frac{\lambda_t + 1}{2} \in [0, 1]$.

Third step: This step is dedicated to show the boundedness of the variables. Let us analyze the dynamics in (5.1) (b). According to the analysis in section 4.4 and given that $\tilde{u}_2 = 0$ for $t \geq t^\star$, it follows that the variables $q(\cdot)$, $\dot{q}(\cdot)$ are bounded on $[t^\star, +\infty)$. Assuming that $\dot{u}_{2d}(\cdot)$, $\dot{q}_d(\cdot)$ and $\ddot{q}_{2d}(\cdot)$ are bounded, then $\ddot{q}(\cdot)$ is also bounded. Therefore,

on $[t^\star, +\infty)$, and given that $r\ddot{\theta} = k_{21}(\dot{q} - \dot{q}_d) + k_{22}(\ddot{q} - \ddot{q}_d) + \dot{u}_{2d}$, it follows that $\ddot{\theta}(\cdot)$ and consequently $\tau(\cdot)$ are bounded. Similarly, $\dot{\theta}(\cdot)$ is bounded on $[t^\star, +\infty)$.
Since $r\dot{\theta}(t) = u_2^d(t)$ on $[t^\star, +\infty)$, it follows that

$$\theta(t) = \theta(t^\star) + \frac{1}{r}\int_{t^\star}^{t}(k_{21}(q(s) - q_d(s)) + k_{22}(\dot{q}(s) - \dot{q}_d(s)) + u_{2d}(s))ds \tag{5.17}$$

A necessary and sufficient condition for the boundedness of pulley's angle is that the integrand in (5.17) be bounded. However, it is important to note that since θ is defined modulo 2π, its boundedness is a secondary issue. The boundedness of all variables on $[0, t^\star)$ is ensured from the fact that there does not exist any finite escape in the closed-loop system, since all the right-hand sides are sums of linear single-valued terms and bounded set-valued terms. □

Case $g_{21} > 0$

This is the case when a force feedback is applied. Recall that $u_2^d \triangleq k_{21}(q - q_d) + k_{22}(\dot{q} - \dot{q}_d) + g_{21}(\lambda_1 - \lambda_{1d}) + u_{2d}$. Using (4.12), the robot-object dynamics (5.1) (a) (b) is equivalently rewritten as:

$$\begin{aligned}
\ddot{q}(t) &= \tfrac{u_1(t)}{m} - \mu g \operatorname{proj}\left([-1,1];\ 2\tfrac{\dot{q}(t) - k_{21}(q(t)-q_d(t)) - k_{22}(\dot{q}(t)-\dot{q}_d(t)) + g_{21}\lambda_{1d}(t) - 2g_{21} - u_{2d}(t) - \tilde{u}_2(t)}{g_{21}}\right) \\
\ddot{\theta}(t) &= \tfrac{\tau(t)}{I} + \tfrac{r\mu mg}{I} \operatorname{proj}\left([-1,1];\ 2\tfrac{\dot{q}(t) - k_{21}(q(t)-q_d(t)) - k_{22}(\dot{q}(t)-\dot{q}_d(t)) + g_{21}\lambda_{1d}(t) - 2g_{21} - u_{2d}(t) - \tilde{u}_2(t)}{g_{21}}\right)
\end{aligned} \tag{5.18}$$

with $\tilde{u}_2 = r\dot{\theta} - u_2^d$. However, the rest of the control input cannot be designed similarly as for the case when $g_{21} = 0$ in (5.11) and (5.12). This is because the multipliers λ_1 and λ_{1d} are not differentiable (and could even be discontinuous), making it impossible to differentiate $u_2^d(q, \dot{q}, \lambda_1, t)$ in order to get (5.7).

Remark 5.3.3. *It is known that backstepping strategy can be adapted to yield different controllers, which do not necessarily all behave identically [35]. Thus, the controller designed above may be modified.*

5.3.2 Analysis of Pulley's Angle Error Dynamics

This section is dedicated to discussing the possibility of designing desired pulley's angle dynamics and then analyzing the corresponding error dynamics. This discussion is useful for proving the boundedness of these dynamics. The closed-loop robot dynamics in (5.1) (b) is given by:

$$\ddot{\theta}(t) \in \frac{1}{r}g(q(t), \dot{q}(t), t) - \frac{1}{r}k_{sl}\operatorname{sgn}(r\dot{\theta}(t) - u_2^d(q(t), \dot{q}(t), t)) + \frac{r\mu mg}{I}\operatorname{sgn}(\dot{q}(t) - r\dot{\theta}(t)) \tag{5.19}$$

Let us interpret (5.19) in terms of the desired trajectory for the pulley's angle. One approach is to define $\tau(\theta, \dot{\theta}, t) = I\ddot{\theta}_d - k_v(\dot{\theta} - \dot{\theta}_d) - k_p(\theta - \theta_d)$, and then find a suitable function $\theta_d(\cdot)$ such that the object dynamics (5.1) (a) is suitably controlled. Let us

consider the framework of (4.1), where $I\ddot{\theta}(t) = \tau(t)$. Let $\tilde{\theta} \triangleq \theta - \theta_d$, then $I\dddot{\tilde{\theta}}(t) + k_v\ddot{\tilde{\theta}}(t) + k_p\dot{\tilde{\theta}}(t) = 0$, so that $\tilde{\theta}$, $\dot{\tilde{\theta}}$ and $\ddot{\tilde{\theta}}$ converge exponentially fast to zero.

The next step is to define $\dot{\theta}_d(t)$ such that (4.1) is controlled as in section 4.2.1, assuming that $r\dot{\theta} = r\dot{\theta}_d$. Specifically, $\dot{\theta}_d(t) = \frac{1}{r}u_2(q,\dot{q},t) = \frac{1}{r}(k_{21}(q-q_d) + k_{22}(\dot{q}-\dot{q}_d) + u_{2d})$. Then, $\ddot{\theta}_d = \frac{1}{r}g(q,\dot{q},t) - \frac{1}{r}k_{22}\mu g\lambda_t$, where the contact force is necessary to define the desired pulley's angle acceleration. Therefore, this control approach is not directly implementable. However, the above backstepping strategy allows us to avoid this issue by correctly interpreting the desired angle acceleration. Let us define $\ddot{\theta}'_d \triangleq \frac{1}{r}g(q,\dot{q},t)$ and $\dddot{\tilde{\theta}}' \triangleq \ddot{\theta} - \ddot{\theta}'_d$, it follows from (5.19) that:

$$\dddot{\tilde{\theta}}'(t) \in -\frac{1}{r}k_{sl}\,\mathrm{sgn}(r\dot{\theta}(t) - u_2^d(q(t),\dot{q}(t),t)) + \frac{r\mu mg}{I}\,\mathrm{sgn}(\dot{q}(t) - r\dot{\theta}(t)). \tag{5.20}$$

Using the expressions of $g(q,\dot{q},t)$ in (5.10), of $u_2^d(\cdot)$, and (5.1) (a), it is possible to show that $g(q,\dot{q},t) = \dot{u}_2^d + k_{22}\mu g\lambda_t$. Therefore,

$$r\dot{\theta}(t) - u_2^d(q(t),\dot{q}(t),t) = r\dot{\theta}(t) - \int_0^t g(q,\dot{q},t)dt + \int_0^t k_{22}\mu g\lambda_t(t)dt = r\dot{\theta}(t) - r\int_0^t \ddot{\theta}_d(t)dt$$

Assuming the initial conditions are correct, it follows from (5.19):

$$\begin{aligned}\dddot{\tilde{\theta}}(t) \;&\in \ddot{\theta}(t) - \tfrac{1}{r}g(q,\dot{q},t) + \tfrac{1}{r}k_{22}\mu g\lambda_t \in \tfrac{1}{r}k_{22}\mu g\lambda_t - \tfrac{1}{r}k_{sl}\,\mathrm{sgn}(r\dot{\theta}(t) - r\dot{\theta}_d(t)) + \tfrac{r\mu mg}{I}\lambda_t \\ &\in -\tfrac{1}{r}k_{sl}\,\mathrm{sgn}(r\ddot{\tilde{\theta}}(t)) + \left(\tfrac{r\mu mg}{I} + \tfrac{1}{r}k_{22}\mu g\right)\lambda_t,\end{aligned} \tag{5.21}$$

with $\lambda_t(t) \in \mathrm{sgn}(\dot{q}(t) - r\dot{\theta}(t))$. Thus, it is possible to reinterpret the above backstepping control strategy with a suitable definition of the desired angle trajectory. Although $\ddot{\theta}_d$ is not realizable because it involves $\lambda_t(t)$ in its definition, the closed-loop error system yields the differential inclusion (5.21). Note that the condition on k_{sl} allows us to deduce that $\ddot{\tilde{\theta}}$ converges to zero in a finite time. By referring to (5.20), it is inferred that:

$$\dddot{\tilde{\theta}}'(t) \in -\frac{1}{r}k_{sl}\,\mathrm{sgn}\left(\ddot{\tilde{\theta}}'(t) + k_{22}\mu g\int_0^t \lambda_t(t)dt\right) + \frac{r\mu mg}{I}\lambda_t(t)). \tag{5.22}$$

In summary, the error system resulting from the backstepping strategy is defined by (5.21), (5.13), and (5.4). Considering the asymptotic tracking for the state of the mass (*i.e.*, $q(t) \to q_d(t)$ and $\dot{q}(t) \to \dot{q}_d(t)$ as $t \to +\infty$), it is inferred that,

$$\begin{aligned} & g(q,\dot{q},t) = k_{21}(\dot{q}-\dot{q}_d) + k_{22}\tfrac{k_{11}(q-q_d)+k_{12}(\dot{q}-\dot{q}_d)+u_{1d}}{m} - k_{22}\ddot{q}_d + \dot{u}_{2d} \\ \to\;& g_\infty(t) \triangleq k_{22}\tfrac{u_{1d}(t)}{m} - k_{22}\ddot{q}_d(t) + \dot{u}_{2d}(t), \text{ as } t \to \infty \end{aligned}$$

Therefore,

Corollary 5.3.4. *The pulley's angular velocity is bounded and it satisfies* $\dot{\theta}(t) \to \frac{1}{r}\left(\frac{k_{22}}{m}\int_0^t u_{1d}(t)dt - k_{22}\dot{q}_d(t) + u_{2d}(t)\right) - \int_0^t k_{22}\mu g\lambda_t(t)dt$.

5.3.3 Numerical Simulations

This section is dedicated for the numerical simulations of the dynamical system in (5.1) after implementing the controller designed in (5.14). The simulations are performed for the nominal case and the case with parametric uncertainties to test the robustness of the controller. The sliding-mode controller guarantees some robustness with respect to uncertainties in μ. According to (5.13) and (5.21), it is sufficient to know an upper-bound on the friction coefficient. However, a complete robustness analysis mimicking section 4.5 does not hold since $g_{21} = 0$ as noted above. Therefore, in this section, a numerical analysis of the controller's robustness is provided when the coefficient of friction is both under-estimated and over-estimated.

In the Nominal Case (known friction coefficient)

Since the controller in (5.14) possesses a set-valued part (the signum, or relay, multi-valued function), it is important to perform the simulations with a suitable numerical integrator. Hence the platform SICONOS is used again. According to the methodology followed to simulate LCS, as explained in Appendix C.1, it is required first to write the closed-loop system of (5.1) in the form of an LCS. This is equivalent to write the LCS of the closed-loop system's dynamics in (5.5) for $\dot{q}$ and (5.19) for $\dot{\theta}$ by considering $\tilde{u}_2$ in (5.13) as an intermediate variable. Let us define the state $x = (q, \dot{q}, \theta, \dot{\theta})^\top$, the desired state to be tracked $x_d = (q_d, \dot{q}_d)^\top$, and the slack variable $\lambda_k \in \operatorname{sgn}(r\dot{\theta} - u_2^d)$. Recall that $\tilde{u}_2 = r\dot{\theta} - u_2^d$, the controllers $u_1 = k_{11}(x_1 - x_{1d}) + k_{12}(x_2 - x_{2d}) + u_{1d}$, $u_2^d = k_{21}(x_1 - x_{1d}) + k_{22}(x_2 - x_{2d}) + u_{2d}$, and $\tau = \frac{k_{11}k_{22}}{rm}(x_1 - x_{1d}) + \left(\frac{k_{12}k_{22}}{rm} + \frac{k_{21}}{r}\right)(x_2 -$

$x_{2d}) + \frac{2k_{22}}{r}\mu g\lambda_{1,d} - \frac{k_{22}}{r}\mu g + \dot{u}_{2d} - \frac{k_{sl}}{r}\lambda_k$. The closed-loop LCS is written as:

$$
\begin{cases}
\dot{x}(t) = \overbrace{\begin{pmatrix} 0 & 1 & 0 & 0 \\ \frac{k_{11}}{m} & \frac{k_{12}}{m} & 0 & 0 \\ 0 & 0 & 0 & 1 \\ \frac{k_{11}k_{22}}{rm} & \frac{k_{21}}{r} + \frac{k_{12}k_{22}}{rm} & 0 & 0 \end{pmatrix}}^{\triangleq A_1} x(t) + \overbrace{\begin{pmatrix} 0 & 0 & 0 & 0 \\ -2\mu g & 0 & 0 & 0 \\ 0 & 0 & 0 & 0 \\ \frac{2r}{I}m\mu g & 0 & -\frac{2}{r}k_{sl} & 0 \end{pmatrix}}^{\triangleq B_1} \lambda(t) + \begin{pmatrix} 0 & 0 \\ \frac{1}{m} & 0 \\ 0 & 0 \\ \frac{k_{22}}{rm} & 0 \end{pmatrix} u_d(t) \\
\quad - \begin{pmatrix} 0 & 0 \\ \frac{k_{11}}{m} & \frac{k_{12}}{m} \\ 0 & 0 \\ \frac{k_{11}k_{22}}{rm} & \frac{k_{21}}{r} + \frac{k_{12}k_{22}}{rm} \end{pmatrix} x_d(t) + \begin{pmatrix} 0 & 0 \\ 0 & 0 \\ 0 & 0 \\ \frac{2k_{22}}{r}\mu g & 0 \end{pmatrix} \lambda_d(t) + \overbrace{\begin{pmatrix} 0 \\ \mu g \\ 0 \\ -\frac{k_{22}}{r}\mu g - \frac{r}{I}m\mu g + \frac{1}{r}\dot{u}_{2d} + \frac{k_{sl}}{r} \end{pmatrix}}^{\triangleq E_1'} \\
0 \leq \lambda(t) \perp w(t) = \underbrace{\begin{pmatrix} 0 & -1 & 0 & r \\ 0 & 0 & 0 & 0 \\ k_{21} & k_{22} & 0 & -r \\ 0 & 0 & 0 & 0 \end{pmatrix}}_{\triangleq C_1} x(t) + \underbrace{\begin{pmatrix} 0 & 1 & 0 & 0 \\ -1 & 0 & 0 & 0 \\ 0 & 0 & 0 & 1 \\ 0 & 0 & -1 & 0 \end{pmatrix}}_{\triangleq D_1} \lambda(t) - \begin{pmatrix} 0 & 0 \\ 0 & 0 \\ k_{21} & k_{22} \\ 0 & 0 \end{pmatrix} x_d(t) \\
\quad + \begin{pmatrix} 0 \\ 1 \\ u_{2d} \\ 1 \end{pmatrix} \geq 0
\end{cases}
\tag{5.23}
$$

where $\lambda \triangleq (\lambda_1,\ \lambda_2,\ \lambda_3,\ \lambda_4)^\top$, $\lambda_1 = \frac{1+\lambda_t}{2}$, and $\lambda_3 = \frac{1+\lambda_k}{2}$. It is noteworthy that the transformation of the signum function into LCP formalism is demonstrated in section 4.2.1, as explained in [42].

Take $k_{sl} = 2\mu g\left|\frac{r^2 m}{I} + k_{22}\right|$. The closed-loop LCS in (5.23) is strictly state passive since the BMI in (4.10) after being transformed into an LMI has a solution given by:

$$
K = \begin{pmatrix} -3.06 & -2.29 \\ -10.77 & -11.08 \end{pmatrix} \quad \text{and} \quad P = \begin{pmatrix} 2.35 & 1.099 \\ 1.099 & 1.23 \end{pmatrix}
$$

with $\epsilon = 1$. Take $\mu = 0.5$, $r = 0.5$, $I = 1kg.m^2$, and $mg = 9.8$. The numerical simulation is performed with the initial values $x(0) = (1, 0, 0, 2)^\top$ and $x_d(0) = (3, -4)^\top$. The desired inputs $u_{1d} = u_{2d} = 0.5m\mu g\cos 2t$ and the time step $h = 0.01$s.

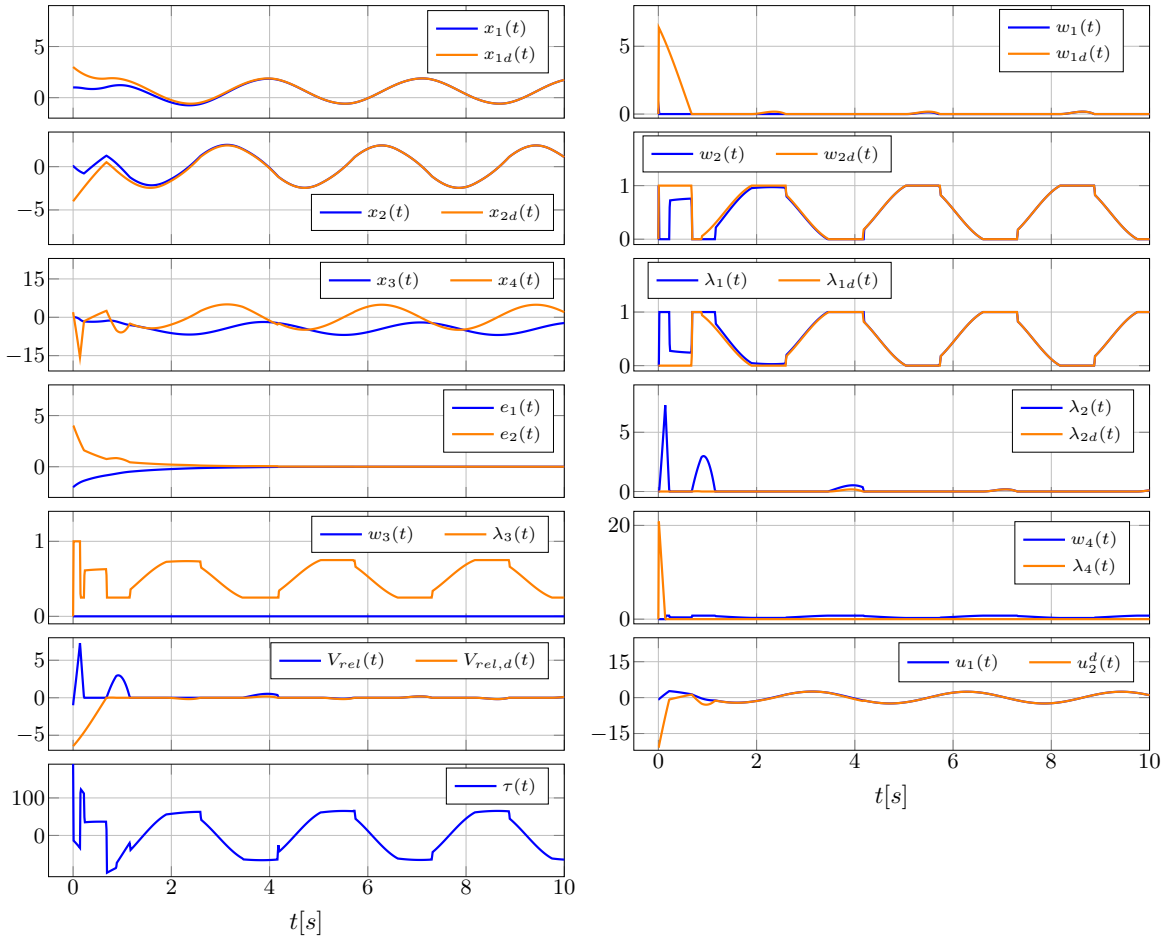

Figure 5.2: Backstepping control of the pulley-belt-mass system.

It is observed in Figure 5.2 that the error of the mass $e = q - q_d$ converges exponentially to zero and that the dynamics of the pulley's angle, as depicted by the plots x_3, x_4 are bounded. These observations confirm the results stated in Proposition 5.3.2. In the steady state response (*i.e.*, $e = 0$), there is a synchronization noticed between the desired and closed-loop complementarity variables $\lambda_{1d}, \lambda_{2d}, w_{1d}, w_{2d}$ and $\lambda_1, \lambda_2, w_1, w_2$, respectively. Moreover, the controller $u = (u_1, u_2^d)^\top$ converges to the desired periodic behaviour $u_d = (u_{1d}, u_{2d})^\top$. In order to analyze the stick/slip behaviour of the desired and the closed-loop system, as shown by the plot $V_{rel} = \dot{q} - u_2^d$, let us observe Figure 5.3:

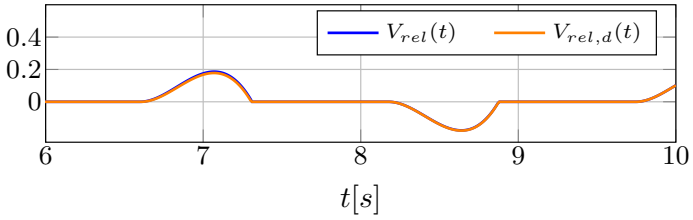

Figure 5.3: Relative velocity in the steady state response

Figure 5.3 shows a part of the plot V_{rel} in Figure 5.2, and it corresponds to the

steady state responses of the desired system $V_{rel,d} = \dot{q}_d - u_{2d}$ and the closed-loop system $V_{rel} = \dot{q} - u_2^d$. The relative velocity of the closed-loop system converges to that of the desired system, and it is observed that the mass exhibits a stick/slip behavior with a small amplitude of the relative velocity, $V_{rel} = 0.2$m/s, during the slip phase.

Let us simulate the intermediate variable $\tilde{u}_2$ in two different ways to verify the consistency of our analysis. The first simulation in Figure 5.4a shows the plot of $\tilde{u}_2$ where $\tilde{u}_2 = r\dot{\theta} - u_2^d$. The second simulation in Figure 5.4b is that of the dynamics of $\tilde{u}_2$ in (5.13).

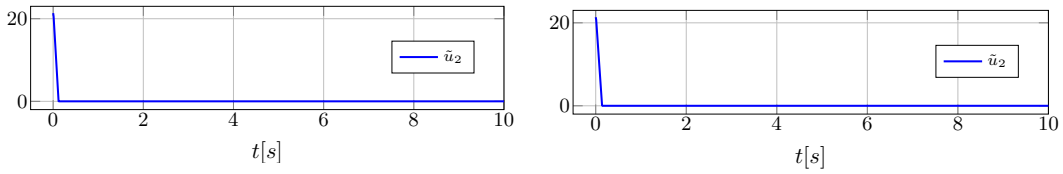

(a) Numerical simulation of $\tilde{u}_2 = r\dot{\theta} - u_2^d$ (b) Numerical simulation of $\tilde{u}_2$ in (5.13)

Figure 5.4: Numerical simulation of $\tilde{u}_2$ using two integration approaches.

It can be observed from Figure 5.4 that the variable $\tilde{u}_2$ shows a finite time convergence to zero (*i.e.*, $\tilde{u}_2 = 0$ for all $t > 0.13$s), as predicted theoretically. Also, there is consistency between Figures 5.4a and 5.4b, which show that deriving $\tilde{u}_2$ from the simulation given in Figure 5.2 as $\tilde{u}_2 = r\dot{\theta} - u_2^d$ gives the same result as simulating directly $\tilde{u}_2$ from its dynamics in (5.13). It is noteworthy that if k_{sl} is decreased such that $k_{sl} = 1.4\mu g \left|\frac{r^2 m}{I} + k_{22}\right|$, the transient response will increase slightly (*i.e.*, $\tilde{u}_2 = 0$ for all $t > 0.21$s). Additionally, if k_{sl} is decreased to $k_{sl} = 1.1\mu g \left|\frac{r^2 m}{I} + k_{22}\right|$, then the transient response will increase to 0.34s.

In the Presence of Parametric Uncertainties (uncertain friction coefficient)

Let us test the robustness with respect to additive parametric uncertainties $\Delta\mu$ in the plant model. The controller is designed from the nominal (known) friction coefficient μ_0. Let $\mu = \mu_0 + \Delta\mu$ be the coefficient of friction of the real plant model. The nominal system of the frictional oscillator with pulley-belt dynamics in (5.1) is written as:

$$\ddot{q}_d(t) \in \frac{u_{1d}(t)}{m} - \mu_0 mg \ \mathrm{sgn}(\dot{q}_d(t) - u_{2d}(t))$$

The plant's model with uncertainties is:

$$\begin{cases} \ddot{q}(t) \in \frac{u_1(t)}{m} - (\mu_0 + \Delta\mu)mg \ \mathrm{sgn}(\dot{q}(t) - r\dot{\theta}(t)) \\ \\ \ddot{\theta}(t) \in \frac{\tau(t)}{I} + \frac{r(\mu_0+\Delta\mu)mg}{I} \mathrm{sgn}(\dot{q}(t) - r\dot{\theta}(t)) \end{cases}$$

where the controller $u_1 = k_{11}(q(t) - q_d(t)) + k_{12}(\dot{q}(t) - \dot{q}_d(t)) + u_{1d}$ and $\tau(t)$ is defined in (5.14). Recall that $\tau(t)$ is given as follows:

$$\frac{r}{I}\tau(t) = \frac{k_{11}k_{22}}{m}(q(t) - q_d(t)) + \left(\frac{k_{12}k_{22}}{m} + k_{21}\right)(\dot{q}(t) - \dot{q}_d(t)) + \mu_0 mg\lambda_{t,d} + \dot{u}_{2d} - k_{sl}\lambda_k$$

where $\lambda_{t,d}(t) \in \text{sgn}(\dot{q}_d(t) - r\dot{\theta}_0(t))$, $\lambda_k \in \text{sgn}(r\dot{\theta}(t) - u_2^d(t))$, $k_{sl} > (\mu_0 + \Delta\mu)g\left|\frac{r^2m}{I} + k_{22}\right|$.

We have $u_2^d(t) = k_{21}(q(t) - q_d(t)) + k_{22}(\dot{q} - \dot{q}(t)) + u_{2d}(t)$. Let us recall that the state $x \stackrel{\Delta}{=} (q,\ \dot{q},\ \theta,\ \dot{\theta})^\top$ and the desired state $x_d = (q_d,\ \dot{q}_d)^\top$, then the closed-loop system with uncertainties is given by the following LCS:

$$\begin{cases} \dot{x}(t) = A_1 x(t) + (B_1 + \Delta B_1)\lambda(t) - \begin{pmatrix} 0 & 0 \\ \frac{k_{11}}{m} & \frac{k_{12}}{m} \\ 0 & 0 \\ \frac{k_{11}k_{22}}{rm} & \frac{k_{21}}{r} + \frac{k_{12}k_{22}}{rm} \end{pmatrix} x_d(t) + \begin{pmatrix} 0 & 0 \\ 0 & 0 \\ 0 & 0 \\ \frac{2k_{22}}{r}\mu_0 g & 0 \end{pmatrix} \lambda_d(t) \\ \qquad\qquad + \begin{pmatrix} 0 & 0 \\ \frac{1}{m} & 0 \\ 0 & 0 \\ \frac{k_{22}}{rm} & 0 \end{pmatrix} u_d(t) + E_1' + \Delta E_1' \\ 0 \le \lambda(t) \perp w(t) = C_1 x(t) + D_1\lambda(t) - \begin{pmatrix} 0 & 0 \\ 0 & 0 \\ k_{21} & k_{22} \\ 0 & 0 \end{pmatrix} x_d(t) + \begin{pmatrix} 0 \\ 1 \\ u_{2d} \\ 1 \end{pmatrix} \ge 0 \end{cases} \tag{5.24}$$

where A_1, B_1, C_1, D_1, and E_1' are defined in (5.23).
By taking $k_{sl} = 2(\mu_0 + \Delta\mu)g\left|\frac{r^2m}{I} + k_{22}\right|$, then

$$\Delta B_1 = \begin{pmatrix} 0 & 0 & 0 & 0 \\ -2\Delta\mu\, g & 0 & 0 & 0 \\ 0 & 0 & 0 & 0 \\ \frac{2mgr}{I}\Delta\mu & 0 & -4\Delta\mu\, g\left|\frac{r^2m}{I} + k_{22}\right| & 0 \end{pmatrix} \quad \text{and} \quad \Delta E_1' = \begin{pmatrix} 0 \\ \Delta\mu\, g \\ 0 \\ -\frac{rmg}{I}\Delta\mu + 2\Delta\mu\left|\frac{r^2m}{I} + k_{22}\right| \end{pmatrix}$$

In the following figures, the coefficient of friction is varied to cover two approaches: overestimated and underestimated friction, in order to observe the behavior of the system and the analyze the robustness of the controller. Recall that $\mu = 0.5$, $r = 0.5$, $I = 1kg.m^2$, and $mg = 9.8$. The numerical simulation is performed with the initial values $x(0) = (1, 0, 0, 2)^\top$ and $x_d(0) = (3, -4)^\top$. The desired inputs $u_{1d} = u_{2d} = 0.5m\mu g\cos 2t$ and the time step $h = 0.01$s.

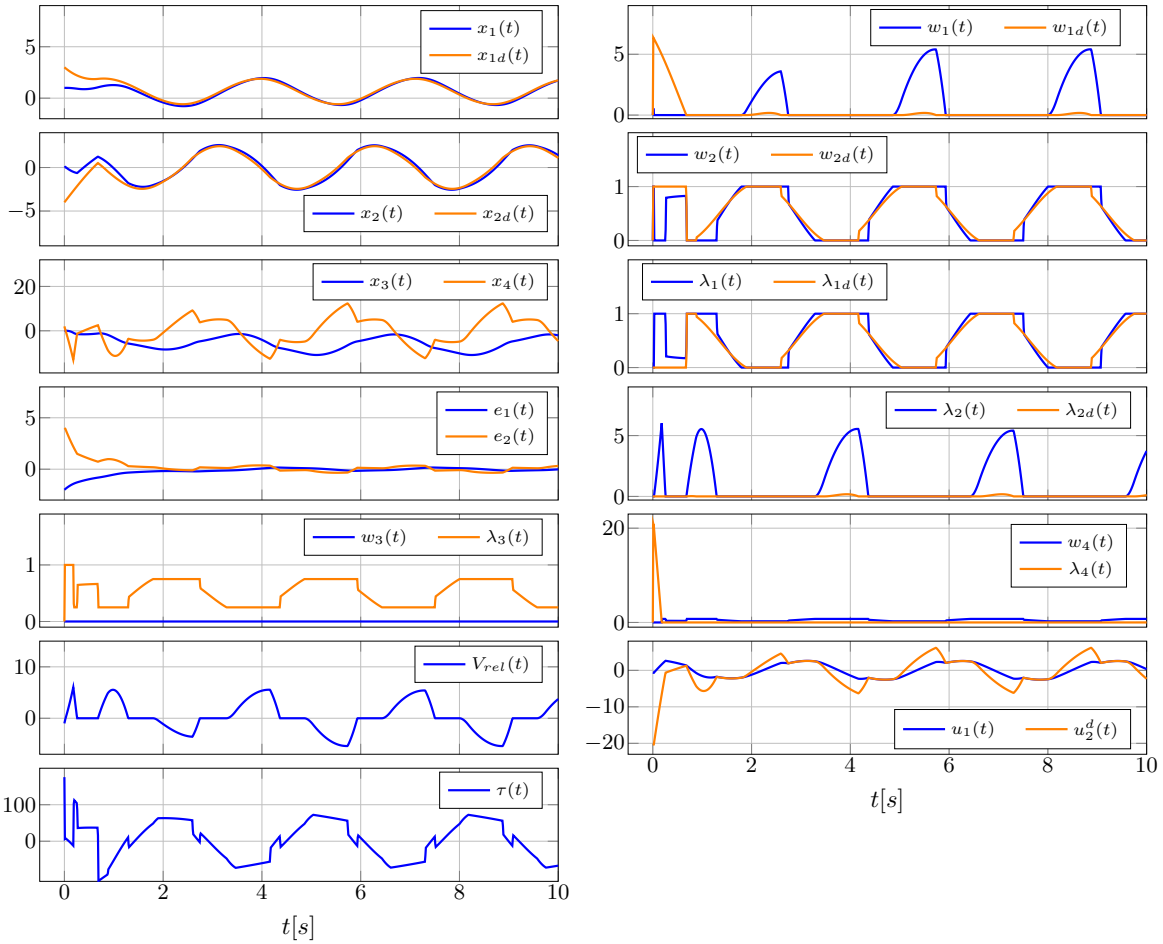

Figure 5.5: Backstepping control of the pulley-belt-mass system with $\Delta\mu = -0.1$

In Figure 5.5, the coefficient of friction is overestimated (*i.e.*, $\mu_0 > \mu_0 + \Delta\mu$). The numerical simulation shows that there is a significant error e between the closed-loop and the desired trajectories such that $\|e_1\|_{[5,10],\infty} = 0.162$ and $\|e_2\|_{[5,10],\infty} = 0.349$. It is important to show that the pulley's angle dynamics $x_3 \triangleq \theta$ and $x_4 \triangleq \dot{\theta}$ are still bounded in the presence of uncertainties in the friction coefficient.
By observing the plot of the relative velocity $V_{rel} = \dot{q} - r\dot{\theta}$, the mass presents a stick/slip behavior with respect to the belt. This behavior can be explained by examining the plot of λ_1. From the complementarity problem in (5.24), we have $w_1 = -x_2 + rx_4 + \lambda_2$ and $w_2 = -\lambda_1 + 1$. Given that $V_{rel} = \dot{q} - r\dot{\theta} \triangleq x_2 - rx_4$, then $w_1 = -V_{rel} + \lambda_2$. At this step, it is possible to solve the complementarity problem $0 \leq (w_1, w_2)^\top \perp (\lambda_1, \lambda_2)^\top \geq 0$ for different values of λ_1, where $\lambda_1 \in [0, 1]$. Solving this problem as in section 4.3 will illustrate the relation between λ_1 and V_{rel}: if $\lambda_1 = 1$, then $V_{rel} = \lambda_2 \geq 0$; if $\lambda_1 = 0$, then $V_{rel} = -w_1 \leq 0$; and if $\lambda_1 \in]0, 1[$, then $V_{rel} = 0$.
The plot of the controller u shows that the u_2^d has the same behavior as x_4 after $\tilde{u}_2$ converges to zero in finite time (0.13s).

Let us now examine the behavior of the system when the friction is underestimated for $\Delta\mu = 0.1$, by observing the numerical simulations in Figure 5.6.

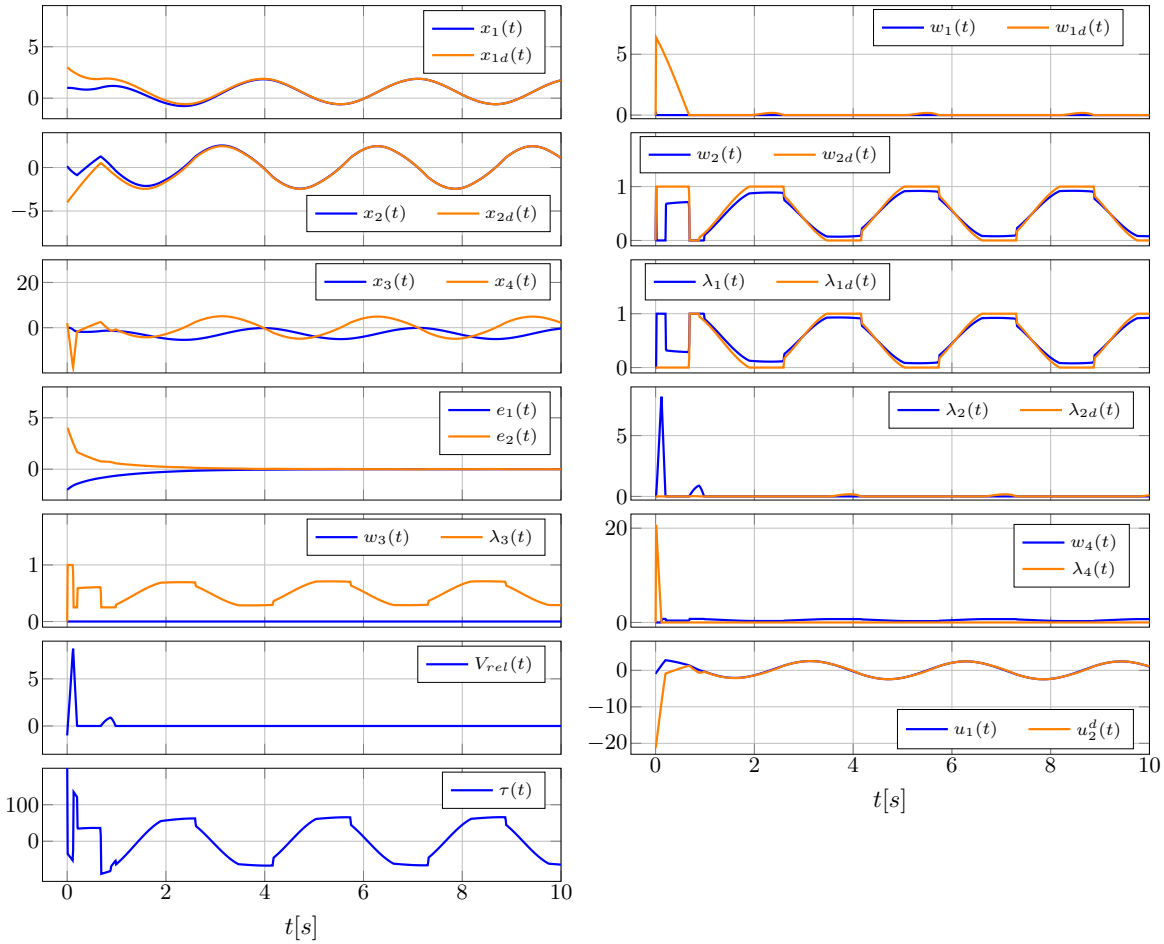

Figure 5.6: Backstepping control of the pulley-belt-mass system with $\Delta\mu = 0.1$

It is interesting to notice that the result of tracking in Figure 5.6, where the friction is underestimated, is better than that in Figure 5.5, with smaller values of error such that $\|e_1\|_{[5,10],\infty} = 0.005$ and $\|e_2\|_{[5,10],\infty} = 0.013$. As well, the pulley's angle dynamics $\theta \triangleq x_3$ and $\dot{\theta} \triangleq x_4$ show boundedness.
In Figure 5.6, the mass exhibits only sticking mode to the belt (*i.e.*, $V_{rel} = \dot{q} - r\dot{\theta} = 0$) in the steady state response. This behaviour is further illustrated by the evolution of the complementarity variable λ_1, where $\lambda_1 \in]0, 1[$ in the steady state response as shown in Figure 5.6.

From the above numerical simulations in Figures 5.5 and 5.6, it is observed that for trajectory tracking in frictional oscillators with pulley-belt dynamics using our approach (*i.e.*, backstepping strategy), it is better to underestimate friction to achieve smaller tracking error. However, in the case of underestimating friction (*i.e.*,$\mu_0 < \mu_0 + \Delta\mu$), the mass never slides. This result is different from the case of overestimating friction (*i.e.*, $\mu_0 > \mu_0 + \Delta\mu$), where the tracking error is larger and the mass shows sliding phases.

To further check the observations from Figures 5.5 and 5.6, let us add the following figures with a larger uncertainty $\Delta\mu = \pm 0.2$.

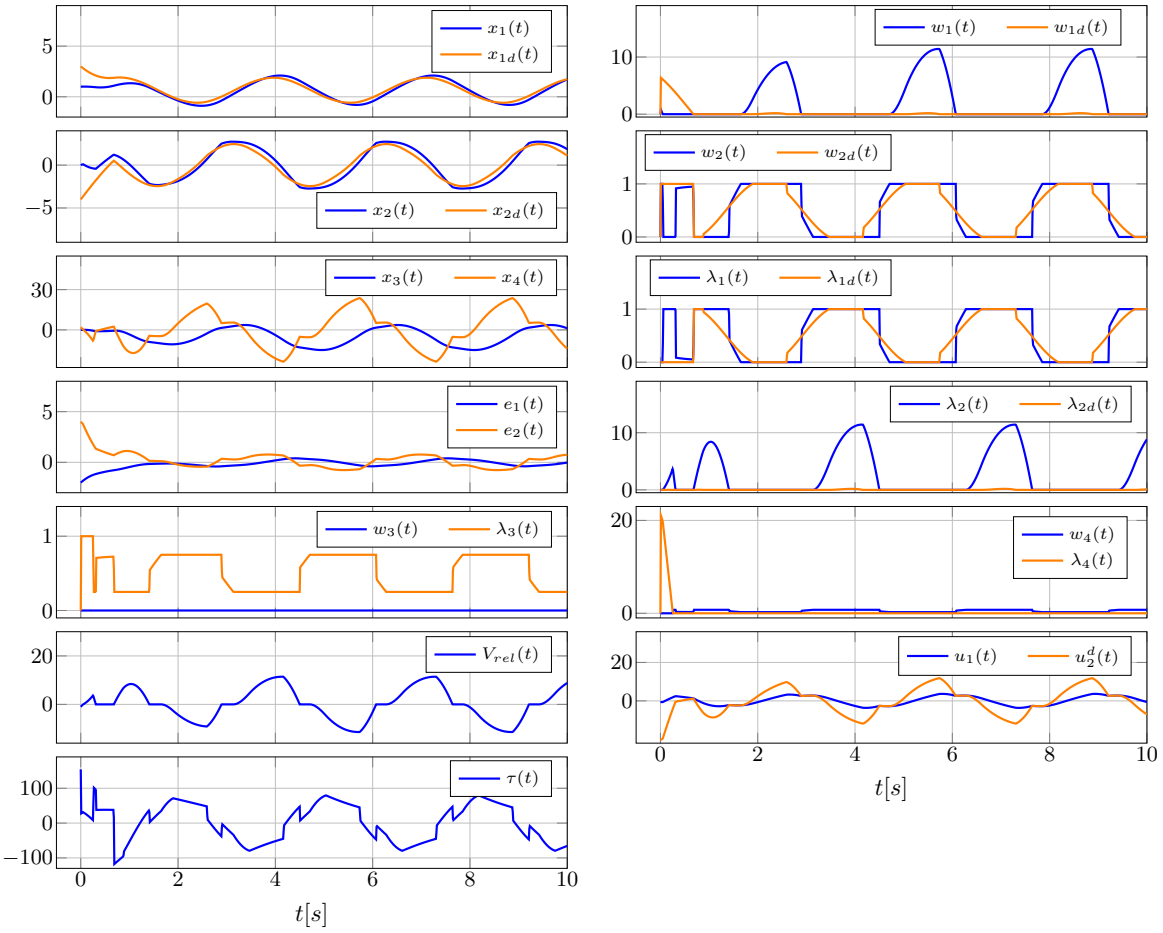

Figure 5.7: Backstepping control of the pulley-belt-mass system with $\Delta\mu = -0.2$

The friction in the numerical simulation in Figure 5.7 is overestimated (*i.e.*, $\mu_0 > \mu_0 + \Delta\mu$) with $\Delta\mu = -0.2$. The tracking error $e = (q - q_d, \dot{q} - \dot{q}_d)^\top$ increases significantly from that in Figure 5.5 where $\Delta\mu = -0.1$, such that $\|e_1\|_{[5,10],\infty} = 0.39$ and $\|e_2\|_{[5,10],\infty} = 0.76$. It can be observed that the pulley's angle dynamics remain bounded as shown in the plots of $x_3 \triangleq \theta$ and $x_4 \triangleq \dot{\theta}$.
The stick/slip behaviour of the mass is still observable as in Figure 5.5 for the case of overestimated friction, as shown by the plot of $V_{rel} = \dot{q} - r\dot{\theta}$ and λ_1. The relation between V_{rel} and λ_1 can be deduced from the complementarity problem in (5.24), which is explained in the comment for Figure 5.5. Moreover, the amplitude of the relative velocity shows a large increase as the overestimation of friction increases, for $\Delta\mu = -0.2$ in Figure 5.7 compared to that for $\Delta\mu = -0.1$ in Figure 5.5. The numerical simulation in Figure 5.7 also presents the plots of the controllers $u = (u_1, u_2^d)^\top$ and $\tau(t)$.

Let us underestimate the friction with $\Delta\mu = 0.2$, and observe the behaviour of the system depicted in Figure 5.8.

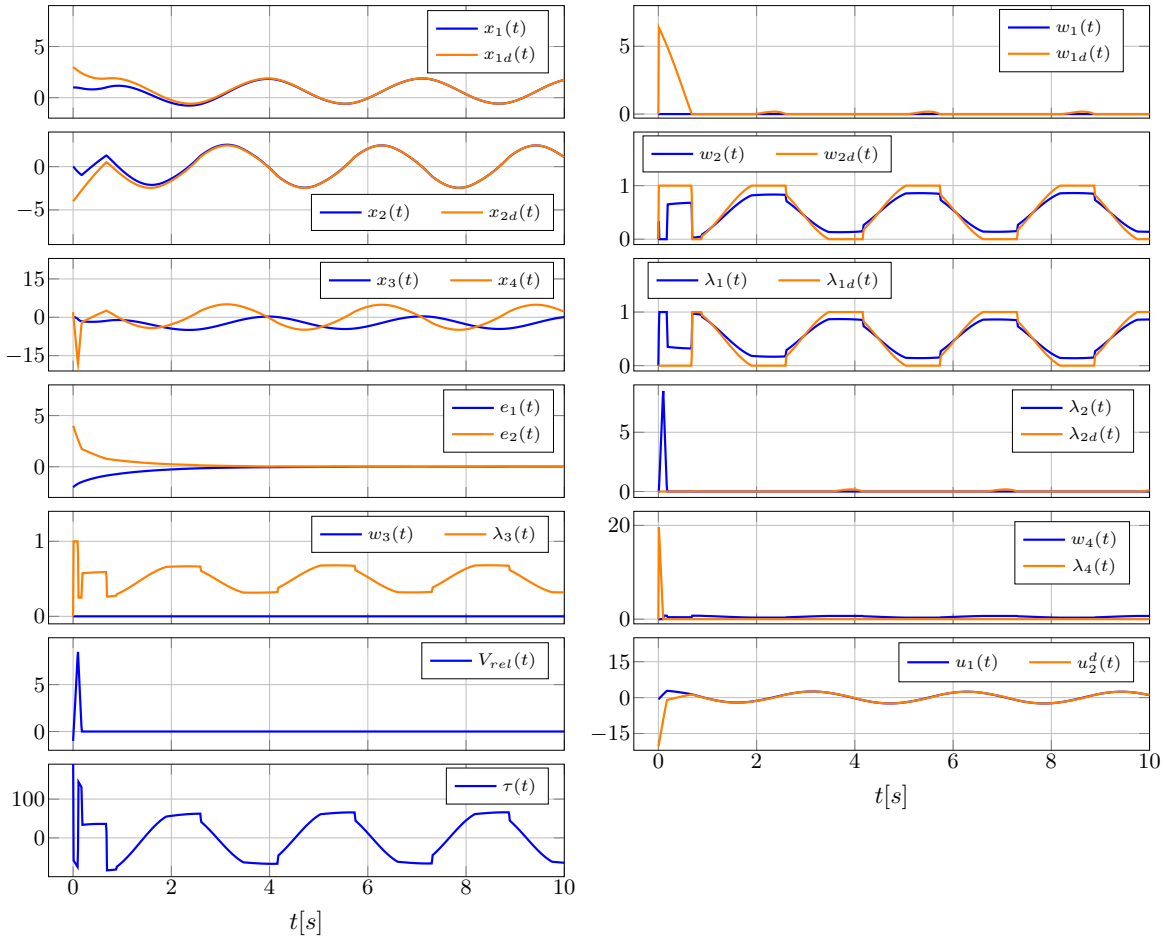

Figure 5.8: Backstepping control of the pulley-belt-mass system with $\Delta\mu = 0.2$

In the numerical simulation of Figure 5.8, the friction is underestimated (*i.e.*, $\mu_0 < \mu_0 + \Delta\mu$) with $\Delta\mu = 0.2$. It is interesting to observe in Figure 5.8 that the tracking result is represented by a small tracking tracking error $e = (q - q_d, \dot{q} - \dot{q}_d)^\top$, as in Figure 5.6 with a slight increase, such that $\|e_1\|_{[5,10],\infty} = 0.006$ and $\|e_2\|_{[5,10],\infty} = 0.014$. The pulley's angle dynamics $x_3 \triangleq \theta$ and $x_4 \triangleq \dot{\theta}$ remain bounded.
Additionally, the mass exhibits sticking behaviour only in the steady steady state system for the case of underestimating friction in Figure 5.8 with $\Delta\mu = 0.2$, which is similar to the behaviour shown in Figure 5.6 with $\Delta\mu = 0.1$. The sticking mode is explained by the plot of λ_1, where $\lambda_1 \in]0, 1[$ in the steady state response, which implies that $V_{rel} = 0$ according to the complementarity problem in (5.24). Note that the controller τ displays a completely different behaviour in Figure 5.8 (when the friction is underestimated) from that in Figure 5.6 (when the friction is overestimated).

To further analyze the robustness of the controller with respect to the uncertainties in the friction coefficient and to demonstrate our observations regarding friction estimation, let us consider a different set of initial values for the states x and x_d. Consider the following figures with the new initial conditions $x_d(0) = (1, 0)^\top$ and $x(0) = (3, -4, 1, -2)^\top$. Recall that $\mu_0 = 0.5$, $r = 0.5$, $I = 1$ kg.m^2, and $mg = 9.8$. The desired inputs $u_{1d} = u_{2d} = 0.5m\mu gcos2t$ and the time step $h = 0.01$.

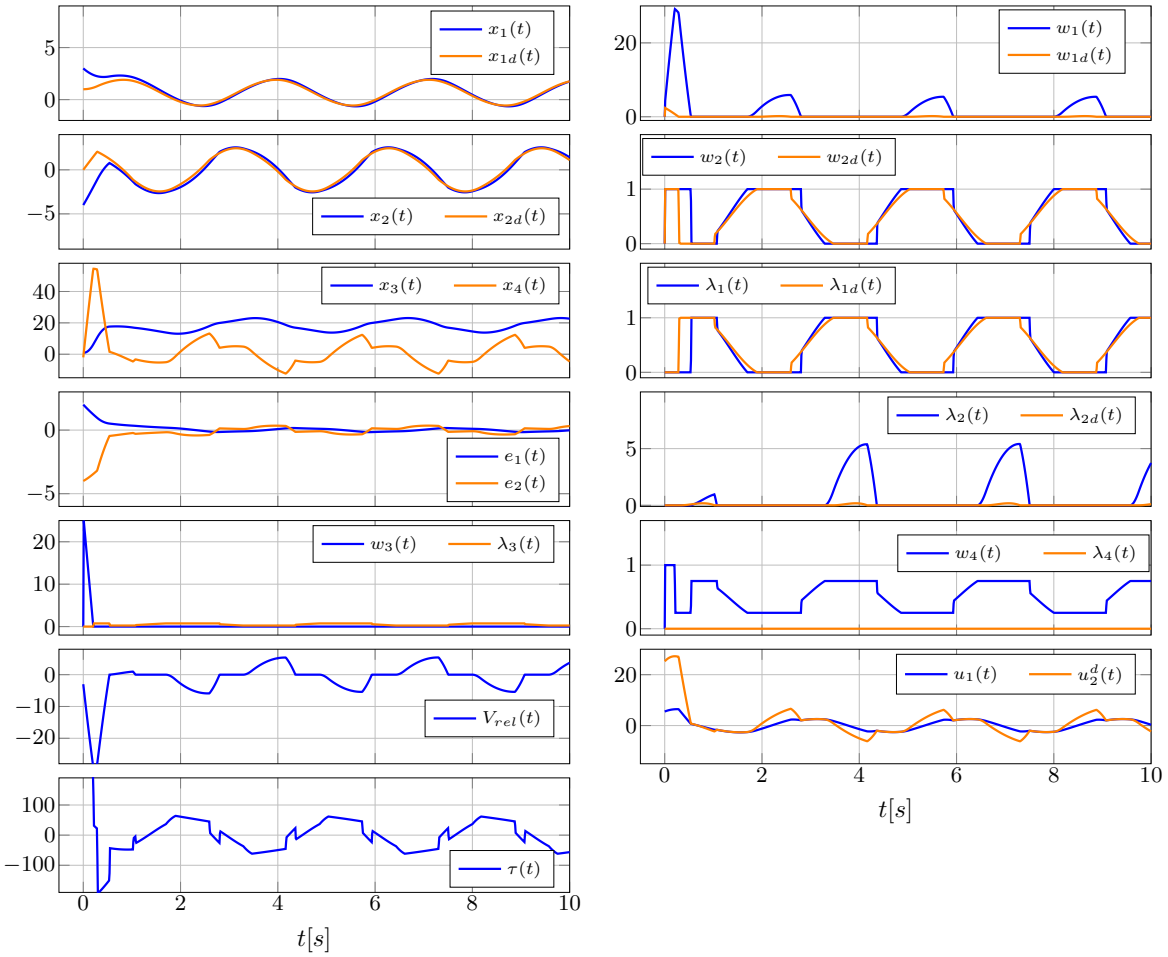

Figure 5.9: Backstepping control of the pulley-belt-mass system with $\Delta\mu = -0.1$ and new initial conditions

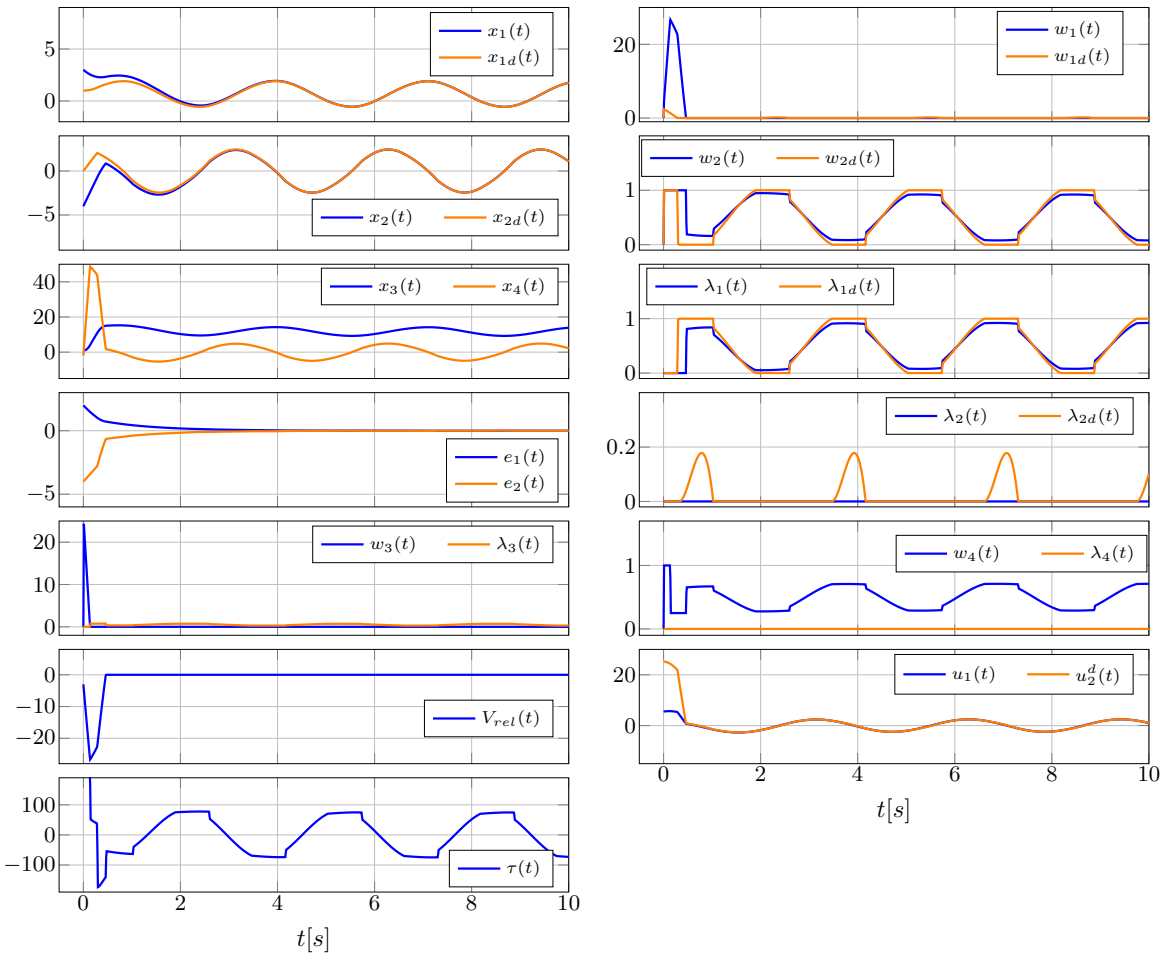

Figure 5.10: Backstepping control of the pulley-belt-mass system with $\Delta\mu = 0.1$ and new initial conditions

From Figures 5.9 and 5.10, it is observed that underestimating friction (I.E., $\Delta\mu = 0.1$) gives better result for the tracking error, where $e = x - x_d$ converges to zero, even with different initial conditions. The same observations were noticed for other initial conditions, but their figures are not presented here for brevity.

5.4 The Backward-Euler Discrete-time Implementation of the Backstepping Controller

The foregoing section presents numerical simulations of the closed-loop dynamics using specific time-stepping schemes available in the SICONOS platform, which is similar to the simulations presented in Chapter 3 for the nonsmooth set-valued electrical circuits (see Appendix C.1). Set-valued sliding-mode controllers have to be implemented in discrete-time using implicit Euler algorithms in order to avoid numerical chattering [36]. Thus, it is crucial to analyze the discrete-time implementation of the controller. The objective of this section is to analyze the discrete-time backstepping controller without feedback from λ_t, as described in section 5.3. To begin this analysis, let us start with a backward (implicit) Euler discretization of the dynamics in (5.1):

$$\begin{cases} (a)\ \ \dot{q}_{k+1} = \dot{q}_k + h\frac{u_{1,k}}{m} - h\mu g\lambda_{t,k+1} \\ (b)\ \ q_{k+1} - q_k = h\dot{q}_k \\ (c)\ \ I\dot{\theta}_{k+1} = I\dot{\theta}_k + h\tau_k + hr\mu mg\lambda_{t,k+1} \\ (d)\ \ \theta_{k+1} = \theta_k + h\dot{\theta}_k \\ (e)\ \ \lambda_{t,k+1} \in \operatorname{sgn}(\dot{q}_{k+1} - r\dot{\theta}_{k+1}) \end{cases} \tag{5.25}$$

with $h > 0$ the timestep. The scheme in (5.25) is called implicit because it deals with the set-valued frictional terms implicitly. This approach avoids chattering at sticking modes [1], and ensures the convergence of piecewise constant discrete solutions to the solutions of the continuous-time plant. In other words, implicit (backward Euler) schemes gives an accurate approximation of the contact force, while explicit (forward Euler) schemes do not. Therefore, the time-discretization in (5.25) is considered an appropriate approach for the system's dynamics. Let us define the implicit controller to be applied on $(t_k, t_{k+1}]$:

$$\tau_k = \frac{I}{r}g(q_k, \dot{q}_k, t_k) - \frac{I}{r}k_{sl}\lambda_{3,k+1}, \quad \lambda_{3,k+1} \in \operatorname{sgn}(\tilde{u}_{2,k+1}), \tag{5.26}$$

with $\tilde{u}_{2,k} = r\dot{\theta}_k - u^d_{2,k}$. Recall that $x_d = (x_{1d}, x_{2d})^\top = (q_d, \dot{q}_d)^\top$, then $u^d_{2,k} = k_{21}(q_k - x_{1d,k}) + k_{22}(\dot{q}_k - x_{2d,k}) + u_{2d,k}$. After some manipulations it is obtained:

$$\begin{aligned} \tfrac{\tilde{u}_{2,k+1}-\tilde{u}_{2,k}}{h} \in\ & -k_{sl}\operatorname{sgn}(\tilde{u}_{2,k+1}) + \mu g\left(k_{22} + \tfrac{r^2 m}{h}\right)\lambda_{t,k+1} - k_{21}\tfrac{x_{1d,k+1}-x_{1d,k}}{h} \\ & - \tfrac{u_{2d,k+1}-u_{2d,k}}{h} - k_{22}\tfrac{x_{2d,k+1}-x_{2d,k}}{h} + k_{22}\dot{x}_{2d,k} + \dot{u}_{2d,k} + k_{21}\dot{x}_{1d,k}. \end{aligned} \tag{5.27}$$

5.4.1 Well-posedness

In this section, the well-posedness of the dynamical system in (5.25), the controller τ in (5.26), and the intermediate variable $\tilde{u}_2$ in (5.27) is discussed, ensuring the existence and uniqueness of solutions.

Study of (5.25) (5.26)

The inclusion in (5.25)(e) is equivalently written as: $\dot{q}_{k+1} - r\dot{\theta}_{k+1} \in \mathcal{N}_{[-1,1]}(\lambda_{t,k+1})$. Using (5.25)(a) (c) and (5.26), then:

$$\dot{q}_k + h\frac{u_{1,k}}{m} - h\mu g\left(1 + \frac{r^2 m}{I}\right)\lambda_{t,k+1} - r\dot{\theta}_k - hg(q_k, \dot{q}_k, t_k) + hk_{sl}\lambda_{3,k+1} \in \mathcal{N}_{[-1,1]}(\lambda_{t,k+1}) \tag{5.28}$$

Given that $\tilde{u}_{2,k+1} = r\dot{\theta}_{k+1} - u^d_{2,k+1}$ and using (5.25) (a) (c), the inclusion $\lambda_{3,k+1} \in \text{sgn}(\tilde{u}_{2,k+1})$ in (5.26) is equivalently written as:

$$\begin{aligned} &r\dot{\theta}_k + hg(q_k, \dot{q}_k, t_k) - hk_{sl}\lambda_{3,k+1} + h\mu g\left(k_{22} + \tfrac{r^2 m}{I}\right)\lambda_{t,k+1} - k_{21}(q_k + h\dot{q}_k - x_{1d,k+1}) \\ &-k_{22}(\dot{q}_k + h\tfrac{u_{1,k}}{m} - x_{2d,k+1}) - u_{2d,k+1} \in \mathcal{N}_{[-1,1]}(\lambda_{3,k+1}) \end{aligned} \tag{5.29}$$

By combining (5.28) and (5.29), the following generalized equation (GE) with the unknowns $(\lambda_{t,k+1}, \lambda_{3,k+1})$ is obtained:

$$H(q_k, \dot{q}_k, t_k) - M_h \begin{pmatrix} \lambda_{t,k+1} \\ \lambda_{3,k+1} \end{pmatrix} \in \mathcal{N}_{[-1,1]^2} \begin{pmatrix} \lambda_{t,k+1} \\ \lambda_{3,k+1} \end{pmatrix} \tag{5.30}$$

with

$$H = \begin{pmatrix} \dot{q}_k + h\frac{u_{1,k}}{m} - r\dot{\theta}_k - hg(q_k, \dot{q}_k, t_k) \\ r\dot{\theta}_k + hg(q_k, \dot{q}_k, t_k) - k_{21}(q_k + h\dot{q}_k - x_{1d,k+1}) - k_{22}(\dot{q}_k + h\frac{u_{1,k}}{m} - x_{2d,k+1}) - u_{2d,k+1} \end{pmatrix}$$

and $M_h = h\begin{pmatrix} \mu g\left(1 + \frac{r^2 m}{I}\right) & -k_{sl} \\ -\mu g\left(k_{22} + \frac{r^2 m}{I}\right) & k_{sl} \end{pmatrix}$.

The generalized equation in (5.30) can be written as an affine variational inequality AVI(K, H, M_h) [67] where $K = [-1, 1]^2$ is a bounded polyhedral set. The GE in (5.30) has a solution according to [67, Corollary 2.2.5], with a result on the uniqueness of solution provided in [67, Theorem 4.3.2]. In order to show the uniqueness of the solution to (5.30), it is required to prove that the matrix M_h is P-matrix [4, Theorem 3]. Given that $k_{sl} > \left|\frac{r^2\mu mg}{I} + k_{22}\mu g\right| > 0$ and $\mu g\left(1 + \frac{r^2 m}{I}\right) > 0$, let us check if $k_{sl}\mu g\left(1 + \frac{r^2 m}{I}\right) - k_{sk}\mu g\left(k_{22} + \frac{r^2 m}{I}\right)$ is positive. The principal minor $k_{sl}\mu g(1 - k_{22}) > 0$ for all $k_{22} < 1$. Thus, the matrix M_h is a P-matrix if $k_{22} < 1$. A stronger condition requires that $M_h \succ 0$. Consequently, the GE in (5.30) is rewritten as:

$$0 \in F\begin{pmatrix} \lambda_{t,k+1} \\ \lambda_{3,k+1} \end{pmatrix},$$

where $F(\cdot)$ is strongly monotone. Therefore, according to [14, Theorem 23.44], the solution is unique.

The existence and uniqueness of the multipliers prove that the difference inclusion in (5.25) (5.26) is well-posed, *i.e.*, there exists a unique solution q_{k+1}, $\dot{q}_{k+1}$, θ_{k+1}, $\dot{\theta}_{k+1}$.

In order to compute the solution it is convenient to rewrite the GE as an LCS. Let $\bar{\lambda}_{k+1} \triangleq \begin{pmatrix} \lambda_{t,k+1} \\ \lambda_{3,k+1} \end{pmatrix}$ and let us define $\mathcal{C}$ as the set of $\bar{\lambda}_{k+1}$ such that $\bar{\lambda}_{k+1} \in [-1,1]^2$, then:

$$\mathcal{C} = \left\{ \bar{\lambda}_{k+1} \in I\!R^2 \mid \begin{pmatrix} 1 & 0 \\ -1 & 0 \\ 0 & 1 \\ 0 & -1 \end{pmatrix} \bar{\lambda}_{k+1} + \begin{pmatrix} 1 \\ 1 \\ 1 \\ 1 \end{pmatrix} \geq 0 \right\} \tag{5.31}$$

Let us define the normal cone to $\mathcal{C}$ at $\bar{\lambda}_{k+1}$ as follows:

$$\begin{aligned} \mathcal{N}_{\mathcal{C}}(\bar{\lambda}_{k+1}) &= \{z \in I\!R^2 \mid z_1 = -\gamma_1 + \gamma_2 \text{ and } z_2 = -\gamma_3 + \gamma_4,\ \gamma_i \geq 0 \text{ for } i \in \{1,2,3,4\}\} \\ &= \{z \in I\!R^2 \mid z = -R^\top \gamma, 0 \leq \gamma \perp R\bar{\lambda}_{k+1} + r \geq 0\} \end{aligned}$$

where $\gamma = (\gamma_1, \gamma_2, \gamma_3, \gamma_4)^\top$ is a slack variable, $R = \begin{pmatrix} 1 & 0 \\ -1 & 0 \\ 0 & 1 \\ 0 & -1 \end{pmatrix}$ and $r = \begin{pmatrix} 1 \\ 1 \\ 1 \\ 1 \end{pmatrix}$. Then, the GE in (5.30) is equivalently written as the MLCP:

$$\begin{cases} M_h \bar{\lambda}_{k+1} - H(q_k, \dot{q}_k, t_k) = R^\top \gamma \\ 0 \leq \gamma \perp R\bar{\lambda}_{k+1} + r \geq 0 \end{cases}$$

Given that M_h is P-matrix, the following LCP is derived:

$$0 \leq \gamma \perp RM_h^{-1}R^\top \gamma + RM_h^{-1}H(q_k, \dot{q}_k, t_k) + r \geq 0 \tag{5.32}$$

By solving (5.32), the variables $\lambda_{t,k+1}$ and $\lambda_{3,k+1}$ are obtained. The matrix $RM_h^{-1}R^\top$ is not a P-matrix, since it has low-rank 2 provided that $k_{22} < 1$. However, it is noteworthy that the 4 constraints defining $\mathcal{C}$ in (5.31) cannot be activated simultaneously. Therefore, an enumeration procedure can be used to compute the solutions.

Study of (5.27)

The input in (5.26) corresponds to (5.11)-(5.12), and (5.27) corresponds to (5.13). The last six terms in (5.27) depend only on the desired system states and inputs, and they vanish as $h \to 0$. However, the lower bound on k_{sl} can be modified compared to the continuous-time case to cope with these terms. The following is stated:

Lemma 5.4.1. *The generalized equation (5.27) has always a unique solution $\tilde{u}_{2,k+1}$. Moreover, for k_{sl} large enough, the sequence $\{\tilde{u}_{2,k}\}_{k\geq 0}$ converges to zero in a finite number of steps.*

The proof is identical to the proofs provided in [2, 36] and it is omitted here.

Let us denote $\xi_k \triangleq -k_{21}\frac{x_{1d,k+1}-x_{1d,k}}{h} - \frac{u_{2d,k+1}-u_{2d,k}}{h} - k_{22}\frac{x_{2d,k+1}-x_{2d,k}}{h} + k_{22}\dot{x}_{2d,k} + \dot{u}_{2d,k} + k_{21}\dot{x}_{1d,k} + \mu g\left(k_{22} + \frac{r^2 m}{h}\right)\lambda_{t,k+1}$, then (5.27) is rewritten equivalently as:

$$\tilde{u}_{2,k} + h\xi_k \in \tilde{u}_{2,k+1} + hk_{sl}\ \mathrm{sgn}(\tilde{u}_{2,k+1}), \tag{5.33}$$

equivalently

$$\tilde{u}_{2,k+1} = J_{\mathrm{sgn}}^{hk_{sl}}(\tilde{u}_{2,k} + h\xi_k), \tag{5.34}$$

where $J_{\mathrm{sgn}}^{hk_{sl}}(\cdot) = (1 + hk_{sl}\ \mathrm{sgn})^{-1}(\cdot)$ is the resolvent of index hk_{sl} of the signum multifunction, known as a single-valued nonexpansive mapping [14]. By induction, it follows that $\tilde{u}_{2,k+1}$ is a single-valued function of $\tilde{u}_{2,0}$ and ξ_0.

Let us study the well-posedness of the closed-loop system in (5.25). This means that it is required to check whether $\dot{q}_k$ and $\dot{\theta}_k$ can be computed in a unique way for $k \geq 1$, as a consequence of Lemma 5.4.1. The first controller to be applied on $(t_k, t_{k+1}]$ is given by:

$$u_{1,k} = k_{11}(q_k - x_{1d,k}) + k_{12}(\dot{q}_k - x_{2d,k}) + u_{1d,k}.$$

Using (5.25) (a), this gives rise to:

$$\begin{aligned}\dot{q}_{k+1} - x_{2d,k+1} = \ & \left(1 + \tfrac{h}{m}k_{12}\right)(\dot{q}_k - x_{2d,k}) + \tfrac{h}{m}k_{11}(q_k - x_{1d,k}) + x_{2d,k} - x_{2d,k+1} \\ & + \tfrac{h}{m}u_{1d,k} - h\mu g\lambda_{t,k+1}\end{aligned} \tag{5.35}$$

Assume that $\tilde{u}_{2,k} = 0$ for all $k > k^\star$ (from Lemma 5.4.1, such a $k^\star < +\infty$ exists), then $r\dot{\theta}_k = u_{2,k}^d$ and thus:

$$\begin{aligned}\dot{q}_{k+1} - x_{2d,k+1} \in \ & \left(1 + \tfrac{h}{m}k_{12}\right)(\dot{q}_k - x_{2d,k}) + \tfrac{h}{m}k_{11}(q_k - x_{1d,k}) + x_{2d,k} - x_{2d,k+1} + \tfrac{h}{m}u_{1d,k} \\ & - h\mu g\ \mathrm{sgn}(\dot{q}_{k+1} - k_{21}(q_{k+1} - x_{1d,k+1}) - k_{22}(\dot{q}_{k+1} - x_{2d,k+1}) - u_{2d,k+1})\end{aligned} \tag{5.36}$$

This difference inclusion is the discrete-time counterpart of (4.19). Let $\zeta_k \triangleq \frac{h}{m}k_{11}(q_k - x_{1d,k}) + x_{2d,k} - x_{2d,k+1} + \frac{h}{m}u_{1d,k}$, and using (5.25) (b), $\beta_k \triangleq -k_{21}(q_k + h\dot{q}_k - x_{1d,k+1}) - u_{2d,k+1} + x_{2d,k+1}$, then (5.36) is rewritten equivalently as:

$$\dot{q}_{k+1} - x_{2d,k+1} \in \left(1 + \frac{h}{m}k_{12}\right)(\dot{q}_k - x_{2d,k}) + \zeta_k - h\mu g\ \mathrm{sgn}((1 - k_{22})(\dot{q}_{k+1} - x_{2d,k+1}) + \beta_k). \tag{5.37}$$

To simplify, let us denote $\dot{\tilde{q}}_k \triangleq \dot{q}_k - x_{2d,k}$. Then, (5.37) is equivalently rewritten as:

$$\begin{aligned}&\dot{\tilde{q}}_{k+1} \in \left(1 + \tfrac{h}{m}k_{12}\right)\dot{\tilde{q}}_k + \zeta_k - h\mu g\ \mathrm{sgn}((1 - k_{22})\dot{\tilde{q}}_{k+1} + \beta_k) \\ &\qquad\qquad \Updownarrow \\ &(1 - k_{22})\dot{\tilde{q}}_{k+1} + \beta_k \in \beta_k + (1 - k_{22})\left(\left(1 + \tfrac{h}{m}k_{12}\right)\dot{\tilde{q}}_k + \zeta_k\right) - (1 - k_{22})h\mu g\ \mathrm{sgn}((1 - k_{22})\dot{\tilde{q}}_{k+1} + \beta_k) \\ &\qquad\qquad \Updownarrow \\ &(1 - k_{22})\dot{\tilde{q}}_{k+1} + \beta_k = J_{\mathrm{sgn}}^{(1-k_{22})h\mu g}\left((1 - k_{22})\left(1 + \tfrac{h}{m}k_{12}\right)\dot{\tilde{q}}_k + (1 - k_{22})\zeta_k + \beta_k\right) \\ &\qquad\qquad \Updownarrow \\ &\dot{\tilde{q}}_{k+1} = \tfrac{1}{1-k_{22}}\left(J_{\mathrm{sgn}}^{(1-k_{22})h\mu g}\left((1 - k_{22})\left(1 + \tfrac{h}{m}k_{12}\right)\dot{\tilde{q}}_k + (1 - k_{22})\zeta_k + \beta_k\right) - \beta_k\right)\end{aligned} \tag{5.38}$$

where we assumed that $1 - k_{22} > 0$, which is consistent with the analytical computations in section 4.4.3 when $G = 0$. As above, $J_{\mathrm{sgn}}^{(1-k_{22})h\mu g}(\cdot)$ is the resolvent of the set-valued signum function with index $(1 - k_{22})h\mu g$. The developments in (5.38) show that

$\dot{q}_{k+1}$ in (5.25) (a) with the controllers $u_{1,k}$ and τ_k as above, can be computed uniquely at each timestep for all $k > k^\star$. This uniqueness stems from the one-step-nonsmooth-problem [1], which is uniquely solvable. For $1 \leq k \leq k^\star$, we have $r\dot{\theta}_k = u^d_{2.k} - \tilde{u}_{2,k}$, where the sequence $\{\tilde{u}_{2,k}\}_{k\geq 0}$ is known (see (5.33) or (5.34)). Therefore, the above reasoning can be applied again by introducing $\tilde{u}_{2,k}$ in (5.36). Specifically, in the expression $\text{sgn}(\dot{q}_{k+1} - k_{21}(q_{k+1} - x_{1d,k+1}) - k_{22}(\dot{q}_{k+1} - x_{2d,k+1}) - u_{2d,k+1} + \tilde{u}_{2,k+1})$ and adjusting β_k accordingly. Hence, it is inferred that $\dot{q}_k$ exists uniquely for all $k \geq 1$. Consequently, from (5.25) (a) (b), it follows that $\lambda_{t,k+1}$ exists uniquely as well.

Consider now (5.25) (c). Following from the foregoing analysis, $\lambda_{t,k+1}$ exists uniquely for all $k \geq 0$, thus it can be treated as an exogenous variable for (5.25) (c). The same applies to $u^d_{2,k}$. Inserting (5.26) into (5.25) (c) yields:

$$
\begin{gathered}
r\dot{\theta}_{k+1} \in r\dot{\theta}_k + hg(q_k, \dot{q}_k, t_k) - hk_{sl}\ \text{sgn}(-u^d_{2,k+1} + r\dot{\theta}_{k+1}) + h\tfrac{r^2\mu mg}{I}\lambda_{t,k+1} \\
\Updownarrow \\
r\dot{\theta}_{k+1} - u^d_{2,k+1} \in r\dot{\theta}_k - u^d_{2,k} + u^d_{2,k} - u^d_{2.k+1} + hg(q_k, \dot{q}_k, t_k) - hk_{sl}\ \text{sgn}(-u^d_{2,k+1} + r\dot{\theta}_{k+1}) \\
+h\tfrac{r^2\mu mg}{I}\lambda_{t,k+1} \\
\Updownarrow \\
r\dot{\theta}_{k+1} - u^d_{2.k+1} \in r\dot{\theta}_k - u^d_{2,k} + \gamma_k - hk_{sl}\ \text{sgn}(r\dot{\theta}_{k+1} - u^d_{2,k+1}) \\
\Updownarrow \\
r\dot{\theta}_{k+1} - u^d_{2,k+1} = (1 + hk_{sl}\text{sgn})^{-1}(r\dot{\theta}_k - u^d_{2,k} + \gamma_k) = J^{hk_{sl}}_{\text{sgn}}(r\dot{\theta}_k - u^d_{2,k} + \gamma_k),
\end{gathered}
$$

with $\gamma_k \triangleq u^d_{2,k} - u^d_{2,k+1} + hg(q_k, \dot{q}_k, t_k) + h\frac{r^2\mu mg}{I}\lambda_{t,k+1}$. It is inferred that $r\dot{\theta}_{k+1} - u^d_{2,k+1}$, hence $\dot{\theta}_{k+1}$ is uniquely defined for all $k \geq 0$. Similarly, from (5.25) (d), θ_{k+1} is also uniquely defined. Therefore, the following is proved:

Proposition 5.4.2. *Consider the difference inclusion in (5.25) (5.26), with bounded initial data q_0, $\dot{q}_0$, θ_0, $\dot{\theta}_0$ and desired signals. Then, the system (5.25) (5.26) is well-posed.*

5.4.2 Stability Analysis

In this section, the stability analysis of (5.36) is studied based on the material presented in section 4.4. The discretization of (4.7) is given by:

$$
\begin{cases}
\dot{q}_{d,k+1} = \dot{q}_{d,k} + \frac{h}{m}u_{1d,k} - h\mu g\lambda_{t,d,k+1} \\
q_{d,k+1} = q_{d,k} + h\dot{q}_{d,k} \\
\lambda_{t,d,k+1} \in \text{sgn}(\dot{q}_{d,k+1} - u_{2d,k})
\end{cases}
\tag{5.39}
$$

Using (5.25) (a) the discrete-time error dynamics are given by:

$$
\begin{cases}
(a)\ \ \dot{\tilde{q}}_{k+1} = \dot{\tilde{q}}_k + h\mu g(\lambda_{t,d,k+1} - \lambda_{t,k+1}) + \frac{h}{m}u_{1,k} - \frac{h}{m}u_{1d,k} \\
(b)\ \ u_{1,k} = k_{11}\tilde{q}_k + k_{12}\dot{\tilde{q}}_k + u_{1d,k} \\
(c)\ \ \lambda_{t,d,k+1} \in \text{sgn}(\dot{q}_{d,k+1} - u_{2d,k}) \\
(d)\ \ \lambda_{t,k+1} \in \text{sgn}(\dot{q}_{k+1} - r\dot{\theta}_{k+1}) = \text{sgn}(\dot{q}_{k+1} - \tilde{u}_{2,k} - u^d_{2,k}) \\
(e)\ \ u^d_{2,k} = k_{21}\tilde{q}_k + k_{22}\dot{\tilde{q}}_k + u_{2d,k} \\
(f)\ \ \tilde{q}_{k+1} = \tilde{q}_k + h\dot{\tilde{q}}_k.
\end{cases}
\tag{5.40}
$$

It is important to note that $\tilde{u}_{2,k}$ vanishes after a finite number of steps $k^\star < +\infty$ (see Lemma 5.4.1) and that all variables exist uniquely for all $k \geq 1$. Hence, it is sufficient to study the difference inclusion (5.40) for $k \geq k^\star$, where (5.40) (d) simplifies to:

$$\lambda_{t,k+1} \in \operatorname{sgn}(\dot{q}_{k+1} - k_{21}\tilde{q}_k - k_{22}\dot{\tilde{q}}_k - u_{2d,k}).$$

Consequently, for $k \geq k^\star$ the discrete error dynamics are given by:

$$\begin{cases} (a)\ \ \dot{\tilde{q}}_{k+1} = \dot{\tilde{q}}_k + \frac{h}{m}k_{11}\tilde{q}_k + \frac{h}{m}k_{12}\dot{\tilde{q}}_k + h\mu g(\lambda_{t,d,k+1} - \lambda_{t,k+1}) \\ (b)\ \ \lambda_{t,k+1} \in \operatorname{sgn}(\dot{q}_{k+1} - k_{21}\tilde{q}_k - k_{22}\dot{\tilde{q}}_k - u_{2d,k}) \\ (c)\ \ \lambda_{t,d,k+1} \in \operatorname{sgn}(\dot{q}_{d,k+1} - u_{2d,k}) \\ (d)\ \ \tilde{q}_{k+1} = \tilde{q}_k + h\dot{\tilde{q}}_k, \end{cases} \tag{5.41}$$

which is the discrete counterpart of (4.20). Recall that $\lambda_t = 2\lambda_1 - 1$, it follows from (5.41) that:

$$e_{k+1} = (I_2 + hA_{cl})e_k + hB_{cl}(\lambda_{k+1} - \lambda_{d,k+1})$$

which represents the discrete counterpart of (4.21). In the complementarity framework, the discrete-time systems read as follows:

$$\begin{cases} e_{k+1} = (I_2 + hA_{cl})e_k + hB_{cl}(\lambda_{k+1} - \lambda_{d,k+1}) \\ 0 \leq \lambda_{d,k+1} \perp w_{d,k+1} = \begin{pmatrix} 0 & 1 \\ 0 & 0 \end{pmatrix} u_{d,k} + \begin{pmatrix} 0 \\ 1 \end{pmatrix} + \begin{pmatrix} 0 & 1 \\ -1 & 0 \end{pmatrix} \lambda_{d,k+1} + \begin{pmatrix} 0 & -1 \\ 0 & 0 \end{pmatrix} x_{d,k+1} \geq 0 \\ 0 \leq \lambda_{k+1} \perp w_{k+1} = \underbrace{\begin{pmatrix} k_{21} & k_{22} - 1 \\ 0 & 0 \end{pmatrix}}_{C_{cl}} e_{k+1} + \begin{pmatrix} 0 \\ 1 \end{pmatrix} + \underbrace{\begin{pmatrix} 0 & 1 \\ -1 & 0 \end{pmatrix}}_{D_{cl}} \lambda_{k+1} \\ \qquad\qquad + \begin{pmatrix} 0 & -1 \\ 0 & 0 \end{pmatrix} x_{d,k+1} + \begin{pmatrix} 0 & 1 \\ 0 & 0 \end{pmatrix} u_{d,k} \geq 0 \end{cases} \tag{5.42}$$

The reasoning in section 4.4.2–(4.22) can be repeated to prove that

$$(w_{k+1} - w_{d,k+1})^\top (\lambda_{k+1} - \lambda_{d,k+1}) \leq 0.$$

where $w_{k+1} - w_{d,k+1} = C_{cl}e_{k+1} + D_{cl}(\lambda_{k+1} - \lambda_{d,k+1})$. The KYP Lemma conditions for passivity in discrete-time systems differ from those in continuous-time systems [39, section 3.15]. Passivity preservation, with same supply rate, storage function, and for all $h > 0$, after discretization with a (θ, γ)-method holds under restrictive conditions [75]. Let us consider the Lyapunov candidate function $V_k = e_k^\top P e_k$, where P is the solution of the continuous-time matrix inequality for strict state passivity in (4.10).

Then,

$$\begin{aligned}
V_{k+1}-V_k &= (e_{k+1}-e_k)^\top P(e_{k+1}+e_k)\\
&= he_k^\top A_{cl}^\top P(e_{k+1}+e_k)+h(\lambda_{k+1}-\lambda_{d,k+1})^\top B_{cl}^\top P(e_{k+1}+e_k)\\
&= \tfrac{h}{2}e_k^\top(A_{cl}^\top P+PA_{cl})e_k+he_k^\top A_{cl}^\top Pe_{k+1}+h(\lambda_{k+1}-\lambda_{d,k+1})^\top C_{cl}(e_{k+1}+e_k)\\
&= \tfrac{h}{2}e_k^\top(A_{cl}^\top P+PA_{cl})e_k+he_k^\top A_{cl}^\top P(I_2+hA_{cl})e_k+h^2e_k^\top A_{cl}^\top PB_{cl}(\lambda_{k+1}-\lambda_{d,k+1})\\
&\quad +h(\lambda_{k+1}-\lambda_{d,k+1})^\top C_{cl}(e_{k+1}+e_k)\\
&= he_k^\top(A_{cl}^\top P+PA_{cl})e_k+h^2e_k^\top A_{cl}^\top PA_{cl}e_k+h^2e_k^\top A_{cl}^\top C_{cl}^\top(\lambda_{k+1}-\lambda_{d,k+1})\\
&\quad +h(\lambda_{k+1}-\lambda_{d,k+1})^\top C_{cl}e_k+h(\lambda_{k+1}-\lambda_{d,k+1})^\top(w_{k+1}-w_{d,k+1}-D_{cl}(\lambda_{k+1}-\lambda_{d,k+1}))\\
&= he_k^\top(A_{cl}^\top P+PA_{cl})e_k+h^2e_k^\top A_{cl}^\top PA_{cl}e_k+h^2e_k^\top A_{cl}^\top C_{cl}^\top(\lambda_{k+1}-\lambda_{d,k+1})\\
&\quad +h(\lambda_{k+1}-\lambda_{d,k+1})^\top C_{cl}e_k+h(\lambda_{k+1}-\lambda_{d,k+1})^\top(w_{k+1}-w_{d,k+1})\\
&\le -h\epsilon\, e_k^\top Pe_k+h^2e_k^\top A_{cl}^\top PA_{cl}e_k+h^2e_k^\top A_{cl}^\top C_{cl}^\top(\lambda_{k+1}-\lambda_{d,k+1})\\
&\quad +h(\lambda_{k+1}-\lambda_{d,k+1})^\top C_{cl}e_k
\end{aligned}$$

Recall that both multipliers $\lambda_{1,k}=\frac{\lambda_{t,k}+1}{2}$ and $\lambda_{1d,k}=\frac{\lambda_{t,d}+1}{2}$ belong to $[0,1]$ by construction. Moreover, $C_{cl}^\top\lambda_k=\begin{pmatrix}k_{21}\lambda_{1,k}\\(k_{22}-1)\lambda_{1,k}\end{pmatrix}$. Therefore,

$$\begin{aligned}
V_{k+1}-V_k &\le -h\epsilon\, e_k^\top Pe_k+h^2e_k^\top A_{cl}^\top PA_{cl}e_k+h^2e_k^\top A_{cl}^\top\begin{pmatrix}k_{21}\\k_{22}-1\end{pmatrix}(\lambda_{1,k+1}-\lambda_{1d,k+1})\\
&\quad +he_k^\top\begin{pmatrix}k_{21}\\k_{22}-1\end{pmatrix}(\lambda_{1,k+1}-\lambda_{1d,k+1})\\
&\le -he_k^\top\left(\epsilon P-hA_{cl}^\top PA_{cl}\right)e_k+\tfrac{h^2}{2}\left\|\begin{pmatrix}k_{21}\\k_{22}-1\end{pmatrix}A_{cl}e_k\right\|^2+\tfrac{h^2}{2}(\lambda_{1,k+1}-\lambda_{1d,k+1})^2\\
&\quad +\tfrac{h}{2}\left\|\begin{pmatrix}k_{21}\\k_{22}-1\end{pmatrix}e_k\right\|^2+\tfrac{h}{2}(\lambda_{1,k+1}-\lambda_{1d,k+1})^2\\
&\le -he_k^\top\left(\epsilon P-hA_{cl}^\top PA_{cl}-\tfrac{h}{2}A_{cl}^\top(k_{21}^2+(k_{22}-1)^2)A_{cl}-\tfrac{1}{2}(k_{21}^2+(k_{22}-1)^2)I_2\right)e_k\\
&\quad +2h^2+2h.
\end{aligned}\tag{5.43}$$

It is inferred from (5.43) that for sufficiently small $h>0$ and sufficiently large $\epsilon>0$, there exists a ball $\mathbb{B}_{r(h)}(0)$ centered at the origin $e=0$, with a radius proportional to h such that $V_{k+1}-V_k<0$ outside $\mathbb{B}_{r(h)}(0)$. Hence, all trajectories of (5.42) converge to this ball and remain inside it. Moreover, all the solutions are bounded for bounded initial data. Thus, the following is proved:

Proposition 5.4.3. *Consider the difference inclusion in (5.41), with bounded initial data. Assume that $h>0$, $\epsilon(k_{11},k_{12})>0$, and K are such that*

$$\epsilon P-hA_{cl}^\top PA_{cl}-\frac{h}{2}A_{cl}^\top(k_{21}^2+(k_{22}-1)^2)A_{cl}-\frac{1}{2}(k_{21}^2+(k_{22}-1)^2)I_2\succ 0,$$

then all trajectories $\{e_k\}_{k\in\mathbb{N}}$ *of the error dynamics in (5.42) are uniformly bounded and converge asymptotically to a ball* $\mathbb{B}_{r(h)}(0)$ *with* $r(h) \to 0$ *as* $h \to 0$.

For all $k \geq k^\star$, according to Lemma 5.4.1, $\tilde{u}_{2,k} = 0$, so $r\dot{\theta}_k = u^d_{2d,k}(q_k, \dot{q}_k, t_k)$. Hence, $\{\dot{\theta}_k\}_{k\geq k^\star}$ is a bounded sequence. Additionally, for $0 \leq k < k^\star$, Proposition 5.4.2 ensures that the sequence is also bounded. Thus, we have proved:

Corollary 5.4.4. *Consider the difference inclusion in (5.25) (c) (d) (e), with bounded initial data. Then, the sequence* $\{\dot{\theta}_k\}_{k\geq 0}$ *is uniformly bounded.*

Conclusion

In this chapter, frictional oscillators with pulley-belt dynamics are considered, which present challenges in the trajectory tracking problem. Hence, a new approach based on the backstepping strategy is proposed for the controller design. The stability analysis shows that the tracking error is exponentially stable and that the pulley's angle dynamics remain bounded. Then, numerical simulations are presented to analyze the robustness of the proposed approach in the cases of underestimated and overestimated friction. In addition, the controller design and the stability analysis are studied in discrete time when using Backward-Euler method for discretization.

Chapter 6

Conclusions and Perspectives

The purpose of this chapter is to provide a summary of the work presented in this thesis and to introduce some research perspectives to be tackled in the future.

6.1 Summary of Contributions

This thesis makes contributions by developing theoretical results to solve the trajectory tracking control problem in linear complementarity systems (LCS) and frictional oscillators. The roles of passivity and maximal monotonicity are crucial in the controller design and stability analysis. The thesis initially focuses on the control design and the stability analysis of the error dynamics in LCS for several cases, including the nominal case without state jumps and the case with initial and further state jumps. These results are extended to address the case with parametric uncertainties, where the boundedness of the tracking error is proved under the assumption of strong passivity. This conservative assumption is relaxed under some conditions to strict state passivity, which is particularly useful for robustness analysis in frictional oscillators.

Numerical applications such as electrical circuits with ideal diodes, mechanical systems with unilateral springs, and networks with unilateral interactions are provided with their numerical simulations to illustrate the theoretical developments. There is a specific focus in this work on electrical circuits with ideal diodes by analyzing their passivity based on different circuit designs. The numerical simulations are implemented using SICONOS platform, which is dedicated to a class of nonsmooth dynamical systems encompassing those studied in this thesis (namely, complementarity dynamical systems).

The work in this thesis progresses to deal with the challenges posed by the trajectory tracking problem in frictional oscillators. The set-valued friction model is refined by including the Stribeck effect in the model. In this case, a new approach to design the control is considered, which involves passifying the friction model. This approach allows us to ensure exponential stability of the tracking error. Then, the backstepping strategy is implemented to design the controller when the pulley-belt dynamics are included in frictional oscillators. This strategy guarantees that the tracking error converges exponentially to zero, where the stability analysis is performed in continuous time and

discrete time domains.

6.2 Research Perspectives

The results developed in this thesis provide some insights for future research work. This section explores possible research perspectives for the trajectory tracking problem in linear complementarity systems and frictional oscillators.

6.2.1 Perspectives in LCS

In the context of LCS, there are several interesting problems that require investigations and are presented as follows:

- Electrical circuits with ideal diodes are studied as numerical applications in this thesis. For future work, the diode model could be enhanced to Shockley's law model which is more realistic. This model poses new challenges for the trajectory tracking problem, including the robustness analysis of the controller in the presence of the refined diode model.

- The main focus in this work is on trajectory tracking in LCS, where a desired state x_d is defined to be tracked. A possible extension is to solve the output tracking problem in LCS, which involves tracking the output (*i.e.*, one of the complementarity variables) $w_d = Hx_d + J\lambda_d + Lu_d$. This problem could be tackled through implementing a state feedback $u = Kx + u_d$ (see *e.g.*, [126]).

- In this thesis, a critical assumption for the controller design is the availability of the state x for measurement. Relaxing this assumption opens a possible future direction, which includes implementing state observers for LCS in the closed-loop [83, 31].

6.2.2 Perspectives in frictional oscillators

This section provides further extensions to the work developed in this thesis on trajectory tracking control in frictional oscillators, as follows:

- This perspective focuses on extending the strategies developed in our work to study the trajectory tracking control in frictional oscillators with two-mass system. A concise discussion is given below on our preliminary work, including the dynamics of the system and main observations.

  If two masses m_1 and m_2 are sliding on a belt, connected one to the other with a linear spring-dashpot, with stiffness $k \geq 0$ and viscous friction coefficient $f \geq 0$, then the dynamics is given by the following, where each mass is acted upon by a force control input u_i, $i = 1, 2$.

$$\begin{cases} (a)\ \ddot{q}_1(t) \in \frac{u_1(t)}{m_1} - \frac{k}{m_1}(q_1(t) - q_2(t)) - \frac{f}{m_1}(\dot{q}_1(t) - \dot{q}_2(t)) - \mu_1 g\ \mathrm{sgn}(\dot{q}_1(t) - u_3(t)) \\ (b)\ \ddot{q}_2(t) \in \frac{u_2(t)}{m_2} - \frac{k}{m_2}(q_2(t) - q_1(t)) - \frac{f}{m_2}(\dot{q}_2(t) - \dot{q}_1(t)) - \mu_2 g\ \mathrm{sgn}(\dot{q}_2(t) - u_3(t)), \end{cases}$$

with $u_3 = r\omega$. The pulley-belt dynamics can be considered similarly as in Chapter 5. The objective is to control the gravity center of masses, while keeping the states of the masses $(q_1, \dot{q}_1)$ and $(q_2, \dot{q}_2)$ bounded. The dynamics are as follows:

$$(m_1 + m_2)\ddot{q}_c(t) \in u_1(t) + u_2(t) - \mu_1 m_1 g \operatorname{sgn}(\dot{q}_1(t) - u_3(t)) - \mu_2 m_2 g \operatorname{sgn}(\dot{q}_2(t) - u_3(t)) \tag{6.1}$$

Knowing that the sum of two maximal monotone operators is maximal monotone (see [14, Corollary 24.4]), a set-valued term is defined such that $\mathcal{F}_t(-u_3) \triangleq \mu_1 m_1 g \operatorname{sgn}(\dot{q}_1(t) - u_3) + \mu_2 m_2 g \operatorname{sgn}(\dot{q}_2(t) - u_3)$. Thus, an analogy is established between the dynamics of the gravity center of mass in (6.1) and the dynamics of frictional oscillator with one mass presented in Chapter 4. Building on this analogy, the basic idea is to mimic the control strategy developed for the nominal case in Chapter 4 in order to achieve trajectory tracking for (6.1).

- After addressing the trajectory tracking problem in the two-mass systems, an interesting future research involves extending the results obtained to frictional oscillators with n-masses (n-mass systems). This may be related to the control of the Burridge-Knopoff contact model [66].

- Oscillators with rocking blocks and stacked blocks as shown in Figure 6.1 present a natural extension of frictional oscillators. It is interesting to study trajectory tracking control in these systems due to their significant applications in seismology and mechanical engineering [152, 73].

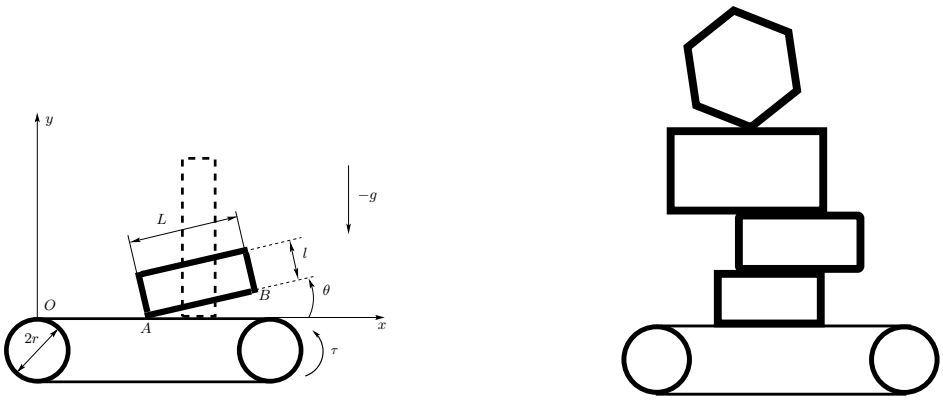

(a) (b)

Figure 6.1: Frictional oscillators with (a) rocking block, (b) stacked blocks.

Appendix

Appendix A

Useful Mathematical Results

A.1 Transformation of BMI to an LMI

The inequalities in (2.7) and (2.56) are bilinear matrix inequalities(BMIs). In order to solve these inequalities, the BMI must be reformulated to an LMI (following a classical technique, *e.g.*, [136, Example 5.5 p.136]). First, the left-hand and the right-hand sides of (2.7) are multiplied by $\begin{pmatrix} Q & 0 \\ 0 & I \end{pmatrix}$, where $Q \triangleq P^{-1}$, and let $N \triangleq KQ$. It follows that

$$\begin{pmatrix} QA^\top + AQ + N^\top E^\top + EN + \epsilon Q & B + EG - QC^\top - N^\top F^\top \\ B^\top + G^\top E^\top - CQ - FN & -D - FG - (D + FG)^\top \end{pmatrix} \preccurlyeq 0 \tag{A.1}$$

This LMI is a feasible problem and it is solved in the new variables $Q = Q^T \succ 0$, G, and N where $K = NQ^{-1}$.

A.2 Uniform and Ultimate Boundedness

The following Lyapunov-like theorem is for showing uniform boundedness and ultimate boundedness.

Theorem A.2.1. *[87, Theorem 4.18] Let $D \subset \mathbb{R}^n$ be a domain that contains the origin and $V : [0, \infty) \times D \to \mathbb{R}$ be a continuously differentiable function such that*

$$\alpha_1(\|x\|) \leq V(x) \leq \alpha_2(\|x\|)$$

$$\frac{\partial V}{\partial t} + \frac{\partial V}{\partial x}\frac{\partial x}{\partial t} \leq -W_3(x), \quad \forall \|x\| \geq \mu > 0$$

for all $t \geq 0$, for all $x \in D$, where α_1 and α_2 are class $\mathcal{K}$ functions and $W_3(\cdot)$ is a continuous positive definite function. Take $r > 0$ such that $B_r \subset D$ and suppose that,

$$\mu < \alpha_2^{-1}(\alpha_1(r))$$

Then, there exists a class $\mathcal{KL}$ function β and for every initial state $x(t_0)$, satisfying $\|x(t_0)\| \leq \alpha_2^{-1}(\alpha_1(r))$, there exists $T > 0$ (dependent on $x(t_0)$ and μ) such that the solution satisfies

$$\|x(t)\| \leq \alpha_1^{-1}(\alpha_2(r)), \quad \forall t \geq t_0 + T \tag{A.2}$$

Moreover, if $D = \mathbb{R}^n$ and α_1 belongs to class $\mathcal{K}_\infty$, then (A.2) holds for any initial state $x(t_0)$, with no restrictions on how large μ is.

A.3 Conditions for Positive (Semi) Definiteness

Lemma A.3.1. *[17, Proposition 8.2.4] Consider the matrix $M = \begin{pmatrix} Q & S \\ S^\top & R \end{pmatrix}$. Assume that $Q = Q^\top$ and $R = R^\top$. Then $M \succcurlyeq 0$ if and only if:*

1. $R \succcurlyeq 0$,
2. $SR^\dagger R = S \Leftrightarrow \mathrm{Im}(S^\top) \subseteq \mathrm{Im}(R)$,
3. $Q \succcurlyeq SR^\dagger S^\top$.

The equivalence in item 2 follows from [17, Remark after Fact 6.4.5]. The next lemma provides some necessary conditions for item 3 to hold.

Lemma A.3.2. *Assume that $Q = Q^\top \succcurlyeq 0$ and $R = R^\top \succcurlyeq 0$. Then $Q \succcurlyeq SR^\dagger S^\top$:*

1. $\Rightarrow \mathrm{Im}(Q) \supseteq \mathrm{Im}(SR^\dagger S^\top) \Longleftarrow \mathrm{Im}(Q) \supseteq \mathrm{Im}(S)$.
2. $\Rightarrow \lambda_i(Q) \geq \lambda_i(SR^\dagger S^\top)$ *for all* $i \in \{1, \ldots, n\}$, *and* $\mathrm{tr}(Q) \geq \mathrm{tr}(SR^\dagger S^\top)$ *and* $\det(Q) \geq \det(SR^\dagger S^\top) \geq 0$.

Proof. 1. From [18, Fact 7.17.24], there exists matrices L such that $Q = LL^\top$ and N such that $SR^\dagger S^\top = NN^\top$, since $R^\dagger$ is symmetric [17, Proposition 6.1.6]. From [18, Theorem 10.6.1] it follows that $LL^\top \succcurlyeq NN^\top \Rightarrow \mathrm{Im}(N) \subseteq \mathrm{Im}(L)$. Using [17, Theorem 2.4.3] we have that $\mathrm{Im}(N) = \mathrm{Im}(NN^\top)$ and $\mathrm{Im}(L) = \mathrm{Im}(LL^\top)$. The first implication is proved. Using [17, Lemma 2.4.1] we have $\mathrm{Im}(SR^\dagger S^\top) \subseteq \mathrm{Im}(S)$. The second implication is proved.

2. From [18, Theorem 10.4.9, Corollary 10.4.10].

□

Notice that $\lambda_i(SR^\dagger S^\top) = \lambda_i(NN^\top) = \sigma_i^2(N)$ (because $R^\dagger \succcurlyeq 0$), and similarly $\lambda_i(Q) = \sigma_i^2(L)$. The matrix inequality in Lemma A.3.1 item 3 can therefore be transformed into a singular values inequality, provided the matrices N and L are computed (Cholesky decomposition [18, Fact 10.10.42], or the Gram matrix decomposition [18, Fact 10.10.41] can be chosen).
An interesting result follows from [18, Theorem 10.6.2] and the same reasoning as in the proof of Lemma A.3.2 item 1: there exists $\alpha > 0$ such that $\alpha Q \succcurlyeq SR^\dagger S^\top \iff \mathrm{Im}(Q) \supseteq \mathrm{Im}(SR^\dagger S^\top)$. A first step may be to check the ranges inclusion, then to calculate an $\alpha > 0$, following the reasoning in the proof of [18, Theorem 10.6.2]: compute the matrices N and L, compute the matrix T such that $N = LT$, and compute $\alpha = \lambda_{\max}(TT^\top)$. If $\alpha \leq 1$ then Lemma A.3.1 item 3 holds true. Following the proof of [18, Theorem 10.6.2], T can be calculated.

Let us provide an excerpt of [51, Theorem 2.11], and a corollary of it. Let us recall that for a given $M \in \mathbb{R}^{n\times n}$, $||M||_{2,2}$ is the induced matricial norm such that $||M||_{2,2} = \sigma_{\max}(M)$ (the largest singular value) [17, Proposition 9.4.9], it is a submultiplicative norm [17, Corollary 9.4.12].

Theorem A.3.3. *[51] Let $M \in \mathbb{R}^{n\times n}$ be a positive definite matrix. Then every matrix*

$$A \in \{A \in \mathbb{R}^{n\times n} \mid \left|\left|\left(\tfrac{M+M^\top}{2}\right)^{-1}\right|\right|_{2,2} ||M - A||_{2,2} < 1\}$$

is positive definite.

Corollary A.3.4. *[24] Let $D = P + N$, where D, P and N are $n \times n$ real matrices, and $P \succ 0$, not necessarily symmetric. If*

$$||N||_{2,2} < \frac{1}{\| \left(\frac{P+P^\top}{2}\right)^{-1} \|_{2,2}}$$

then $D \succ 0$.

Fact A.3.5. *[67] Let $\mathbb{R}^{m\times m} \ni M = M^\top \succ 0$, $x \in \mathbb{R}^m$, $q \in \mathbb{R}^m$ and $K \subseteq \mathbb{R}^m$ be a closed nonempty convex set. Then:*

$$M(x-q) \in -\mathcal{N}_K(x) \Leftrightarrow x = \mathrm{proj}_M[K;q] \Leftrightarrow x = \operatorname*{argmin}_{z\in K} \frac{1}{2}(z-q)^\top M(z-q), \quad \text{(A.3)}$$

where proj_M is the orthogonal projection in the metric defined by M. Moreover such a x is unique.

Appendix B

Supplementary Mathematical Developments

B.1 Optimization problem in (1.11) for the example in section 2.2

In this section, the optimization problem in (1.11) is solved using KKT conditions. In this case, KKT conditions are necessary and sufficient conditions for the optimal value because the following optimization problem

$$x(t^+) = \text{argmin}_{x\in\mathcal{K}} \frac{1}{2}(x - x(t^-))^\top P(x - x(t^-)).$$

is convex knowing that $P = P^\top \succ 0$, $x(t)$ and $x(t^-) \in I\!R$. The optimization problem is solved for the two systems.

B.1.1 Desired system in (2.23)

It is required to find $x_d(t^+)$ which is the optimal value to minimize the following

$$\begin{aligned} f_d(x_d) &= \min \tfrac{1}{2}(x_d - x_d^-)^2 \\ \text{s.t. } & x_d \in \mathcal{K}_d \end{aligned}$$

where $P = 1$ and $\mathcal{K}_d = \{x_d \in I\!R \mid cx_d + u_{2d}(t^+) \geq 0\} = \{x_d \in I\!R \mid -cx_d - u_{2d}^+ \leq 0\}$. Let us write the Lagrangian function of the minimization problem

$$\mathcal{L}(x_d, \mu) = \frac{1}{2}(x_d - x_d^-)^2 - \mu(-cx_d - u_{2d}^+)$$

where μ is the lagrangian multiplier. Let us state KKT conditions to be satisfied:

$$\begin{cases} \frac{\partial \mathcal{L}}{\partial x_d} = 0 \Leftrightarrow x_d - x_d^- + c\mu = 0 \Leftrightarrow x_d = x_d^- - c\mu \\ \mu(-cx_d - u_{2d}^+) = 0 \Leftrightarrow \mu(c^2\mu - cx_d^- - u_{2d}^+) = 0 \\ \mu \leq 0 \\ -cx_d - u_{2d}^+ \leq 0 \Leftrightarrow c^2\mu - cx_d^- - u_{2d}^+ \leq 0 \end{cases}$$

KKT conditions are written in the form of a LCP:

$$0 \leq -\mu \perp -c^2\mu + cx_d^- + u_{2d}^+ \geq 0$$

The LCP(c^2, $cx_d^- + u_{2d}^+$) has a unique solution defined by:

$$-\mu = \begin{cases} 0 & \text{if } cx_d^- + u_{2d}^+ \geq 0 \\ -\frac{1}{c}x_d^- - \frac{1}{c^2}u_{2d}^+ & \text{if } cx_d^- + u_{2d}^+ < 0 \end{cases}$$

Let us substitute the values of the solution in the KKT condition $\frac{\partial \mathcal{L}}{\partial x_d} = 0$ to calculate x_d as follows:

$$x_d = \begin{cases} x_d^- & \text{if } cx_d^- + u_{2d}^+ \geq 0 \\ -\frac{1}{c}u_{2d}^+ & \text{if } cx_d^- + u_{2d}^+ < 0 \end{cases} \tag{B.1}$$

B.1.2 Closed-loop system in (2.25)

It is required to find the optimal value $x(t^+)$ in order to minimize the following

$$\begin{gathered} f(x) = \min \tfrac{1}{2}(x - x^-)^2 \\ \text{s.t. } x \in \mathcal{K} \end{gathered}$$

where $\mathcal{K} = \{x \in I\!R \mid (c+k_3)x - k_3x_d(t^+) + u_{2d}(t^+) \geq 0\} = \{x \in I\!R \mid -(c+k_3)x + k_3x_d(t^+) - u_{2d}(t^+) \leq 0\}$. Let us write the Lagrangian function

$$\mathcal{L}(x,\mu) = \frac{1}{2}(x-x^-)^2 - \mu\left(-(c+k_3)x + k_3x_d^+ - u_{2d}^+\right)$$

The necessary and sufficient conditions to be satisfied are the following:

$$\begin{cases} \frac{\partial \mathcal{L}}{\partial x} = 0 \Leftrightarrow x - x^- + \mu(c+k_3) = 0 \Leftrightarrow x = x^- - \mu(c+k_3) \\ \mu\left(-(c+k_3)x + k_3x_d^+ - u_{2d}^+\right) = 0 \Leftrightarrow \mu\left(-(c+k_3)x^- + \mu(c+k_3)^2 + k_3x_d^+ - u_{2d}^+\right) = 0 \\ \mu \leq 0 \\ -(c+k_3)x + k_3x_d^+ - u_{2d}^+ \leq 0 \Leftrightarrow -(c+k_3)x^- + \mu(c+k_3)^2 + k_3x_d^+ - u_{2d}^+ = 0 \end{cases}$$

KKT conditions are written in the form of a LCP as:

$$0 \leq -\mu \perp -(c+k_3)^2\mu + (c+k_3)x^- - k_3x_d^+ + u_{2d}^+ \geq 0$$

The LCP$\left((c+k_3)^2, (c+k_3)x^- - k_3x_d^+ + u_{2d}^+\right)$ has a unique solution defined by:

$$-\mu = \begin{cases} 0 & \text{if } \quad (c+k_3)x^- - k_3x_d^+ + u_{2d}^+ \geq 0 \\ -\frac{1}{(c+k_3)}x^- + \frac{k_3}{(c+k_3)^2}x_d^+ - \frac{1}{(c+k_3)^2}u_{2d}^+ & \text{if } (c+k_3)x^- - k_3x_d^+ + u_{2d}^+ < 0 \end{cases}$$

Let us substitute the values of the solution in the KKT condition $\frac{\partial \mathcal{L}}{\partial x} = 0$ to calculate x as follows:

$$x = \begin{cases} x^- & \text{if } (c+k_3)x^- - k_3x_d^+ + u_{2d}^+ \geq 0 \\ -\frac{k_3x_d^+ - u_{2d}^+}{(c+k_3)} & \text{if } (c+k_3)x^- - k_3x_d^+ + u_{2d}^+ < 0 \end{cases}$$

B.2 Proof of the DI in (2.16)

Let us remind the transformation of an LCP into a differential inclusion of the first-order sweeping process (FOSwP) with perturbation type, as proposed in [37, 22, 38]. It is assumed that the constraint qualification stated after (2.16) holds true. Recall the closed-loop system in (2.3) with $D = 0$ and $G = 0$ as follows:

$$\begin{cases} \dot{x}(t) = (A + EK)x(t) + B\lambda(t) - EKx_d(t) + Eu_d(t) \\ 0 \leq \lambda(t) \perp w(t) = (C + FK)x(t) - FKx_d(t) + Fu_d(t) \geq 0 \end{cases} \tag{B.2}$$

As a result of convex analysis, the linear complementarity problem (LCP) is written in the form of a differential inclusion DI as follows:

$$0 \leq w \perp \lambda \geq 0 \Leftrightarrow w \in -\mathcal{N}_{\mathbb{R}^m_+}(\lambda) \Leftrightarrow \lambda \in -\mathcal{N}_{\mathbb{R}^m_+}(w)$$

By applying this property to the LCP in (B.2), then

$$\lambda(t) \in -\mathcal{N}_{\mathbb{R}^m_+}\left((C + FK)x(t) - FKx_d(t) + Fu_d(t)\right) \;\Leftrightarrow\; \lambda(t) \in -\mathcal{N}_{S(t)}\left((C + FK)x(t)\right)$$

where $S(t) = \left\{v \in \mathbb{R}^m_+ \mid v - FKx_d(t) + Fu_d(t) \in \mathbb{R}^m_+\right\}$. Given that the quadruple of the closed-loop system $(A+EK, B, C+FK, 0)$ is strictly passive, then $PB = (C+FK)^\top$ for some $P = P^\top \succ 0$. The closed-loop system in (B.2) is written as DI:

$$\dot{x} \in (A + EK)x(t) - B\mathcal{N}_{S(t)}\left((C + FK)x(t)\right) - EKx_d(t) + Eu_d(t) \tag{B.3}$$

Let $R^2 = P$ such that $R = R^\top \succ 0$ and $\zeta = Rx$, then the DI in (B.3) is written as:

$$\dot{\zeta}(t) = R\dot{x}(t) \in R(A+EK)R^{-1}\zeta(t) - RB\mathcal{N}_{S(t)}\left((C + FK)R^{-1}\zeta(t)\right) - REKx_d(t) + REu_d(t) \tag{B.4}$$

But

$$RB = R^{-1}PB = R^{-1}(C + FK)^\top$$

By using the following property from the convex analysis (the chain rule):

$$M^\top \mathcal{N}_{S(t)}(Mx) = \mathcal{N}_{\phi(t)}(x)$$

where $\phi(t) = \{z \mid Mz \in S(t)\}$. Then,

$$R^{-1}(C + FK)^\top \mathcal{N}_{S(t)}\left((C + FK)R^{-1}\zeta(t)\right) = \mathcal{N}_{\phi(t)}(\zeta(t))$$

where $\phi(t) = \{Rx \mid (C + FK)x(t) \in S(t)\}$. Thus, the differential inclusion DI in (B.4) is written as follows:

$$\dot{\zeta} \in R(A + EK)R^{-1}\zeta(t) + R\left(-EKx_d(t) + Eu_d(t)\right) - \mathcal{N}_{\phi(t)}(\zeta(t))$$

Appendix C

Numerical Simulations and Computations

C.1 Numerical Simulations with SICONOS

SICONOS is an open-source software that aims to provide objects and functions for modeling and simulating Non-smooth Dynamical Systems (NSDS). Dynamical systems with non-smooth time evolution are called NSDS and they have a large field of applications such as mechanical systems, electrical circuits, and robotics. The user can build simulations with SICONOS using C_{++} programs or Python scripts. The two main points of any SICONOS simulation is to build the Model that describes the NSDS and then to define the simulation strategy to be used in order to simulate it during a given period of time. Thus, a good understanding of the structure of SICONOS is necessary to build and simulate a non-smooth problem. In the following, a concise description is provided about the main steps required to model and simulate LCS in (1.1), as performed in this thesis.

C.1.1 Modelling

Consider the LCS in (1.1), then the first step is to define the Model. Our system is defined by a class inherited from the `DynamicalSystem` class, represented as follows:

`FirstOrderLinearTIDS`. This class describes the first order linear time-invariant dynamical system as:

$$M\dot{x}(t) = Ax(t) + b + r$$

with M is $n \times n$ for $n-$dimensional system, b is the exogeneous input and r is the input due to the non-smooth behaviour. The matrix M is considered an identity matrix by default.

The simulations of the electrical circuits, the unilateral network, and the mechanical frictional oscillator with Coulomb friction fit in this formalism in Chapter 3 and sections 4.4.3 and 4.5.3 in Chapter 4. The corresponding part of the code:

```
class my_dynamics(sk.FirstOrderLinearTIDS):
    ndof =  # number of states
    x0 = np.zeros(ndof)           #the initial state
    A = np.zeros((ndof, ndof))    #initialize the matrix A
    b0 = np.zeros(ndof)           #initialize the vector b0

    def __init__(self):
        super().__init__(self.x0, self.A, self.b0)
  # A is empty and will be updated at each time step with a call to computeA.
    def computeA(self, time):
        # Define the matrix A here

    def computeb(self, time):
        # Define b ≙ Eu_d in this function
```

It is important to note that the vector r defines the non-smooth relation in the dynamical system which corresponds to $B\lambda$ in our LCS and is defined later in the relation.

The numerical simulation implemented for the Stribeck effect in section 4.6 uses a different class for modeling which is defined as:

`FirstOrderNonLinearDS`. This class describes the nonlinear first order dynamical system as:

$$M\dot{x}(t) = f(t, x(t), z) + r$$

where $f(t, x, z)$ is the smooth vector field and $z \in \mathbb{R}^s$ is a set of discrete states, and it is taken to be zero in our work. To simulate this type of system, the Jacobian $\nabla_x f(t, x, z)$ must be provided explicitly in the code. More information is given in the documentation [1] about modeling NSDS under the class `DynamicalSystem` in SICONOS.

The second part for modeling in SICONOS is the interaction. The object `Interaction` describes the link between dynamical systems and it is composed of the `Relation` and the `NonSmoothLaw` which will be illustrated below. The class `Relation` is introduced to define the mapping between these local variables. In this thesis, we mainly used the following class:

`FirstOrderLinearR`. First order linear and time invariant relations:

$$\begin{aligned} y &= C(t, z)x + D(t, z)\lambda + e(t) \\ r &= B(t, z)\lambda \end{aligned}$$

where C, D and B represent the same matrices as in the LCS (1.1). The vector e is considered as the exogeneous input to the signal Fu_d.

[1] https://nonsmooth.gricad-pages.univ-grenoble-alpes.fr/siconos/users_guide/dynamical_systems.html

```
class my_relation(sk.FirstOrderLinearR):
    # There is a function defined called compute_K0G0()
    #that solves the LMI and returns
    #the values of the control gains K_0 and G_0
    def __init__(self, K_0, G_0):
        # Initialize operators
        C = np.zeros((, ))  # Define dimensions for C

        D = np.zeros((, ))  # Define dimensions for D

        B = np.zeros((, ))  # Define dimensions for B

        e = np.zeros(())  # Define dimensions for e

        # Initialize relation with operators
        super(my_relation, self).__init__(C, B)

        # Set pointers for D and e
        self.setDPtr(D)
        self.setePtr(e)

    def computeC(self, time, z, C):
        # Define matrix C here

    def computeB(self, time, z, B):
        # Define matrix B here

    def computeD(self, time, z, D):
        # Define matrix D here

    def computee(self, time, z, e):
        # Define Fu_d here

    #Define the output y due to the non-smooth behaviour
    def computeh(self, time, x, ll, z, y):
        self.computeC(time, z, self.C())
        np.matmul(self.C(), x, y)
        self.computeD(time, z, self.D())
        self.computee(time, z, self.e())
        y[...] += np.matmul(self.D(), ll) + self.e()

 #Define the input r due to the non-smooth behaviour
    def computeg(self, time, ll, z, r):
        self.computeB(time, z, self.B())
        r[...] += np.matmul(self.B(), ll)
```

For the simulation of frictional oscillator in the presence on Stribeck effect in section 4.6, another relation is used:

`FirstOrderNonLinearR.` This is the standard first order nonlinear relation:

$$y = h(t, x, \lambda, z)$$
$$r = g(t, \lambda, x, z)$$

In this case, the functions h and g and their jacobians according to x and λ (*i.e.*, $\nabla_x h$, $\nabla_\lambda h$, $\nabla_x g$ and $\nabla_\lambda g$ are explicitly defined with some plug-in functions. More information about the class `Relations` is given in the documentation [2] for SICONOS.

In the final step of modeling, it is required to define your non-smooth law which describes the mapping between y and λ. In our simulation, the non-smooth law is defined by the complementarity problem in (1.1)(b). In SICONOS, it is defined by the class:

[2] https://nonsmooth.gricad-pages.univ-grenoble-alpes.fr/siconos/users_guide/relations.html

`ComplementarityConditionNSL`. It is a class which models the following complementarity conditions:

$$0 \leq y \perp \lambda \geq 0$$

The corresponding code is given by

```
# Create interactions
relation = ex.my_relation(K_0, G_0)

# Declare a nonsmooth law.
# Its size must match the size of the system,
# defining the constraints
# i.e., the length of y and lambda vectors of the relation.
nslaw = sk.ComplementarityConditionNSL(2)
inter = sk.Interaction(nslaw, relation)
```

C.1.2 Integration of the Dynamics

In this section, the Moreau-Jean's time stepping scheme used to integrate the dynamics over a time-step is presented. This method involves the time-discretization of the entire system including the dynamics, the relations, and the non-smooth law. The integration of the ODE of the first order nonlinear system over the interval $[t_k, t_{k+1}]$ results in:

$$\int_{t_k}^{t_{k+1}} \dot{x}dt = \int_{t_k}^{t_{k+1}} f(t, x, z)dt + \int_{t_k}^{t_{k+1}} rdt$$

The left-hand side is equivalent to $x_{k+1} - x_k$ and the terms in the right-hand side are approximated using θ-method, specifically implicit Euler method, as follows:

$$\begin{aligned} \textstyle\int_{t_k}^{t_{k+1}} f(t, x, z)dt &\approx h\theta f(t_{k+1}, x_{k+1}, z) + h(1-\theta)f(t_k, x_k, z) \\ &\approx h\theta f_{k+1} + h(1-\theta)f_k \end{aligned}$$

where $\theta \in [0, 1]$, and the other approximation is

$$\int_{t_k}^{t_{k+1}} rdt \approx hr_{k+1}$$

This discretization scheme is applied directly to the ODE presented in the LCS in (1.1) and gives the following:

$$x_{k+1} - x_k = h\theta Ax_{k+1} + hA(1-\theta)x_k + hB\lambda_{k+1} + hE\theta u_{k+1} + hE(1-\theta)u_k$$

Assume that $W \triangleq (1 - hA\theta)$ which is invertible, then

$$x_{k+1} = x_k + hW^{-1}Ax_k + hW^{-1}B\lambda_{k+1} + hEW^{-1}\left(\theta u_{k+1} + (1-\theta)u_k\right)$$

The non-smooth law is discretized as follows:

$$0 \leq y_{k+1} \perp \lambda_{k+1} \geq 0$$

which is equivalent to

$$0 \leq M\lambda_{k+1} + q_{k+1} \perp \lambda_{k+1} \geq 0 \tag{C.1}$$

The LCP in (1.1)(b) approximated according to this time-stepping scheme as:

$$0 \leq Cx_{k+1} + D\lambda_{k+1} + Fu_{k+1} \perp \lambda_{k+1} \geq 0$$

which fits with the LCP given by (C.1) after substituting x_{k+1} obtained before with

$$\begin{aligned} M &= hCW^{-1}B + D \\ q_{k+1} &= CW^{-1}(1 + hA)x_k + hEW^{-1}C\left(\theta u_{k+1} + (1-\theta)u_k\right) + Fu_{k+1} \end{aligned}$$

C.2 Numerical computation of state-jump times in (3.25)

Let us check numerically that the state jumps and the state-jump times are independent of the matrix solution of the passivity LMI, as predicted by theoretical arguments [43, 37, 75]. It is also shown in [75] that the event-capturing time-stepping Moreau-Jean scheme that is implemented in the SICONOS software package, does approximate this state-jump rule. Hence the numerical results obtained from SICONOS can be taken as the correct state-jump times when the chosen time-step is small enough.

For the desired system:

Knowing that at the time of discontinuity $t = 1$, the values of the desired state from simulation in Figure 3.18 at $t = 1^-$ is given by the numerical solver SICONOS as follows:

$$x_d(1^-) = \begin{pmatrix} 3.4615397 \\ -1.832126 \\ 0.238885 \\ 2.91881 \end{pmatrix}$$

In order to calculate the values of the states at $t = 1^+$, the optimization problem in (1.11) is solved using MOSEK solver with $P = P_d$ which is the solution of the LMI for the passivity of the desired system in (1.8). We solved the optimization problem for different values of the solution P_d (*i.e.,* the solution P_d is not unique). The results is obtained below:

Values of P_d	Values of $x_d(1^+)$
$P_{d1} = \begin{pmatrix} 1.2165869 & 1.1915869 & 0 & -1.1915867 \\ 1.1915869 & 1.2165866 & 0 & -1.191587 \\ 0 & 0 & 0.02499 & 0 \\ -1.1915867 & -1.191587 & 0 & 1.2165868 \end{pmatrix}$	$\begin{pmatrix} 3.4615397 \\ -1.832121 \\ 10 \\ 2.91881 \end{pmatrix}$
$P_{d2} = \begin{pmatrix} 0.9388826 & 0.9138827 & 0 & -0.9138835 \\ 0.9138827 & 0.9388826 & 0 & -0.9138835 \\ 0 & 0 & 0.024999 & 0 \\ 0.9138835 & -0.9138835 & 0 & 0.9388818 \end{pmatrix}$	$\begin{pmatrix} 3.4615397 \\ -1.832126 \\ 10 \\ 2.91881 \end{pmatrix}$
$P_{d3} = \begin{pmatrix} 0.016668 & -0.008336 & 0 & 0.008332 \\ -0.008336 & 0.016673 & 0 & 0.008336 \\ 0 & 0 & 0.025 & 0 \\ 0.008332 & 0.008336 & 0 & 0.016668 \end{pmatrix}$	$\begin{pmatrix} 3.4615397 \\ -1.832126 \\ 10 \\ 2.91881 \end{pmatrix}$

It is noteworthy that the different values P_{d1}, P_{d2} and P_{d3} comes from solving the BMI in (1.8), after being transformed into LMI as in Appendix A.1, using MOSEK, CVXOPT and SCS solvers respectively. The numerical solver SICONOS computes the jump automatically and gives $x_d(1^+) = \begin{pmatrix} 3.499868 \\ -1.798264 \\ 10 \\ 2.932387 \end{pmatrix}$ when the time step $h = 0.001$ as well as $x_d(1^+) = \begin{pmatrix} 3.466 \\ -1.834 \\ 10 \\ 2.92 \end{pmatrix}$ when the time step $h = 0.00001$.

For the closed-loop system:

At the time of discontinuity $t = 1$, the value of the closed-loop state is given by:

$$x(1^-) = \begin{pmatrix} 3.391813 \\ -2.0267 \\ 0.723447 \\ 3.42975 \end{pmatrix}$$

The value of the state jump is the solution of the optimization problem in (1.11). The table below shows the values of $x(1^+)$ for different value of the storage function matrix P being the solution of BMI in (4.10) for strict passivity.

Values of P	Values of $x(1^+)$
$P_1 = \begin{pmatrix} 0.029 & 0.001 & -0.006 & -0.004 \\ 0.001 & 0.033 & 0.016 & 0.001 \\ -0.006 & 0.016 & 0.032 & 0.01 \\ -0.004 & 0.001 & 0.01 & 0.0304 \end{pmatrix}$	$\begin{pmatrix} 3.397125 \\ -2.0267 \\ 9.9417 \\ 3.431 \end{pmatrix}$
$P_2 = \begin{pmatrix} 0.04589 & 0.006245 & -0.005963 & -0.006264 \\ 0.006245 & 0.03969 & 0.015618 & -0.001698 \\ -0.005963 & 0.015618 & 0.032439 & 0.009719 \\ -0.006264 & -0.001698 & 0.009719 & 0.034227 \end{pmatrix}$	$\begin{pmatrix} 3.3952 \\ -2.0269 \\ 9.9415 \\ 3.431 \end{pmatrix}$
$P_3 = \begin{pmatrix} 0.03844 & 0.00339 & -0.00596 & -0.00489 \\ 0.00399 & 0.03742 & 0.01562 & 0 \\ -0.005963 & 0.015618 & 0.032439 & 0.009719 \\ -0.00489 & 0 & 0.009719 & 0.03262 \end{pmatrix}$	$\begin{pmatrix} 3.3958 \\ -2.0268 \\ 9.9415 \\ 3.431 \end{pmatrix}$

The numerical solver SICONOS computes the jump automatically and gives $x(1^+) = \begin{pmatrix} 3.4299 \\ -1.9915 \\ 9.9262 \\ 3.4462 \end{pmatrix}$ when the time step $h = 0.001$ as well as $x(1^+) = \begin{pmatrix} 3.3986 \\ -2.029 \\ 9.93 \\ 3.4233 \end{pmatrix}$ when the time step $h = 0.00001$.

According to the results shown above, the value of the jump in the desired state and closed-loop state x_d and x respectively given by SICONOS converges to the value of the jump which is the solution of the optimization problem in (1.11) as the time step $h \to 0$ [75, Definition 8].

Appendix D

Electrical Circuits' Dynamics

Let us recall some useful mathematical relations between the voltage V and the current i of the electrical components $\mathbf{R}$, $\mathbf{C}$ and $\mathbf{L}$ as follows:

- For the resistor, let us recall Ohm's Law: $V_{\mathbf{R}} = \mathbf{R}i_{\mathbf{R}}$ where $\mathbf{R}$ is the resistance of the resistor.
- For the capacitor, we have the relations: $Q_{\mathbf{C}} = \mathbf{C}V_{\mathbf{C}}$ where $\mathbf{C}$ is the capacitance and $Q_{\mathbf{C}}$ is the charge on the capacitor and $\dot{Q}_{\mathbf{C}} = i_{\mathbf{C}}$
- For the inductor, the relation is $V_{\mathbf{L}} = \mathbf{L}\frac{di_{\mathbf{L}}}{dt}$ where $\mathbf{L}$ is the inductance of the inductor.

Circuit in Figure 3.1

Recall that the state x_1 is the charge on the capacitor and the state x_2 is the current passing through the inductor. By applying KVL (Kirchhoff's Voltage Law) we can write the following equations:

$$-u + V_{\mathbf{C}} - V_{\mathbf{L}} = 0 \Leftrightarrow -u + \frac{x_1}{\mathbf{C}} - \mathbf{L}\dot{x}_2 = 0 \Leftrightarrow \dot{x}_2 = \frac{1}{\mathbf{LC}}x_1 - \frac{u}{\mathbf{L}}$$

$$-V_{\mathbf{C}} - V_{\mathbf{R}} + w = 0 \Leftrightarrow -\frac{x_1}{\mathbf{C}} - \mathbf{R}\lambda + w = 0 \Leftrightarrow w = \frac{x_1}{\mathbf{C}} + \mathbf{R}\lambda$$

Let us apply KCL (Kirchhoff's Current Law) at the point of connection between the capacitor $\mathbf{C}$ and the voltage source u, then:

$$i_{\mathbf{C}} + i_{\mathbf{L}} = i_{\mathbf{R}} \Leftrightarrow \dot{x}_1 + x_2 = \lambda \Leftrightarrow \dot{x}_1 = -x_2 + \lambda$$

The equations derived, along with the complementarity relation (*i.e.*, $0 \leq \lambda \perp w \geq 0$), are consistent with the LCS in (3.1).

Circuit in Figure 3.7

Recall that the state x_1 is the charge on the capacitor and the state x_2 is the current passing through the inductor. By applying KVL for the lower loop of the circuit, then:

$$V_{\mathbf{R}} = V_{\mathbf{L}} + u_2$$

Now, let us apply KVL for the upper loop of the circuit, then:

$$u_1 + V_{\mathbf{C}} - \lambda + V_{\mathbf{R}} = 0 \quad \Leftrightarrow u_1 + V_{\mathbf{C}} - \lambda + V_{\mathbf{L}} + u_2 = 0$$

$$\Leftrightarrow L\dot{x}_2 = -\tfrac{x_1}{\mathbf{C}} + \lambda - u_1 - u_2$$

By applying KCL at any node, then:

$$i_{\mathbf{C}} = i_{\mathbf{R}} + i_{\mathbf{L}} \Leftrightarrow \dot{x}_1 = -\frac{x_1}{\mathbf{RC}} + x_2 + \frac{\lambda}{\mathbf{R}} - \frac{u_1}{\mathbf{R}}$$

Given from the circuit that $i_{\mathbf{C}} = w$, then we can have the equation of the complementaity variable. Thus, the dynamics of the LCS in (3.7) are recovered.

Circuit in Figure 3.12

Recall that the states x_1, x_2, x_3 and x_4 are the voltages across the capacitors $\mathbf{C}_1$, $\mathbf{C}_2$, $\mathbf{C}_3$ and $\mathbf{C}_4$ respectively, and that $\mathbf{C}_1 = \mathbf{C}_2 = \mathbf{C}_3 = \mathbf{C}_4 = \mathbf{C}$.
The current passing through $\mathbf{C}_1$ is $C\dot{x}_1$ where $C\dot{x}_1 = i_1 = \lambda_1$. Let us apply KCL on the node connection the two resistors $\mathbf{R}$ and $\mathbf{C}_4$, then:

$$i_1 = i_4 + i_{\mathbf{R}} \Leftrightarrow \lambda_1 = C\dot{x}_4 + \frac{V_{\mathbf{R}}}{\mathbf{R}}$$

Given that: $V_{\mathbf{R}} = x_1 + x_2 + x_3$ by applying KVL on the second (*i.e.*, right-handed) loop, hence:

$$C\dot{x}_4 = \frac{-x_1 - x_2 - x_3}{\mathbf{R}} + \lambda_1$$

Now, let us apply KCL on the node that connects between $\mathbf{C}_1$, $\mathbf{C}_2$, and $\mathbf{C}_4$, then:

$$i_4 = i_1 + i_2 \Leftrightarrow C\dot{x}_4 = \lambda_1 + C\dot{x}_2$$

By substituting the dynamics of x_4, the dynamics of x_2 is written as:

$$C\dot{x}_2 = \frac{-x_2 - x_3 - x_4}{\mathbf{R}}$$

Let us apply KCL again on the node connecting $\mathbf{C}_2$, $\mathbf{C}_3$, and the second diode, the dynamics of x_3 are obtained as follows:

$$i_2 + \lambda_2 = i_3 \Leftrightarrow C\dot{x}_3 = \frac{-x_2 - x_3 - x_4}{\mathbf{R}} + \lambda_2$$

For the LCP, the capacitor $\mathbf{C}_3$ is connected in parallel with the second diode, hence

$$w_2 = x_3$$

By applying KVL on the first (*i.e.*, left-handed) loop, thus:

$$V_{\mathbf{R}} - u - w_1 + V_{\mathbf{C}_1} + V_{\mathbf{C}_4} = 0 \Leftrightarrow w_1 = R\lambda_1 - u + x_1 + x_4$$

The dynamics derived, along with the complementarity equations which satisfy $0 \leq \lambda \perp w \geq 0$, allows us to write the LCS in (3.16).

Circuit in Figure 3.19

Recall that x_1 is the current passing through the inductor $\mathbf{L}$, x_2 is the voltage across the capacitor $\mathbf{C}_1$, x_3 is the voltage across the capacitor $\mathbf{C}_2$, $\lambda(t) \triangleq (i_{DF1},\ i_{DR1},\ -v_{DF2},\ i_{DR2})^\top$, and $w(t) \triangleq (-v_{DF1},\ -v_{DR1},\ i_{DF2},\ -v_{DR2})^\top$.
By applying KVL in the **LC** loop, we have: $V_{\mathbf{C}_1} = V_{\mathbf{L}}$, then $x_2 = L\dot{x}_1$. Given that $i_{\mathbf{R}} = \frac{V_{\mathbf{R}}}{\mathbf{R}} = \frac{x_3}{\mathbf{R}}$, let us apply KCL at the node connecting D_{F_1}, D_{R_1} and the output load, then:

$$i_{D_{R_1}} + i_{D_{F_1}} = i_{\mathbf{R}} + i_{\mathbf{C}_2} \Leftrightarrow \mathbf{C}_2\dot{x}_3 = \lambda_1 + \lambda_2 - \frac{x_3}{\mathbf{R}}$$

Another KCL is applied at the node connecting D_{F_2}, D_{R_2} with the output load, hence:

$$i_{D_{R_2}} + i_{D_{F_2}} = i_{\mathbf{R}} + i_{\mathbf{C}_2} \Leftrightarrow w_3 + \lambda_4 = \lambda_1 + \lambda_2$$

In order to derive the dynamics of x_2, let us apply KCL at the node connecting D_{F_2}, D_{R_1} and the input load, then:

$$i_{D_{R_1}} = i_{D_{F_2}} + i_{\mathbf{L}} + i_{\mathbf{C}_1} \Leftrightarrow \mathbf{C}_1\dot{x}_2 = -x_1 - w_3 + \lambda_2 \Leftrightarrow \mathbf{C}_1\dot{x}_2 = -x_1 - \lambda_1 + \lambda_4$$

If we apply KVL in the loop of D_{F_2}, D_{R_1} and $\mathbf{C}_2$, then: $w_2 = x_3 - \lambda_3$. Another KVL in the loop of $\mathbf{C}_1$, u, D_{F_1}, and D_{R_1}, the following is derived:

$$V_{\mathbf{C}_1} + w_1 - w_2 + u = 0 \Leftrightarrow w_1 = -x_2 + x_3 - \lambda_3 - u$$

For the equation of w_4, let us apply KVL in the loop of D_{F_1}, D_{R_2}, and $\mathbf{C}_2$, then: $w_4 = \lambda_3 + x_2 + u$.
From the dynamics derived above, and the equations of the complementarity variables that satisfy $0 \leq \lambda \perp w \geq 0$, the LCS in (3.30) is obtained.

Bibliography

[1] V. Acary and B. Brogliato. *Numerical Methods for Nonsmooth Dynamical Systems: Applications in Mechanics and Electronics*. Vol. 35. Springer Verlag, 2008, p. 526.

[2] V. Acary, B. Brogliato, and Y. Orlov. "Chattering-free digital sliding-mode control with state observer and disturbance rejection". In: *IEEE Transactions on Automatic Control* 57.5 (2012), pp. 1087–1101.

[3] Vincent Acary et al. *An introduction to Siconos*. Technical Report RT-0340. INRIA, Nov. 2019, p. 97. URL: https://inria.hal.science/inria-00162911.

[4] K. Addi, B. Brogliato, and D. Goeleven. "A qualitative mathematical analysis of a class of variational inequalities via semi-complementarity problems. Applications in electronics". In: *Mathematical Programming* 126 (2011), pp. 31–67. DOI: 10.1007/s10107-009-0268-7.

[5] S. Adly, D. Goeleven, and R. Oujja. "Well-posedness of nonsmooth Lurie dynamical systems involving maximal monotone operators". In: *Mathematical Analysis in Interdisciplinary Research*. Ed. by I.N. Parasidis, E. Provids, and T.M. Rassias. Vol. 179. Springer International Publishing, 2021.

[6] S. Adly, H. Hantoute, and B.K. Le. "Nonsmooth Lur'e dynamical systems in Hilbert space". In: *Set-Valued and Variational Analysis* 24 (2016), pp. 13–35.

[7] U. Andreaus and P. Casini. "Dynamics of friction oscillators excited by a moving base and/or driving force". In: *Journal of Sound and Vibration* 245 (2001), pp. 685–699. DOI: 10.1006/jsvi.2000.3555.

[8] D. Angeli. "A Lyapunov approach to incremental stability properties". In: *IEEE Transactions on Automatic Control* 47.3 (2002), pp. 410–421. DOI: 10.1109/9.989067.

[9] MOSEK ApS. *MOSEK Optimizer API for Python*. 2023. URL: https://docs.mosek.com/10.1/pythonapi.pdf.

[10] Ch. E. Arroud and G. Colombo. "A Pontryagin maximum principle for the controlled sweeping process". In: *Set-Val. Var. Anal.* 26 (2018), pp. 607–629.

[11] A. Aydinoglu et al. "Stabilization of complementarity systems via contact-aware controllers". In: *IEEE Transactions on Robotics* 38.3 (2022), pp. 1735–1754.

[12] M. Barreau, S. Tarbouriech, and F. Gouaisbaut. "Lyapunov stability analysis of a mass–spring system subject to friction". In: *Systems and Control Letters* 150 (2021), p. 104910.

[13] J. Bastien, M. Schatzman, and C. Lamarque. "Study of an elastoplastic model with an infinite number of internal degrees of freedom". In: *European Journal of Mechanics - A/Solids* 21.2 (2002), pp. 199–222.

[14] H.H. Bauschke and P.L. Combettes. *Convex Analysis and Monotone Operator Theory in Hilbert Spaces*. Canadian Mathematical Society–Société mathématique du Canada. Springer Science+Business Media, 2011.

[15] E.J. Berger. "Friction modeling for dynamic system simulation". In: *Applied Mechanics Reviews* 55.6 (Oct. 2002), pp. 535–577.

[16] M. di Bernardo et al. *Piecewise-smooth Dynamical Systems. Theory and Applications*. Applied Mathematical Sciences 163. London: Springer-Verlag, 2008.

[17] D.S. Bernstein. *Matrix Mathematics. Theory, Facts and Formulas*. 2nd Ed. Princeton Univ. Press, 2009.

[18] D.S. Bernstein. *Scalar, Vectors, and Matrix Mathematics. Theory, Facts and Formulas*. 3rd Ed. Princeton Univ. Press, 2018.

[19] S. Bhat and D. Bernstein. "Finite-Time Stability of Continuous Autonomous Systems". In: *SIAM Journal on Control and Optimization* 38.3 (2000), pp. 751–766. URL: https://doi.org/10.1137/S0363012997321358.

[20] B. Biemond and N. van de Wouw. "Tracking control for hybrid systems with state-triggered jumps". In: *IEEE Transactions on Automatic Control* 58.4 (2012), pp. 876–890.

[21] J.M. Bourgeot and B. Brogliato. "Tracking Control of Complementarity Lagrangian Systems". In: *International Journal of Bifurcation and Chaos* 15.6 (2005), pp. 1839–1866.

[22] B. Brogliato. "Absolute stability and the Lagrange–Dirichlet theorem with monotone multivalued mappings". In: *Systems and Control Letters* 51.5 (2004), pp. 343–353.

[23] B. Brogliato. "Dissipative dynamical systems with set-valued feedback loops: Well-posed set-valued Lur'e dynamical systems". In: *IEEE Control Systems* 42.3 (2022), pp. 93–114.

[24] B. Brogliato. "Kinetic quasi-velocities in unilaterally constrained Lagrangian mechanics with impacts and friction". In: *Multibody System Dynamics* 32 (2014), pp. 175–216.

[25] B. Brogliato. "Modeling, analysis and control of robot–object nonsmooth underactuated Lagrangian systems: A tutorial overview and perspectives". In: *Annual Reviews in Control* 55 (2023), pp. 297–337.

[26] B. Brogliato. *Nonsmooth Mechanics. Models, Dynamics, and Control*. 3rd. Communications and Control Eng. Springer Int. Pub. Switzerland, 2016.

[27] B. Brogliato. "Some perspectives on the analysis and control of complementarity systems". In: *IEEE Transactions on Automatic Control* 48.6 (2003), pp. 918–935.

[28] B. Brogliato and D. Goeleven. "Existence, uniqueness of solutions and stability of nonsmooth multivalued Lur'e dynamical systems". In: *Journal of Convex Analysis* 20.3 (2013), pp. 881–900.

[29] B. Brogliato and D. Goeleven. "The Krasovskii-LaSalle invariance principle for a class of unilateral dynamical systems". In: *Mathematics of Control, Signals and Systems* 17 (2005), pp. 57–76.

[30] B. Brogliato and D. Goeleven. "Well-posedness, stability and invariance results for a class of multivaled Lur'e dynamical systems". In: *Nonlinear Analysis. Theory, Methods and Applications* 74 (2011), pp. 195–212.

[31] B. Brogliato and W.P.M.H. Heemels. "Observer design for Lur'e systems with multivalued mappings: A passivity approach". In: *IEEE Transactions on Automatic Control* 54.8 (2009), pp. 1996–2001.

[32] B. Brogliato, S. Niculescu, and M.D.P. Monteiro Marques. "On tracking control of a class of complementary-slackness hybrid mechanical systems". In: *Systems & Control Letters* 39.4 (2000), pp. 255–266.

[33] B. Brogliato, S.I. Niculescu, and P. Orhant. "On the control of finite-dimensional mechanical systems with unilateral constraints". In: *IEEE Transactions on Automatic Control* 42.2 (1997), pp. 200–215.

[34] B. Brogliato and P. Orhant. "Contact stability analysis of a one-degree-of-freedom robot". In: *Dynamcics and Control* 8.1 (1998), pp. 37–53.

[35] B. Brogliato, R. Ortega, and R. Lozano. "Globally stable nonlinear controllers for flexible joint manipulators: a comparative study". In: *Automatica* 31.7 (1995), pp. 941–956.

[36] B. Brogliato and A. Polyakov. "Digital implementation of sliding-mode control via the implicit method: A tutorial". In: *International Journal of Robust and Nonlinear Control* 31.9 (2021), pp. 3528–3586.

[37] B. Brogliato and A. Tanwani. "Dynamical systems coupled with monotone set-valued operators: Formalisms, applications, well-posedness, and stability". In: *SIAM Review* 62.1 (2020), pp. 3–129.

[38] B. Brogliato and L. Thibault. "Existence and uniqueness of solutions for non-autonomous complementarity systems". In: *Journal of Convex Analysis* 17.3-4 (2010), pp. 961–990.

[39] B. Brogliato et al. *Dissipative Systems Analysis and Control*. 3rd. Communications and Control Eng. Springer Nature Switzerland AG, 2020.

[40] B. Brogliato et al. "On the equivalence between complementarity systems, projected systems and differential inclusions". In: *Systems and Control Letters* 55 (2006), pp. 45–51.

[41] A. Cabboi, L. Marino, and A. Cicirello. "A comparative study between Amontons–Coulomb and Dieterich–Ruina friction laws for the cyclic response of a single degree of freedom system". In: *European Journal of Mechanics - A/Solids* 96 (2022), p. 104737.

[42] K. Camlibel. “Complementarity Methods in the Analysis of Piecewise Linear Dynamical Systems”. ISBN 90 5668 079 X. PhD thesis. Tilburg, NL: Katholieke Universiteit Brabant, 2001.

[43] M.K. Camlibel, W.P.M.H. Heemels, and J.M. Schumacher. “On linear passive complementarity systems”. In: *European Journal of Control* 58 (2002), pp. 220–237.

[44] M.K. Camlibel, L. Iannelli, and A. Tanwani. “Convergence of proximal solutions for evolution inclusions with time-dependent maximal monotone operators”. In: *Mathematical Programming Ser. A* 145 (2021). https://doi.org/10.1007/s10107-021-01666-7, pp. 1017–1059.

[45] M.K. Camlibel, L. Iannelli, and F. Vasca. “Passivity and Complementarity”. In: *Mathematical Programming Ser. A* 145 (2014), pp. 531–563.

[46] M.K. Camlibel, J.S. Pang, and J. Shen. “Lyapunov stability of complementarity and extended systems”. In: *SIAM Journal on Control and Optimization* 17.4 (2006), pp. 1056–1101.

[47] M.K. Camlibel and J.M. Schumacher. “Linear passive systems and maximal monotone mappings”. In: *Mathematical Programming Ser. B* 157 (2016), pp. 397–420.

[48] T. H. Cao et al. “Applications of controlled sweeping processes to nonlinear crowd motion models with obstacles”. In: *IEEE Control Systems Letters* 6 (2022), pp. 740–745.

[49] T. H. Cao et al. “Optimization of controlled free-time sweeping processes with applications to marine surface vehicle modeling”. In: *IEEE Control Systems Letters* 6 (2022), pp. 782–787.

[50] H. Cartan. *Cours de Calcul Différentiel*. 3rd. Paris, F: Hermann, 1967.

[51] X. Chen and S. Xiang. “Perturbation bounds of P-matrix linear complementarity problems”. In: *SIAM J. Optimization* 18.4 (2007), pp. 1250–1265.

[52] E.A. Coddington and Levinson. *Theory of Ordinary Differential Equations*. 6th reprint. New Delhi: Tata McGraw Hill Publishing Company LTD, 1982.

[53] G. Colombo, P. Gidoni, and E. Vilches. “Stabilization of periodic sweeping processes and asymptotic average velocity for soft locomotors with dry friction”. In: *Discr. Cont. Dyn. Syst.* 42.2 (2022), pp. 737–757.

[54] G. Colombo, B. S. Mordukhovich, and Dao Nguyen. “Optimal control of sweeping processes in robotics and traffic flow models”. In: *J. Optim. Theory Appl.* 182 (2019), pp. 439–472.

[55] G. Colombo, B. S. Mordukhovich, and Dao Nguyen. “Optimization of a perturbed sweeping process by con- strained discontinuous controls”. In: *SIAM Journal on Control and Optimization* 58 (2020), pp. 2678–2709.

[56] G. Colombo and M. Palladino. “The minimum time function for the controlled Moreau’s sweeping process”. In: *SIAM Journal on Control and Optimization* 54 (2016), pp. 2036–2062.

[57] G. Colombo et al. “Optimal control of the sweeping process”. In: *Dynamics of Continuous, Discrete and Impulsive Systems* B19 (2012), pp. 117–159.

[58] G. Colombo et al. “Optimal control of the sweeping process: the polyhedral case”. In: *J. Differential Eqs.* 260 (2016), pp. 3397–3447.

[59] A.G.S. Conceicao, M.D. Correia, and L. Martinez. “Modeling and friction estimation for wheeled omnidirectional mobile robots”. In: *Robotica* 34.9 (2016), pp. 2140–2150. DOI: 10.1017/S0263574715000065.

[60] M. Corless and G. Leitmann. “Continuous State Feedback Guaranteeing Uniform Ultimate Boundedness for Uncertain Dynamic Systems”. In: *IEEE Transactions on Automatic Control* 26.5 (1981), pp. 1139–1144.

[61] R.W. Cottle, J.S. Pang, and R.E. Stone. *The Linear Complementarity Problem*. Academic Press, 1992.

[62] G. Csernák and G. Licskó. “Asymmetric and chaotic responses of dry friction oscillators with different static and kinetic coefficients of friction”. In: *Meccanica* 56 (June 2021). DOI: 10.1007/s11012-021-01382-8.

[63] G. Csernák and G. Stépán. “On the periodic response of a harmonically excited dry friction oscillator”. In: *Journal of Sound and Vibration* 295.3 (2006), pp. 649–658.

[64] J. Das and A.K. Mallik. “Control of friction driven oscillation by time-delayed state feedback”. In: *Journal of Sound and Vibration* 297.3 (2006), pp. 578–594. DOI: https://doi.org/10.1016/j.jsv.2006.04.013.

[65] J. P. Den Hartog. “Forced Vibrations With Combined Coulomb and Viscous Friction”. In: *Transactions of the American Society of Mechanical Engineers* 53.2 (1930), pp. 107–115.

[66] B. A. Erickson, B. Birnir, and D. Lavallee. “Periodicity, chaos and localization in a Burridge–Knopoff model of an earthquake with rate-and-state friction”. In: *Geophysical Journal International* 187 (Aug. 2011), pp. 178–198. DOI: 10.1111/j.1365-246X.2011.05123.x.

[67] F. Facchinei and J. S. Pang. *Finite-Dimensional Variational Inequalities and Complementarity Problems*. Springer New York, NY, 2003. URL: https://api.semanticscholar.org/CorpusID:118457067.

[68] R. San Felice and B. Biemond. “An embedding approach for the design of state-feedback tracking controllers for references with jumps”. In: *Int. Journal of Robust and Nonlinear Control* 24 (2014), pp. 1585–1608.

[69] J.E. Fenel and L. Thibault. “BV solutions of nonconvex sweeping process differential inclusion with perturbation”. In: *Journal of Differential Equations* 226 (2006), pp. 135–179.

[70] F. Forni, A.R. Teel, and L. Zaccarian. “Follow the Bouncing Ball: Global Results on Tracking and State Estimation With Impacts”. In: *IEEE Transactions on Automatic Control* 58.6 (2013), pp. 1470–1485.

[71] S. Galeani, L. Menini, and A. Potini. "Trajectory tracking for a particle in elliptical billiards". In: *International Journal of Control* 81.2 (2008), pp. 189–213.

[72] B.C. Gegg, A.C.J. Luo, and Steve C. Suh. "Grazing bifurcations of a harmonically excited oscillator moving on a time-varying translation belt". In: *Nonlinear Analysis: Real World Applications* 9.5 (2008), pp. 2156–2174. DOI: https://doi.org/10.1016/j.nonrwa.2007.07.004.

[73] A. Giouvanidis and E. Dimitrakopoulos. "Nonsmooth dynamic analysis of sticking impacts in rocking structures". In: *Bulletin of Earthquake Engineering* 15 (May 2017). DOI: 10.1007/s10518-016-0068-4.

[74] D. Goeleven and B. Brogliato. "Stability and instability matrices for linear evolution variational inequalities". In: *IEEE Transactions on Automatic Control* 49.4 (2004), pp. 521–534.

[75] S. Greenhalgh, V. Acary, and B. Brogliato. "On preserving dissipativity properties of linear complementarity dynamical systems with the theta-method". In: *Numerische Mathematik* 125.4 (2013), pp. 601–637.

[76] T. H.Cao et al. "Optimization and discrete approximation of sweeping processes with controlled moving sets and perturbations". In: *Journal of Differential Equations* 274 (2021), pp. 461–509.

[77] T. H.Cao et al. "Optimization of fully controlled sweeping processes". In: *Journal of Differential Equations* 295 (2021), pp. 138–186.

[78] D. Heck et al. "Guaranteeing stable tracking of hybrid position–force trajectories for a robot manipulator interacting with a stiff environment". In: *Automatica* 63 (2016), pp. 235–247.

[79] M. A. Heckl and I.D. Abrahams. "Active Control of Friction-Driven Oscillations". In: *Journal of Sound and Vibration* 193.1 (1996), pp. 416–426. DOI: https://doi.org/10.1006/jsvi.1996.0285.

[80] W. P. M. H. Heemels et al. "Time-stepping methods for constructing periodic solutions in maximally monotone set-valued dynamical systems". In: *53rd IEEE Conference on Decision and Control*. 2014, pp. 3095–3100. DOI: 10.1109/CDC.2014.7039866.

[81] W.P.M.H. Heemels and B. Brogliato. "The Complementarity Class of Hybrid Dynamical Systems". In: *European Journal of Control* 9.2 (2003), pp. 322–360.

[82] W.P.M.H. Heemels et al. "Computation of periodic solutions in maximal monotone dynamical systems with guaranteed consistency". In: *Nonlinear Analysis: Hybrid Systems* 24 (2017), pp. 100–114. DOI: https://doi.org/10.1016/j.nahs.2016.10.006.

[83] W.P.M.H. Heemels et al. "Observer-based control of linear complementarity systems". In: *Int. J. of Robust and Nonlinear Control* 21.10 (2011), pp. 1193–1218.

[84] N. Hinrichs, M. Oestreich, and K. Popp. "On the Modelling of Friction Oscillators". In: *Journal of Sound and Vibration* 216.3 (1998), pp. 435–459. DOI: https://doi.org/10.1006/jsvi.1998.1736.

[85] Roger A. Horn and Charles R. Johnson. *Matrix Analysis*. 2nd. Cambridge University Press, 2013.

[86] M. Kamenskii, O. Makarenkov, and L.N. Wadippuli. "A continuation principle for periodic BV-continuous state-dependent sweeping processes". In: *SIAM Journal on Mathematical Analysis* 52.6 (2020), pp. 5598–5626.

[87] H.K. Khalil. *Nonlinear Systems*. 3rd. Upper Saddle River, NJ: Prentice Hall, 2002.

[88] R. Kikuuwe et al. "A nonsmooth quasi-static modeling approach for hydraulic actuators". In: *Transactions of ASME: Journal of Dynamic Systems, Measurement, and Control* 143.12 (2021), p. 121002.

[89] R. Kikuuwe et al. "Proxy-based sliding mode control: A safer extension of PID position control". In: *IEEE Transactions on Robotics* 26.4 (2010), pp. 670–683.

[90] Y. B. Kim and S. T. Noah. "Stability and Bifurcation Analysis of Oscillators With Piecewise-Linear Characteristics: A General Approach". In: *Journal of Applied Mechanics* 58.2 (June 1991), pp. 545–553. DOI: 10.1115/1.2897218.

[91] M. Kunze. *Non-smooth Dynamical Systems*. Lecture Notes in Mathematics 1744. Berlin Heidelberg: Springer-Verlag, 2000.

[92] B.K. Le. "On a class of Lur'e dynamical systems with state-dependent set-valued feedback". In: *Set-Valued and Variational Analysis* (2020).

[93] B.K. Le. "Well-posedness and nonsmooth Lyapunov pairs for state-dependent maximal monotone differential inclusions". In: *Optimization* 69.6 (2020), pp. 1187–1217.

[94] Mathias Legrand and Christophe Pierre. "A compact, equality-based weighted residual formulation for periodic solutions of systems undergoing frictional occurrences". In: *Journal of Structural Dynamics* 2 (2024), pp. 144–170. URL: https://hal.science/hal-04189699.

[95] D H Leine R I van Campen. "Discontinuous bifurcations of periodic solutions". In: *Mathematical and Computer Modelling* 36 (2002), pp. 259–273. DOI: 10.1006/jsvi.2000.3555.

[96] R.I. Leine, D. Campen, and B. Vrande. "Bifurcations in Nonlinear Discontinuous Systems". In: *Nonlinear Dynamics* 23 (2000), pp. 105–164.

[97] R.I. Leine and H. Nijmeijer. *Dynamics and Bifurcations of Non-Smooth Mechanical Systems*. Lecture Notes in Applied and Computational Mechanics 18. Berlin Heidelberg: Springer-Verlag, 2004.

[98] R.I. Leine and N. van de Wouw. "Uniform convergence of monotone measure differential inclusions: with application to the control of mechanical systems with unilateral constraints". In: *International Journal of Bifurcations and Chaos* 18.5 (2008), pp. 1435–1457.

[99] R.I. Leine et al. “Stick-slip vibrations induced by alternate friction models”. In: *Nonlinear Dynamics* 16.1 (1998), pp. 41–54.

[100] Y. Li and Z.C Feng. “Bifurcation and chaos in friction-induced vibration”. In: *Communications in Nonlinear Science and Numerical Simulation* 9.6 (2004), pp. 633–647. DOI: https://doi.org/10.1016/S1007-5704(03)00058-3.

[101] Z. Li, Q. Wang, and H.-P. Gao. “Control of friction oscillator by Lyapunov redesign based on delayed state feedback”. In: *Acta Mechanica Sinica* 25 (2009), pp. 257–264.

[102] Z. Li et al. “An improved iterative approach with a comprehensive friction model for identifying dynamic parameters of collaborative robots”. In: *Robotica* 42.5 (2024), pp. 1500–1522.

[103] Z. Li et al. “Non-stationary friction-induced vibration with multiple contact points”. In: *Nonlinear Dynamics* 111 (2023), pp. 9889–9917.

[104] C.-S. Liu and W.-T. Chang. “Frictional behaviour of a belt-driven and periodically excited oscillator”. In: *Journal of Sound and Vibration* 258.2 (2002), pp. 247–268. DOI: https://doi.org/10.1006/jsvi.2002.5108.

[105] Y. F. Liu et al. “Experimental comparison of five friction models on the same test-bed of the micro stick-slip motion system”. In: *Mechanical Sciences* 6 (2015), pp. 15–28.

[106] R. Lozano and B. Brogliato. “Adaptive control of robot manipulators with flexible joints”. In: *IEEE Transactions on Automatic Control* 37.2 (1992), pp. 174–181.

[107] A.C. J. Luo and M.T. Patel. “Bifurcation and Stability of Periodic Motions in a Periodically Forced Oscillator With Multiple Discontinuities”. In: *Journal of Computational and Nonlinear Dynamics* 4.1 (Dec. 2008), p. 011011. DOI: 10.1115/1.3007902.

[108] A.C.J. Luo and B.C. Gegg. “Periodic Motions in a Periodically Forced Oscillator Moving on an Oscillating Belt With Dry Friction”. In: *Journal of Computational and Nonlinear Dynamics* 1.3 (Mar. 2006), pp. 212–220. DOI: 10.1115/1.2198874.

[109] D.S. Madeira and J. Adamy. “On the equivalence between strict positive realness and strict passivity of linear systems”. In: *IEEE Transactions on Automatic Control* 61.10 (2016), pp. 3091–3095.

[110] S. Manfredi and D. Angeli. “Necessary and sufficient conditions for consensus in nonlinear monotone networks with unilateral interactions”. In: *Automatica* 77 (2017), pp. 51–60.

[111] L. Marino and A. Cicirello. “Experimental investigation of a single-degree-of-freedom system with Coulomb friction”. In: *Nonlinear Dynamics* 99 (2020), pp. 1781–1799.

[112] M.D.P. Monteiro Marques. *Differential Inclusions in Nonsmooth Mechanical Problems. Shocks and Dry Friction*. Vol. 9. Progress in Nonlinear Differential Equations and their Applications. Basel: Birkhäuser Verlag, 1993.

[113] K. Mehran et al. “Stability Analysis of Sliding–Grazing Phenomenon in Dry-Friction Oscillator Using Takagi–Sugeno Fuzzy Approach”. In: *Journal of Computational and Nonlinear Dynamics* 10.6 (Nov. 2015), p. 061010. DOI: 10.1115/1.4029663.

[114] L. Menini, C. Possieri, and A. Tornambe. “Algebraic Methods for Multiobjective Optimal Design of Control Feedbacks for Linear Systems”. In: *IEEE Transactions on Automatic Control* 63.12 (2018), pp. 4188–4203.

[115] L. Menini, C. Possieri, and A. Tornambe. “Trajectory tracking of a bouncing ball in a triangular billiard by unfolding and folding the billiard table”. In: *International Journal of Control* 95 (2021), pp. 1–14.

[116] L. Menini and A. Tornambe. “Asymptotic tracking of periodic trajectories for a simple mechanical system subject to nonsmooth impacts”. In: *IEEE Transactions on Automatic Control* 46.7 (2001), pp. 1122–1126.

[117] C.I. Morarescu and B. Brogliato. “Passivity-based switching control of flexible-joint complementarity mechanical systems”. In: *Automatica* 46.1 (2010), pp. 160–166.

[118] C.I. Morarescu and B. Brogliato. “Trajectory tracking control of multiconstraint complementarity Lagrangian systems”. In: *IEEE Transactions on Automatic Control* 55.6 (2010), pp. 1300–1313.

[119] B. S. Mordukhovich and D. Nguyen. “Discrete approximations and optimal control of nonsmooth perturbed sweeping processes”. In: *Journal of Convex Analysis* 28.2 (2021), pp. 655–688.

[120] J.J. Moreau. “Evolution problem associated with a moving convex set in a Hilbert space”. In: *Journal of Differential Equations* 26.3 (1977), pp. 347–374. DOI: https://doi.org/10.1016/0022-0396(77)90085-7.

[121] J.J. Moreau. “La notion de surpotentiel et les liaisons unilatŕales en élastostatique”. In: *C. R. Acad. Sci. Paris Sér. A-B* (1968), A954–A957.

[122] J.J. Moreau. *Rafle par un convexe variable (Deuxième partie)*. Article dans ”Séminaire d’analyse convexe”, Montpellier, exposé n°3. 1972. URL: https://hal.science/hal-02309457.

[123] J.J. Moreau. *Rafle par un convexe variable (Première partie)*. Article dans ”Séminaire d’analyse convexe”, Montpellier, exposé n°15. 1971. URL: https://hal.science/hal-02309451.

[124] J.J. Moreau. “Unilateral Contact and Dry Friction in Finite Freedom Dynamics”. In: *Nonsmooth Mechanics and Applications*. Ed. by J. J. Moreau and P. D. Panagiotopoulos. Vol. 302. International Center for Mechanical Sciences. https://link.springer.com/chapter/10.1007/978-3-7091-2624-0_1. Vienna: Springer Verlag, 1988, pp. 1–82.

[125] M. Oestreich, N. Hinrichs, and K. Popp. “Bifurcation and stability analysis for a non-smooth friction oscillator”. In: *Archive of Applied Mechanics* 66.5 (1996), pp. 301–314. DOI: 10.1007/s004190050070.

[126] F. Padula, L. Ntogramatzidis, and E. Garone. “MIMO tracking control of LTI systems: A geometric approach”. In: *Systems and Control Letters* 126 (2019), pp. 8–20.

[127] A. Pavlov and L. Marconi. “Incremental passivity and output regulation”. In: *Systems & Control Letters* 57 (May 2008), pp. 400–409.

[128] Q. H. Pham and B. Brogliato. “Correction to "Analysis of the Implicit Euler Time-Discretization of a Class of Descriptor-Variable Linear Cone Complementarity Systems", J. Convex Analysis 29/2 (2022) 481–517”. In: *Journal of Convex Analysis* 31.3 (2024), pp. 1035–1037.

[129] K. Popp and P. Stelter. “Stick-Slip Vibrations and Chaos”. In: *Philosophical Transactions: Physical Sciences and Engineering* 332.1624 (1990), pp. 89–105. DOI: http://www.jstor.org.sid2nomade-1.grenet.fr/stable/76822..

[130] M. Posa, M. Tobenkin, and R. Tedrake. “Stability analysis and control of rigid-body systems with impacts and friction”. In: *IEEE Transactions on Automatic Control* 61.6 (2016), pp. 1423–1437.

[131] M. Rijnen, A. Saccon, and H. Nijmeijer. “Reference spreading: Tracking performance for impact trajectories of a 1DoF setup”. In: *IEEE Transactions on Control Systems Technology* 28.3 (2019), pp. 1124–1131.

[132] M. Rijnen et al. “Hybrid systems with state-triggered jumps: Sensitivity-based stability analysis with application to trajectory tracking”. In: *IEEE Transactions on Automatic Control* 65.11 (2020), pp. 4568–4583.

[133] G. Rill, T. Schaeffer, and M. Schuderer. “LuGre or not LuGre”. In: *Multibody System Dynamics* 60 (2024), pp. 191–218.

[134] R.T. Rockafellar. *Convex Analysis*. New Jersey: Princeton University Press, 1970.

[135] R.T. Rockafellar and R.J.B. Wets. *Variational Analysis*. Vol. 317. Grundlehren der mathematischen Wissenschaften. Corrected Third Printing. Berlin Heidelberg: Springer Verlag, 2009.

[136] C. Scherer and S. Weiland. *Linear Matrix Inequalities in Control*. https://www.imng.uni-stuttgart.de/mst/files/LectureNotes.pdf. 2015.

[137] M. Schuderer et al. “Friction modeling from a practical point of view”. In: *Multibody System Dynamics* (2024). DOI: https://doi.org/10.1007/s11044-024-09978-0.

[138] V. Sessa et al. “A complementarity approach for the computation of periodic oscillations in piecewise linear systems”. In: *Nonlinear Dynamics* 85 (July 2016).

[139] S. W. Shaw. “On the dynamic response of a system with dry friction”. In: *Journal of Sound and Vibration* 108 (1986), pp. 305–325.

[140] J. Shen. “Robust non-Zenoness of piecewise affine systems with applications to linear complementarity systems”. In: *SIAM Journal on Optimization* 24.4 (2014), pp. 2023–2056.

[141] J. Shen and J.S. Pang. "Linear complementarity systems: Zeno states". In: *SIAM Journal on Optimization* 44 (2005), pp. 1040–1066.

[142] E. Sontag. "Contractive Systems with Inputs". In: vol. 398. Mar. 2010, pp. 217–228. DOI: 10.1007/978-3-540-93918-4_20.

[143] E.D. Sontag. *Mathematical Control Theory: Deterministic Finite Dimensional Systems.* Texts in Applied Mathematics. New York: Springer, 2013.

[144] M.W. Spong. "Modeling and control of elastic joint robots". In: *ASME J. Dyn. Systems Measurement and Control* 109.4 (1987), pp. 310–319.

[145] A. Tanwani, B. Brogliato, and C. Prieur. "Well-posedness and output regulation for implicit time-varying evolution variational inequalities". In: *SIAM Journal on Control and Optimization* 56.2 (2018), pp. 751–781.

[146] L. Thibault. "Sweeping process with regular and nonregular sets". In: *Journal of Differential Equations* 193 (2003), pp. 1–26.

[147] J.J. Thomsen. "Using Fast Vibrations to Quench Friction-Induced Oscillations". In: *Journal of Sound and Vibration* 228.5 (1999), pp. 1079–1102. DOI: https://doi.org/10.1006/jsvi.1999.2460.

[148] J.J. Thomsen and A. Fidlin. "Analytical approximations for stick–slip vibration amplitudes". In: *International Journal of Non-Linear Mechanics* 38 (Apr. 2003), pp. 389–403. DOI: 10.1016/S0020-7462(01)00073-7.

[149] P. Vigué et al. "Regularized friction and continuation: Comparison with Coulomb's law". In: *Journal of Sound and Vibration* 389 (2017), pp. 350–363.

[150] A.A. Vladimirov. "Nonstationary dissipative evolution equations in a Hilbert space". In: *Nonlinear Analysis: Theory, Methods & Applications* 17.6 (1991), pp. 499–518.

[151] L. Niwanthi Wadippuli, I. Gudoshnikov, and O. Makarenkov. "Global asymptotic stability of nonconvex sweeping processes". In: *Discrete and Continuous Dynamical Systems - B* 25.3 (2020), pp. 1129–1139.

[152] H. Zhang, B. Brogliato, and C. Liu. "Dynamics of planar rocking-blocks with Coulomb friction and unilateral constraints: Comparisons between experimental and numerical data". In: *Multibody System Dynamics* 32 (June 2013). DOI: 10.1007/s11044-013-9356-9.